



# Wind power in cold climates

Ice mapping methods

Elforsk report 13:10



Hans Bergström, Esbjörn Olsson, Stefan Söderberg,  
Petra Thorsson, Per Undén

March 2013

# Wind power in cold climates

Ice mapping methods

Elforsk report 13:10

Hans Bergström, Esbjörn Olsson, Stefan Söderberg,  
Petra Thorsson, Per Undén

March 2013

## Preface

This report is the final report from the Vindforsk III project V-313, Wind Power in Cold Climate.

Vindforsk – III is funded by ABB, Arise windpower, AQSystem, E.ON Elnät, E.ON Vind Sverige, Energi Norge, Falkenberg Energi, Fortum, Fred. Olsen Renewables, Gothia wind, Göteborg Energi, Jämtkraft, Karlstads Energi, Luleå Energi, Mälarenergi, O2 Vindkompaniet, Rabbalshede Kraft, Skellefteå Kraft, Statkraft, Stena Renewable, Svenska Kraftnät, Tekniska Verken i Linköping, Triventus, Wallenstam, Varberg Energi, Vattenfall Vindkraft, Vestas Northern Europe, Öresundskraft and the Swedish Energy Agency.

Reports from Vindforsk are available from [www.vindforsk.se](http://www.vindforsk.se)

The project has been led by Hans Bergström at Uppsala University. The work has been carried out by Uppsala University, WeatherTech Scandinavia, and SMHI

Comments on the work have been given by a reference group with the following members:

Sven-Erik Thor, Vattenfall Vindkraft  
Daniel Eriksson, Skellefteå Kraft  
Fredrik Stighall, Jämtkraft  
Göran Ronsten, WindRen AB (repr för O2)  
Helena Hedblom, Fortum  
Martin Lindholm, E.ON Vind Sverige AB  
Måns Håkansson, Statkraft  
Anders Björck, Elforsk  
Stockholm March 2013



Anders Björck

Programme manager Vindforsk-III

Electricity- and heatproduction, Elforsk



## Sammanfattning

I Vindforsk V-313 projektet "Vindkraft i kallt klimat" har målet varit att utveckla metoder för att konstruera en högupplöst (1x1 km<sup>2</sup>) klimatologi för isbildning på vindkraftverk. Detta är en mycket krävande uppgift eftersom instrumentella observationer av isbildning bara har varit rutinmässigt tillgängliga i Sverige under tre vintersäsonger och endast på ett dussintal platser. Termen klimatologi i klassisk meteorologi betyder statistik över 30 års data, och oftast i form av direkta eller indirekta observationer. Exempel är medeltemperaturen (årlig, månatlig, maximum etc.), antal frostdagar, växtsäsong, variabilitet, antal dagar med nederbörd, medelvind, molnighet, solinstrålning, för att nämna några.

I projektet har forskare från Uppsala universitet, WeatherTech Scandinavia och SMHI samarbetat. Observationer har analyserats och "state-of-the-art" numeriska väderprognosermodeller har tillämpats i fallstudier och testats i ett flertal känslighetsstudier. Omfattande modellverifieringar har utförts. Modellerad islast och beräknade produktionsförluster har också jämförts med mätningar. Flera metoder testades med syfte att erhålla en metod med vilken man kan representera en långsiktig klimatologi baserad på endast ett fåtal års data.

Projektet har belyst osäkerheterna i modellering av islast och isklimat. Slutresultaten beror inte enbart på vilken mesoskalig modell som används utan även på hur modellen är uppsatt. För att förbättra modellerna behövs mer exakta mätningar av islast. Observationer av mängden molnvatten och fördelningen av droppstorlek kan också vara av stort värde för att bättre förstå varför modellerna inte lyckas beskriva den islast som observationerna ger.

*Några viktiga resultat är:*

### **Observationer - Avsnitt 3**

Observationerna har främst hämtats från O2:s Vindpilotprojekt vilka gjordes tillgängliga för V-313-projektet. Mätplatserna instrumenterades under de tre vintersäsongerna 2009/2010-2011/2012, alla platser var inte tillgängliga från början. Det har också förekommit avbrott i mätningarna under längre eller kortare perioder på vissa platser. Ismätningarna har granskats noggrant och kontrollerats för att vara i överensstämmelse med t.ex. temperaturdata från samma platser. Korrigeringar för förskjutningar av nollnivå hos instrumenten har gjorts. Islasterna befanns också vara mycket brusiga och en filtrering har därför tillämpats. Dessa korrigeringar kunde inte automatiseras utan måste göras manuellt.

Det måste betonas att dessa resultat INTE kan tas som klimatologiska värden för islast. Mängden data är alltför begränsad och kvaliteten på islastdata kan ifrågasättas. Det är välkänt att mätning av islast är en svår uppgift och de instrument som finns har alla sina styrkor och svagheter. Resultat av Vindforsk projektet V-363 redovisas i rapporten "Experiences of different ice measurements methods", visar att ingen teknik och inget instrument för att mäta islast eller istillväxt i dagsläget kan användas med tillförsikt i alla situationer.

**Modellering av islast - Avsnitten 4 och 5**

Tre mesoskaliga modeller på km-skalan, WRF, Arome och COAMPS<sup>®</sup>, har använts i projektet. Först och främst har de använts för att validera både mätningar mot modell och modellernas prestanda mot mätningar.

Dessa "state-of-the-art" mesoskaliga modeller kan simulera utvecklingen med tiden av tryck, temperatur, vind och fukt (och även sikt) ganska väl. En drift eller bias i instrumenten för ismätningar kan ganska lätt upptäckas när man jämför mot modellerade värden. Skillnader mellan de olika modellernas resultat har sannolikt sin grund i skillnader mellan modellernas beskrivning av terräng och geomorfologiska egenskaper, samt skillnader i modellernas parameterisering av fysiken. Till exempel har det visat sig att modellernas turbulens-scheman spelar en stor roll för vind- och temperaturprofiler, vilka i sin tur påverkar modellerat molnvatten.

Vid utvärdering av modellresultat och observationer är det av vikt att beakta att mätningar representerar tillståndet i atmosfären vid eller mycket nära en exakt punkt i rummet, medan modellerna representerar ett genomsnitt över en eller ett par kvadratkilometer (en modells grid-ruta). Detta innebär att mätningarna representerar mycket mindre skalor än modellerna. Den småskaliga variationen återspeglas i varianserna som ses i verifikationerna. Även ett perfekt modellresultat kan aldrig förväntas ligga närmare observationerna än vad som beskrivs av variansen på dessa små skalor. Trots detta visar en jämförelse av resultaten från tre olika modeller, med olika parameteriseringar, initial- och randvillkor, ändå jämförbara värden vilket ökar tillförlitligheten hos resultaten.

För att uppskatta istillväxten användes den så kallade Makkonens formel. Indata till denna är vindhastighet, temperatur och molnkondensat, vilka tas från vädermodellerna. Droppkoncentration antogs ha ett konstant värde på  $100 \text{ cm}^{-1}$ . De observerade isbildningsepisoderna fångas ofta väl i tiden av modellerna. Överensstämmelsen mellan den modellerade islastens storlek, jämfört med de uppmätta islasterna, förbättrades efter att man korrigerat för skillnaden mellan modellernas terränghöjd och den verkliga terrängens höjd. Hävning av luften till högre höjd för de fall modellernas terränghöjd var lägre än mätplatsernas terränghöjd, och omräkning av tillståndet i den volym av luft som lyftes, resulterade i mer molnvatten och större isbildning. Det ska här påpekas att modellresultaten jämförs med den mest osäkra kvantiteten som mäts, nämligen islasten. En osäkerhet är iskast som i viss mån kan korrigeras för i mätningarna, men som inte är rakt på sak att modellera. Att minska osäkerheten i den observerade islasten är nödvändigt för att förbättra modellerna. I projektet har det också framkommit att istillväxten ofta påverkas av både flytande och frysta molnpartiklar, att innefatta båda i beräkningarna ökar den beräknade islasten ytterligare. Mer forskning om hur detta bör göras behövs dock.

Kartor som visar antal timmar med aktiv nedisning, isbildning överstigande 10 g/h, för alla tre mesoskaliga modellerna och för de tre vintersäsongerna, visar ett samband mellan topografihöjd och istimmar. Speciellt är det de lokala skillnaderna i terränghöjd som är av betydelse, mer isbildning återfinns på bergstoppar jämfört med i dalarna. Det visade sig att islasterna har en stor säsongsvariation i antalet timmar med isbildning. Inte bara avseende timmar med nedisning i en viss punkt utan också i vilken del av landet som mest

isbildning hittades. Denna förståelse är viktig vid valet av metod för att skapa en isklimatologi. Dessutom visades det att slutresultatet inte enbart berodde på vilken mesoskalig modell som används utan även på hur modellen är uppsatt.

### **Modellering av isklimatet - Avsnitt 6**

Det är uppenbart att det inte är möjligt att kartlägga ett isklimat enbart utgående från observationer, speciellt inte med det antalet platser som finns idag, (även om dessa utgör ett unikt och värdefullt nätverk i sig) och det kommer aldrig att bli möjligt att skapa ett nätverk med tillräckligt stort antal mätplatser på grund av kostnader och logistik. Sedan är det tidsaspekten. En datamängd som täcker några årtionden (t.ex. 30 år som för konventionella meteorologiska observationer) kommer att krävas, men branschen och beslutsfattare kan inte vänta så länge.

Sålunda måste en klimatologi vara modellbaserad och göras med så hög upplösning som möjligt för att fånga den lokala variationen i isklimatet. Att köra modellerna med 1 km upplösning för hela landet under 30 år skulle vara mycket krävande vad det gäller datorresurserna. Beroende på hur mycket resurser som kan investeras i ett sådant projekt kan det ta från år till decennier att slutföra. Av den anledningen har metoder som kräver kortare beräkningstider undersökts. Med förhoppningen att det genom att välja representativa månader skulle kunde bara tillräckligt att modellera några år. Av de metoder som testats här framstod en metod som det bästa alternativet, en metod grundad på bästa anpassningen av temperatur och vindhastighet till långtidsmedlet. Men ytterligare insatser behövs för att förbättra metodens representativitet för isbildning, innan den kan tillämpas för att kartlägga isklimatet.

Nedskalningstekniker där man utgår från lägre modellupplösning är en annan väg som undersökts. En modell med 9 km upplösning är fullt möjligt att köra i 30 år och sedan används statistiska samband mellan resultaten från en 1 km modell, över ett visst område och tid, med 9 km modellen. Skillnaderna i terränghöjd är den fysiska grunden till skillnaderna och de flesta av variationen i en 1 km modell kan förklaras av dessa, åtminstone vad det gäller tidsmedelvärden. Det har visats att lokala områden med hög isbildningsfrekvens kan reproduceras från en 9 km modell på detta sätt.

De två tillgängliga alternativ som har testats här (om man utelämnar fem år på rad som inte rekommenderas) har olika fördelar och nackdelar. Nedskalningstekniken, som är baserad på modellkörningar med lägre upplösning, gör det möjligt att använda en tillräckligt lång period så att osäkerheten om klimatologisk representativitet kommer att vara liten. Å andra sidan har vi infört en osäkerhet genom nedskalningen själv.

Med metoden som använder representativa månader introducerar vi istället en osäkerhet om hur representativa de utvalda kortare perioderna faktiskt är för klimatet. Istället minskar osäkerheten genom att det blir möjligt att göra modellberäkningarna med 1 km upplösning direkt för klimatologin. Men sedan har det också visats att valet av modell som används för detta kan medföra stora skillnader i resultaten.

Kanske det bästa alternativet skulle vara att först med hjälp av flera olika modeller göra klimatologier över hela landet med lägre modellupplösning.

Sedan genom en ensembleteknik beräknas den statistiskt mest sannolika isklimatologin på denna skala, för att slutligen tillämpa nedskalningstekniken för att komma till en isklimatologi med 1 km upplösning. Men denna teknik har inte testats hittills.

### ***Mesoskalig modellering av produktionsförluster - Avsnitt 7***

I projektet har observationer av islast på turbinblad inte funnits tillgängliga. För att uppskatta produktionsförlust orsakade av nedisning, har istället empiriska relationer utvecklats mellan observerad islast med IceMonitorn och observerade produktionsförluster.

Det visade sig att förlusterna verkar vara större vid lägre vindhastigheter och att produktionsförluster främst uppträder under istillväxt. Produktionen ökar igen ganska snabbt när istillväxten upphör, medan den uppmätta islasten ligger kvar på konstant nivå. Det finns även en uppenbar skillnad i isläpp och sublimering mellan IceMonitorn och turbinblad. Därför är det möjligen inte bästa metoden att gå vidare med att ytterligare utveckla modeller som uppskattar produktionsförluster som en funktion av vindhastighet och islast. En möjlig alternativ väg framåt som diskuteras är att istället utveckla en modell där produktionsförlusten beror på den potentiella istillväxten över hela rotordiametern. Data från många vindparker med många typer av turbiner behövs sannolikt för att göra en generell modell av produktionsförlusterna.

## Summary

In the Vindforsk V-313 project "Vindkraft i kallt klimat" the goal was to arrive at a methodology to construct a high resolution (1x1 km<sup>2</sup>) climatology of icing on wind power turbines. This is a very demanding task since observations of icing on instruments have only been routinely available in Sweden during three winter seasons and at a dozen locations. The term climatology in classical meteorology means statistics over 30 years of data, and usually in the form of direct or indirect measurements. Examples are mean temperatures (annual, monthly, maximum etc.), number of frost days, growing season, variability, number of days of precipitation, mean winds, cloudiness, solar radiation, to name a few.

In the project researchers from Uppsala University, WeatherTech Scandinavia, and SMHI have been collaborating. Observations have been analysed and state-of-the-art numerical weather prediction models have been applied in case studies and tested in several sensitivity studies. Extensive model verification has been carried out. Modelled ice load and estimated production losses were also compared to measurements. The question of how to arrive at a method using only a few years to represent the long-term climatology was addressed and several methods were tested.

The project has shed light on the uncertainties in modelling ice load and icing climate. The end results not only depend on which mesoscale model that is used but also on how the model is set up. In order to improve the models more accurate measurements of ice load is needed. Observations of liquid cloud water content and droplet size distributions could also be of significant value to better understand why the ice load models fail in capturing the observed ice load.

*Some important results are:*

### **Observations – Section 3**

The observations are mainly results from O2's Wind Pilot project and were made available to the V-313 project. The sites were established during the three winter seasons 2009/2010-2011/2012; all sites were not available from the beginning. There have also been outages at some sites for longer or shorter periods. The data have been scrutinised meticulously and checked for consistency, e.g. with co-located temperature data. Corrections for zero-level of the ice load instruments have been made, but the ice load data were also found to be quite noisy and a filtering procedure has been applied. These corrections could not be done automatically and manual inputs were needed.

It must be emphasised that these results can NOT be taken as climatological values of the ice load. The amount of data is far too sparse and the quality of the ice load data could be doubted. It is well known that measuring ice load is a difficult task and all instruments have their strengths and weaknesses. Results of the Vindforsk project V-363 with report "Experiences of different ice measurements methods" indicate that no technique and no instrument for measuring ice load or ice accretion can be trusted in every icing situation.

**Modelling of ice load – Sections 4 and 5**

Three meso-scale km scale resolution models, WRF, AROME and COAMPS®, have been employed in this work. First and foremost, they have been used to validate both the measurements against the model and the model performance against the measurements.

The state-of-the-art meso-scale models are able to simulate the time evolution of pressure, temperature, wind, and humidity (and also visibility in fact) quite accurately. A drift or bias in the instruments for ice measurements can quite easily be detected when comparing against the model values. Differences in results between the models are likely due to differences between model terrain and other physiographic fields of the models and also the physical parameterisations. For instance it is shown that the turbulence schemes in the models play a major role for the wind and temperature profiles, which in turn have an effect on the modelled cloud liquid water.

When evaluating model results and observations it is of importance to consider that measurements represent the state of the atmosphere at or very close to a precise point in space, whereas the models represent an average over one or a few square km (a model grid box). This means that the measurements represent much smaller scales than the models. The small-scale variability is reflected in the variances seen in the verifications. Even a perfect model can never verify closer to perfect observations than those variances at small scales. In spite of this three different models using different parameterisations, initial and boundary conditions, still producing quite comparable results, which increases the reliability of the results.

To estimate the ice accretion, the so-called Makkonen formula was employed. Input to this model, wind speed, temperature and cloud condensates, was taken from the weather prediction models. Droplet number concentration was assumed to have a constant value of  $100 \text{ cm}^{-3}$ . The observed icing episodes are most often captured well in time. The predicted magnitudes of the ice loads, compared with the measured ones, were improved after taking the difference between model terrain height and the real terrain height of the site into account. Lifting of the air in cases of higher terrain height than model terrain height and re-calculating the state in a volume of air lifted results in more cloud condensate and more icing. It must here be pointed out that the model results are compared to the most uncertain quantity monitored, namely the ice load. One uncertainty is ice shedding which to some extent can be corrected for in the measurements but not straight forward to model. Reducing the uncertainties in the observed ice load is necessary for improving the models. In the project it was also found that icing often involves a mix of liquid and frozen cloud particles, and taking this into account increases the estimated ice load further. More research on how to include this is, however, needed.

Maps with number of hours with active icing, ice accretion exceeding 10 g/h, for all three meso-scale models and the three winter seasons show a relation between topographic height and icing hours. In particular it is the local differences in terrain height that are of importance, more icing is found on hilltops than in valleys. It is found that the maps show a high inter-seasonal variation in the numbers of icing hours. Not only in the number of icing hours in a single point but also in which part of the country that most icing is found.

This understanding is of importance for choosing a method to create an icing climatology. Moreover, it is shown that the end results not only depend on which mesoscale model that is used but also on how the model is set up.

### ***Modelling the icing climate – Section 6***

It is clear that it is not possible to map an icing climate with observations alone, certainly not with the number of sites available today, (even if this is a unique and valuable network in itself) and it will never be possible to establish a dense enough network due to cost and logistics. Then there is the time aspect. A dataset covering a few decades (e.g. 30 years as for conventional meteorological observations) will be required, but the industry and decision makers cannot wait that long.

Thus, a climatology has to be model based and preferably with as high as possible resolution to capture the local variability in the icing climate. To run the models at 1 km model grid resolution for the whole country for some 30 years would be very computationally expensive. Depending on how much resource that can be invested in such a project, it can take from a year to decades to finish. Therefore investigations of methods employing less computational time have been carried out. One could hope that by choosing representative months, only a few years of modelling could be sufficient. Of the methods tested here, one method stood out as being the best option, the so-called best fit of temperature and wind speed. But, further work is needed to improve the representation of the icing climate before it can be applied to map the icing climate.

Downscaling techniques from coarser resolution models is another avenue that was explored. A 9 km resolution model is quite feasible to run for 30 years and then to use statistical relationships between a 1 km model, over a certain area and time, with the 9 km model. The differences in terrain height is the physical reason for the differences and most of the variability in a 1 km model can be described in this way, at least for time averaged values. It is demonstrated that local areas of high icing frequency can be reproduced from a 9 km model in this way.

The two options available and tested here (excluding five consecutive years which is not recommended) have different advantages and disadvantages. The downscaling technique, which is based on coarse resolution model runs, allows a long enough period to be used so that the uncertainty regarding climatological representativeness will be small. On the other hand we introduce an uncertainty through the downscaling itself. With the representative months method we instead introduce an uncertainty regarding how representative the chosen shorter periods actually are for the climate. Instead we reduce uncertainty in that it will become feasible to make the 1 km resolution climatology using high-resolution model runs directly. But then again, it has been demonstrated that the choice of model used for this can make quite a difference to the results.

Maybe the best option would be to first make coarse resolution climatology over the whole country using several different models. Then use some ensemble technique to get the statistically most probable icing climatology on that scale, and finally applying the downscaling technique to arrive at the 1 km resolution icing climatology. But this technique has not been tested so far.

***Meso-scale modelling of production losses – Section 7***

In the project, observations of ice load on turbine blades have not been available. To estimate the production loss due to icing, empirical relationships between observed ice load on the IceMonitor and observed production losses were instead developed.

It was found that the losses seem to be greater at lower wind speeds and that production losses primarily occur during ice build-up. The production picks up again rather quickly when the build-up stops while the measured ice load stays at a constant level. There is an evident difference in ice shedding and sublimation between the IceMonitor and turbine blades. Hence, to further develop models that estimate production losses as a function of wind speed and ice load only might not be the best approach. A possible way forward discussed is to instead develop a model in which the production loss depends on the potential icing over the entire rotor disc. Many wind farm datasets with many types of turbines is likely needed to make a general production loss model.

<b>1</b>	<b>Introduction</b>	<b>2</b>
<b>2</b>	<b>Background</b>	<b>6</b>
2.1	Summary of Chapter 2 .....	10
<b>3</b>	<b>Observations</b>	<b>11</b>
3.1	Instrumentation .....	11
3.2	Measurement results.....	13
3.3	Summary of Chapter 3 .....	25
<b>4</b>	<b>Meso-scale modelling of ice load</b>	<b>28</b>
4.1	Description of models.....	28
4.1.1	AROME .....	32
4.1.2	COAMPS® .....	35
4.1.3	WRF .....	38
4.2	Comparisons with observations .....	42
4.2.1	Meteorological data .....	42
4.2.2	Ice load data .....	89
4.3	Sensitivity of results to model parameterizations and boundary condition.....	96
4.4	Summary of Chapter 4 .....	113
<b>5</b>	<b>Results from modelling of ice load during three winter seasons</b>	<b>115</b>
5.1	AROME 2.5km.....	115
5.2	COAMPS® and WRF 3km.....	120
5.3	COAMPS® and WRF 1km.....	126
5.4	Summary of Chapter 5 .....	132
<b>6</b>	<b>Modelling the icing climate</b>	<b>133</b>
6.1	Using representative months or periods.....	134
6.1.1	Comparison between different representative period methods.	135
6.1.2	Modelling the icing .....	138
6.1.3	Comparison between the different methods.....	139
6.1.4	Comments on the results.....	163
6.1.5	A discussion on the length of the representative period.....	164
6.2	Using downscaling techniques .....	166
6.2.1	Results using statistical downscaling .....	169
6.3	Summary of Chapter 6 .....	189
<b>7</b>	<b>Meso-scale modelling of production losses</b>	<b>190</b>
7.1	Method .....	190
7.2	Results from winter season 2011/2012 .....	192
7.3	Summary of Chapter 7 .....	195
<b>8</b>	<b>Discussion and future work</b>	<b>196</b>
	<b>References</b>	<b>202</b>
	<b>Publications and conference proceedings in the project</b>	<b>205</b>
	<b>Appendix A</b>	<b>207</b>
	<b>Appendix B</b>	<b>227</b>



# 1 Introduction

## Description of the Project work and staff involved

The first part of the Project dealt a lot with setting up and configuring the models to run and simulate the icing in Sweden and at the measurements sites, for three winter (half year) seasons. They needed to be run at as high resolution as possible with computer resources available. WeatherTech and SMHI have different approaches as regards coupling (forcing) from global models and to analysis data to start forecasts. Furthermore, SMHI has the capability (and the normal experience) of running its model over the whole domain of interest (Sweden) whereas WeatherTech applies the commonly used telescope technique to be able to focus on a limited number of sites at high resolution. The first season SMHI ran with a grid resolution of 2.5 km over the northern part of Sweden whereas WeatherTech could go down to 1 km around the sites of interest.

Many tests and comparisons and introduction of latest up to date model versions and configurations were made during the first year. Model differences, and even choices within one model, turned out to be much more important than the external forcing approaches (boundaries and analyses). Ulf Andrae and Per Undén from SMHI and Stefan Söderberg, WeatherTech, and Hans Bergström, Uppsala University, were the main persons involved in this part of the work.

Observations, mainly from the sites of the O2 Wind Pilot project, were used from the start, as they came on line. Even though the models showed reasonable agreements with icing observations, it was realized from the beginning that the observations needed thorough quality control and adjustments. Also the associated meteorological observations were sometimes in error. Petra Thorsson was recruited as PhD student at Uppsala University and she did extensive quality control over the seasons 2009/2010 and 2010/2011 of data and provided quality controlled data. Hans Bergström was also involved and later on in the project he developed and employed corrections and filtering to the ice load observation.

Petra Thorsson started her PhD work with an extensive study of the icing processes and surveyed the literature for the different known methods of calculation. The report (Thorsson, 2010) serves as reference and background for not only the V-313 project but can be recommended for anybody who wants to find out more about the icing on structures.

The model simulations continued and with new model versions and increase of resolution or area in the case of AROME at SMHI (to cover practically all of Sweden at 2.5 km and one area in the middle part of the country at 1 km). WeatherTech started to employ WRF at this stage, as a complement to COAMPS<sup>®</sup>. WRF is a more developed modelling system with several options of e.g., microphysics schemes. Esbjörn Olsson, SMHI, joined the project from

the second year and did most of the modelling and data (observation handling) work and later replaces Ulf Andrae. At WeatherTech Magnus Baltscheffsky worked with WRF and later also Andreas Grantinger helped with the extensive runs and production of data. Much of this production was made on the SMHI computing facilities at NSC, Linköping. The extensive cluster computing time was provided as in kind contribution following Energimyndigheten's directives. In kind contributions of computing facilities was also provided by WeatherTech for all COAMPS<sup>®</sup> simulations and WRF sensitivity tests. WeatherTech also provided a 30-year database of WRF runs on a 9-km model grid. During the last year Björn Stensen and Lisa Bengtsson became involved from the SMHI side (on observations of visibility and on model representation of cloud species).

During the second half of the project the modelling of the ice accretion from meteorological model parameters was enhanced with a lifting method accounting for differences between real site height and model topography and having it flow dependent. It showed to be important in order to reach the right amount of ice load as seen from the measurements. Care was taken to use identical calculations for all the models involved. Extensive data extraction from the models were made in a coordinated manner between the participants in order to prepare for the report and show results both for sites as well as seasonal maps of icing hours.

The first part of the Project had been mainly dedicated to set up, run and, at times, re-run model simulations and verify against observation and improve some aspects. The model runs, either for the whole country at 2.5 km, or around the sites at 1 km, required a lot of dedicated computer and manpower resources and it was obvious that the whole of Sweden cannot be modelled at 1 km grid resolution for several decades as would be required for a climate simulation. Building on work elsewhere (FMI and Kjeller Vindteknikk), ways were explored how to construct an icing climatology from either limited time periods or low resolution data.

A classical way of classifying the large scale atmospheric flow into flow regimes was explored and attempts were made to associate icing frequency to certain flow patterns. It was done both from re-analyses at relatively low resolution and from Swedish observations. This was met with limited success and only the mean situation could be used. From re-analysis data a lot of calculations were made to see how long periods (years) were needed to reasonably cover the long term (30 year) climate. It showed some promise that a 5 year periods may suffice, provided for each month the used years were chosen in a way that they best represented the long-time average. Another, third method, is to derive statistical relations between high resolution and low resolution runs over certain areas, and then run long low resolution runs for e.g. 30 years. These tasks were carried out by Esbjörn Olsson, Petra Thorsson, Hans Bergström and Per Undén.

### **The contents of the report**

Chapter 2 gives a background to what the term **climatology** means and how it can be derived. It deals with the correlation scales for different meteorological variables and what is required to sample their natural variability from observations. The main available tools, analyses or models,

and their advantages and limitations are discussed. Different parameters in an icing climatology are briefly discussed and from a user perspective.

The availability of observations of ice load and meteorological parameters at sites has been central to the Project and a detailed account of the different instruments and their quality is given in Chapter 3. Most of the observations have been provided through O2's Pilot Project to which WeatherTech and SMHI have been contributing and benefited from. Measurements of icing before and after smoothing of noisy data are shown for the different sites. The data availability and their quality are described for each site. At the end of Chapter 3 there are some conclusions and a summary table for the three seasons.

Chapter 4 (4.1) gives a broad overview of the concept of meso-scale modelling, the physical parameterisation and particularly how cloud constituents are represented. The steps and the methods for estimating ice accretion from model output and the decay of icing are described. Then there is more in depth information about the models. Three different meso-scale models have been employed in the Project: AROME at SMHI (which is used and developed at more than a dozen weather services in Europe), COAMPS<sup>®</sup> at WeatherTech Scandinavia, and some time into the project, also WRF. COAMPS<sup>®</sup> is developed by the Naval Research Lab, Monterey, California and WRF is a US open source model, which is widely used for research and forecasting. The integration areas are shown as well as the location of the model levels near to the surface.

In 4.2.1 follows comprehensive verification statistics of the three models against the meteorological observations at the 12 sites. They are shown in terms of distribution curves and in tables. In the beginning there are some general conclusions about the performance.

4.2.2 shows comparative results for ice load data for three selected sites and interesting periods (when there were icing conditions and available good quality data). There are large uncertainties of what goes into the Makkonen formula as seen both from curves and tables. Results are summarized at the end of the chapter.

The investigations of sensitivities to lateral boundary forcing as well as the initial conditions (analysis) have been investigated in 4.3 for one of the models, WRF. The differences are small, but the choice of the different physical parameterisations has a larger impact particularly in the atmospheric boundary layer. The cloud scheme affects the cloud water content itself, but the turbulence scheme has a more profound impact on wind and temperature profiles as well as the cloud water. Results are shown for a few sites and compared with the three original models. In terms of icing hours the variations are large, between models and particularly physics schemes.

The report so far, the first half, has tried to explain the subject and requirements and the properties and quality of both observations and of the model tools that have been employed. Now, the second half of the report aims to give answers to the question how to derive a high resolution icing climatology. As already alluded to above, there is no straightforward method to do this, with the so far available observations or computing power.

The first approach is to run a high resolution model simulation over as many seasons as possible. Chapter 5 shows results from the three winter seasons that have been simulated in the Project and shows examples of maps of icing hours. There is a question of what are the most desirable user parameters, but it must be rather user (site and model) dependent. From model data like these it is possible to derive other parameters for specific users.

The approaches in the following chapters investigate how long high resolution model runs and from which years or months they should be done in order to approximate a long term climatology.

In Chapter 6 four different approaches to representative periods are described and thoroughly investigated. The methods are first explored over the ERA Interim re-analysis set. One is to find the years (for a particular month) with the best fit to the long term mean (e.g. 30 years). This method is novel and shows the best performance of the four. Random days to form a climatology is clearly inferior, at least for as short periods as monthly climatologies. Best fit to Lamb classes (circulation patterns) is akin to the first one, but shows clear disadvantages compared to the first one (too low winds). The method of choosing 5 consecutive years works well for some variables but is sensitive to which 5 years are used.

Then the methods are tested on a 9 km grid 30 year WRF model simulation. Again the best fit method is the most satisfactory one for temperature. For ice load all methods seem to work.

In 6.1.4 and 6.1.5 the conclusions and recommendations on the four methods are presented.

Another alternative, which does not suffer from reduced sampling in time, is the statistical downscaling technique described in Section 6.2. Statistical regressions between temperature and winds at coarse (9 km) grid resolution and 1 km grid have been derived and with an adjustment of humidity and water content. Results are shown for two models, COAMPS<sup>®</sup> and WRF. The high resolution runs can be reproduced quite well also for icing hours. The differences between the models may actually be larger than the downscaling error. In the end the pros and cons of the different methods are discussed.

Chapter 7 deals with the most difficult task, to estimate production losses. Empirical tables have been derived for one site where ample data was available. They are shown both from icing rate and ice load. As a first attempt the tables have been applied for other sites and production losses estimated from the different model runs. There are substantial uncertainties and also variations between the models. In spite of this for some sites and months there are general agreements with the observed values.

Chapter 8 gives a concluding discussion of what has been learned from the observations and models. The uncertainties in observations and between models have been shown and these must be handled in future work. The project has shown that there are a few, mainly two methods that are feasible for an icing climatology.

## 2 Background

In the Vindforsk V-313 project "Vindkraft i kallt klimat" the goal is to arrive at a methodology to construct a high resolution ( $1 \times 1 \text{ km}^2$ ) climatology of icing on wind power turbines. The term climatology in classical meteorology means statistics over 30 years of data, and usually in the form of direct or indirect measurements. Examples are mean temperatures (annual, monthly, maximum etc.), number of frost days, growing season, variability, number of days of precipitation, mean winds, cloudiness, solar radiation, to name a few. Most variables are simple scalars but also derived quantities such as growing season may be considered.

### **Measurements**

Direct measurements are instruments installed at discrete sites, located as to represent the conditions in a particular area as accurately as possible. Errors in representativeness are always encountered to a certain extent when interpreting the measurements. A temperature sensor can measure within  $0.1^\circ$  but short-term variations of around  $1^\circ$  may occur due to convective motions of the air. The height of the station relative to surrounding terrain may have even larger effects. Winds over land are more difficult due to turbulent motions with large variability in time and space.

Meteorological quality stations need to be well sited, well equipped and regularly maintained. There is thus a significant cost for a large network and this limits the density of the network. Therefore sampling of weather and climate can only be done at a limited number of locations. The Swedish climate network for precipitation has about 700 stations of which about 130 also measure temperature and can be collected in real time twice a day. The hourly (almost all automatic) stations are close to 200 but they have more advanced instrumentation than the basic climate stations.

Even for the most basic measurements the country can only be sampled at about  $30 \times 30 \text{ km}$ , and for e.g. precipitation the errors in representativeness may be substantial. There is a lot of variability down to (and below) the km scale. Climatological analyses (maps of monthly precipitation e.g.) have been produced through some intelligent (subjective) horizontal pattern analysis using meteorological experience in addition to the point measurements.

### **Analyses**

Objective analyses of observations with wide representativeness, such as pressure, wind and temperature in the free atmosphere, have successfully been employed for Numerical Weather Prediction (NWP) since the 1950's. Horizontal scales of several hundred km are well analysed in this way and it is done with a NWP model short range forecast as a background, filling in information not given by observations. (This is the concept of Data Assimilation).

The NWP based analyses have successfully been extended to so-called re-analyses of climatological time scales of more than 30 years and now even in

some cases for the whole of last century. This is achieved using as complete observation data sets as possible and the current state-of-the-art analysis and forecasting model. The assimilation system is kept the same over the whole time period so trends over decades are caused by the observations. The resulting re-analyses are as good, or in some aspects better, than any pure observational data sets that exist. The climate trends are realistic and also available in areas or levels that are not normally observed.

The global ECMWF (European Centre for Medium Range Weather Forecasts) datasets (ERA-40 and ERA-Interim foremost) have become established datasets for climate monitoring, observation studies, model validation and many other research and customer applications (Uppala et al., 2005).

With its spatial and temporal resolution of 125km/6hours the ERA-40 re-analyses were made from 1957 to 2001. After that the period 1979 - today (2012) is re-analysed at the higher resolution of ~80 km compared to the ~125 km of ERA-40. Also, ERA-Interim is made with 4-dimensional variational analysis (ERA-40 was 3-dimensional) and with an upgraded analysis system and forecast model. In particular a new variational bias-control of satellite radiances was been introduced. The same observations were presented to both data assimilations.

In the US, NCEP (National Centres for Environmental Prediction) and NCAR (National Center for Atmospheric Research) have also made re-analyses (Kalnay et al., 1996). In the NCEP/NCAR Reanalysis 1 project, state-of-the-art analysis/forecast system has been used to perform data assimilation from 1948 to the present. The spatial resolution is T62, ~209 km with 6 hours temporal resolution.

The fine scales associated with clouds, precipitation and surface variables are much harder to analyse objectively. Specially devised meso-scale analysis systems have been developed, like MESAN at SMHI (Häggmark et al., 1990) that can be applied on the 5-10 km scale. There are similar, or other, approaches that have been applied in other countries. (See section 4.1 for the definition of meso-scale).

For climate analyses there are also long term gridded data sets where just daily observations of temperature and precipitation have been interpolated statistically e.g. with kriging and with resolutions of 25-50 km. For sub-regions of Europe or individual nations, there are high resolution data sets at 1-10 km resolution.

### **Remote sensing**

Indirect measurements are cloud images from satellites or radar returns as a proxy for precipitation intensity. These data may have large errors, particularly for precipitation, but the advantage is that they are area covering and at resolutions down to 1x1 km.

These indirect measurements are very difficult to combine with traditional large scale representative observations in objective analyses. There are on the other hand several very useful satellite derived cloud data sets that can be used for model validation and also for climate studies.

### **Icing climatology**

For icing the climatology is much more complex than for the basic variables. Icing is a derived quantity from several variables that are generally not measured, except maybe on some special masts, or even more rarely at the sites of the wind power turbines. Icing is a function of air temperature, total moisture content (vapour, liquid and solid to some extent) and wind speed throughout the height range that the turbine blades sweep. Moreover there are aero-dynamical effects that may vary between manufacturers and also effects of turbulence from surface objects and neighbouring turbines.

Direct measurements of icing have now been established in Sweden through the Pilot project, which uses about a dozen instrument sites. Icing measurements to such an extent are rather unique. Still the representativeness of each measurement must be considered to be very local due to the elevation and surrounding topography, and sometimes questionable placement position of the measurement (e.g. within a park). Thus, there will never be any complete or comprehensive measurements of these variables covering the whole area at km scale resolution. An objective analysis of icing data often 100's of km apart is also not an option. The high resolution (a few km scale) data have to be model generated. Today's sophisticated meteorological prediction models include all the main variables needed for icing calculations. Pressure, temperature, wind, humidity, and cloud water are accurately simulated from the large-scale analysis and model integrations. Such high-resolution models are used over a limited area (inner model), and driven with information of the large-scale flow through the boundary conditions from an external model. The external model has data assimilation of large scale variables and defines the general flow well. Within the high resolution inner model, the surface conditions are those that matter most for data assimilation and for model performance. High resolution input data sets of fixed surface properties are used (such as topography and vegetation).

The clouds and particularly the liquid water content and drop size distribution are not yet directly analysed from any observations but model generated from the larger scales and by the high resolution model's interaction with local topography, mainly. In AROME and COAMPS<sup>®</sup>, the drop size distribution is not yet predicted but assumed whereas there are schemes in WRF that are predictive (two-moment scheme).

The models are tested and icing calculations may be tuned with the aid of the ice measurement sites that have been established in Sweden. In this way the models are used to transfer the information derived from the tuning at the measurement sites (and during the seasons that they have existed) in space and in time to construct the best possible climatology over say the last 30 years. This way of using models has rather successfully been applied for many other applications like winds, temperatures and precipitation (re-analyses mentioned above). The models provide an internally multi-variate consistent regularly spaced atmospheric state of the variables involved.

### **Models and climatology**

High resolution meso-scale models are designed and run at resolutions of 1-2 km typically. The equations of motions are used at their almost unapproximated form and high speed gravity and sound waves are permitted. The mean vertical advection is assumed to describe the dynamics of deep convection, and the process is thus explicitly represented by the model's equations. The high resolution results in a large number of grid points in order to represent Sweden or even parts of the country. The time steps are quite short, a minute or less. This means that the computation time for each model simulation (like a one day forecast) takes several hours of execution time even on a large cluster computer.

Combined with the fact that reasonable number of icing observations only exists for the last three years in Sweden, the model simulations and observed icing climatology, at this stage (2012) will have to be based on a very short sampling with respect to the classical 30 year period. An icing climatology based on a shorter period may be sufficient, e.g. of 10 years. It depends on the required accuracy and especially if one needs to know the real extremes or not. Moreover, the result will depend on which 10-year period the climatology is based on.

In the project, different approaches have been tested to deal with this problem. Flow patterns from the large-scale flow have been used for other climatological studies and it is clear from the downscaling of the ERA-Interim re-analysis that the large scale flow has a large impact on the icing, at least when accumulated over a month or a season. Also downscaling methods can be used and make use of relatively coarse resolution model simulations.

### **User expectations of icing climatologies**

During the project a few different parameters have been computed that may answer questions on icing climatology. Three main candidates were established:

- a) Number of icing hours over a certain accretion rate
- b) Number of days with ice load above a certain limit
- c) Period of ice load on structures (i.e. including how long it lasts)

From the experience in the project a) seems to be the most feasible quantity since it is directly related to meteorological parameters in the models or in measurements. The other ones are much more difficult since it depends on evaporation (sublimation) and fall-off. Whereas the first one may be estimated to some extent, the fall-off is almost impossible to model. From output power data we have seen that this fall-off seems to rather immediate and (less than a day or so) and this gives some hope of not having to try to model c) and the fall-off to any large degree.

The user (being the owner or operator of the turbine of wind power park) is eventually interested in the resulting production loss for their particular installation. This is likely to be different both between manufacturers and locally at each individual site. Of course also the type of ice, clear or porous, is determining the production loss. In the project empirical lookup tables or functions have been derived and applied with some success, but it may be

very risky to take important investment decisions from oversimplified and very uncertain "loss" climatology. A number of parameters plus local considerations for each site will be needed. Furthermore the shape of the ice formation has not been modelled. It is far beyond the scope of this project but may be necessary for future enhancement.

## 2.1 Summary of Chapter 2

The climatology may be constructed mainly in three different ways: Observations themselves, if available for long enough periods may be used, but only at their location or within their correlation scale. **Analyses** of observations on to regular grids and **re-analyses** are the most important tools for climatologies as well as for weather forecasting. **Numerical Weather Prediction** models, apart from being used for forecasting, are also an important component for most analyses. This is due to their physical descriptions of the flow also where observations are sparse. The **icing climatology** depends on mainly three different meteorological parameters of which one, cloud water, is almost never observed. Furthermore, the observations of icing only exist at a limited number of places and for the few most recent years. Thus, it is necessary to use the most advanced meso-scale models at km scale grid distance to derive climatologies of icing. Which parameters should be used in an icing climatology is hard to decide on. Number of icing hours over a certain amount or ice load (accumulation) and number of hours with ice accretion above a certain rate are the most obvious choices. Then the effect on the production is related to these, but is rather site dependent.

## 3 Observations

### 3.1 Instrumentation

Observations of ice load and meteorological parameters have been made available to the project mainly through O2's Vindpilot project concerning wind power in cold climates. The measurements sites are located from northern to southern Sweden, but due to confidentiality issues their exact locations may not be revealed. They are only identified by the Electricity Price Region in Sweden in which they are located, see Figure 3-1. Region 1 is Northern Norrland, region 2 is Southern Norrland, region 3 is Svealand and Northern Götaland, and region 4 is southern Götaland. A summary of the site locations are given in Table 3-1, together with measurement periods and instrumentation used.

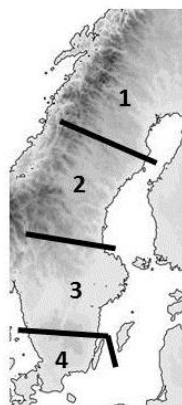


**Figure 3-1: Map showing borders between the Swedish Electricity Price Regions.**

**Table 3-1: Summary of measurement sites giving: Area (Swedish Electricity Price Region). Height above ground level. Measurement period. Instrumentation (M=multisensor, I=ice load/detection, V=visibility, C=cloud height).**

Site	Area	Height (m)	Measurement period	Instrumentation
E1	1	78	Sep 2009 – April 2012	M I
E2	1	150	Sep 2011 – April 2012	M I
E3	1	40	Sep 2011 – April 2012	M I V C
E4	1	80	Sep 2011 – April 2012	M I V
E5	2	80	Sep 2009 – April 2012	M I V C
E6	2	100	Sep 2010 – April 2012	M I V C
E7	2	200	Sep 2010 – April 2012	M I V
E8	2	70	Sep 2010 – April 2012	M I V C
E9	2	155	Sep 2010 – April 2012	M I V
E10	3	80	Jan 2011 – April 2012	M I V C
E11	2	60	Sep 2010 – April 2012	M I V C
E12	3	100	Sep 2011 – April 2012	M I V
E13	3	150	Sep 2011 – April 2012	M I V
E14	3	100	Dec 2011 – April 2012	M I V

Meteorological data was measured using the Quatro-Ind multisensor from Lambrecht. This instrument measures wind speed and direction, temperature, relative humidity, and air pressure. This type of sensor is not a precision instrument with high accuracy. According to the operating manual for the instrument the accuracies are  $\pm 0.5$  m/s for wind speed,  $\pm 3^\circ$  for wind direction,  $\pm 1$  °C for air temperature,  $\pm 4$  % for relative humidity, and  $\pm 3$  hPa for air pressure. At site E1 instead the Vaisala WXT510 multisensor was used.

The ice load was measured using the IceMonitor from Combitech. The weight of ice getting caught by a 0.5 m long rotating cylinder having a 30 mm diameter is measured using a load cell. In practice many problems are however identified with this type of instrument. One is that the cylinder stops rotating and further ice growth will be located only on the windward side of the instrument, thus the output weight cannot be trusted anymore and also the resulting bias in load will enhance the probability for ice drop from the instrument purely as a consequence of cracks developing in the ice that is stack on one side of the cylindrical rod.

Another problem is that growing ice may "lift" the rod so that the measured load is incorrect. It is also well known that a load cell is more or less temperature sensitive such that a zero-drift may occur. This would be straight forward to account for if no other shifts in zero-value would occur, but this is not so. Now and then sudden jumps in zero-level seem to occur and need to be identified before data is being used.

Also the output signal from the IceMonitor is quite noisy making some kind of filtering of the measured load needed before analyses. This is illustrated in Figure 3-2, which shows time series of ice load and temperature during two months. The thin green line shows measured ice load in N/0.5 m. It is obvious that the ice load signal is quite spiky, typically within  $\pm 1$  N/0.5 m. Occasionally much more as for example at the end of December. The reason for this is not obvious but the consequence is that the raw signal has to be filtered in order to arrive at a smooth time series, which could readily be used for analyses. Directly using the measured ice load it would not be possible to for example make an analysis of ice accretion as a time series of this would then be extremely spiky with unrealistically large both positive and small numbers. The thick red line gives the result after this smoothing.

Another issue to be considered regarding ice load measurements is that ice load sometimes decreases also during periods with temperatures well below 0 °C. Ice load may decrease not only by melting but also due to sublimation, i.e. a phase shift from solid ice to water vapour. But the decrease in ice load is now and then too rapid to be caused by the sublimation processes. A plausible explanation is that ice is dropped from the measuring instrument due to impairments in the ice leading to cracks in the ice and finally some piece of ice may simply fall off. Some of the more rapid decreases in ice load during January in Figure 3-2 may be due to this happening.

At some of the sites a visibility sensor from Vaisala (PWD20W) was installed, capable of measuring visibility in the range 10-2000 m. Some sites also include cloud height measurements using the CBME80 ceilometer from MicroStep-MIS.

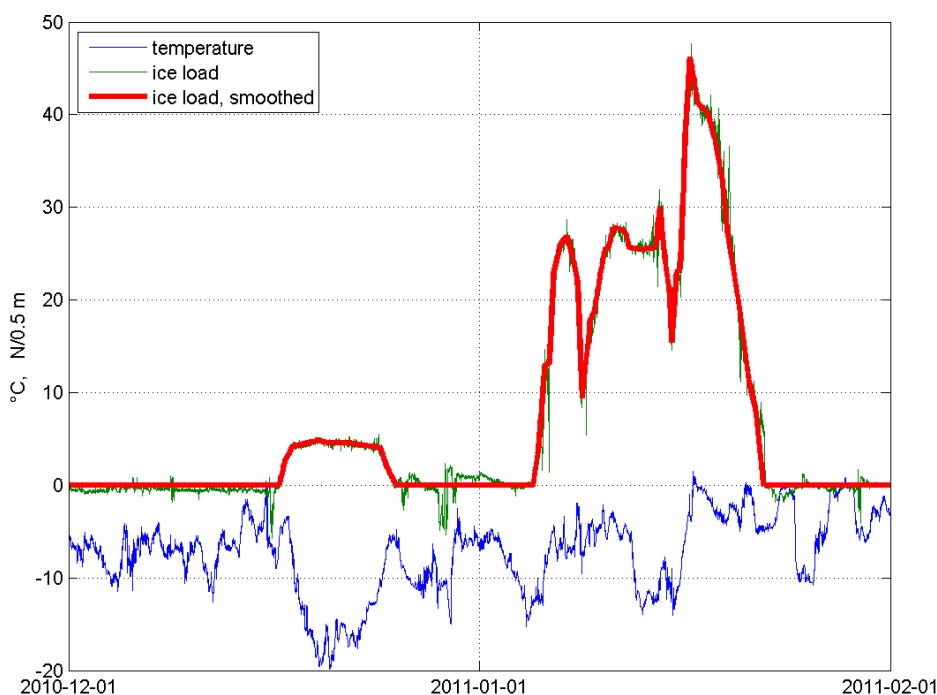


**Figure 3-2: Example of time series of temperature and ice load during a period of two months. The measured ice load is shown by the thin green line and the smoothed ice load by the thick red line.**

## 3.2 Measurement results

A general overview of the measurement results are presented in graphs showing time series of ice load and temperature for the different sites and winter seasons. The cumulative distributions of ice load are also shown.

In addition to the actually measured ice load, which often is very spiky, a smoothed time series is also shown. It proved very difficult to accomplish this smoothed curve automatically using a mathematical filtering as this gave frequent unrealistic variations ("over-shooting") not seen in the original observations. Thus a filtering was made simply by plotting the observations and manually using a digital input technique to arrive at the smoothed results.

As ice drop is a known problem using the IceMonitor to measure ice load, a third curve is included where an attempt to account for this has been applied to the smoothed ice load series. The assumption is then that ice load cannot decrease by other means than ice melt and sublimation (direct transition from ice to vapour). The melting is left accounted for as it is measured such that drop of ice is still accepted for temperatures above 0 °C. But a decrease in ice load in excess of what could be accounted for by sublimation is not accepted for temperatures below freezing. The "no drop" ice load time series is thus arrived at by estimating the sublimation of ice at each observation time using

the measured wind speed, temperature and relative humidity. If the measured ice load corresponds to a larger decrease than is expected to be accounted for by sublimation the value is kept at the observed ice load value for the preceding time only reduced by a value corresponding to the estimated sublimation.

*Site E1:*

The results for site E1 is shown in Figure 3-3 for three winter seasons. The winter 2009-2010 started with an icing period in late October reaching almost 5 kg/m, followed by several icing episodes in November-December when the maximum measured ice load reached 13 kg/m in mid-November. Next major icing event occurred in January with a peak at 12 kg/m. Comparing the measured ice load and the ice load corrected for ice drop we see that the difference is large especially for the January ice event. The rapid drop in measured ice load in late January following the peak at 12 kg/m is probably not correct. It seems to be following a rapid decrease in temperature, which might have added to the ice drop making the ice more brittle which could have formed a crack in the ice. The cumulative distribution shows that for the winter 2009-2010 as a whole, icing occurred 37 % of the time according to the measurements. Correcting for drop of ice this increase to 46 %.

During the winter season 2010-2011 the maximum ice load was smaller at site E1, only 3 kg/m according to measurement and 5 kg/m correcting for ice drop. Icing however occurred most of the time from early November to the beginning of March. Icing occurred seen over the whole season 36 % of the time.

There was a gap in the measurements during the first half of the winter season 2011-2012. From early January until the first days of March severe icing dominated with measured ice load reaching 12 kg/m and the ice load corrected for ice drop reached 25 kg/m. The cumulative distribution shows that measured icing occurred 42 % of the time and 52 % of the time correcting for ice drop.

*Site E2:*

Measurements at site E2 show that the winter season 2011-2012 also at this site was quite severe, with measured ice load reaching 12 kg/m, see Figure 3-4. The result after correcting for ice drop however seems unrealistic. Probably the data are somehow faulty as is obvious during September, where ice load measurements show an extremely spiky data series at the same time as a measured ice load of 4-5 kg/m are found simultaneously with temperatures between 5 and 10 °C. This type of error probably continued throughout the winter but is not as obvious for temperatures below zero. But this affects the correction for ice drop leading to the unrealistically large corrected ice load values. The amount of time with icing was at this site 20 % according the observations.

*Sites E3 and E4:*

No reliable icing measurements were available from these two sites.

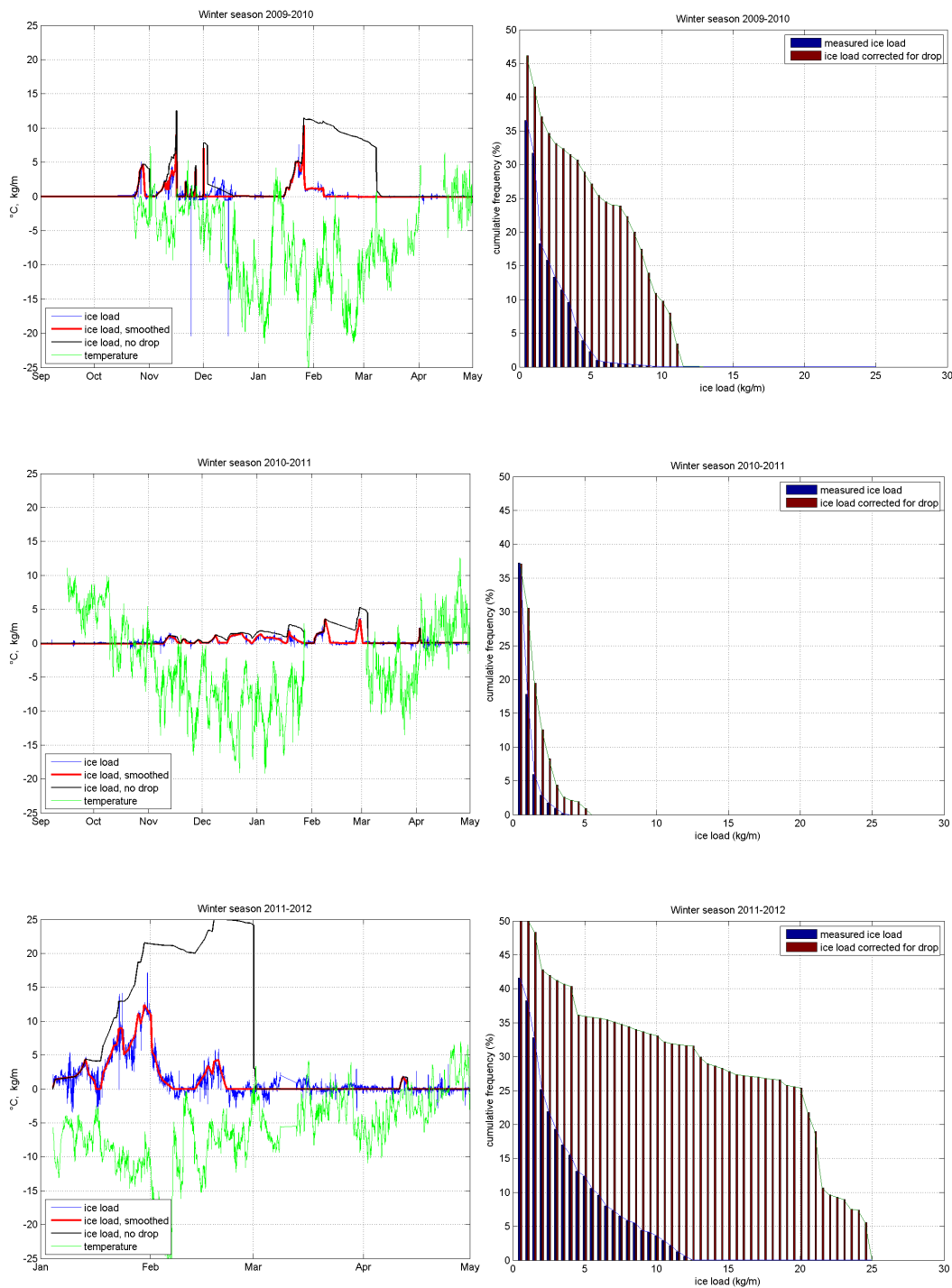


**Figure 3-3: Results for site E1 for top-down winter seasons 2009-10, 2010-11 and 2011-12. Left hand graphs show time series of ice load and temperature. Right hand graphs show cumulative distributions of ice load.**

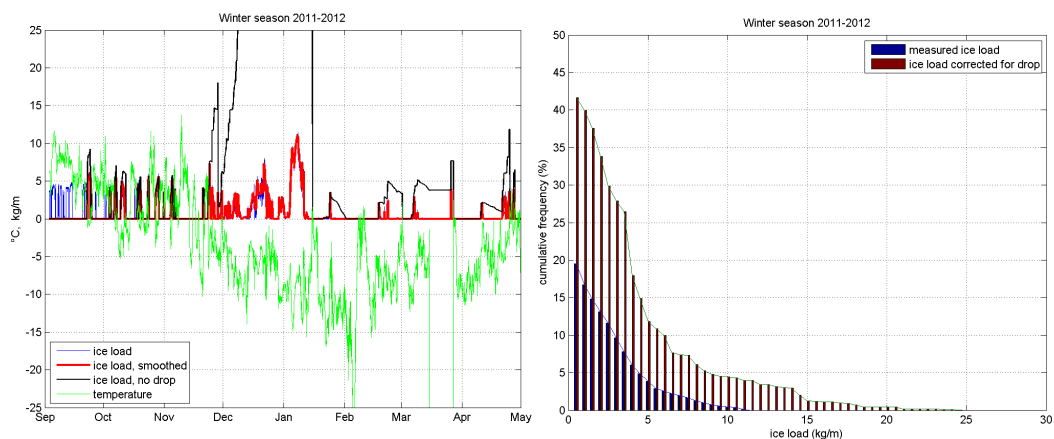


**Figure 3-4: Results for site E2 for winter season 2011-12. Left hand graph shows time series of ice load and temperature. Right hand graph shows cumulative distributions of ice load.**

#### *Site E5:*

Ice load measurements are available from site E5 for all three winter seasons 2009-2010 to 2011-2012, see Figure 3-5. The winter 2009-2010 started with a first icing event in late September. From late October icing got more severe and lasted until mid-January ended by a period with temperatures reaching +5 °C. The maximum ice load measured was 21 kg/m and correcting for ice drop increased this maximum to 24 kg/m. After the period with temperatures above zero in January, the icing was less severe. But icing occurred into the beginning of April. For the winter as such icing occurred during 36 % of the time according to the measurements. After correction for ice drop this time increased to 45 %.

The winter season 2010-2011 was less severe at this site. The maximum observed ice load was 3 kg/m, 6 kg/m after correction for ice drop. The result for this winter is however uncertain as hardly any measurements are available for the period late November until early January. Also this year a late icing event occurred in early April. For the winter as a whole icing was observed 13 % of the time, but this rather low number is probably not correct due to the gap in the observation from November to January.

The risk of underestimating the icing during the winter 2010-2011 gets obvious looking at the results for the winter season 2011-2012. The dominant icing event this season occurred in December with maximum ice loads reaching 20 kg/m. Icing was observed during the rest of the winter with a peak in the beginning of February reaching 8 kg/m. The fast decrease in measured ice load following this peak is probably not correct judging from the measured temperature, which is below zero. While the measured ice load consequently is small after the peak in early February, the ice load corrected for ice drop remains high throughout February after which the temperature for a period was above freezing. The cumulative distribution shows that for the whole winter period icing occurred 26 % of the time according to the measurements, while correcting for ice drop increased this to 39 %.

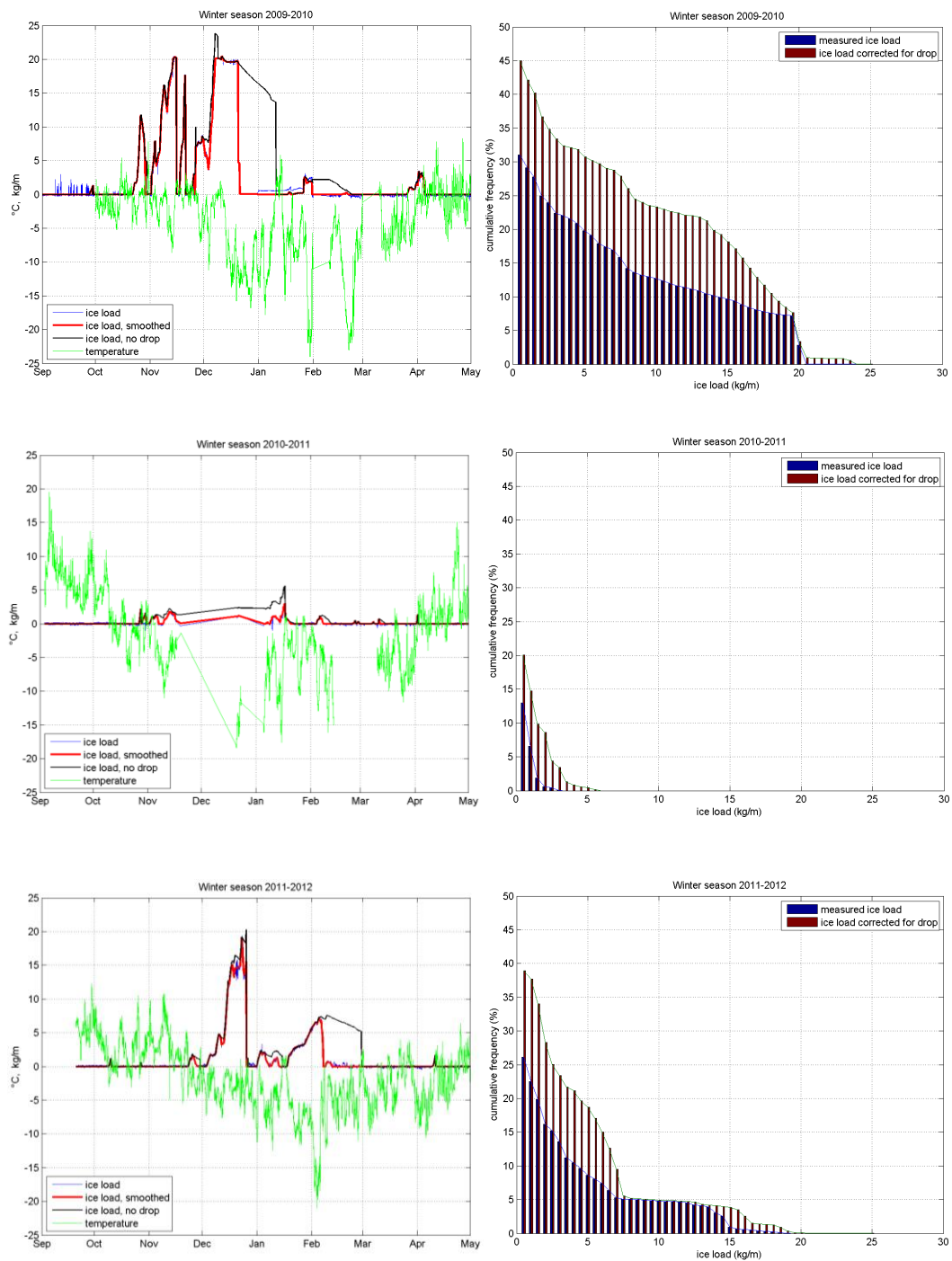


**Figure 3-5: Results for site E5 for top-down winter seasons 2009-10, 2010-11 and 2011-12. Left hand graphs show time series of ice load and temperature. Right hand graphs show cumulative distributions of ice load.**

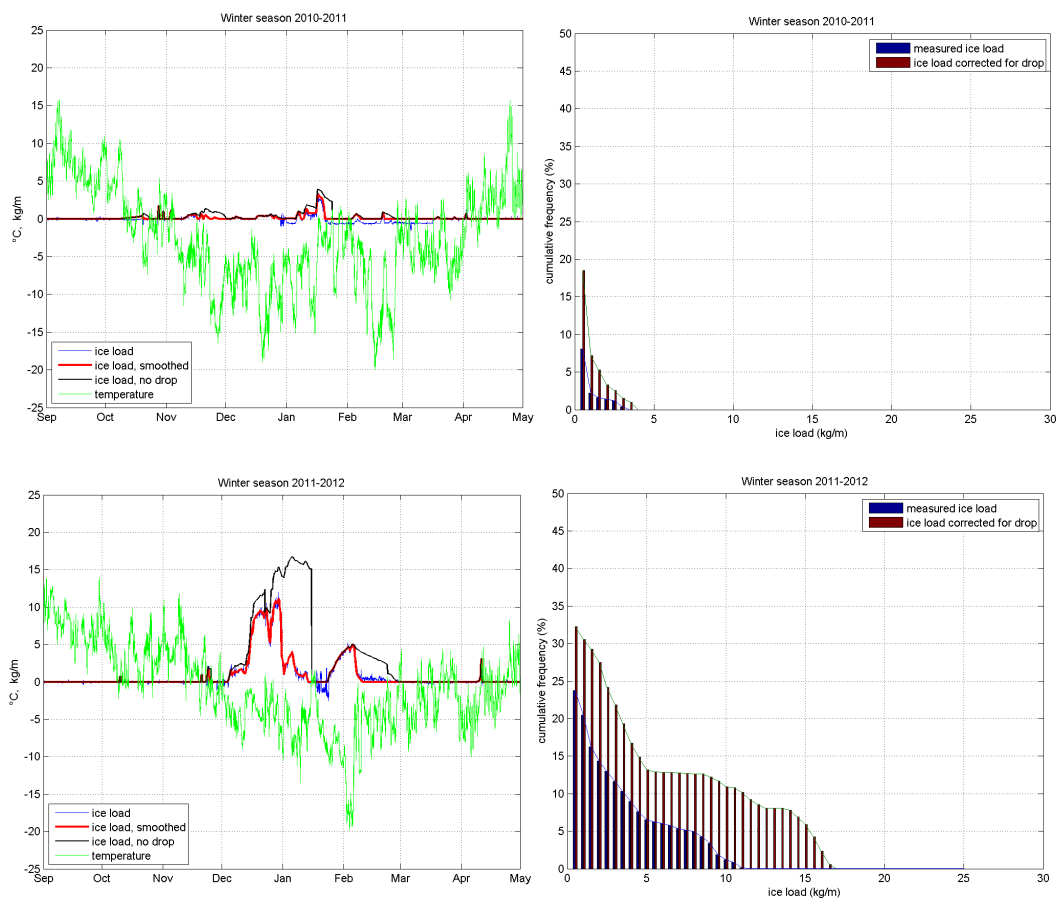


**Figure 3-6: Results for site E6 for top-down winter seasons 2010-11 and 2011-12. Left hand graphs show time series of ice load and temperature. Right hand graphs show cumulative distributions of ice load.**

#### Site E6:

At site E6 the results for the ice winter 2010-2011 show a less severe winter, see Figure 3-6. Icing occurred during most of the winter from mid-October, ending with an icing episode in early April. But the maximum ice load remained as low as 3-4 kg/m. The part of the whole winter having icing was as a whole just 8 % of the time, but after correction for ice drop this time increased to 18 %.

The winter season 2011-2012 showed more icing according to the measurements at site E6. After only some minor icing events in October and November, ice load grew from early December. The maximum observed ice load was 11 kg/m in late December, but again a fast decrease of measured ice load was observed during a period with temperatures well below zero. Correcting for this the ice load continued to increase well into January reaching 17 kg/m. After a melting period a new maximum in ice load in late January and February was observed. Also at this site a late icing event in mid-April was noted for this winter. For the winter season as a whole icing occurred during 24 % of the time, a number which increased to 32 % after correction for ice drop.

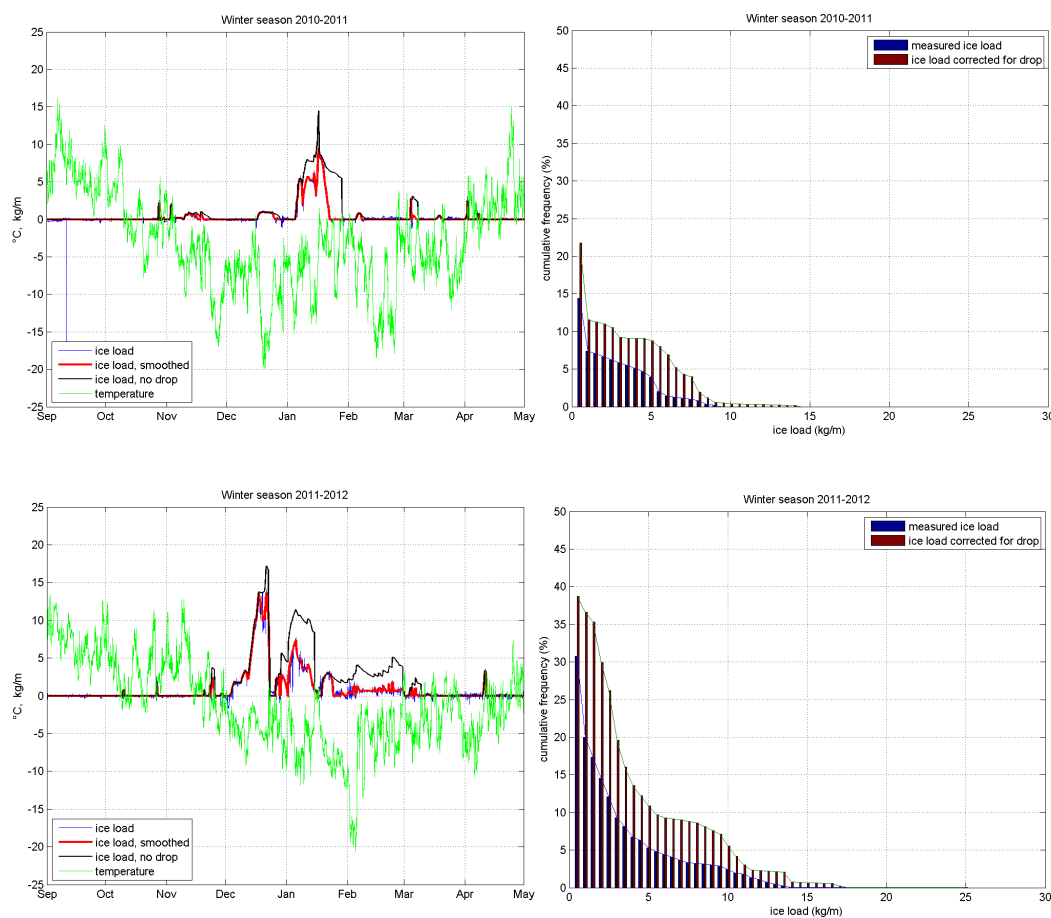


**Figure 3-7: Results for site E7 for top-down winter seasons 2010-11 and 2011-12. Left hand graphs show time series of ice load and temperature. Right hand graphs show cumulative distributions of ice load.**

#### *Site E7:*

The winter season 2010-2011 as site E7 show a similar pattern as for site E6, but with slightly more ice load especially during January with an observed maximum of 9 kg/m and a corrected maximum reaching 14 kg/m, see Figure 3-7. This is not surprising as the two measurements were taken on the same tower, but at different heights. Site E6 is at 100 m height, while site E7 is at 200 m. One could expect icing to increase with height due to increased probability of getting into the clouds. But this is not always found according to the observations. Some icing events are found at 100 m height but not at 200 m height or being somewhat more pronounced at 200 m. But the cumulative distribution of ice load show the expected trend towards larger part of time having icing at the upper level, site E7, where icing is observed 14 % of the time, a number which increases to 22 % correcting for ice drop.

The same general picture is found for the winter season 2011-2012. But a period with decrease in ice load at 200 m, occurring in late December, not observed at 100 m height, shows that ice load could decrease with height during some situations, this time due to a temperature inversion. At 200 m the temperature rises above zero, leading to melting, while at 100 m the temperature remains below zero. In spite of this the part of time with icing

still was larger at 200 m than at 100 m. The numbers at 200 m show that 31 % of the time icing was observed, while this number increased to 38 % correcting for ice drop.

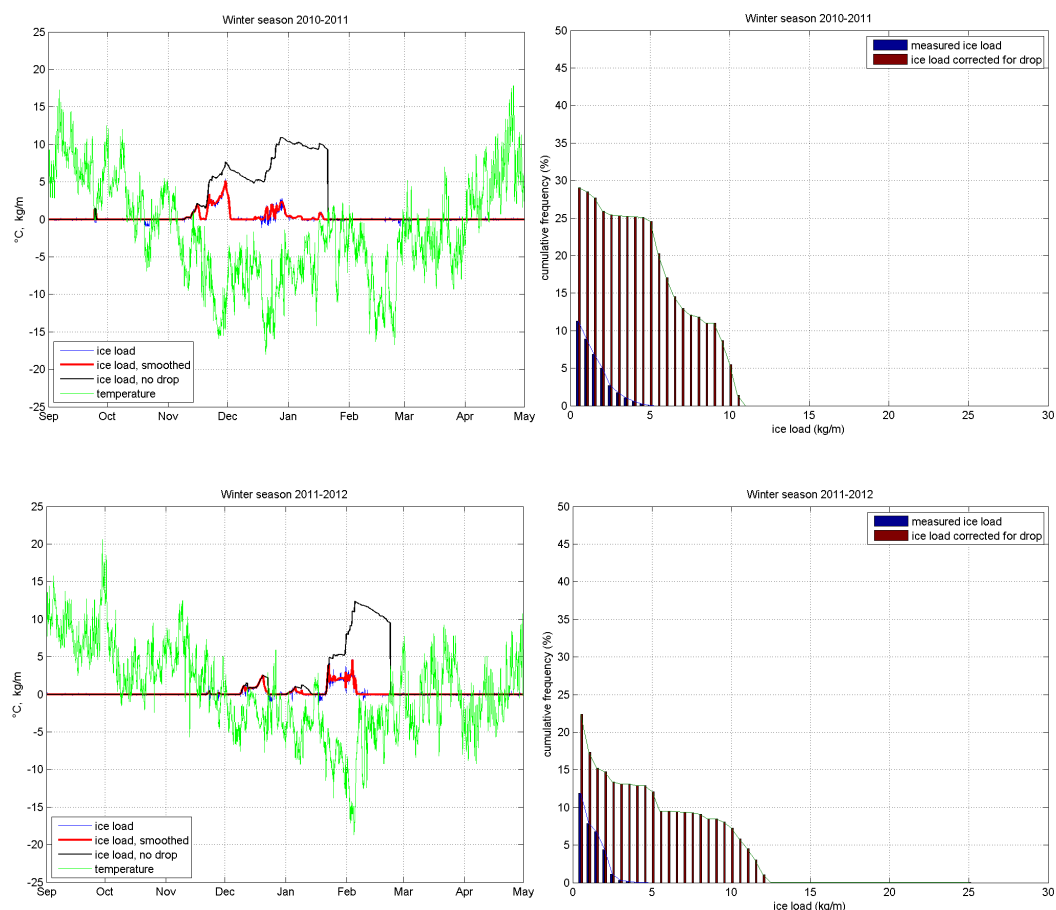


**Figure 3-8: Results for site E8 for top-down winter seasons 2010-11 and 2011-12. Left hand graphs show time series of ice load and temperature. Right hand graphs show cumulative distributions of ice load.**

#### *Site E8:*

The winter season 2010-2011 started with a short icing event already in September, see Figure 3-8. October had no icing according to the measurements and the true icing period started in the middle of November and the measured ice load increased to 5 kg/m just before 1<sup>st</sup> December. A rapid drop of ice load following this maximum but again during a period of temperatures below zero making this decrease unrealistically large. Similar rapid decreases in ice load occurred in the measured several times in December. As a consequence the ice load arrived at after correction for erroneous ice drop from the IceMonitor instrument increases to 11 kg/m as a maximum. No icing was measured after mid-January. The cumulative distribution of ice load shows that icing occurred 11 % of time during this winter. After correction for ice drop this increased to 29 %.

The winter season 2011-2012 started at site E8 with some minor events in October to early January. In mid-January ice load increased to a maximum of almost 5 kg/m, a maximum that increased to 12 kg/m correcting for ice drop. Ice load occurred seen over the whole winter 12 % of the time according to the observations, increasing to 23 % after correction for ice drop.

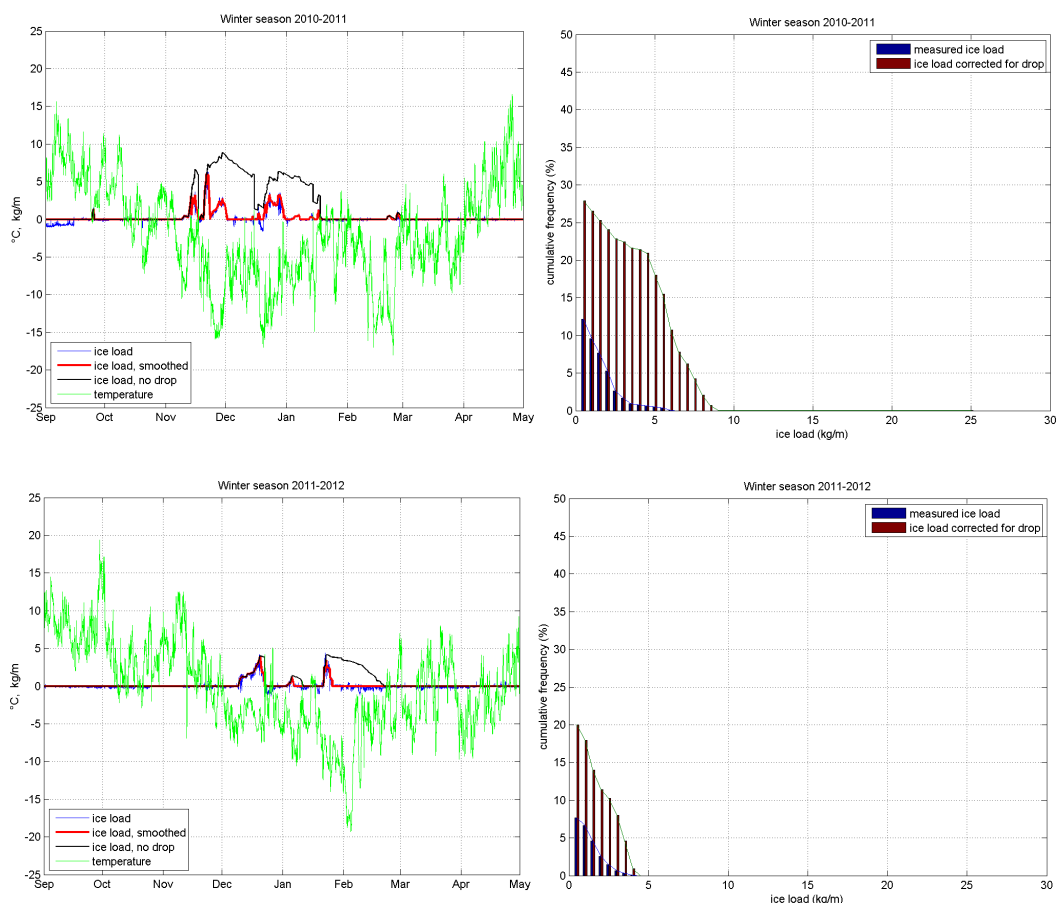


**Figure 3-9: Results for site E9 for top-down winter seasons 2010-11 and 2011-12. Left hand graphs show time series of ice load and temperature. Right hand graphs show cumulative distributions of ice load.**

#### *Site E9:*

This site is at the same location as site E8, but at 155 m height instead of at 70 m. As when comparing sites E6 and E7, the upper level should be expected to have a larger ice load due to low cloud heights, but this is only partly seen in the observations for the winter 2010-2011, see Figure 3-9. Also in mid-December temperature increases to above zero at 155 m height while it remains below freezing at 70 m due to a temperature inversion. The effect of this is not seen much on the measurements directly as the ice load was small at the time, but affects the ice load corrected for ice drop. For the whole winter icing occurs 12 % of the time according to the observation and 28 % of the time according to the ice load corrected for ice drop.

The same general results are also valid for the winter 2011-2012. The icing in December and early January is slightly larger at 155 m, while the icing event

in late January prevails longer at 70 m height, both in the measurements and in the drop corrected ice load. Icing during this winter occurred 8 % of the time according to the observations and increase to 20 % correcting for ice drop.

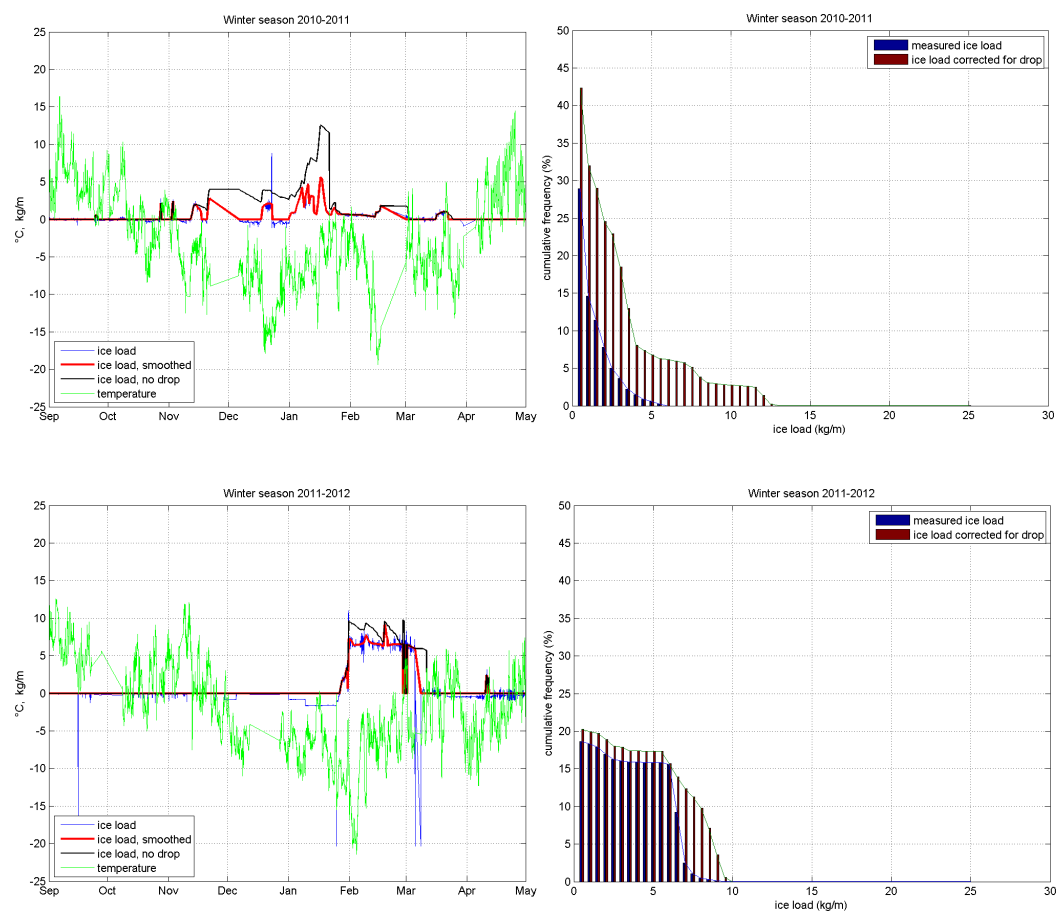


**Figure 3-10: Results for site E11 for top-down winter seasons 2010-11 and 2011-12. Left hand graphs show time series of ice load and temperature. Right hand graphs show cumulative distributions of ice load.**

*Site E10:*

No ice load measurements were available from site E10.

*Site E11:*

At this site the icing winter 2010-2011 starts with minor icing already in September, see Figure 3-10. Later icing occurred most of the time, although there are some gaps in the data, with a maximum ice load reaching 6 kg/m according to the measurements and after correcting for ice drop reaching 12 kg/m. Icing occurred 29 % of the time according to observations and 42 % of the time after correction for ice drop.

During the winter season 2011-2012 the ice load measurements were out of order until the end of January. Icing lasted throughout February until beginning of March with a maximum ice load of 9-10 kg/m. Icing occurred 18 % of the time despite the gap in the measurements during the beginning of the winter season.

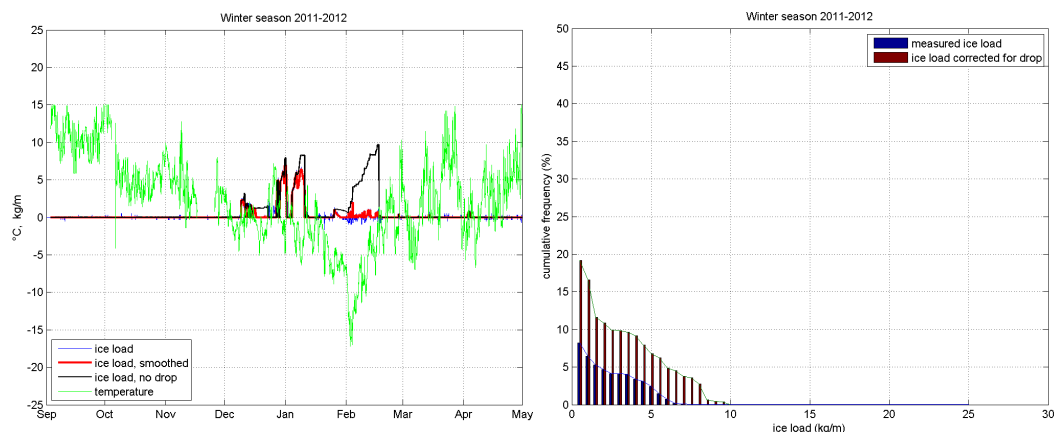


**Figure 3-11: Results for site E13 for winter season 2011-12. Left hand graph shows time series of ice load and temperature. Right hand graph shows cumulative distributions of ice load.**

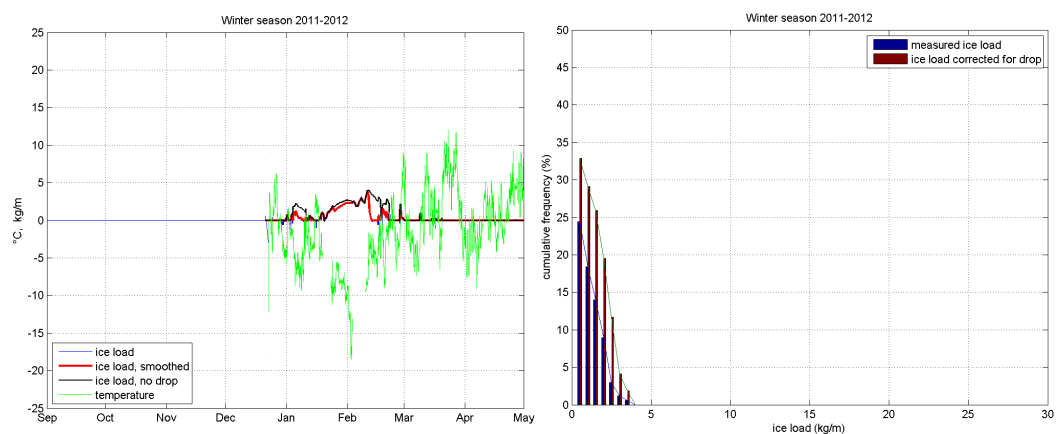


**Figure 3-12: Results for site E14 for winter season 2011-12. Left hand graph shows time series of ice load and temperature. Right hand graph shows cumulative distributions of ice load.**

#### *Site E13:*

Icing measurements for the winter season 2011-2012 started at this site in December and lasted until mid-February, see Figure 3-11. The maximum measured ice load was 8 kg/m and after correction for ice drops the maximum increased to 10 kg/m. The cumulative distribution shows that icing occurred 8 % of the time according to the observation. After correcting for ice drop this increased to 19 % of the time.

#### *Site E14:*

The measurements at this site started in late December of the winter season 2011-2012. Icing lasted through February and ended with some minor events in March. Maximum ice load was 4 kg/m. Part of time with ice load was 24 % according to observations and increased to 33 % correcting for ice drop.

For the sites having observations of visibility, the relation between ice accretion,  $dM/dt$  g/h/m, and visibility has been studied. Such a relation has

earlier been reported and is expected, at least principally. Low visibility usually will mean a higher concentration of small liquid water drops.

The results found for our data also show that the speed of ice accretion increases with decreasing visibility, although there are rather large differences between the different sites, se Figure 3-13.

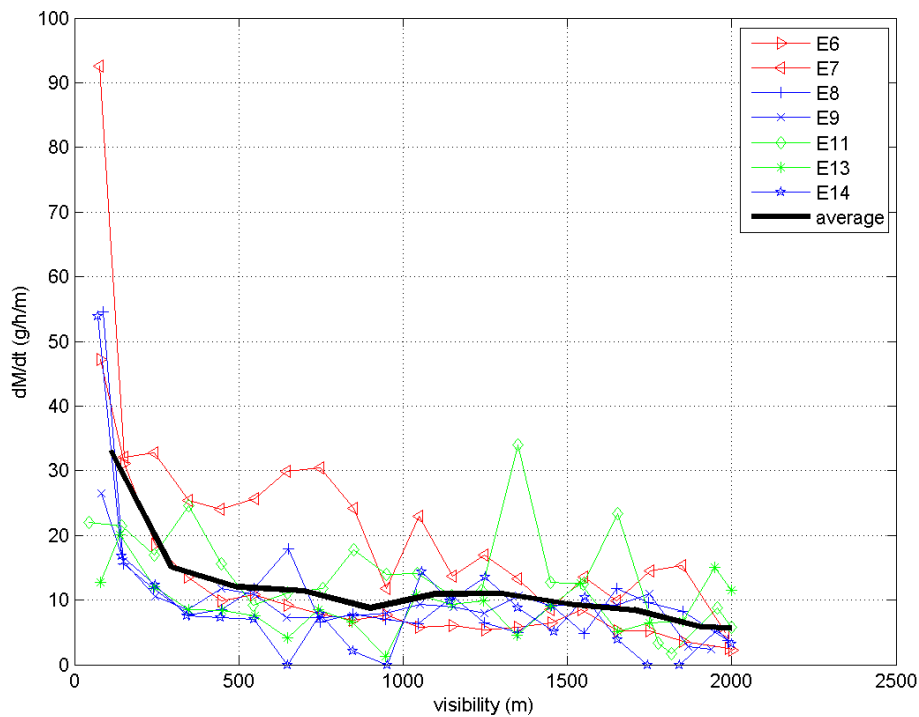


**Figure 3-13: Ice accretion versus visibility.**

### 3.3 Summary of Chapter 3

The results presented above indicate that an ice load reaching about 20 kg/m is certainly to be expected for both Area 1 and Area 2 judging from measurements during 2-3 winter seasons. The results from Area 3 are just for one winter season, but indicate that an ice load reaching 10-15 kg/m could be expected.

It must however be emphasised that these results could NOT be taken as climatological values of the ice load. The amount of data is far too sparse for that; also the quality of the ice load data could be doubted. It is well known that measuring ice load is a difficult task and that no technique and instrument for doing this exist today which can be trusted in every icing situation.

The technique to correct the measured data for drop of ice from the instrument could be expected to give ice load numbers, which are potentially more correct. But the accuracy of the result is dependent on that the measured, and smoothed, signal is not too spiky. It was in many cases not obvious if the measured variability was only due to electric noise or if there was some true variability included. It was evident that the variability was erroneous to some extent e.g. regarding site E2 (Figure 3-4), but it was not obvious if this was always so. There may be more variability in the data, which should have been smoothed out, if so leading to too large ice drop corrections.

The ice load data has also been analysed as regards ice accretion. It was then necessary to use the smoothed ice load data; otherwise the spiky original measurement signal would have drastically affected the statistics of ice accretion. The monthly results are presented in Table 3-2 for each site and winter season. The upper number in each cell of the table shows the number of hours for which the ice accretion speed was above 10 g/h, sometimes called hours with active icing. The bottom number gives the percentage of time for which data was available. There are large differences between both sites and winter season, but typical numbers seem to be around 50 hours with active icing per month. The highest monthly number is 271 hours measured at site E5 during November 2009. Monthly numbers exceeding 100 hours of active icing have occurred during 5 months at one or several of the sites. One month during the winter 2009-2010 and two months during both of the winters 2010-2011 and 2011-2012, respectively. Due to the limited amount of data, both as regards number of sites and as regards availability of data during the measurement periods, this should not be regarded as any exact numbers of any larger climatological significance. In connection to this the sometimes poor quality of the data should be kept in mind.

In Figure 3-14 all results have been put together to make monthly statistics of the number of active icing hours, also partitioning the results into the three areas from which ice load measurements were available. The general impression is that active icing is more common in Area 1, Northern Norrland, than in the other areas. This is true for all but one of the winter months. For February Area 3 show the highest number, but it should be remembered that this is based on data from just one winter season from this area. Otherwise the season for active icing according to the measurements started later in Area 3 than in the other two areas. While active icing started already in

September in Areas 1 and 2, no active was observed in Area 3 until in December. Regarding the active icing in late winter and spring, the difference between the areas were smaller. The icing season ended in April for all areas.

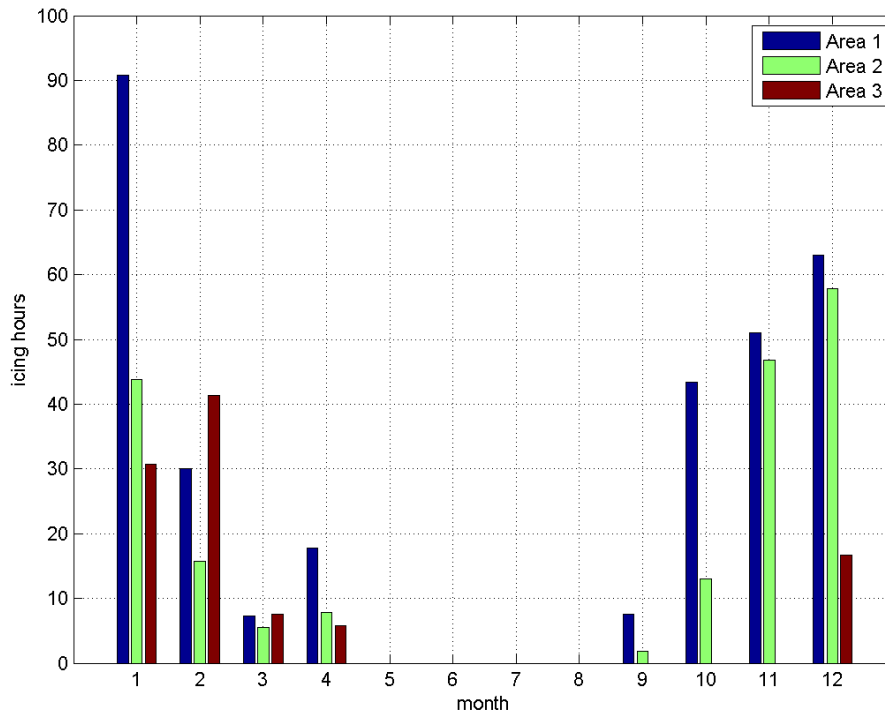


**Figure 3-14: Monthly average numbers of icing hours according the measurements. Results presented for the three areas defined earlier.**

**Table 3-2: Monthly numbers of icing hours for each site given by the upper number in each cell. The bottom number gives percentage of data availability.**

Year-mon	E 1	E 2	E 3	E 4	E 5	E 6	E 7	E 8	E 9	E10	E11	E12	E13	E14
2009-09	0 3				8 96									
2009-10	38 27				65 96									
2009-11	82 99				271 97									
2009-12	3 99				87 96									
2010-01	80 99				17 96									
2010-02	6 99				3 40									
2010-03	0 80				13 43									
2010-04	0 95				22 93									
2010-09	0 95				0 86	0 95	0 93	3 95	9 89		4 85			
2010-10	0 95				30 94	20 95	13 94	0 95	0 94		12 90			
2010-11	18 95				17 32	30 95	30 95	81 95	110 95		54 60			
2010-12	29 94				1 8	11 95	8 95	58 95	55 94		18 77			
2011-01	18 93				34 84	35 96	92 94	10 95	16 94	17 63	114 95			
2011-02	55 94				18 95	12 95	7 95	0 96	11 91	14 89	8 45			
2011-03	0 94				10 97	4 94	14 96	0 95	0 94	6 98	7 78			
2011-04	16 95				11 99	6 94	14 95	0 95	0 94	19 98	0 80			
2011-09		15 95			0 34	0 95	0 94	0 94	0 95				0 92	
2011-10		92 100			14 97	6 95	10 95	0 94	0 95				0 100	
2011-11		53 100			16 97	21 95	20 95	5 94	0 94				0 100	
2011-12		157 100			158 98	138 95	158 95	28 95	33 95				50 100	
2012-01	161 83	104 100			77 98	61 95	70 95	60 95	32 96		38 94		49 100	57 100
2012-02	41 97	18 100			22 100	12 99	50 98	19 99	0 100		24 97		57 100	53 100
2012-03	0 80	29 100			0 98	0 96	26 96	0 95	0 94		0 86		6 100	18 100
2012-04	13 93	42 100			14 98	13 96	22 96	0 94	0 95		13 96		10 100	0 100

## 4 Meso-scale modelling of ice load

### 4.1 Description of models

The class of Numerical Weather Prediction models that are used for high-resolution simulations, predictions for wind energy, and increasingly also for general purpose forecasting, are referred to as meso-scale models.

#### **Meso-scale resolution**

The scale often referred to as meso-scale is the meso- $\gamma$  scale being between 2-20 km in resolved phenomena and from 1/2 hour to about 6 hour's duration, Orlanski (1975). Examples are thunderstorms and meso-scale convective systems (MCSs), sea breeze, urban effects and clear air turbulence (CAT). Below the meso- $\gamma$  scale are the micro scales that deals with processes on the scales of near surface turbulence. . The synoptic scales of 20-200 km belong to the meso- $\beta$  scale even if we don't consider them particularly meso-scale today. Global NWP models have reached resolutions of 15-25 km and can thus resolve the meso- $\beta$  scale.

In order to resolve scales of 2-20 km in dynamical NWP models, the horizontal grid resolution needs to be of the order of a km and meso-scale models are generally run at one or a few km model grid resolution. There are huge computational demands to run the highest resolutions of 1 km. (The cost of the NWP model increases with the inverse of resolution in cube).

Generally (in a model with so called second order accuracy) some 3 gridpoints are required to resolve half a wavelength.

#### **The equations**

In NWP, the state of the atmosphere at some future time is determined using the primitive equations of fluid dynamics and thermodynamics based on an analysis of the current conditions. These equations are derived from various forms of the Navier-Stokes equations of motion. The equations are non-linear partial differential equations, which are impossible to solve exactly through analytical methods. Therefore, the equations are solved using numerical methods by discretization either in spatial or spectral space to yield approximate solutions. There are various forms of simplifications based on scale analysis of the contribution of different terms and their combined effect. Large scale models such as ECMWF's IFS and HIRLAM at SMHI and its sister institutes (and also the meso-scale MIUU model) employ the hydrostatic diagnostic relationship between temperature and geopotential. The acceleration of vertical velocity is neglected and this has the effect of eliminating sound waves and stabilising the model (for moderate resolution).

For high resolution (a few km) over terrain and in convective situations, this hydrostatic assumption is not valid and normal meso-scale models use the so-called elastic set of equations.

**Parameterisation of unresolved scales**

Processes contributing to the evolution of the primitive equations that are not resolved in space or time on the numerical grid need to be represented by a parameterization. In a parameterization the sub-grid scale processes are described as a function of the resolved scale variables, and the mean effect of the sub-grid tendency (such as heating, cooling, moistening, drying) is added to the time-derivative of the state variable.

It must be stressed that all models require some parameterisation, however, the scales of the phenomena that lie sub-grid of a, for instance, 20 km resolution model, are arguably different from the scales of the phenomena that lie sub-grid in a 2 km resolution model.

In coarse resolution NWP models the vertical transport of heat, moisture and momentum due to deep convection is represented by a parameterization. The most common way to describe the effect of convection on its environment is by applying a so-called mass-flux scheme. Most mass-flux parameterizations employ a so-called bulk approach, first suggested by Yanai et al. (1973), in which all active cloud elements are represented in one steady state updraught representing the whole cloud ensemble. In the mass-flux approach, the amount of air rising through each model layer in the clouds is determined by a one-dimensional cloud model.

The meso-scale models on the km-scale do normally not employ a parameterisation of deep convection. The introduction of a time-derivative of the vertical velocity and pressure in the non-hydrostatic meso-scale models, and the small grid-box sizes, allows for an explicit representation of deep convection. This is a major reason for going to meso-scale models, that the convection is represented explicitly (convection permitting models) and that it is thus included in a more physical way than in the large scale models.

Other physical processes such as turbulence, cloud microphysics, condensation, precipitation and radiation need not be inherently different from advanced large scale models, but the most advanced schemes are used in the meso-scale models. For instance, it is necessary to introduce more ice/water categories in the microphysics scheme in order to correctly describe explicit deep convective clouds. This is because the transformation between the liquid and the ice is accompanied by a significant latent heat release, which can contribute to a further growth of convective clouds aloft or cooling beneath by precipitating particles falling in an unsaturated environment. Furthermore, a higher order turbulent kinetic energy prediction scheme (Mellor and Yamada level 2 or 2.5) is really necessary, as the horizontal scales of the phenomena resolved are reduced. The models usually include fully advective cloud and precipitation species (liquid and frozen). Radiation needs to be quite complex and interact e.g., with clouds and sloping surfaces.

### Ice accumulation formula, orographic lift and sublimation

Significant ice loads can form when cloud droplets, raindrops, or a mixture of rain, snow and ice collide with an object. One formula often used to estimate ice load has been formulated by Makkonen (2000). The growth rate, or icing intensity  $dM/dt$  for a surface perpendicular to the airflow can be estimated by:

$$\frac{dM}{dt} = \alpha_1 \alpha_2 \alpha_3 w \cdot A \cdot V, \quad (1)$$

where  $w$  is liquid water content (LWC),  $A$  the cross-section area of the object and  $V$  the wind speed perpendicular to  $A$ .  $\alpha_1$  is the collision efficiency,  $\alpha_2$  is the sticking efficiency, and  $\alpha_3$  is the accretion efficiency.

The collision efficiency  $\alpha_1$  represents the relative number of particles that collide or get in contact with the object in question. It is a function of drop size, wind speed, and water. It also depends on the droplet diameter  $d$ , which can be estimated by the mean volume droplet diameter,

$$D_{mv} = \left( \frac{6 V}{\pi N} \right)^{1/3}, \quad (2)$$

where  $N$  is the cloud droplet concentration. It has however been suggested that the Median Volume Diameter (MVD) is better to use when estimating the collision efficiency (Finstad et al., 1988). In this study  $d$  has been estimated by MVD using the formulation found in the Thompson scheme (26 August 2011) in WRF (see section 4.1.3).

The sticking efficiency,  $\alpha_2$ , is the relative number of particles that stick to and remain on the object. It is set 1 except for snow when it is set to  $1/V$ .

$\alpha_3$  is the accretion efficiency that represents the relative number of particles that collect and form ice. In dry conditions this is 1 but in wet conditions water will run off or blow off. It depends on an energy balance between one hand the latent heat released during freezing and the heat content of the air and on the other hand the cooling effect of flowing air, the evaporation, the heating of accreted droplets and also radiative effects.

A more detailed description of the formula can be found in Thorsson (2010).

The icing calculations have been performed with the Makkonen ice accretion model applied on a 1 m tall cylinder with 30 mm diameter. In the calculations the diameter has been held constant. The meteorological input data for this model are wind speed, pressure, liquid water content, temperature and droplet concentration. Since we do not model the droplet concentration  $N$ , which is used in the estimation of MVD, a constant value of  $100 \text{ cm}^{-3}$  is assumed.

The other parameters are adjusted vertically to account for the difference between model terrain height and real topography. The method used for this vertical adjustment is chosen depending on the low level vertical stability. In stable conditions the air is assumed to rather flow around the mountain than over it, and in this case the parameters are collected at the model level that corresponds to the location height. In unstable conditions the vertical adjustment is done using an adiabatic lift of the air from model height to the

location height. If the cooling associated with this lift results in condensation, the condensed water will be added to the original liquid cloud water from the model before it is used in the ice accretion calculation. Melting of ice is calculated using an energy balance equation, which includes an empirical ice shedding.

The ice load observations shows that ice also falls off/sublimates in below-zero conditions. This effect is not included in the Makkonen model, so in this case formula (3) (Mazin et al., 2001) is used:

$$subl = \frac{\lambda Nu l \xi \phi_0 R_\alpha}{c_p R_v P_\alpha} (e_i - e_a), \quad (3)$$

$$Nu = A Re^n, \quad (4)$$

$$Re = \frac{\rho D V}{\mu}, \quad (5)$$

Constants used:

$$\lambda = 0.02, l = 1, \xi = 1.41, \phi_0 = 1.48$$

This formula takes wind speed ( $V$ ) and relative humidity ( $e_i - e_a$ ) into account so high wind speed and dry air result in a high sublimation rate. All of the variables needed in the calculation e.g. the Nusselt number  $Nu$  are available in the Makkonen formulas so it is relatively easy to add this effect to the ice load calculations.

#### 4.1.1 AROME

AROME (Application Recherche Operationalisation Meso-Echelle) is the meso-scale (km resolution) version of the ALADIN model (Aire Limitée Adaption Dynamique International) (<http://www.crn.meteo.fr/aladin>) (Seity et al., 2012). ALADIN (including AROME) shares code with the global ECWMF IFS (European Centre for Medium Range Weather Forecasts, Integrated Forecasting System). ALADIN is a spectral limited area model and has been developed to use the full non-hydrostatic equations (Euler elastic form of Navier Stoke's equations). As described above, all meso-scale models (1-2 km) are formulated in this way since the vertical velocity is large at the resolved scales due to convection and orographic forcing.

The radiation scheme is of the two-stream type and surface slopes are taken into account. It is based on the radiation scheme used in the ECMWF model, and scientific documentation is available online at <http://www.ecmwf.int/research/ifsdocs/CY23r4/>. The radiation scheme calculates the radiative fluxes taking into account absorption-emission of longwave radiation and reflection, scattering and absorption of solar radiation by the earth's atmosphere and surfaces.

Deep convection is explicitly resolved but there is vertical sub-grid transport due to turbulence and shallow convection, which is described by a so-called Eddy Diffusion Mass-Flux (EDMF) scheme. The scheme computes vertical transport due to dry and moist convective plumes, as well as turbulent mixing in the boundary layer. Organized strong updrafts are parameterized by the mass flux part while the remaining turbulence is parameterized using K-theory, which is using a prognostic closure using turbulent kinetic energy (TKE) (De Rooy and Siebesma, 2008 and Siebesma et. al, 2007).

The main source of clouds in AROME is the mean vertical advection. But other processes may be contributing to the generation of clouds: radiative cooling, ED mixing and of course subgrid cloudy plumes. Clouds are described using a statistical cloud scheme, where the adjustment to saturation is instantaneous (time scale much shorter than the time step). The statistical cloud scheme (Chaboureau and Bechtold, 2005) uses a probability density function (PDF) of "distance to saturation", where the variance of the PDF is a function of turbulence and mass-flux.

The microphysics for warm clouds is described by the "Kessler" scheme (Kessler 1969). It is a one-moment scheme that prognoses the mixing ratio of cloud and rain water. The processes considered are evaporation/condensation, rain evaporation, accretion of cloud droplets by raindrops, conversion of cloud droplets into raindrops (autoconversion), and rain sedimentation. The size distribution of raindrops is assumed to follow a Marshall-Palmer distribution. The mixed phase cloud parameterization is explained in Pinty and Jabouille (1998) and Caniaux et. al (1994). For ice clouds the scheme contains prognostic equation for the primary ice mixing ratio, the snowflakes mixing ratio, and the rimed crystals mixing ratio. The total number concentration of the primary ice is diagnosed, while the total number concentration of the snowflakes and of the rimed crystals follow  $N = C\lambda^*x$ . Where  $\lambda$  is a slope parameter. Both  $C$  and  $x$  depend on the ice category and must be specified from physical arguments. The size distribution of the ice categories follows a gamma distribution.

The surface scheme (SURFEX, Le Moigne, 2012) computes averaged fluxes for momentum, sensible and latent heat and possibly chemical species and dust fluxes and then sends these quantities back to the atmosphere with the addition of a radiative surface temperature, surface direct and diffuse albedo and also surface emissivity. In SURFEX, each model grid box is represented by four surface types: sea or ocean, water bodies (e.g. lakes), urban areas, and nature (soil and vegetation). The coverage of each of these surfaces is obtained with the global ECOCLIMAP database (Masson et al. 2003).

SMHI and its HIRLAM sister institutes work on and run AROME under a long-term co-operation agreement with the ALADIN consortium. HIRLAM (Undén et al, 2002) (High Resolution Limited Area Model) is the previous but still operational regional hydrostatic model for a bit larger scales than AROME (5-20 km resolutions typically). It has a more approximate form of Navier Stoke's equations (assuming hydrostatic balance between pressure and temperature) and the physical parameterisation is simpler, particularly the cloud scheme.

AROME is used for 2.5 km runs, and the initial conditions and boundaries are, in this study, provided by the operational HIRLAM 5 km model. The model has 10 levels in the lowest 300 m, see Table 4-1.

**Table 4-1: The lowest 10 model levels in AROME.**

Model level	Height (m)
10	287
9	247
8	211
7	177
6	146
5	117
4	89
3	63
2	38
1	12

Figure 4-1 shows the AROME area in red that has been used for the two last winter season's simulations. The model has been run in a 6-hour cycle, with data assimilation of surface observations. The 06 and 18UTC forecasts are run up to 6 hours to produce a first guess for the 00 and 12UTC surface analysis. At 00 and 12UTC the model has been run up to 24 hours. Forecast lengths 7-18 hours have been used to construct hourly time series of the relevant parameters.

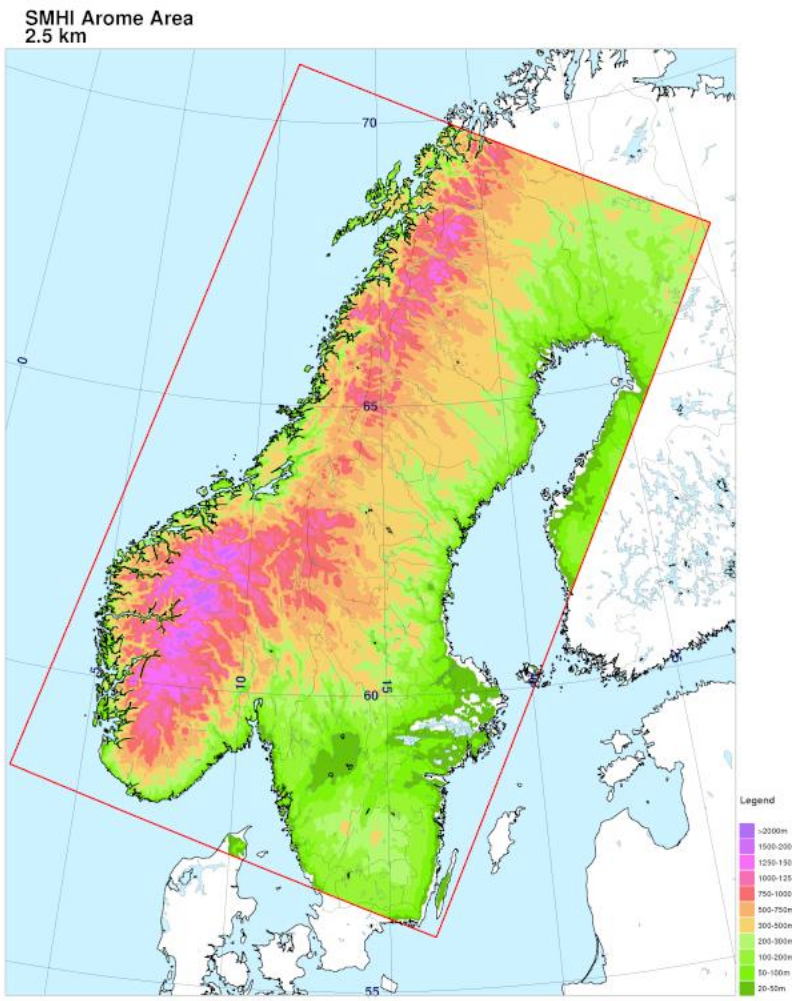


Figure 4-1: SMHI 2011/2012 AROME area.

#### 4.1.2 COAMPS®

COAMPS® (Coupled Ocean/Atmosphere Mesoscale Prediction System) is a numerical mesoscale model developed at the US Naval Research Lab, Monterey, California. Here, version 3.1.1 of the system has been used. It is a non-hydrostatic compressible model with a terrain-following sigma-z vertical coordinate. The model has prognostic equations for the mean variables  $u$  (wind in the east-west direction),  $v$  (wind in the north-south direction),  $w$  (vertical wind),  $\Theta$  (potential temperature), and the Exner function (pressure perturbation). Turbulence is parameterised with a level-2.5 turbulence closure (Mellor and Yamada, 1982); hence, TKE (turbulent kinetic energy) is a prognostic variable. Moist physics is parameterised using a mixing ratio scheme (Rutledge and Hobbs, 1983). Predictions of mixing ratios are given for the microphysical variables water vapour, pristine ice, snow, graupel, rain, and cloud water. Other physical parameterisation schemes included in COAMPS® are long- and shortwave radiation (Harshvardan et al., 1987) and cumulus convection (Kain and Fritsch, 1990). Ground surface temperature is computed using a surface energy balance scheme. High resolution for a given area of interest can be achieved by using nested grids in idealised and real-case simulations. A more complete model description is found in Hodur (1997).

COAMPS® is used operationally by the US Navy to produce forecasts. Examples of areas in which COAMPS® is used on a daily basis are along the US West Coast and in the Mediterranean Sea. In Sweden, COAMPS® is used as a research tool at Uppsala University and Stockholm University, and operationally by WeatherTech Scandinavia AB to produce wind forecasts. The model has also been used in numerous research studies, e.g. on coastal jets (Burk and Thompson 1996, Burk et al. 1999) and katabatic flow (Söderberg and Parmhed 2005).

In order to cover the measurement sites and reduce CPU-usage, separate computational model domains were set up. The sites were grouped in different geographical areas and the desired model grid resolution was achieved by using nested grids. The outer mesh and nest levels 1 to 3 are illustrated in Figure 4-2. The model grid resolution in the outer mesh is  $27 \times 27 \text{ km}^2$  and increase with a factor 3 to  $9 \times 9 \text{ km}^2$ ,  $3 \times 3 \text{ km}^2$ , and  $1 \times 1 \text{ km}^2$  model grid resolution in nest level 1 to 3. The model was set up with 40 vertical levels ranging from 34330 m to 5 m above ground; 11 of the levels are in the lowest 300 m, see Table 4-2.

The model was run for 3 "icing seasons", 2009/2010, 2010/2011, and 2011/2012. Each "icing season" includes the months September to April during which icing events are expected to occur.

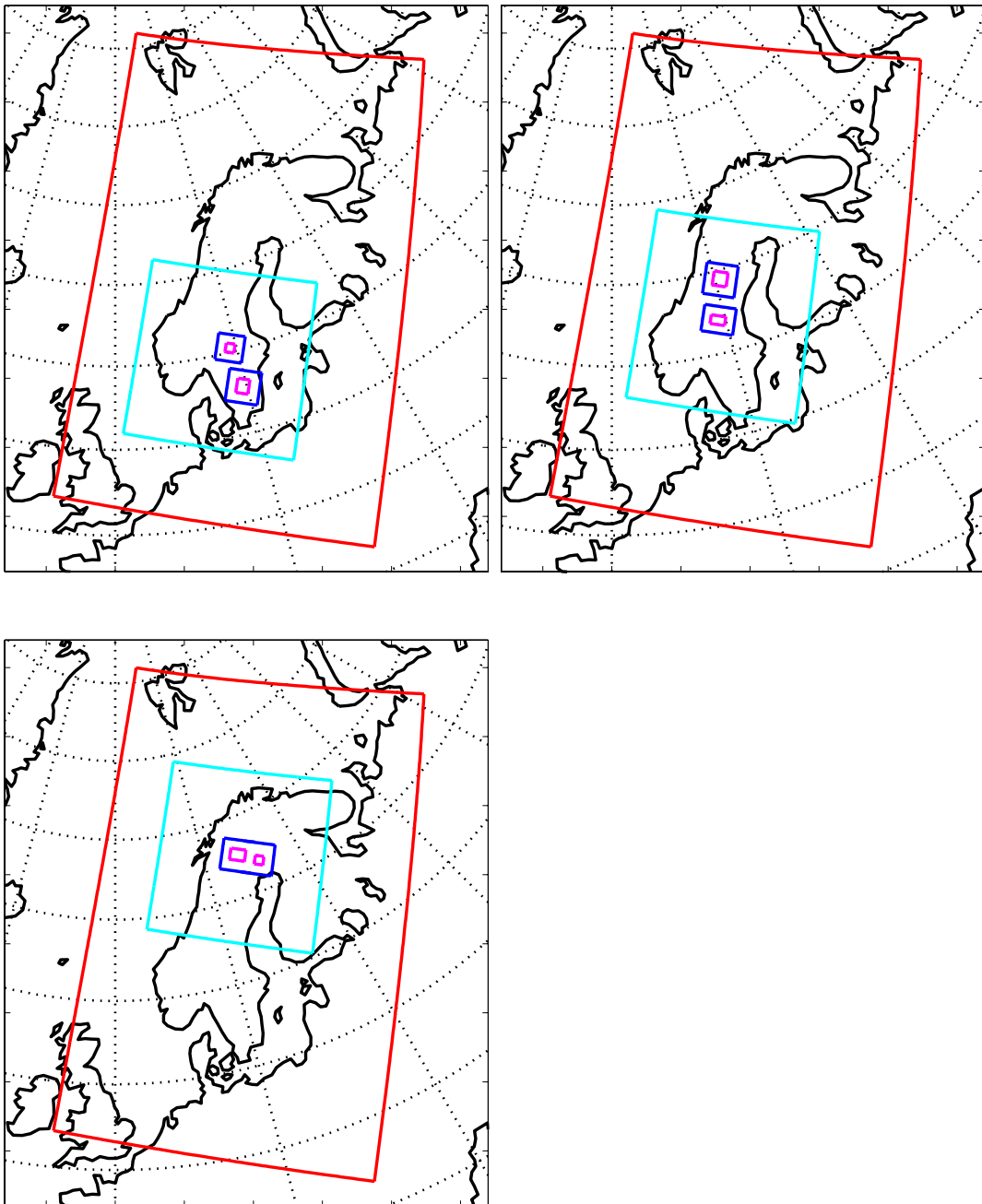


**Figure 4-2: COAMPS® model domains. Outer domain, 27x27 km<sup>2</sup> model grid (red), nest level 1, 9x9 km<sup>2</sup> model grid (green), nest level 2, 3x3 km<sup>2</sup> model grid (blue), and nest level 3, 1x1 km<sup>2</sup> model grid (magenta).**

Initial and lateral boundary conditions were provided using NCEP FNL (Final) Operational Global Analysis data (U.S. National Centers for Environmental Prediction). NCEP FNL is prepared operationally every six hours on 1.0x1.0 degree global grid. Observational data from the Global Telecommunications

System (GTS) and other sources are continuously collected in the Global Data Assimilation System (GDAS). The FNLs are made with the same model NCEP uses in the Global Forecast System (GFS). The analyses are available on the surface, at pressure levels from 1000mb to 10mb, and in the surface boundary layer. Parameters include surface pressure, sea level pressure, geopotential height, temperature, sea surface temperature, soil values, ice cover, relative humidity, u- and v- winds, vertical motion, vorticity and ozone.

Outer mesh boundary conditions are updated every 6 h (00, 06, 12 and 18 UTC). The model is run in 18 h cycles and cold-started at 00 and 12 UTC. The first 6 h of the simulation is not used allowing for model spin-up, necessary for e.g., turbulence kinetic energy and cloud physics. Inner mesh lateral boundary conditions are one-way interactive and continuously updated during the simulation.

Surface characteristics applied to the lower boundary are given by a database included in the model system. Roughness and ground wetness over land is determined by a land-use classification in a 1 km global landuse dataset (USGS). Terrain height is given by a 1 km global terrain database.

**Table 4-2: The lowest 11 levels in COAMPS®.**

Model level	Height (m)
30	285
31	220
32	165
33	120
34	85
35	60
36	45
37	35
38	25
39	15
40	5

### 4.1.3 WRF

The Weather Research and Forecasting (WRF) model is a mesoscale numerical weather prediction system that is suitable for modelling the atmosphere with high-resolution. The system supports two dynamical solvers: the Advanced Research WRF (ARW) and the nonhydrostatic Mesoscale Model (NMM). In the present study WRF ARW v3.2 has been used. It is a community model for which the development is supervised primarily by National Centers for Environmental Prediction (NCEP) and National Center for Atmospheric Research (NCAR) in USA. The solver in WRF consists of a set of Eulerian equations that is fully compressible, non-hydrostatic and conservative for scalar variables. WRF includes prognostic variables for the horizontal and vertical velocity components, perturbation potential temperature, perturbation geopotential, and perturbation surface pressure of dry air. The model has terrain-following vertical coordinates and uses a staggered Arakawa-C grid. The solver uses a time-split integration with a 2nd- or 3rd-order Runge-Kutta scheme (Skamarock et al., 2008).

The WRF model consists of many different physics schemes that are available to use with the ARW solver. These include different descriptions for microphysics, cumulus parameterizations, surface physics, surface layer physics, planetary boundary layer physics and atmospheric radiation physics. For a full list and description of the schemes available see Skamarock et al. (2008). A brief description of the categories and the physics options used in this work follows but for a more comprehensive list with thorough descriptions of all the options available see the ARW technical note (Skamarock et al., 2008).

The microphysics in WRF includes explicitly resolved water vapour, cloud and precipitation processes. In this work the Thompson scheme is used. It is a bulk microphysical parameterization that explicitly predicts the mixing ratios of cloud water, rain, cloud ice, snow, and graupel as well as the droplet number concentrations of cloud ice and rain (but not cloud droplet concentration  $N$  which is assumed to have a constant value of  $100 \text{ cm}^{-3}$ , see also section 4.1). This scheme is developed to be more similar to full double-moment schemes and many of the techniques used are usually found in more advanced spectral/bin microphysical schemes (Thompson et. al, 2004, and 2008).

Cumulus parameterization schemes compute the convective precipitation resulting from sub-grid-scale effects of convective clouds. The schemes represent vertical fluxes originating from updrafts and downdrafts that the model cannot resolve. The parameterizations are only valid on grid sizes that are larger than the scale of convective eddies and should therefore not be used when the model grid size is fine enough for the model to resolve the eddies itself (Skamarock et al., 2008). For this work the modified Kain-Fritsch scheme (Kain, 2004 cited by Skamarock et al., 2008) was chosen for cumulus parameterization. It includes effects from detrainment and entrainment in a simple cloud model with moist updrafts and downdrafts. This scheme was turned off for model domains with a grid size smaller than 9 km.

The surface layer schemes are responsible for calculating friction velocities and exchange coefficients that are needed by the planetary boundary layer and land surface schemes. Over water the surface layer scheme also

calculates the surface fluxes. The scheme used is called the Eta surface layer scheme (Janjic, 1996, 2002 cited by Skamarock et al., 2008) and it is based on the similarity theory by Monin and Obukhov (1954) including parameterizations of a viscous sub-layer following Janjic (1994, cited by Skamarock et al., 2008).

The land-surface models (LSMs) in WRF use input data from many of the other schemes to calculate heat and moisture fluxes. The Noah LSM, which was used in this work, was developed by NCAR and NCEP and is similar to the code used in the NCEP North American Mesoscale Model (NAM).

The planetary boundary layer (PBL) schemes compute tendencies of temperature, moist and horizontal momentum by determining the vertical flux profiles in the well-mixed boundary layer and the stable layer (Skamarock et al., 2008). The surface fluxes needed in the PBL schemes are provided by the surface layer and land-surface schemes. The Yonsei University (YSU) PBL scheme (Hong et al., 2006 cited Skamarock et al., 2008) was used in this work. It uses counter-gradient terms to represent fluxes and has an explicit term handling the entrainment layer at the PBL top. The PBL top is defined from the buoyancy profile.

The atmospheric radiation schemes handle longwave and shortwave radiation in the atmosphere. The simulated processes include absorption and emission of longwave radiation by gases and surfaces and absorption, reflection and scattering of shortwave radiation in the atmosphere and at surfaces. The radiation schemes takes model predicted cloud and water vapour distributions into account. The longwave radiation scheme chosen in this work is called Rapid Radiative Transfer Model (RRTM). RRTM is based on Mlawer et al. (1997, cited in Skamarock et al., 2008) and represents longwave processes due to water vapor, ozone and CO<sub>2</sub>. The shortwave radiation scheme used is the Dudhia scheme. This scheme is based on Dudhia et al. (1989, cited in Skamarock et al., 2008) and accounts for clear-air scattering, water vapor absorption and cloud albedo and absorption (Skamarock et al., 2008).

To cover all the measurement sites, separate computational model domains in which the sites were grouped in different geographical areas were set up. The outer mesh and nest levels 1 to 3 are illustrated in Figure 4-3. The model grid resolution in the outer mesh is 27x27 km<sup>2</sup> and increase with a factor 3 to 9x9 km<sup>2</sup>, 3x3 km<sup>2</sup>, and 1x1 km<sup>2</sup> model grid resolution in nest level 1 to 3. The model was set up with 45 vertical levels with 11 levels in the lowest 300 m, see Table 4-3.

Table 4-3

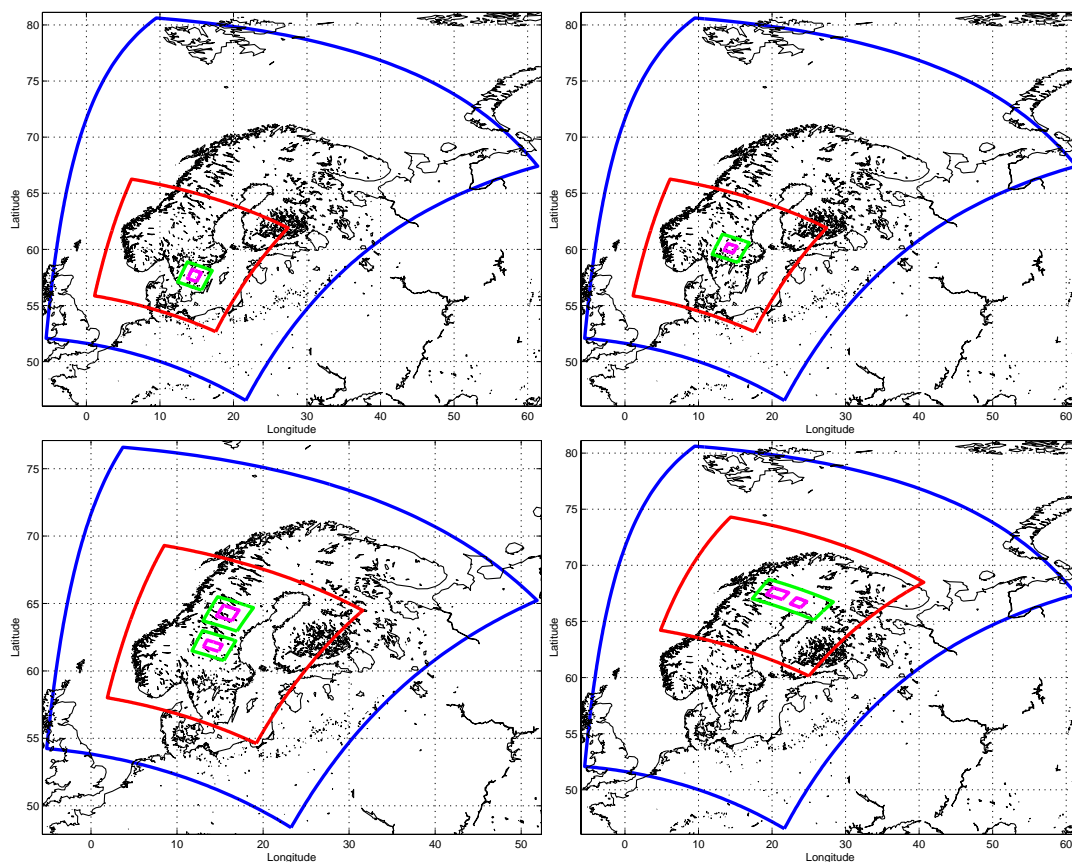


**Figure 4-3: WRF model domains. Outer domain,  $27 \times 27 \text{ km}^2$  model grid (blue), nest level 1,  $9 \times 9 \text{ km}^2$  model grid (red), nest level 2,  $3 \times 3 \text{ km}^2$  model grid (green), and nest level 3,  $1 \times 1 \text{ km}^2$  model grid (magenta).**

The model was run for 2 “icing seasons”, 2010/2011 and 2011/2012. In each “icing season”, the months September to April are included. Meteorological initial and lateral boundary conditions are taken from FNL data, see section 4.1.2. Outer mesh boundary conditions are updated every 6 h (00, 06, 12 and 18 UTC). The model is run in 18 h cycles and cold-started at 00 and 12 UTC. The first 6 h of the simulation is not used allowing for model spin-up, necessary for e.g., turbulence kinetic energy and cloud physics. Inner mesh lateral boundary conditions are one-way interactive.

The data describing the lower surface is extracted from several databases including e.g. topographic and landuse data. These databases are included in the standard WRF source package.

**Table 4-3: The lowest 11 levels in WRF.**

Model level	Height (m)
11	303
10	259
9	222
8	188
7	156
6	127
5	100
4	75
3	53
2	37
1	15

In a recent update of WRF a bug fix of interest for this work was included. In version 3.4.1 with release date August 16, 2012, an updated version to the YSU PBL scheme was included:

- YSU: fix for stable surface conditions (Thanks to Heather Richardson and Sukanta Basu at North Carolina State University) and consistency with thermal roughness length. The change may result in improvement in surface wind forecast at night.
- YSU: a bug fix for nest starting at later time due to introduction of 'topo\_wind' option, even if the option isn't used.

See also <http://www.mmm.ucar.edu/wrf/users/wrfv3.4/updates-3.4.1.html>

Compared to WRF and COAMPS<sup>®</sup> model results and the PBL sensitivity tests, FNL results displayed a less stable boundary layer. This indicates that the YSU-scheme treated stable conditions differently. It is, however, uncertain how the model results would be different over whole winter season. A further investigation is required to draw any firm conclusions.

## 4.2 Comparisons with observations

### 4.2.1 Meteorological data

Prior to estimating ice load it is important to find out how well the numerical weather prediction models are able to reproduce the observed state of the atmosphere. A comparison between modelled and observed values of wind speed, wind direction, temperature, and pressure has been performed and is presented here. For each measurement site, model data have been extracted from the nearest model grid point. No interpolation in the horizontal has been carried out. In Table 4-4, observation height, real terrain height at the measurement site, and model terrain height is given for each site.

**Table 4-4: Observation height, real terrain height at the measurement site, and model terrain height in the closest model grid point for all sites and all models.**

Site	E1	E2	E3	E4	E5	E6	E7	E8	E9	E10	E11	E12	E13	E14
Site obs height	78	150	40	80	80	100	200	70	155	80	60	100	150	100
Site terrain height	390	676	715	593	730	631	631	718	718	508	980	294	345	520
AROME terrain height	229	547	566	452	549	537	537	605	605	433	863	256	318	453
COAMPS terrain height	267	587	626	576	616	615	615	583	583	475	911	261	324	480
WRF terrain height	308	648	656	575	623	617	617	579	579	473	967	263	324	464

It is clear from Table 4-4 that there are differences between model terrain heights and the measurements sites terrain height. The differences are the largest in areas with steep terrain. Note also the differences in terrain height between the models. The differences are due to different model grid resolutions, differences between terrain databases used by the models, and methods used in the models to estimate a representative model terrain height for the grid box.

Several methods can be used to evaluate model performance. Here we have focused on comparing time series of model grid point data to point measurements. No evaluation of model output and routine meteorological observations such as 10-m wind speed and 2-m temperature from weather stations or weather balloon soundings has been done. The observed near-surface data is most cases influenced by local terrain and vegetation that the mesoscale models cannot represent. Furthermore, in many cases the near-surface data is not representative for winds and temperatures at 100-m height or above. Thus only data from the measurement sites listed above with observations taken at heights relevant for estimating icing conditions at typical turbine heights are used in the model evaluation.

For each site and winter season, statistics have been calculated for time periods when both model data and observations are available. The arithmetic mean is defined as:

$$Mean = \frac{1}{N} \sum_{i=1}^N x_i , \quad (6)$$

where  $N$  is the number of values in the data series. The *Median* in a data series is the number found in the middle after having arranged the numbers from the lowest to the highest number. When the median differs from the mean, the data series has a skewed distribution.

In statistics, Bias is an estimator of the mean error in the model. It quantifies systematic errors and tells if the model tends to overestimate or underestimate the modelled variable:

$$Bias = \frac{1}{N} \sum_{i=1}^N x_i - y_i , \quad (7)$$

where  $x$  is the modelled value and  $y$  is the observed value. The mean absolute error disregards the sign of the errors:

$$MAE = \frac{1}{N} \sum_{i=1}^N |x_i - y_i| , \quad (8)$$

and is a measure of the magnitude of the errors. The root mean square error is often used in evaluations of model performance:

$$RMSE = \sqrt{\frac{1}{N} \sum_{i=1}^N (x_i - y_i)^2} \quad (9)$$

and give information on the spread of the error magnitude. In this estimator, outliers are given much weight and only a relatively few bad data points can influence the magnitude of the *RMSE*.

Model skill is not only given by error estimates but also by how well the magnitude of the variability in the two data series agree. The variability in the series is described by the standard deviation:

$$Std = \sqrt{\frac{1}{N} \sum_{i=1}^N (x_i - \bar{x})^2}, \quad (10)$$

where  $\bar{x}$  is the arithmetic mean.

Another statistical measure often used is the correlation coefficient:

$$r = \frac{\frac{1}{N} \sum_{i=1}^N (x_i - \bar{x})(y_i - \bar{y})}{Std(x)Std(y)}, \quad (11)$$

which gives a measure of the linear dependence between the modelled and observed values.

As noted above, outliers often have a large impact on *RMSE*. Moreover, a difficulty in numerical weather prediction is timing the changes in the state of the atmosphere. For example, assume that the temperature can be described by a sinusoidal function and that the amplitude is perfectly predicted. A relatively small phase error will still give a high *RMSE*. Hence, in the analysis of model data and point measurements one has to be aware of that *RMSE* suffers from uncertainties in both time and space. This is sometimes referred to as the “double-penalty” error. To better recognise the influence of phase errors in skill scores, the squared *RMSE* can be decomposed into (Murphy 1988, Horvath et al. 2012):

$$\begin{aligned} \frac{1}{MN} \sum_{k=1}^M \sum_{i=1}^N (x_{i,k} - y_{i,k})^2 = \\ \frac{1}{M} \sum_{k=1}^M (\bar{x}_k - \bar{y}_k)^2 + [Std_k(x) - Std_k(y)]^2 + 2Std_k(x)Std_k(y)[1 - r_k(x, y)] \end{aligned}, \quad (12)$$

where  $k$  and  $i$  are indices in space and time,  $M$  is the number of stations, and bars denote time-means. The first term on the right hand side is the square of the *Bias*, the second term is the square of the bias of the standard deviations, and the third term is the square of the phase error. In this study, each model time series is compared to one point measurement only and the expression simplifies to:

$$RMSE^2 = Bias^2 + [Std(x) - Std(y)]^2 + 2Std(x)Std(y)[1 - r(x, y)] \quad (13)$$

An overview of the results is presented in graphs showing distributions of wind speed, wind direction and temperature and vertical profiles of wind speed and temperature. For each site, statistics and statistical scores are given in tables.

General comments to the model results are:

- The wind speed distributions given by AROME are most often narrower than the other two models and peaks at lower wind speeds than COAMPS<sup>®</sup> and WRF. The negative wind speed bias could in part be due to a lower model terrain height for most sites.
- The wind direction distributions are similar for all three models. For sites where wind directions are observed a good agreement between model data and observations is found.
- The temperature distributions from all three models agree quite well with observations. All models have a cold bias, which also is seen in the mean temperature profiles.
- The mean temperature profiles suggest that COAMPS<sup>®</sup> and AROME have a more stably stratified boundary layer than WRF.
- The vertical wind shear in AROME and COAMPS<sup>®</sup> are more similar to each other than to WRF; this can be a consequence of the differences in the boundary layer stability.
- The mean wind speed profiles from WRF and COAMPS<sup>®</sup> often intersect. The height at which the profiles cross varies from site to site, ~50 and ~200 m height above the model terrain. The variation in intersection height can partly be explained by differences in model terrain height. Below the intersection height, WRF has a higher wind speed than COAMPS<sup>®</sup>, above WRF has a lower wind speed than COAMPS<sup>®</sup>.
- Pressure statistics show that all models perform well in describing variations of the atmospheric pressure.
- Temperature statistics show that the models are able to predict temperature well. The correlation numbers are high even though the largest errors are due to phase errors, which is the dominant component of the *RMSE*.
- Wind speed statistics show that for most sites, AROME has a lower mean wind speed than COAMPS<sup>®</sup> and WRF. For many sites AROME has a negative bias while COAMPS<sup>®</sup> and WRF has a positive bias. The winds modelled in WRF and COAMPS<sup>®</sup> have a somewhat larger variability seen in the larger values of *Std*. The dominant component in *RMSE* is in most cases the phase error.

Site E1:

Model results and observations for site E1 are shown in Figure 4-4 and Figure 4-5 for the winter seasons 2010/2011 and 2011/2012. Statistics is summarized in Table 4-5.

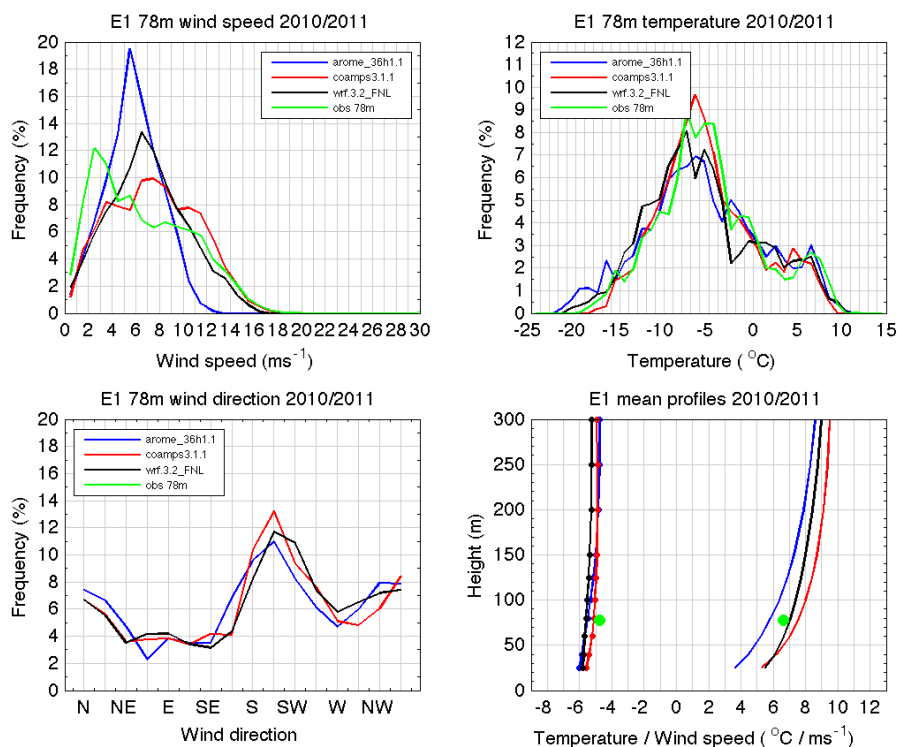


**Figure 4-4: Model results and observations for site E1, winter season 2010/2011. Upper left: wind speed distributions; Upper right: temperature distributions; Lower left: wind direction distributions; Lower right: profiles of mean temperature (solid/dotted) and mean wind speed (solid).**

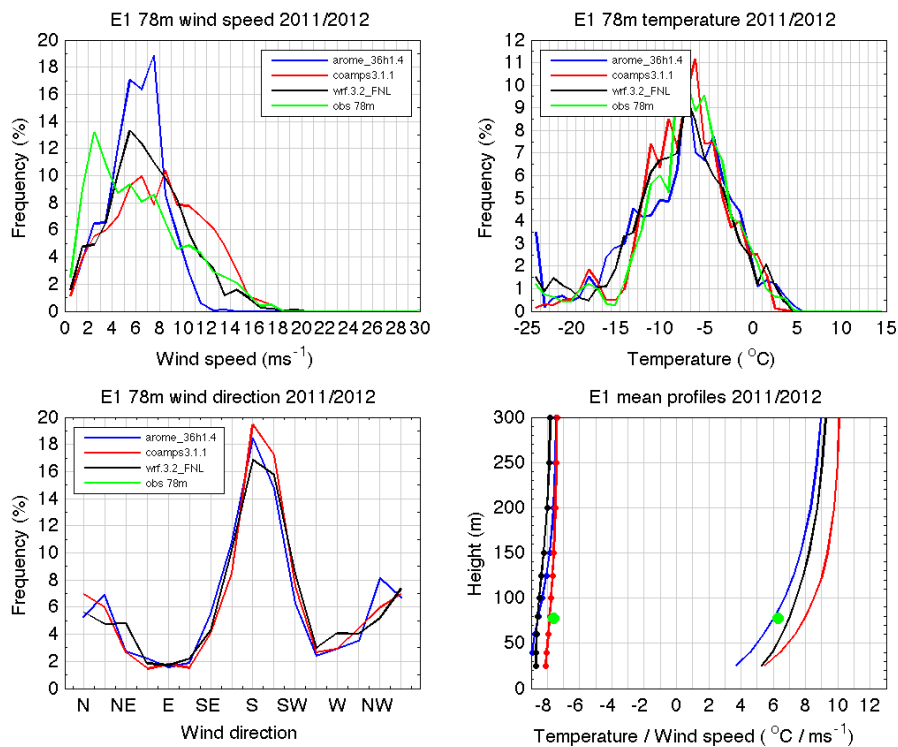


**Figure 4-5: Model results and observations for site E1, winter season 2011/2012. Upper left: wind speed distributions; Upper right: temperature distributions; Lower left: wind direction distributions; Lower right: profiles of mean temperature (solid/dotted) and mean wind speed (solid).**

**Table 4-5: Observation and model statistics and statistical scores for site E1.**

E1 2010/2011											
wind speed											
Data	Mean	Max	Min	Median	Std	MAE	r	RMSE	Bias	Bias Std	PhaseE
arome_36h1.1	5,79	12,67	0,21	5,77	2,28	2,22	0,76	2,78	-0,85	1,67	2,06
coamps3.1.1	7,55	19,02	0,09	7,46	3,63	2,10	0,79	2,63	0,90	0,32	2,45
wrf.3.2_FNL	7,03	16,97	0,07	6,83	3,26	1,92	0,80	2,43	0,37	0,69	2,30
obs78m	6,65	19,10	0,10	5,90	3,95	-	-	-	-	-	-
temperature											
Data	Mean	Max	Min	Median	Std	MAE	r	RMSE	Bias	Bias Std	PhaseE
arome_36h1.1	-5,50	10,28	-21,53	-6,01	6,63	1,91	0,94	2,42	-0,73	0,74	2,19
coamps3.1.1	-5,12	8,52	-17,87	-5,92	5,45	1,35	0,96	1,71	-0,35	0,44	1,62
wrf.3.2_FNL	-5,60	10,09	-20,58	-6,48	6,23	1,71	0,94	2,26	-0,79	0,36	2,08
obs78m	-4,78	11,10	-19,00	-5,40	5,89	-	-	-	-	-	-
pressure											
Data	Mean	Max	Min	Median	Std	MAE	r	RMSE	Bias	Bias Std	PhaseE
arome_36h1.1	948,4	974,6	922,3	947,0	12,36	1,70	1,00	1,85	-1,67	0,15	0,78
coamps3.1.1	950,0	976,8	922,5	948,8	12,65	0,87	1,00	1,12	-0,06	0,14	1,11
wrf.3.2_FNL	950,7	976,6	925,1	949,3	12,41	0,82	1,00	1,05	0,60	0,12	0,85
obs78m	950,0	977,0	924,0	949,0	12,51	-	-	-	-	-	-
E1 2011/2012											
wind speed											
Data	Mean	Max	Min	Median	Std	MAE	r	RMSE	Bias	Bias Std	PhaseE
arome_36h1.4	6,03	13,24	0,09	6,19	2,26	2,21	0,69	2,83	-0,27	1,57	2,33
coamps3.1.1	7,97	17,79	0,20	7,93	3,75	2,42	0,78	3,03	1,67	0,08	2,53
wrf.3.2_FNL	6,97	19,17	0,23	6,67	3,29	2,07	0,76	2,62	0,67	0,54	2,48
obs78m	6,30	18,00	0,20	5,60	3,83	-	-	-	-	-	-
temperature											
Data	Mean	Max	Min	Median	Std	MAE	r	RMSE	Bias	Bias Std	PhaseE
arome_36h1.4	-8,57	4,53	-29,60	-7,64	6,24	1,89	0,94	2,44	-0,96	1,06	1,97
coamps3.1.1	-7,84	3,17	-25,74	-7,44	4,74	1,28	0,95	1,69	-0,23	0,43	1,62
wrf.3.2_FNL	-8,61	3,85	-28,05	-7,94	5,73	1,80	0,93	2,31	-1,00	0,56	2,01
obs78m	-7,61	4,10	-27,90	-7,20	5,18	-	-	-	-	-	-
pressure											
Data	Mean	Max	Min	Median	Std	MAE	r	RMSE	Bias	Bias Std	PhaseE
arome_36h1.4	952,1	990,1	920,4	950,5	17,10	1,36	1,00	1,51	-1,33	0,21	0,68
coamps3.1.1	953,6	991,5	919,5	951,8	17,59	0,77	1,00	0,99	0,17	0,28	0,93
wrf.3.2_FNL	954,5	992,7	922,2	953,0	17,32	1,17	1,00	1,35	1,13	0,01	0,75
obs78m	953,4	992,0	921,0	952,0	17,31	-	-	-	-	-	-

Site E2:

Model results and observations for site E2 are shown in Figure 4-6 for the winter season 2011/2012. Statistics is summarized in Table 4-6.

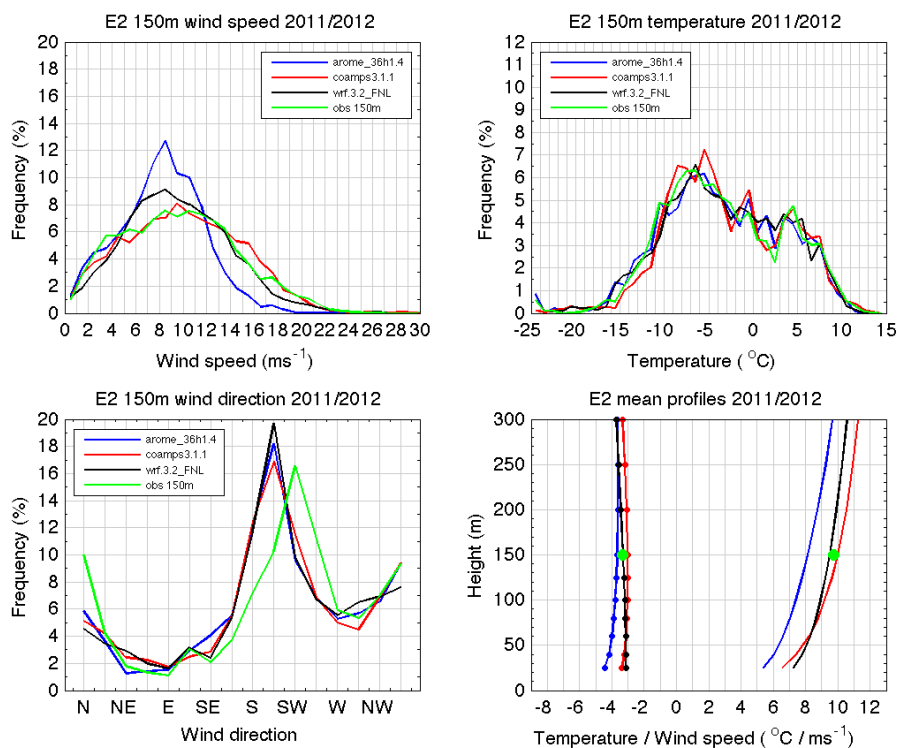


**Figure 4-6: Model results and observations for site E2, winter season 2011/2012. Upper left: wind speed distributions; Upper right: temperature distributions; Lower left: wind direction distributions; Lower right: profiles of mean temperature (solid/dotted) and mean wind speed (solid).**

**Table 4-6: Observation and model statistics and statistical scores for site E2.**

E2 2011/2012												
wind speed												
Data	Mean	Max	Min	Median	Std	MAE	r	RMSE	Bias	Bias Std	PhaseE	
arome_36h1.4	8,14	22,32	0,25	8,26	3,52	2,74	0,77	3,48	-1,60	1,33	2,79	
coamps3.1.1	10,00	29,22	0,18	9,84	4,85	2,48	0,76	3,34	0,26	0,00	3,33	
wrf.3.2_FNL	9,50	26,54	0,11	9,19	4,38	2,68	0,72	3,50	-0,23	0,47	3,46	
obs150m	9,74	26,10	0,20	9,60	4,85	-	-	-	-	-	-	
temperature												
Data	Mean	Max	Min	Median	Std	MAE	r	RMSE	Bias	Bias Std	PhaseE	
arome_36h1.4	-3,66	11,95	-29,50	-4,02	6,92	1,09	0,98	1,54	-0,33	0,18	1,49	
coamps3.1.1	-3,02	13,67	-25,20	-3,94	6,47	1,07	0,98	1,47	0,31	0,28	1,41	
wrf.3.2_FNL	-3,31	11,57	-27,35	-3,61	6,75	1,05	0,98	1,45	0,02	0,00	1,45	
obs150m	-3,33	13,20	-29,50	-4,00	6,75	-	-	-	-	-	-	
pressure												
Data	Mean	Max	Min	Median	Std	MAE	r	RMSE	Bias	Bias Std	PhaseE	
arome_36h1.4	904,5	942,0	865,3	904,2	14,78	24,99	0,77	27,58	-24,99	3,58	11,12	
coamps3.1.1	905,5	943,3	863,3	905,3	15,19	23,94	0,76	26,73	-23,93	3,17	11,49	
wrf.3.2_FNL	906,3	944,3	863,2	906,0	14,97	23,20	0,77	25,94	-23,18	3,39	11,14	
obs150m	929,5	988,0	872,0	927,0	18,36	-	-	-	-	-	-	

Site E3:

Model results and observations for site E3 are shown in for the winter seasons 21010/2011 and 2011/2012 in Figure 4-7 and Figure 4-8. Statistics is summarized in Table 4-7.

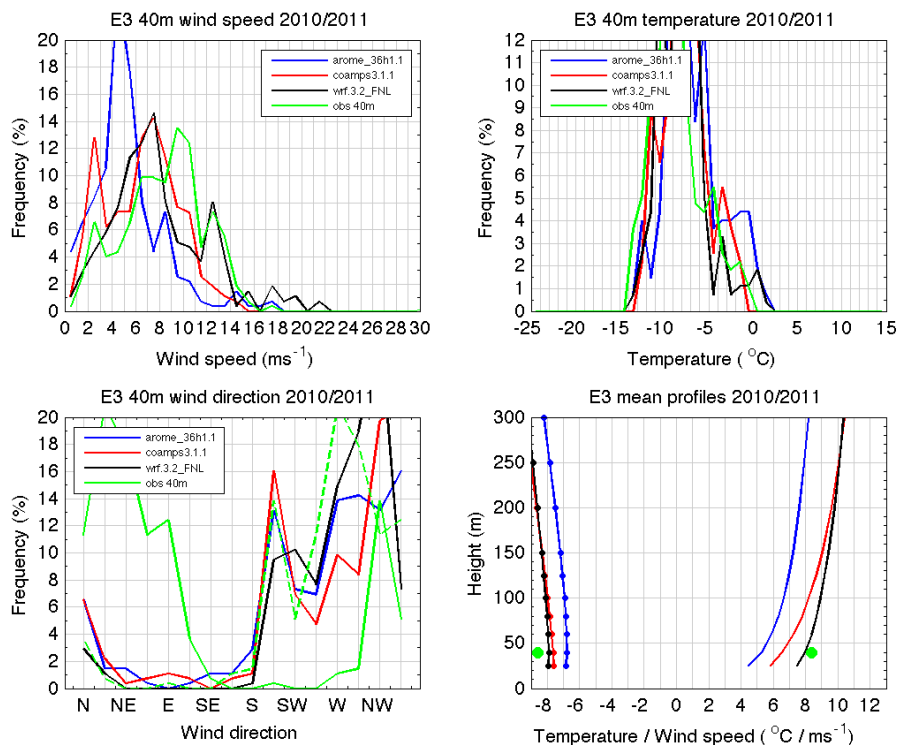


**Figure 4-7: Model results and observations for site E3, winter season 2010/2011. Upper left: wind speed distributions; Upper right: temperature distributions; Lower left: wind direction distributions; Lower right: profiles of mean temperature (solid/dotted) and mean wind speed (solid).**

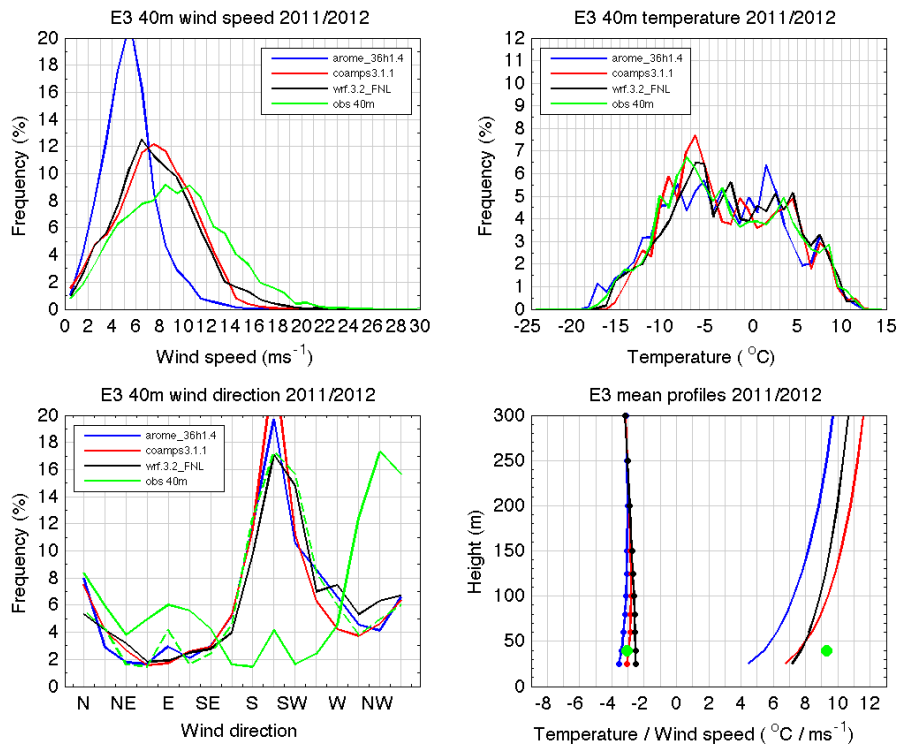


**Figure 4-8: Model results and observations for site E3, winter season 2011/2012. Upper left: wind speed distributions; Upper right: temperature distributions; Lower left: wind direction distributions; Lower right: profiles of mean temperature (solid/dotted) and mean wind speed (solid).**

**Table 4-7: Observation and model statistics and statistical scores for site E3.**

E3 2010/2011												
wind speed												
Data	Mean	Max	Min	Median	Std	MAE	r	RMSE	Bias	Bias Std	PhaseE	
arome_36h1.1	5,27	17,78	0,13	4,87	3,00	3,71	0,51	4,43	-3,09	0,38	3,16	
coamps3.1.1	6,55	17,20	0,04	6,57	3,13	2,75	0,60	3,43	-1,81	0,25	2,91	
wrf.3.2_FNL	7,98	21,85	0,48	7,32	4,01	2,57	0,59	3,43	-0,38	0,64	3,35	
obs40m	8,36	17,10	0,70	8,70	3,38	-	-	-	-	-	-	
temperature												
Data	Mean	Max	Min	Median	Std	MAE	r	RMSE	Bias	Bias Std	PhaseE	
arome_36h1.1	-6,78	1,09	-13,19	-7,38	3,17	1,90	0,92	2,17	1,80	0,38	1,15	
coamps3.1.1	-7,63	-1,22	-12,65	-7,61	2,50	1,28	0,90	1,54	0,94	0,29	1,19	
wrf.3.2_FNL	-7,90	1,20	-13,61	-7,98	2,64	1,31	0,87	1,55	0,67	0,15	1,39	
obs40m	-8,57	-0,60	-13,70	-9,00	2,79	-	-	-	-	-	-	
pressure												
Data	Mean	Max	Min	Median	Std	MAE	r	RMSE	Bias	Bias Std	PhaseE	
arome_36h1.1	907,2	919,0	896,3	905,7	5,92	5,54	0,99	5,63	-5,54	0,16	1,01	
coamps3.1.1	908,5	919,5	895,0	907,0	5,68	4,25	0,98	4,42	-4,25	0,40	1,17	
wrf.3.2_FNL	908,5	920,7	896,6	906,8	6,16	4,19	0,98	4,32	-4,19	0,08	1,08	
obs40m	912,7	924,0	900,0	911,0	6,08	-	-	-	-	-	-	
E3 2011/2012												
wind speed												
Data	Mean	Max	Min	Median	Std	MAE	r	RMSE	Bias	Bias Std	PhaseE	
arome_36h1.4	5,45	17,97	0,11	5,36	2,24	4,13	0,75	4,86	-3,87	1,96	2,17	
coamps3.1.1	7,61	23,00	0,10	7,65	3,24	2,77	0,70	3,48	-1,71	0,97	2,87	
wrf.3.2_FNL	7,74	24,34	0,04	7,52	3,47	2,67	0,73	3,30	-1,59	0,74	2,80	
obs40m	9,32	25,60	0,30	9,20	4,21	-	-	-	-	-	-	
temperature												
Data	Mean	Max	Min	Median	Std	MAE	r	RMSE	Bias	Bias Std	PhaseE	
arome_36h1.4	-3,39	11,28	-18,09	-3,56	6,60	1,13	0,98	1,49	-0,32	0,06	1,46	
coamps3.1.1	-2,94	12,27	-15,52	-3,91	6,22	1,04	0,98	1,35	0,13	0,32	1,31	
wrf.3.2_FNL	-2,53	11,66	-17,28	-2,78	6,37	1,11	0,98	1,46	0,54	0,16	1,34	
obs40m	-3,07	12,00	-17,50	-3,80	6,54	-	-	-	-	-	-	
pressure												
Data	Mean	Max	Min	Median	Std	MAE	r	RMSE	Bias	Bias Std	PhaseE	
arome_36h1.4	913,3	951,7	873,3	913,1	14,87	4,64	1,00	4,84	-4,64	0,29	1,34	
coamps3.1.1	911,5	949,6	869,1	911,3	15,27	6,43	0,99	6,63	-6,43	0,10	1,62	
wrf.3.2_FNL	914,8	953,4	873,9	914,5	15,08	3,16	1,00	3,42	-3,16	0,08	1,30	
obs40m	917,9	958,0	878,0	918,0	15,16	-	-	-	-	-	-	

Site E4:

Model results and observations for site E4 are shown in Figure 4-9 for the winter season 2011/2012. Statistics is summarized in Table 4-8.

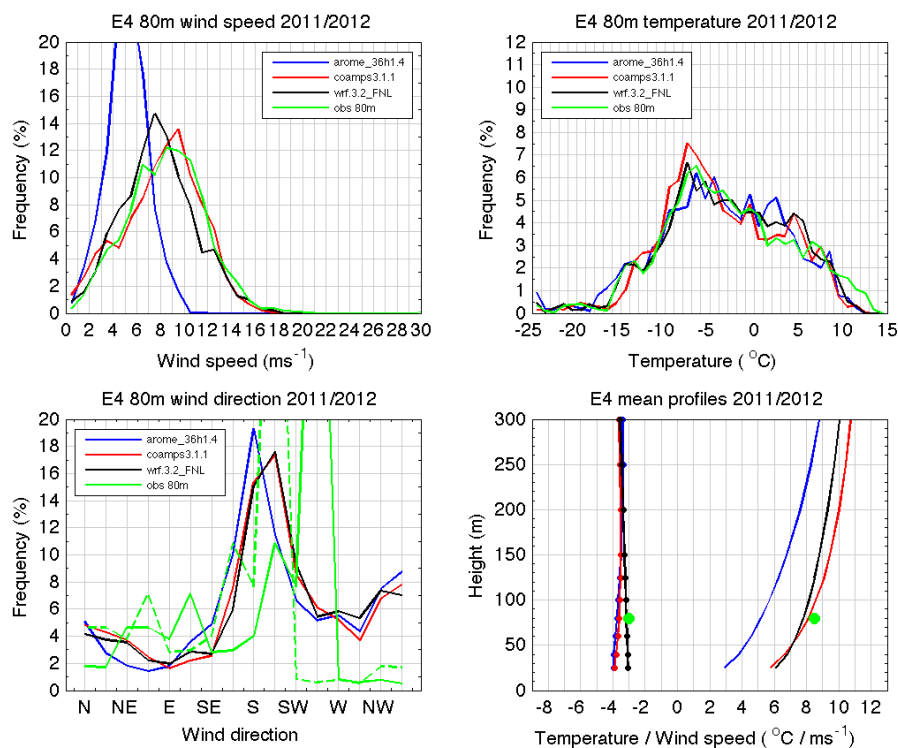


**Figure 4-9: Model results and observations for site E4, winter season 2011/2012. Upper left: wind speed distributions; Upper right: temperature distributions; Lower left: wind direction distributions; Lower right: profiles of mean temperature (solid/dotted) and mean wind speed (solid).**

**Table 4-8: Observation and model statistics and statistical scores for site E4.**

E4 2011/2012												
wind speed												
Data	Mean	Max	Min	Median	Std	MAE	r	RMSE	Bias	Bias Std	PhaseE	
arome_36h1.4	5,18	11,49	0,13	5,22	1,73	3,42	0,76	3,96	-3,31	1,46	1,62	
coamps3.1.1	8,11	17,65	0,21	8,44	3,24	1,93	0,71	2,48	-0,38	0,05	2,45	
wrf.3.2_FNL	7,81	17,61	0,20	7,72	3,08	1,78	0,77	2,25	-0,68	0,11	2,15	
obs80m	8,49	20,70	0,70	8,60	3,19	-	-	-	-	-	-	
temperature												
Data	Mean	Max	Min	Median	Std	MAE	r	RMSE	Bias	Bias Std	PhaseE	
arome_36h1.4	-3,74	11,62	-30,59	-3,82	7,14	1,38	0,97	1,83	-0,73	0,02	1,68	
coamps3.1.1	-3,61	12,30	-26,46	-4,42	6,57	1,36	0,98	1,72	-0,60	0,59	1,50	
wrf.3.2_FNL	-3,15	11,96	-27,70	-3,31	6,86	1,27	0,97	1,66	-0,14	0,31	1,62	
obs80m	-3,01	13,70	-28,30	-3,60	7,17	-	-	-	-	-	-	
pressure												
Data	Mean	Max	Min	Median	Std	MAE	r	RMSE	Bias	Bias Std	PhaseE	
arome_36h1.4	921,5	953,3	884,0	923,6	13,32	9,04	0,99	9,18	-9,04	0,26	1,57	
coamps3.1.1	924,7	957,0	883,8	927,0	13,78	5,82	0,99	6,03	-5,82	0,20	1,56	
wrf.3.2_FNL	925,1	957,2	884,9	927,3	13,51	5,40	0,99	5,61	-5,40	0,07	1,52	
obs80m	930,5	964,0	892,0	932,0	13,58	-	-	-	-	-	-	

Site E5:

Model results and observations for site E5 are shown in Figure 4-10 to Figure 4-12 for the winter seasons 2009/2010, 2010/2011, and 2011/2012. Statistics is summarized in Table 4-9.

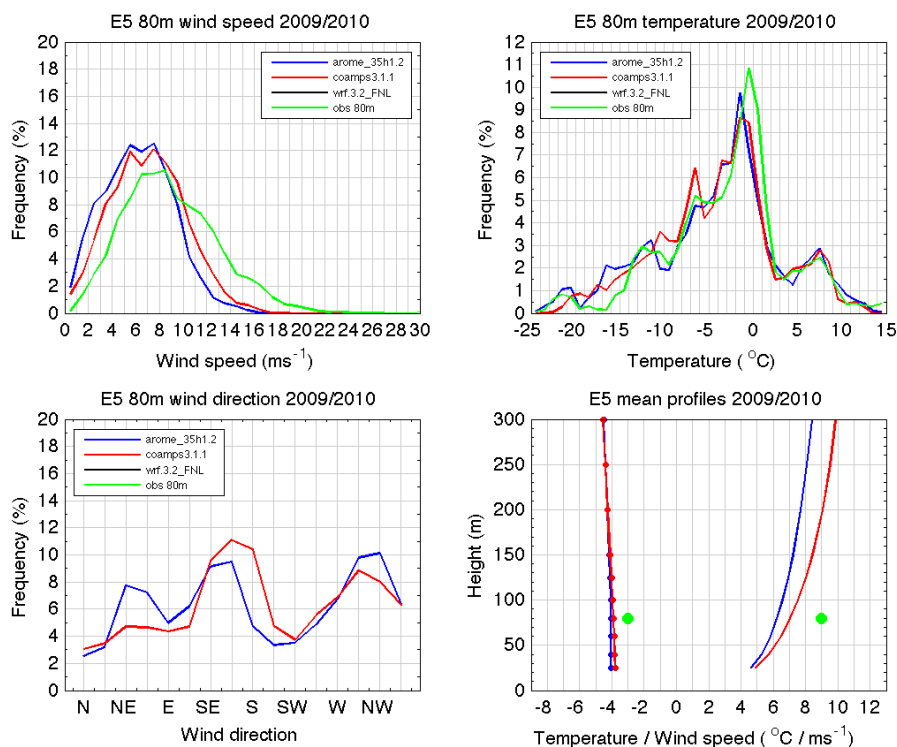


**Figure 4-10: Model results and observations for site E5, winter season 2009/2010. Upper left: wind speed distributions; Upper right: temperature distributions; Lower left: wind direction distributions; Lower right: profiles of mean temperature (solid/dotted) and mean wind speed (solid).**

7

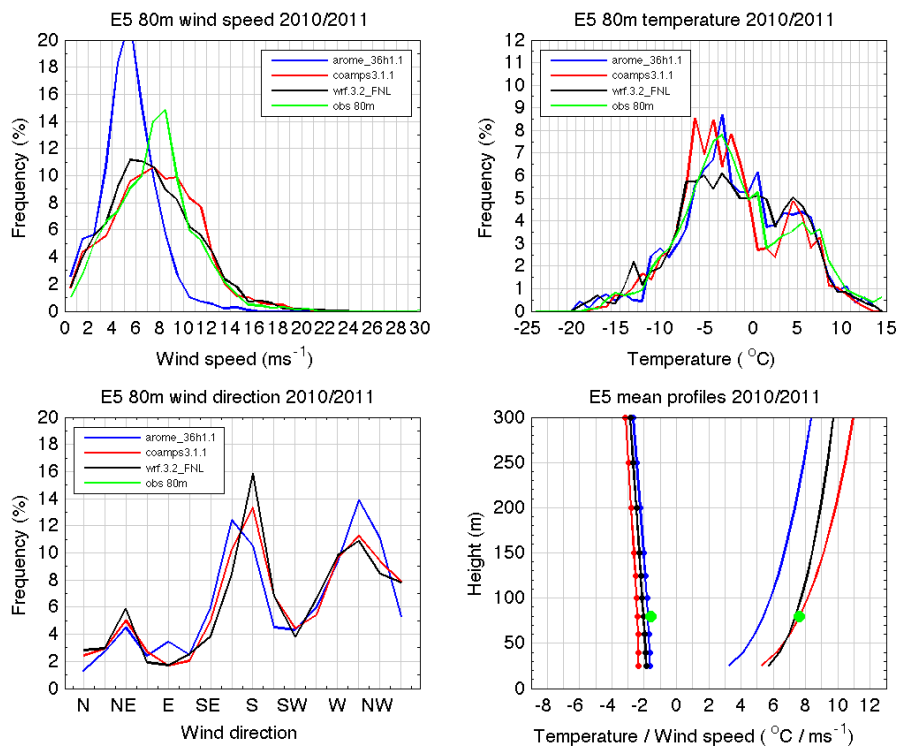


**Figure 4-11: Model results and observations for site E5, winter season 2010/2011. Upper left: wind speed distributions; Upper right: temperature distributions; Lower left: wind direction distributions; Lower right: profiles of mean temperature (solid/dotted) and mean wind speed (solid).**

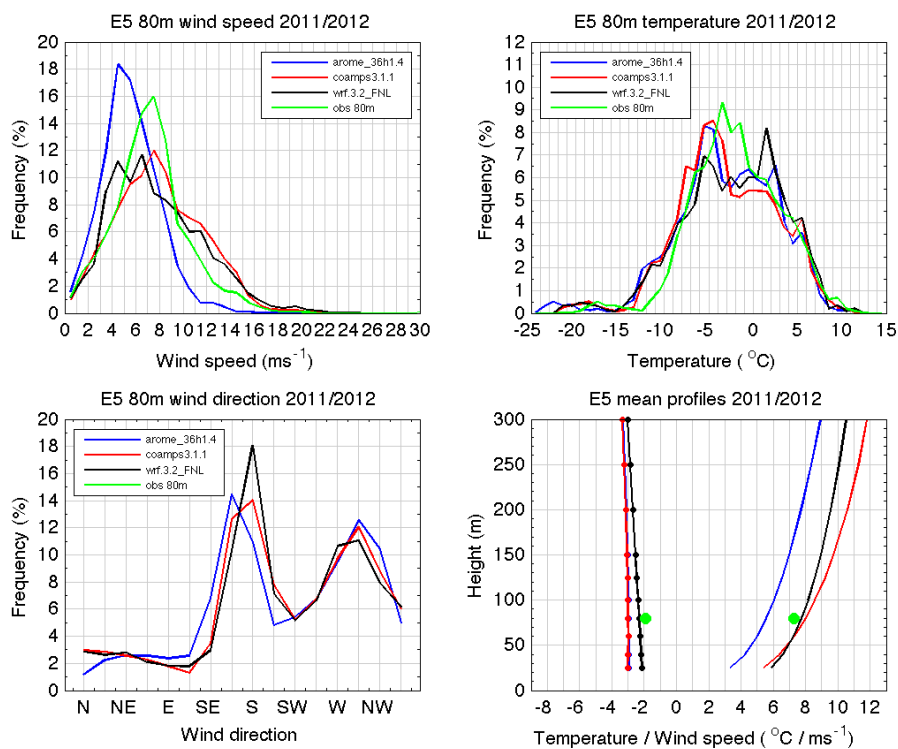


**Figure 4-12: Model results and observations for site E5, winter season 2011/2012. Upper left: wind speed distributions; Upper right: temperature distributions; Lower left: wind direction distributions; Lower right: profiles of mean temperature (solid/dotted) and mean wind speed (solid).**

**Table 4-9: Observation and model statistics and statistical scores for site E5.**

E5 2009/2010												
wind speed												
Data	Mean	Max	Min	Median	Std	MAE	r	RMSE	Bias	Bias Std	PhaseE	
arome_35h1.2	6,23	16,82	0,07	6,16	2,91	3,21	0,70	3,94	-2,76	1,03	2,62	
coamps3.1.1	7,05	18,69	0,07	7,01	3,11	2,71	0,70	3,42	-1,90	0,82	2,73	
wrf.3.2_FNL	-	-	-	-	-	-	-	-	-	-	-	
obs80m	9,00	26,80	0,30	8,60	3,94	-	-	-	-	-	-	
temperature												
Data	Mean	Max	Min	Median	Std	MAE	r	RMSE	Bias	Bias Std	PhaseE	
arome_35h1.2	-4,05	14,40	-24,54	-3,13	7,41	1,59	0,97	2,17	-1,05	0,74	1,75	
coamps3.1.1	-3,90	12,71	-23,14	-3,21	6,76	1,38	0,97	1,85	-0,88	0,08	1,63	
wrf.3.2_FNL	-	-	-	-	-	-	-	-	-	-	-	
obs80m	-3,00	16,50	-24,00	-2,10	6,66	-	-	-	-	-	-	
pressure												
Data	Mean	Max	Min	Median	Std	MAE	r	RMSE	Bias	Bias Std	PhaseE	
arome_35h1.2	907,2	936,9	877,2	907,8	12,01	5,80	0,97	6,23	-5,37	0,12	3,17	
coamps3.1.1	913,6	939,2	883,3	913,4	12,16	1,27	1,00	1,54	1,07	0,03	1,10	
wrf.3.2_FNL	-	-	-	-	-	-	-	-	-	-	-	
obs80m	912,5	939,0	883,0	912,0	12,13	-	-	-	-	-	-	
E5 2010/2011												
wind speed												
Data	Mean	Max	Min	Median	Std	MAE	r	RMSE	Bias	Bias Std	PhaseE	
arome_36h1.1	5,39	15,59	0,04	5,34	2,28	2,61	0,71	3,17	-2,19	0,98	2,07	
coamps3.1.1	7,65	22,08	0,05	7,58	3,61	2,06	0,71	2,66	0,04	0,34	2,63	
wrf.3.2_FNL	7,39	23,75	0,07	7,07	3,66	2,03	0,72	2,61	-0,20	0,39	2,57	
obs80m	7,59	20,80	0,10	7,70	3,27	-	-	-	-	-	-	
temperature												
Data	Mean	Max	Min	Median	Std	MAE	r	RMSE	Bias	Bias Std	PhaseE	
arome_36h1.1	-1,77	13,80	-19,82	-2,21	6,15	1,28	0,96	1,69	-0,15	0,17	1,67	
coamps3.1.1	-2,41	12,42	-18,20	-3,09	5,81	1,16	0,98	1,54	-0,68	0,45	1,30	
wrf.3.2_FNL	-2,04	13,64	-19,96	-2,24	6,36	1,40	0,96	1,89	-0,42	0,05	1,84	
obs80m	-1,61	19,50	-18,30	-2,50	6,32	-	-	-	-	-	-	
pressure												
Data	Mean	Max	Min	Median	Std	MAE	r	RMSE	Bias	Bias Std	PhaseE	
arome_36h1.1	910,0	934,4	884,5	909,6	11,78	1,84	1,00	2,11	1,80	0,42	1,02	
coamps3.1.1	910,7	936,2	883,1	910,3	12,28	2,67	1,00	2,88	2,65	0,12	1,10	
wrf.3.2_FNL	911,2	935,8	884,8	910,9	12,00	3,06	1,00	3,22	3,06	0,19	1,01	
obs80m	908,2	934,0	883,0	908,0	12,20	-	-	-	-	-	-	

Table 4-9 **continued.**

E5 2011/2012

wind speed											
Data	Mean	Max	Min	Median	Std	MAE	r	RMSE	Bias	Bias Std	PhaseE
arome_36h1.4	5,57	17,51	0,08	5,33	2,40	2,37	0,67	2,90	-1,72	0,71	2,22
coamps3.1.1	8,02	22,94	0,08	7,74	3,65	2,24	0,66	2,92	0,74	0,54	2,77
wrf.3.2_FNL	7,76	24,61	0,05	7,13	3,88	2,26	0,66	3,01	0,48	0,77	2,87
obs80m	7,28	20,60	0,20	7,20	3,11	-	-	-	-	-	-
temperature											
Data	Mean	Max	Min	Median	Std	MAE	r	RMSE	Bias	Bias Std	PhaseE
arome_36h1.4	-2,96	11,61	-24,28	-2,88	5,67	1,68	0,93	2,32	-1,06	0,72	1,93
coamps3.1.1	-2,99	11,61	-22,00	-3,37	5,49	1,39	0,97	1,83	-1,09	0,55	1,36
wrf.3.2_FNL	-2,29	11,85	-21,98	-1,95	5,67	1,52	0,94	1,98	-0,39	0,73	1,80
obs80m	-1,90	12,10	-21,00	-2,10	4,94	-	-	-	-	-	-
pressure											
Data	Mean	Max	Min	Median	Std	MAE	r	RMSE	Bias	Bias Std	PhaseE
arome_36h1.4	909,1	945,9	867,8	909,0	15,50	1,18	1,00	1,44	0,95	0,40	1,02
coamps3.1.1	909,7	946,9	867,2	909,8	16,00	2,16	0,99	2,49	1,56	0,10	1,94
wrf.3.2_FNL	910,6	947,4	868,5	910,7	15,76	2,51	1,00	2,69	2,49	0,14	1,00
obs80m	908,1	944,0	867,0	908,0	15,90	-	-	-	-	-	-

Site E6:

Model results and observations for site E6 are shown in Figure 4-13 and Figure 4-14 for the winter seasons 2010/2011 and 2011/2012. Statistics is summarized in Table 4-10.

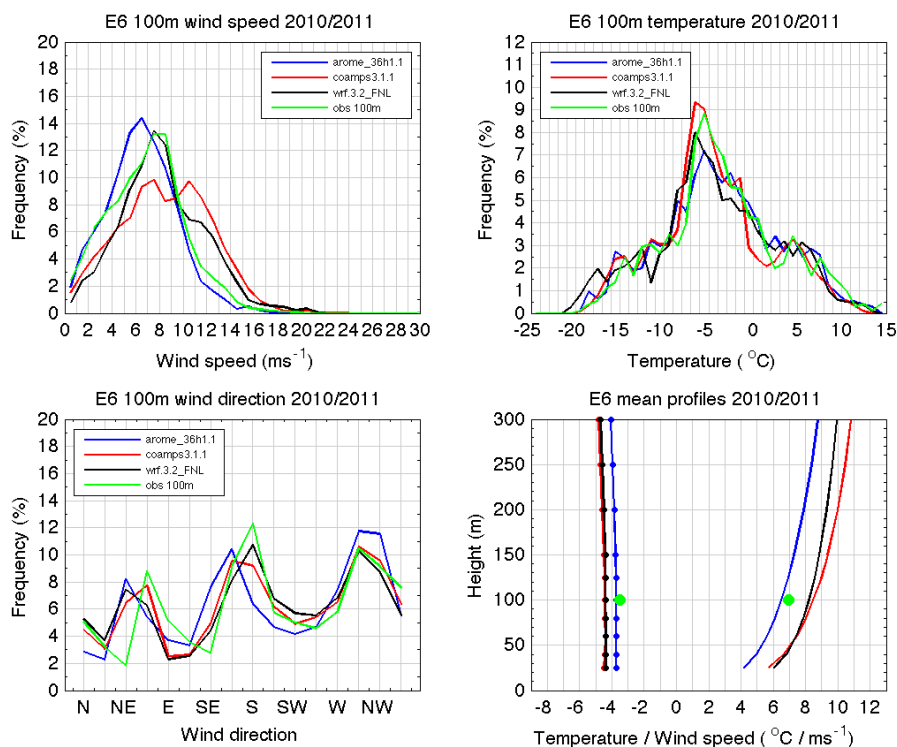


**Figure 4-13: Model results and observations for site E6, winter season 2010/2011. Upper left: wind speed distributions; Upper right: temperature distributions; Lower left: wind direction distributions; Lower right: profiles of mean temperature (solid/dotted) and mean wind speed (solid).**

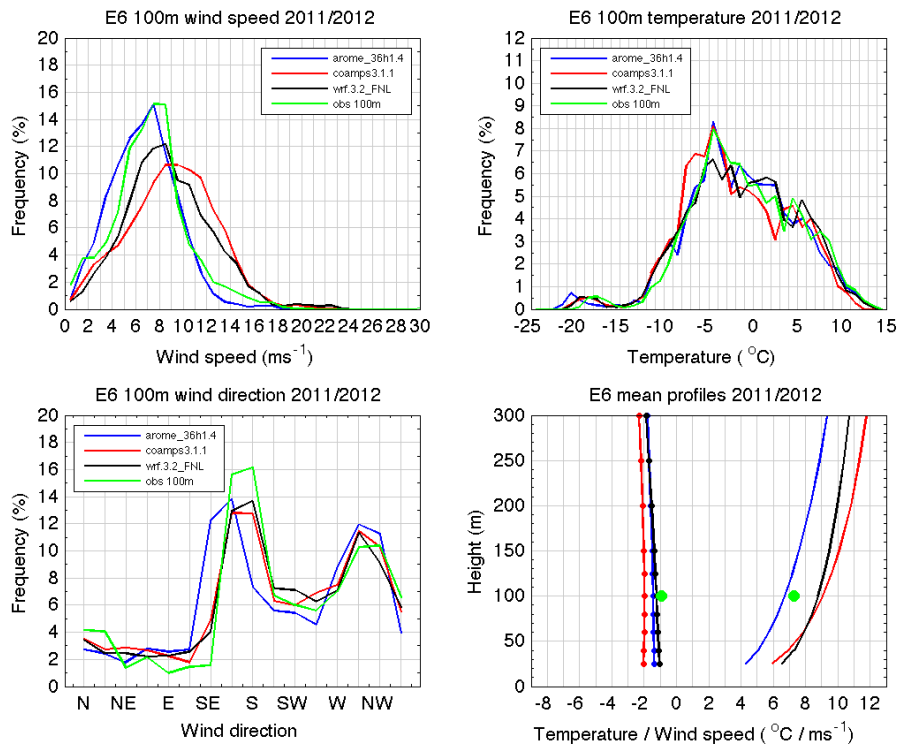


**Figure 4-14: Model results and observations for site E6, winter season 2011/2012. Upper left: wind speed distributions; Upper right: temperature distributions; Lower left: wind direction distributions; Lower right: profiles of mean temperature (solid/dotted) and mean wind speed (solid).**

**Table 4-10: Observation and model statistics and statistical scores for site E6.**

E6 2010/2011											
wind speed											
Data	Mean	Max	Min	Median	Std	MAE	r	RMSE	Bias	Bias Std	PhaseE
arome_36h1.1	6,49	18,04	0,07	6,44	2,92	2,05	0,65	2,64	-0,48	0,31	2,58
coamps3.1.1	8,48	23,63	0,19	8,46	3,83	2,41	0,71	3,16	1,53	0,59	2,70
wrf.3.2_FNL	8,21	21,97	0,18	7,93	3,54	2,19	0,69	2,94	1,25	0,30	2,65
obs100m	6,97	19,70	0,10	7,10	3,24	-	-	-	-	-	-
temperature											
Data	Mean	Max	Min	Median	Std	MAE	r	RMSE	Bias	Bias Std	PhaseE
arome_36h1.1	-3,72	13,90	-19,56	-4,01	6,68	1,16	0,97	1,53	-0,23	0,12	1,51
coamps3.1.1	-4,43	12,49	-19,38	-4,98	6,24	1,27	0,98	1,63	-0,93	0,34	1,29
wrf.3.2_FNL	-4,37	13,39	-20,84	-4,74	6,87	1,29	0,98	1,72	-0,87	0,31	1,45
obs100m	-3,49	15,70	-19,50	-4,10	6,56	-	-	-	-	-	-
pressure											
Data	Mean	Max	Min	Median	Std	MAE	r	RMSE	Bias	Bias Std	PhaseE
arome_36h1.1	928,6	951,2	900,9	929,2	12,14	5,84	1,00	5,92	5,84	0,17	0,97
coamps3.1.1	921,9	945,7	892,1	922,5	12,59	1,13	1,00	1,36	-0,84	0,23	1,05
wrf.3.2_FNL	922,3	945,3	893,6	922,9	12,26	0,81	1,00	1,04	-0,45	0,05	0,93
obs100m	922,7	947,0	895,0	923,0	12,31	-	-	-	-	-	-
E6 2011/2012											
wind speed											
Data	Mean	Max	Min	Median	Std	MAE	r	RMSE	Bias	Bias Std	PhaseE
arome_36h1.4	6,69	20,90	0,10	6,72	2,78	2,01	0,63	2,64	-0,61	0,39	2,54
coamps3.1.1	9,05	22,30	0,16	9,15	3,64	2,55	0,69	3,24	1,74	0,47	2,70
wrf.3.2_FNL	8,78	23,57	0,30	8,46	3,63	2,44	0,66	3,19	1,46	0,46	2,80
obs100m	7,31	20,10	0,10	7,30	3,17	-	-	-	-	-	-
temperature											
Data	Mean	Max	Min	Median	Std	MAE	r	RMSE	Bias	Bias Std	PhaseE
arome_36h1.4	-1,44	13,32	-21,54	-1,65	6,00	1,10	0,97	1,53	-0,50	0,11	1,44
coamps3.1.1	-1,98	11,97	-20,99	-2,70	5,92	1,36	0,97	1,68	-1,04	0,03	1,32
wrf.3.2_FNL	-1,22	13,46	-20,69	-1,30	6,07	1,01	0,98	1,31	-0,28	0,18	1,27
obs100m	-0,94	13,70	-19,30	-1,50	5,89	-	-	-	-	-	-
pressure											
Data	Mean	Max	Min	Median	Std	MAE	r	RMSE	Bias	Bias Std	PhaseE
arome_36h1.4	925,9	964,3	885,2	926,0	15,38	5,81	1,00	5,90	5,81	0,26	0,99
coamps3.1.1	919,5	956,9	876,4	919,7	15,84	1,01	1,00	1,25	-0,67	0,20	1,04
wrf.3.2_FNL	919,8	957,6	878,4	919,9	15,51	0,74	1,00	0,95	-0,26	0,14	0,90
obs100m	920,1	957,0	879,0	920,0	15,64	-	-	-	-	-	-

*Site E7:*

Model results and observations for site E7 are shown in Figure 4-15 and Figure 4-16 for the winter seasons 2010/2011 and 2011/2012. Statistics is summarized in Table 4-11.

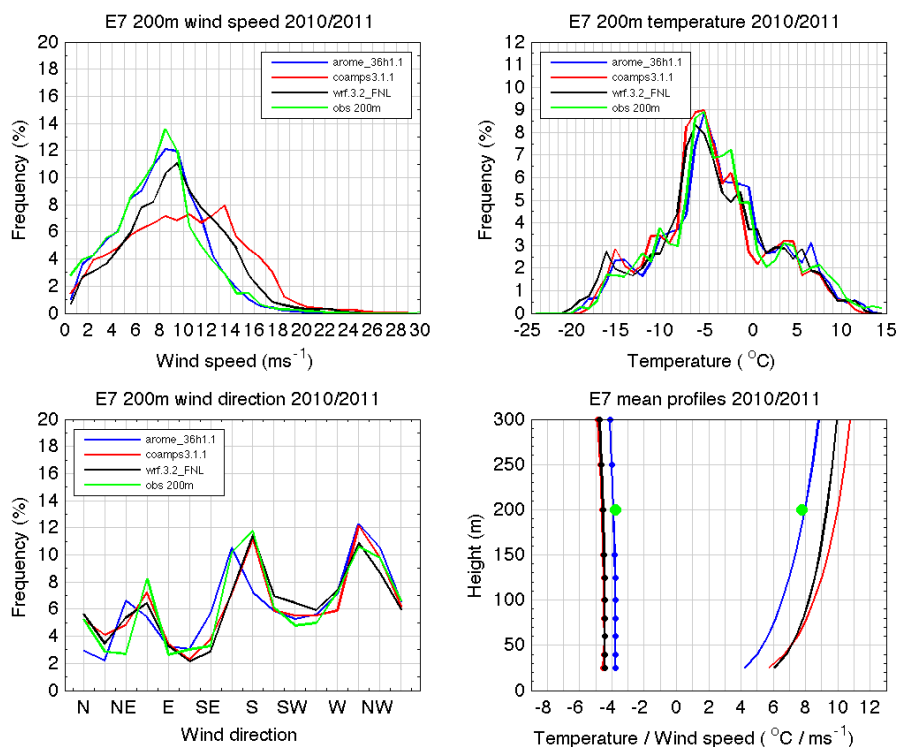


**Figure 4-15: Model results and observations for site E7, winter season 2010/2011. Upper left: wind speed distributions; Upper right: temperature distributions; Lower left: wind direction distributions; Lower right: profiles of mean temperature (solid/dotted) and mean wind speed (solid).**

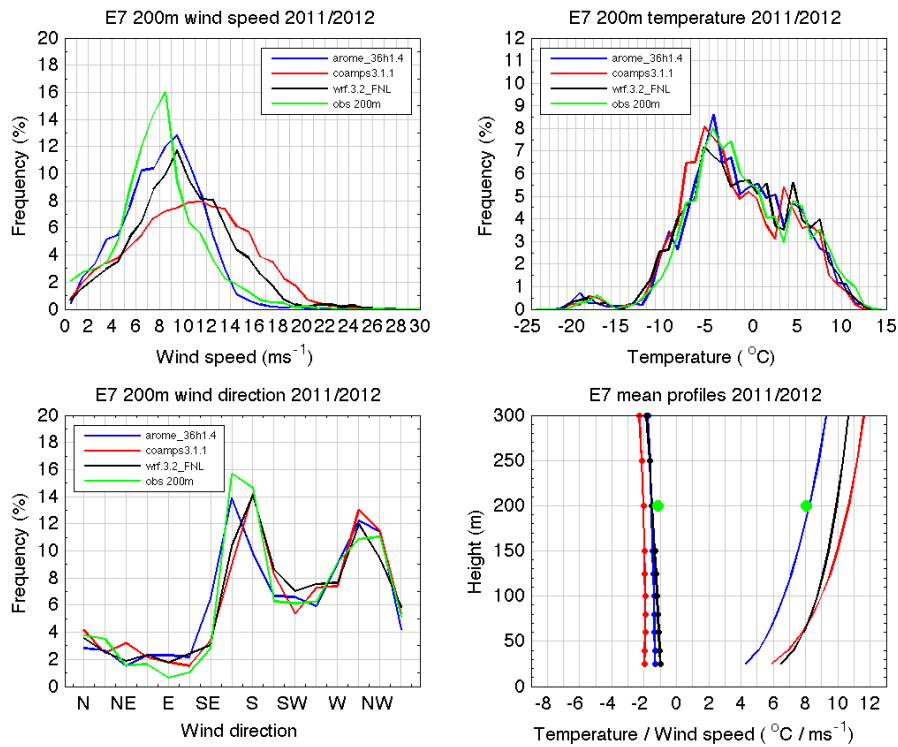


**Figure 4-16: Model results and observations for site E7, winter season 2011/2012. Upper left: wind speed distributions; Upper right: temperature distributions; Lower left: wind direction distributions; Lower right: profiles of mean temperature (solid/dotted) and mean wind speed (solid).**

**Table 4-11: Observation and model statistics and statistical scores for site E7.**

E7 2010/2011											
wind speed											
Data	Mean	Max	Min	Median	Std	MAE	r	RMSE	Bias	Bias Std	PhaseE
arome_36h1.1	7,97	20,47	0,04	8,10	3,45	1,99	0,72	2,65	0,19	0,21	2,64
coamps3.1.1	10,01	28,36	0,08	10,05	4,79	3,02	0,74	3,95	2,24	1,13	3,04
wrf.3.2_FNL	9,33	24,52	0,22	9,27	4,02	2,40	0,73	3,25	1,55	0,36	2,84
obs200m	7,78	23,30	0,10	7,90	3,66	-	-	-	-	-	-
temperature											
Data	Mean	Max	Min	Median	Std	MAE	r	RMSE	Bias	Bias Std	PhaseE
arome_36h1.1	-3,89	13,08	-19,24	-4,36	6,42	1,06	0,98	1,39	-0,11	0,01	1,39
coamps3.1.1	-4,62	11,45	-18,98	-5,17	6,12	1,20	0,98	1,57	-0,83	0,34	1,29
wrf.3.2_FNL	-4,53	12,69	-20,95	-5,00	6,57	1,15	0,98	1,53	-0,74	0,14	1,33
obs200m	-3,79	15,40	-19,70	-4,30	6,44	-	-	-	-	-	-
pressure											
Data	Mean	Max	Min	Median	Std	MAE	r	RMSE	Bias	Bias Std	PhaseE
arome_36h1.1	916,9	939,7	889,5	917,3	12,02	6,07	1,00	6,15	6,07	0,19	0,96
coamps3.1.1	910,2	934,3	881,0	910,6	12,45	0,99	1,00	1,24	-0,56	0,20	1,08
wrf.3.2_FNL	910,6	933,9	882,4	911,0	12,12	0,74	1,00	0,95	-0,19	0,10	0,93
obs200m	910,8	935,0	883,0	911,0	12,21	-	-	-	-	-	-
E7 2011/2012											
wind speed											
Data	Mean	Max	Min	Median	Std	MAE	r	RMSE	Bias	Bias Std	PhaseE
arome_36h1.4	8,26	25,52	0,08	8,44	3,22	2,03	0,68	2,68	0,21	0,23	2,66
coamps3.1.1	10,68	26,22	0,23	10,74	4,67	3,34	0,68	4,32	2,63	1,22	3,21
wrf.3.2_FNL	9,92	27,92	0,08	9,73	4,09	2,74	0,66	3,69	1,87	0,65	3,11
obs200m	8,05	26,70	0,10	7,90	3,45	-	-	-	-	-	-
temperature											
Data	Mean	Max	Min	Median	Std	MAE	r	RMSE	Bias	Bias Std	PhaseE
arome_36h1.4	-1,53	12,61	-21,20	-2,02	5,86	1,07	0,97	1,49	-0,40	0,06	1,44
coamps3.1.1	-2,04	11,38	-20,70	-2,79	5,82	1,24	0,98	1,55	-0,91	0,09	1,25
wrf.3.2_FNL	-1,49	12,60	-20,80	-1,75	6,02	0,95	0,98	1,24	-0,34	0,11	1,18
obs200m	-1,13	13,10	-20,60	-1,80	5,91	-	-	-	-	-	-
pressure											
Data	Mean	Max	Min	Median	Std	MAE	r	RMSE	Bias	Bias Std	PhaseE
arome_36h1.4	914,7	951,9	874,0	914,8	15,04	4,55	1,00	4,68	4,55	0,35	1,06
coamps3.1.1	908,3	944,6	865,3	908,6	15,46	1,90	1,00	2,10	-1,83	0,07	1,04
wrf.3.2_FNL	908,7	945,2	867,4	908,9	15,13	1,53	1,00	1,74	-1,43	0,26	0,95
obs200m	910,1	946,0	869,0	910,0	15,39	-	-	-	-	-	-

Site E8:

Model results and observations for site E8 are shown in Figure 4-17 to Figure 4-19 for the winter seasons 2009/2010, 2010/2011, and 2011/2012. Statistics is summarized in Table 4-12.

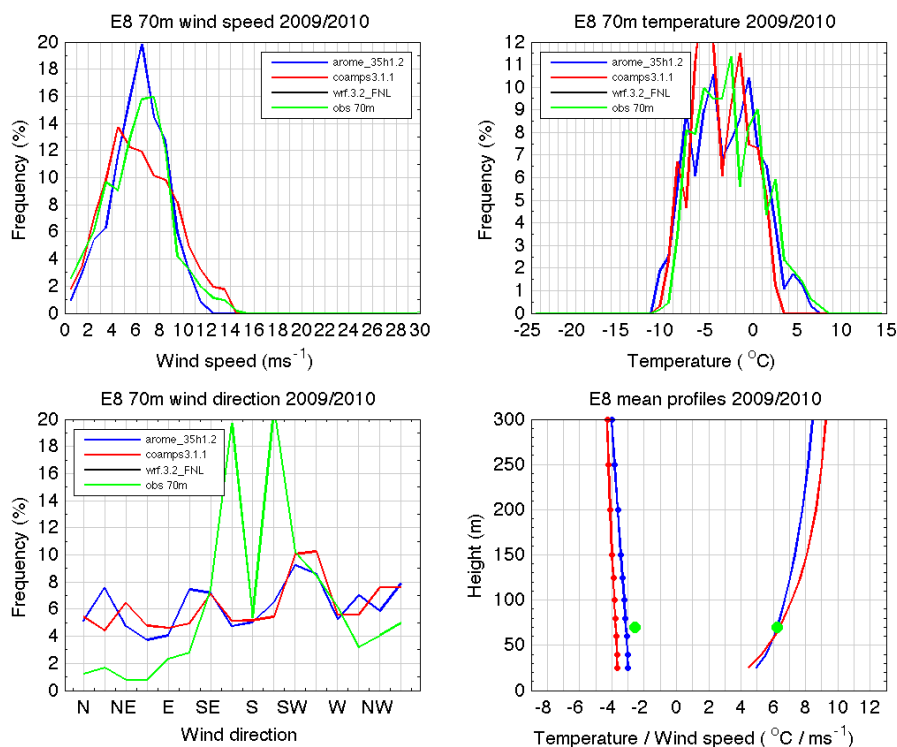


**Figure 4-17: Model results and observations for site E8, winter season 2009/2010. Upper left: wind speed distributions; Upper right: temperature distributions; Lower left: wind direction distributions; Lower right: profiles of mean temperature (solid/dotted) and mean wind speed (solid).**

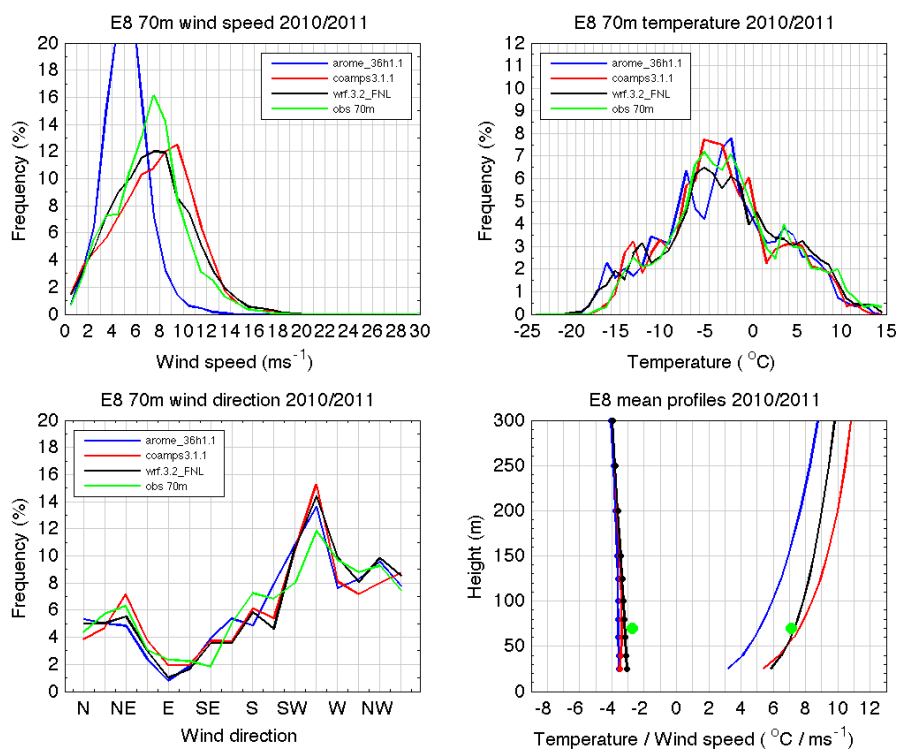


**Figure 4-18: Model results and observations for site E8, winter season 2010/2011. Upper left: wind speed distributions; Upper right: temperature distributions; Lower left: wind direction distributions; Lower right: profiles of mean temperature (solid/dotted) and mean wind speed (solid).**

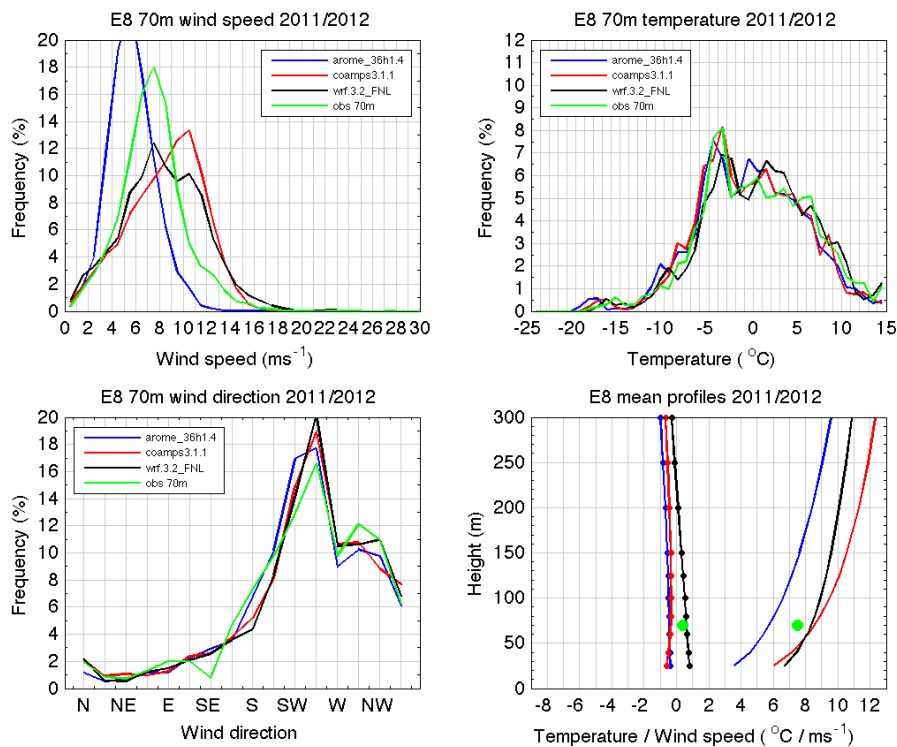


**Figure 4-19: Model results and observations for site E8, winter season 2011/2012. Upper left: wind speed distributions; Upper right: temperature distributions; Lower left: wind direction distributions; Lower right: profiles of mean temperature (solid/dotted) and mean wind speed (solid).**

**Table 4-12: Observation and model statistics and statistical scores for site E8.**

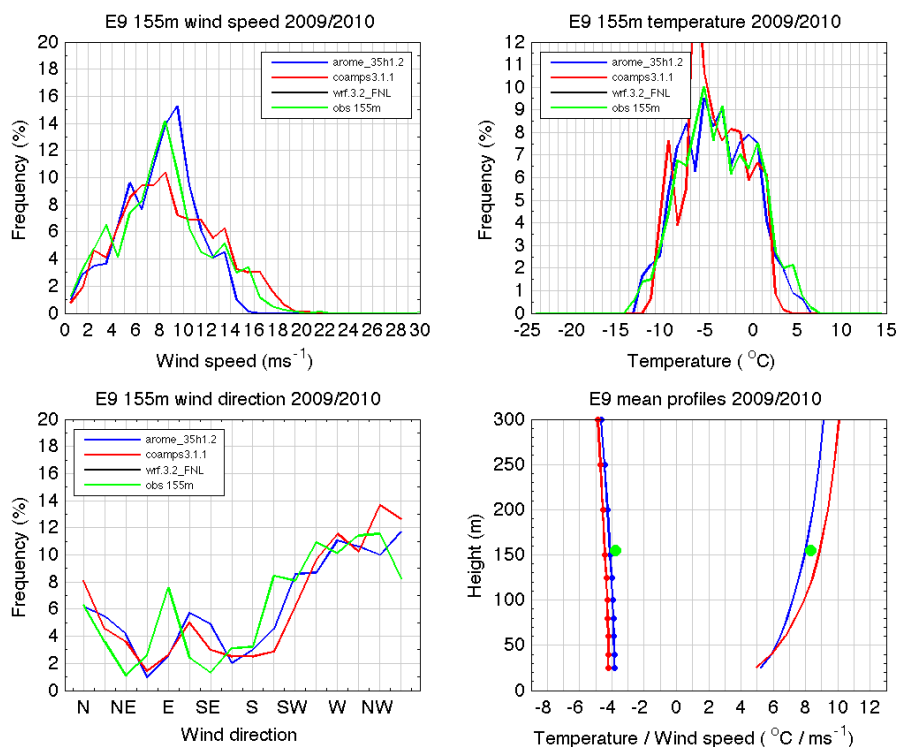
E8 2009/2010											
wind speed											
Data	Mean	Max	Min	Median	Std	MAE	r	RMSE	Bias	Bias Std	PhaseE
arome_35h1.2	6,24	11,61	0,19	6,37	2,22	1,36	0,76	1,73	-0,01	0,44	1,67
coamps3.1.1	6,38	13,94	0,23	6,10	2,90	1,65	0,71	2,11	0,13	0,24	2,10
wrf.3.2_FNL	-	-	-	-	-	-	-	-	-	-	-
obs70m	6,25	14,20	0,50	6,40	2,66	-	-	-	-	-	-
temperature											
Data	Mean	Max	Min	Median	Std	MAE	r	RMSE	Bias	Bias Std	PhaseE
arome_35h1.2	-3,11	6,21	-10,81	-3,08	3,72	1,07	0,94	1,33	-0,53	0,12	1,22
coamps3.1.1	-3,75	2,56	-10,13	-4,21	2,99	1,44	0,92	1,88	-1,16	0,62	1,35
wrf.3.2_FNL	-	-	-	-	-	-	-	-	-	-	-
obs70m	-2,59	8,00	-10,20	-2,90	3,61	-	-	-	-	-	-
pressure											
Data	Mean	Max	Min	Median	Std	MAE	r	RMSE	Bias	Bias Std	PhaseE
arome_35h1.2	905,8	923,4	892,3	905,2	6,74	7,18	0,99	7,21	-7,18	0,07	0,68
coamps3.1.1	909,7	928,4	894,8	909,3	6,97	3,19	0,99	3,28	-3,19	0,16	0,77
wrf.3.2_FNL	-	-	-	-	-	-	-	-	-	-	-
obs70m	912,9	930,0	899,0	912,0	6,81	-	-	-	-	-	-
E8 2010/2011											
wind speed											
Data	Mean	Max	Min	Median	Std	MAE	r	RMSE	Bias	Bias Std	PhaseE
arome_36h1.1	5,17	13,98	0,23	5,15	1,81	2,29	0,75	2,76	-1,96	1,07	1,62
coamps3.1.1	7,60	18,92	0,12	7,81	3,22	1,83	0,73	2,31	0,46	0,33	2,24
wrf.3.2_FNL	7,31	19,69	0,20	7,22	3,26	1,78	0,73	2,30	0,18	0,38	2,26
obs70m	7,13	18,10	0,50	7,20	2,88	-	-	-	-	-	-
temperature											
Data	Mean	Max	Min	Median	Std	MAE	r	RMSE	Bias	Bias Std	PhaseE
arome_36h1.1	-3,59	13,25	-18,56	-3,44	6,62	1,35	0,97	1,80	-0,86	0,20	1,57
coamps3.1.1	-3,39	12,34	-17,93	-3,84	6,14	1,19	0,97	1,59	-0,61	0,28	1,45
wrf.3.2_FNL	-3,18	14,31	-20,24	-3,42	6,83	1,37	0,96	1,89	-0,44	0,41	1,79
obs70m	-2,73	17,10	-17,90	-3,20	6,42	-	-	-	-	-	-
pressure											
Data	Mean	Max	Min	Median	Std	MAE	r	RMSE	Bias	Bias Std	PhaseE
arome_36h1.1	918,5	942,9	886,9	919,3	11,62	1,16	1,00	1,36	-1,05	0,29	0,81
coamps3.1.1	916,6	941,4	883,9	917,4	12,12	2,96	1,00	3,10	-2,96	0,20	0,91
wrf.3.2_FNL	917,0	941,5	884,6	917,7	11,78	2,56	1,00	2,68	-2,55	0,14	0,80
obs70m	919,6	944,0	888,0	920,0	11,92	-	-	-	-	-	-

Table 4-12 **continued.**

E8 2011/2012											
wind speed											
Data	Mean	Max	Min	Median	Std	MAE	r	RMSE	Bias	Bias Std	PhaseE
arome_36h1.4	5,72	18,94	0,18	5,55	1,95	2,16	0,72	2,62	-1,80	0,80	1,74
coamps3.1.1	8,56	23,54	0,13	8,92	3,16	2,14	0,65	2,71	1,05	0,41	2,46
wrf.3.2_FNL	8,34	23,45	0,18	8,24	3,45	2,07	0,68	2,69	0,82	0,69	2,46
obs70m	7,51	27,90	0,50	7,40	2,75	-	-	-	-	-	-
temperature											
Data	Mean	Max	Min	Median	Std	MAE	r	RMSE	Bias	Bias Std	PhaseE
arome_36h1.4	-0,45	15,96	-19,96	-0,46	5,98	1,24	0,97	1,68	-0,83	0,15	1,46
coamps3.1.1	-0,35	15,49	-18,59	-0,60	5,83	1,26	0,97	1,67	-0,73	0,31	1,48
wrf.3.2_FNL	0,64	18,53	-17,87	0,71	6,02	1,19	0,97	1,52	0,27	0,11	1,49
obs70m	0,38	20,50	-18,70	0,10	6,13	-	-	-	-	-	-
pressure											
Data	Mean	Max	Min	Median	Std	MAE	r	RMSE	Bias	Bias Std	PhaseE
arome_36h1.4	917,2	952,2	878,6	918,2	14,85	1,17	1,00	1,39	-0,92	0,44	0,94
coamps3.1.1	915,3	949,6	873,1	916,4	15,38	2,86	1,00	3,04	-2,85	0,09	1,05
wrf.3.2_FNL	915,7	950,1	874,3	916,6	15,01	2,43	1,00	2,60	-2,41	0,29	0,94
obs70m	918,1	952,0	877,0	919,0	15,29	-	-	-	-	-	-

Site E9:

Model results and observations for site E9 are shown in Figure 4-20 to Figure 4-22 for the winter seasons 2009/2010, 2010/2011, and 2011/2012. Statistics is summarized in Table 4-13.



**Figure 4-20: Model results and observations for site E9, winter season 2009/2010. Upper left: wind speed distributions; Upper right: temperature distributions; Lower left: wind direction distributions; Lower right: profiles of mean temperature (solid/dotted) and mean wind speed (solid).**

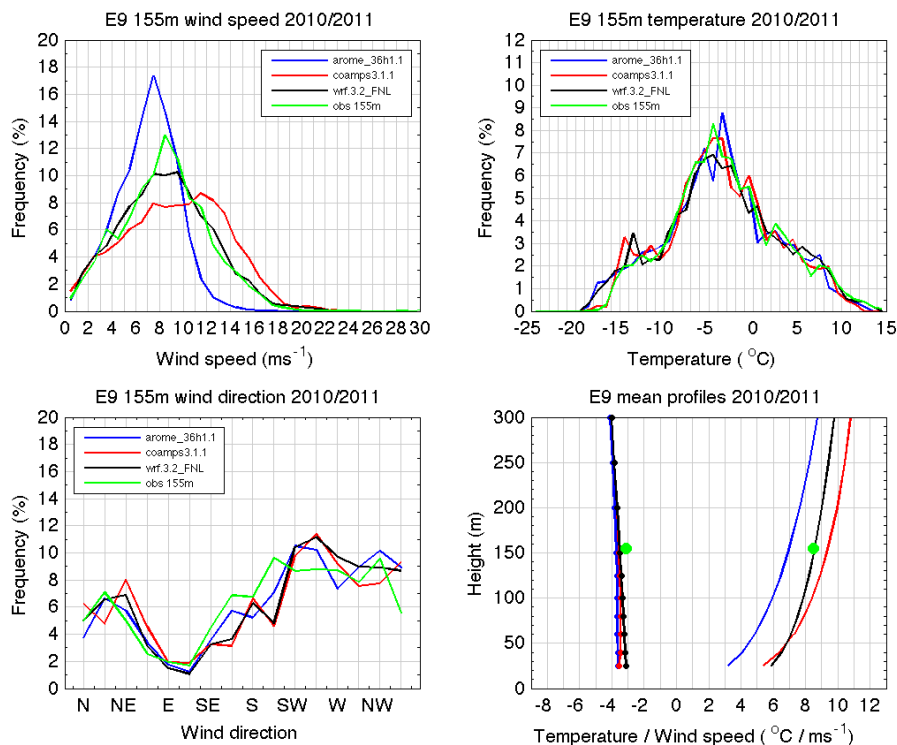


**Figure 4-21: Model results and observations for site E9, winter season 2010/2011. Upper left: wind speed distributions; Upper right: temperature distributions; Lower left: wind direction distributions; Lower right: profiles of mean temperature (solid/dotted) and mean wind speed (solid).**

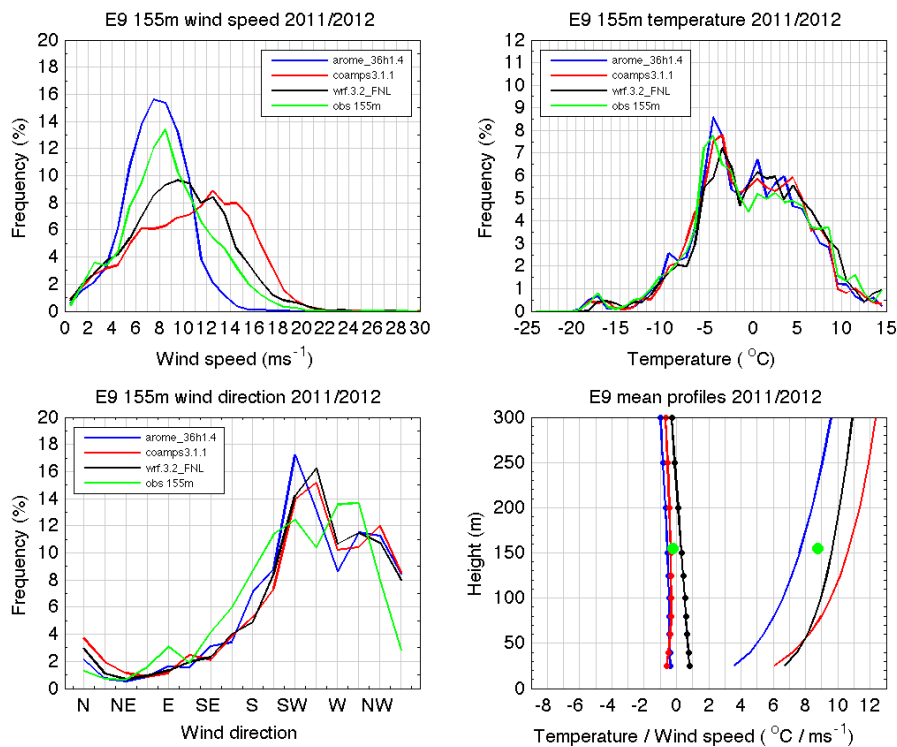


**Figure 4-22: Model results and observations for site E9, winter season 2011/2012. Upper left: wind speed distributions; Upper right: temperature distributions; Lower left: wind direction distributions; Lower right: profiles of mean temperature (solid/dotted) and mean wind speed (solid).**

**Table 4-13: Observation and model statistics and statistical scores for site E9.**

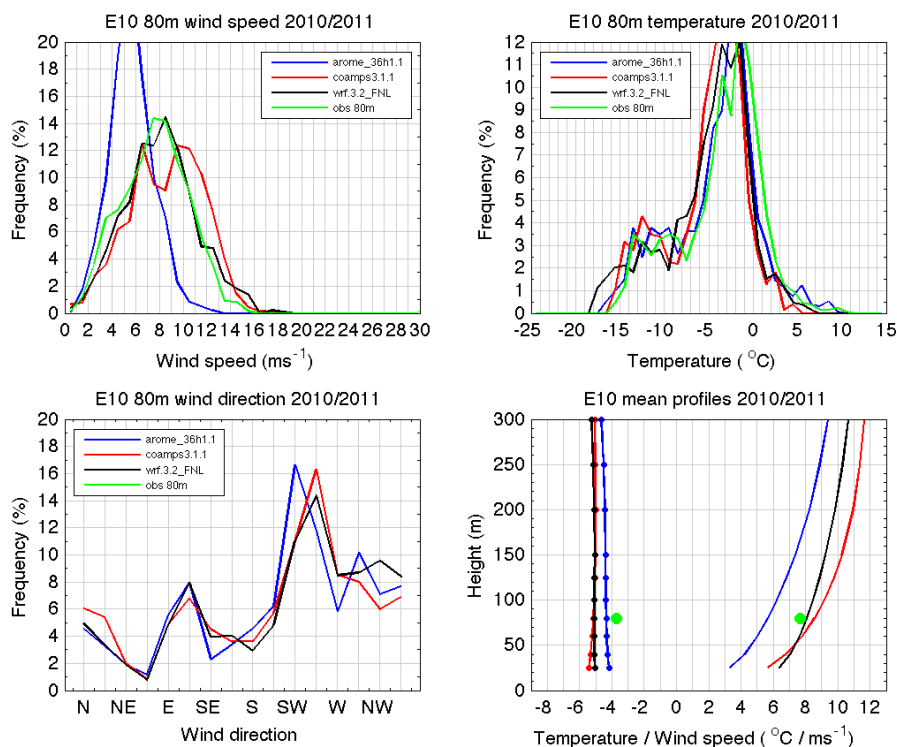
E9 2009/2010											
wind speed											
Data	Mean	Max	Min	Median	Std	MAE	r	RMSE	Bias	Bias Std	PhaseE
arome_35h1.2	8,00	15,48	0,10	8,31	3,06	1,58	0,85	2,03	-0,34	0,76	1,86
coamps3.1.1	8,89	20,83	0,42	8,45	4,05	1,92	0,80	2,53	0,55	0,23	2,46
wrf.3.2_FNL	-	-	-	-	-	-	-	-	-	-	-
obs155m	8,34	21,50	0,40	8,30	3,82	-	-	-	-	-	-
temperature											
Data	Mean	Max	Min	Median	Std	MAE	r	RMSE	Bias	Bias Std	PhaseE
arome_35h1.2	-4,10	5,40	-12,66	-4,21	3,96	1,09	0,94	1,45	-0,33	0,17	1,40
coamps3.1.1	-4,43	3,12	-11,85	-4,75	3,44	1,23	0,93	1,70	-0,66	0,69	1,41
wrf.3.2_FNL	-	-	-	-	-	-	-	-	-	-	-
obs155m	-3,77	6,50	-13,30	-3,90	4,13	-	-	-	-	-	-
pressure											
Data	Mean	Max	Min	Median	Std	MAE	r	RMSE	Bias	Bias Std	PhaseE
arome_35h1.2	898,4	915,9	882,9	897,1	8,36	5,22	1,00	5,26	-5,22	0,18	0,68
coamps3.1.1	902,4	920,2	885,4	901,3	8,64	1,30	1,00	1,49	-1,24	0,11	0,81
wrf.3.2_FNL	-	-	-	-	-	-	-	-	-	-	-
obs155m	903,6	922,0	887,0	902,0	8,54	-	-	-	-	-	-
E9 2010/2011											
wind speed											
Data	Mean	Max	Min	Median	Std	MAE	r	RMSE	Bias	Bias Std	PhaseE
arome_36h1.1	6,99	17,38	0,04	7,21	2,57	2,10	0,80	2,69	-1,49	1,08	1,96
coamps3.1.1	9,39	23,88	0,14	9,55	4,29	2,13	0,80	2,75	0,90	0,63	2,52
wrf.3.2_FNL	8,56	23,40	0,14	8,44	3,86	1,89	0,79	2,46	0,07	0,21	2,45
obs155m	8,49	28,10	0,10	8,50	3,65	-	-	-	-	-	-
temperature											
Data	Mean	Max	Min	Median	Std	MAE	r	RMSE	Bias	Bias Std	PhaseE
arome_36h1.1	-3,71	12,85	-18,55	-3,69	6,34	1,17	0,97	1,60	-0,60	0,20	1,46
coamps3.1.1	-3,56	11,96	-18,31	-3,83	6,08	1,10	0,97	1,52	-0,42	0,06	1,46
wrf.3.2_FNL	-3,51	13,66	-18,83	-3,78	6,59	1,26	0,97	1,76	-0,39	0,46	1,65
obs155m	-3,11	14,80	-18,00	-3,60	6,14	-	-	-	-	-	-
pressure											
Data	Mean	Max	Min	Median	Std	MAE	r	RMSE	Bias	Bias Std	PhaseE
arome_36h1.1	908,6	933,0	877,4	909,2	11,55	1,02	1,00	1,26	0,80	0,36	0,91
coamps3.1.1	906,7	931,4	874,4	907,3	12,03	1,26	1,00	1,47	-1,09	0,12	0,98
wrf.3.2_FNL	907,1	931,5	875,2	907,6	11,70	0,93	1,00	1,14	-0,69	0,22	0,88
obs155m	907,8	932,0	877,0	908,0	11,91	-	-	-	-	-	-

Table 4-13 **continued.**

E9 2011/2012											
wind speed											
Data	Mean	Max	Min	Median	Std	MAE	r	RMSE	Bias	Bias Std	PhaseE
arome_36h1.4	7,71	23,61	0,08	7,76	2,59	2,28	0,69	2,83	-1,08	1,01	2,42
coamps3.1.1	10,69	30,08	0,13	11,10	4,44	3,02	0,67	3,87	1,90	0,85	3,27
wrf.3.2_FNL	9,66	27,52	0,10	9,65	4,07	2,50	0,67	3,27	0,88	0,47	3,12
obs155m	8,78	32,10	0,20	8,60	3,60	-	-	-	-	-	-
temperature											
Data	Mean	Max	Min	Median	Std	MAE	r	RMSE	Bias	Bias Std	PhaseE
arome_36h1.4	-0,56	15,28	-19,30	-0,63	5,84	1,00	0,98	1,44	-0,35	0,47	1,32
coamps3.1.1	-0,34	15,91	-19,02	-0,48	5,82	1,06	0,98	1,44	-0,14	0,49	1,35
wrf.3.2_FNL	0,30	17,87	-18,52	0,34	6,02	1,18	0,98	1,49	0,51	0,30	1,37
obs155m	-0,20	19,40	-19,30	-0,50	6,31	-	-	-	-	-	-
pressure											
Data	Mean	Max	Min	Median	Std	MAE	r	RMSE	Bias	Bias Std	PhaseE
arome_36h1.4	908,8	932,3	873,2	908,8	11,91	1,33	0,99	1,93	0,55	0,62	1,75
coamps3.1.1	907,1	930,8	869,2	907,2	12,29	1,73	0,99	1,99	-1,07	0,24	1,66
wrf.3.2_FNL	907,3	931,4	870,0	907,2	12,03	1,73	0,99	2,00	-0,86	0,51	1,73
obs155m	908,2	933,0	873,0	909,0	12,53	-	-	-	-	-	-

Site E10:

Model results and observations for site E10 are shown in Figure 4-23 and Figure 4-24 for the winter seasons 2010/2011 and 2011/2012. Statistics is summarized in Table 4-14.



**Figure 4-23: Model results and observations for site E10, winter season 2010/2011. Upper left: wind speed distributions; Upper right: temperature distributions; Lower left: wind direction distributions; Lower right: profiles of mean temperature (solid/dotted) and mean wind speed (solid).**

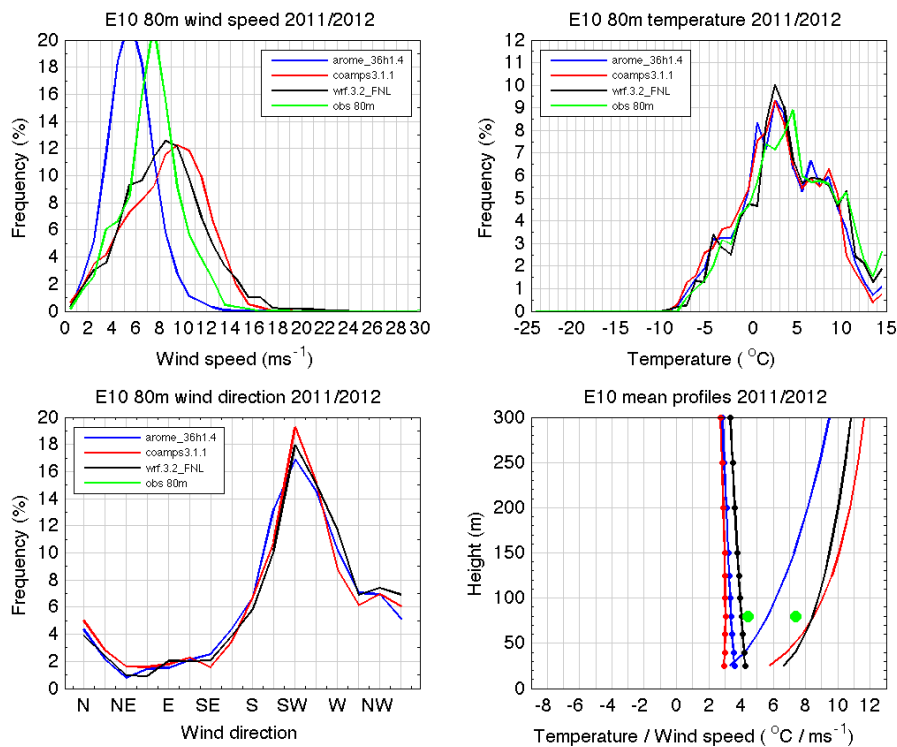


**Figure 4-24: Model results and observations for site E10, winter season 2011/2012. Upper left: wind speed distributions; Upper right: temperature distributions; Lower left: wind direction distributions; Lower right: profiles of mean temperature (solid/dotted) and mean wind speed (solid).**

**Table 4-14: Observation and model statistics and statistical scores for site E10.**

E10 2010/2011												
wind speed												
Data	Mean	Max	Min	Median	Std	MAE	r	RMSE	Bias	Bias Std	PhaseE	
arome_36h1.1	5,65	12,32	0,17	5,56	1,84	2,19	0,80	2,62	-1,99	0,93	1,43	
coamps3.1.1	8,56	17,16	0,36	8,75	3,08	1,81	0,76	2,22	0,91	0,30	2,01	
wrf.3.2_FNL	8,10	18,57	0,56	8,09	2,98	1,49	0,79	1,92	0,46	0,20	1,86	
obs80m	7,65	15,30	0,70	7,80	2,77	-	-	-	-	-	-	
temperature												
Data	Mean	Max	Min	Median	Std	MAE	r	RMSE	Bias	Bias Std	PhaseE	
arome_36h1.1	-4,35	9,25	-16,10	-3,17	4,82	1,18	0,95	1,61	-0,61	0,15	1,49	
coamps3.1.1	-5,15	4,84	-15,89	-4,11	4,25	1,68	0,94	2,10	-1,42	0,41	1,49	
wrf.3.2_FNL	-5,07	6,46	-17,95	-3,97	4,76	1,68	0,92	2,29	-1,33	0,09	1,86	
obs80m	-3,74	10,20	-15,70	-2,80	4,67	-	-	-	-	-	-	
pressure												
Data	Mean	Max	Min	Median	Std	MAE	r	RMSE	Bias	Bias Std	PhaseE	
arome_36h1.1	943,9	962,3	913,1	945,3	10,39	2,89	1,00	3,01	2,89	0,34	0,78	
coamps3.1.1	943,4	962,6	911,9	945,0	10,78	2,37	1,00	2,51	2,36	0,05	0,88	
wrf.3.2_FNL	944,0	962,7	913,5	945,5	10,46	2,96	1,00	3,08	2,96	0,27	0,78	
obs80m	941,0	961,0	910,0	942,0	10,74	-	-	-	-	-	-	
E10 2011/2012												
wind speed												
Data	Mean	Max	Min	Median	Std	MAE	r	RMSE	Bias	Bias Std	PhaseE	
arome_36h1.4	5,65	16,36	0,47	5,55	1,99	2,11	0,67	2,54	-1,75	0,45	1,79	
coamps3.1.1	8,52	20,07	0,19	8,82	3,24	2,08	0,68	2,63	1,13	0,79	2,24	
wrf.3.2_FNL	8,44	23,27	0,12	8,40	3,35	1,95	0,69	2,65	1,05	0,90	2,26	
obs80m	7,39	18,30	0,50	7,45	2,45	-	-	-	-	-	-	
temperature												
Data	Mean	Max	Min	Median	Std	MAE	r	RMSE	Bias	Bias Std	PhaseE	
arome_36h1.4	3,39	16,80	-8,72	3,21	4,82	1,31	0,96	1,73	-1,05	0,26	1,35	
coamps3.1.1	3,04	15,56	-8,71	2,93	4,79	1,67	0,95	2,11	-1,40	0,30	1,55	
wrf.3.2_FNL	4,04	17,52	-9,66	3,69	4,96	1,00	0,97	1,34	-0,39	0,13	1,27	
obs80m	4,44	19,60	-7,90	4,20	5,09	-	-	-	-	-	-	
pressure												
Data	Mean	Max	Min	Median	Std	MAE	r	RMSE	Bias	Bias Std	PhaseE	
arome_36h1.4	941,8	965,0	897,3	943,6	12,43	2,78	1,00	2,91	2,78	0,33	0,81	
coamps3.1.1	941,6	964,8	895,7	943,5	12,91	2,50	1,00	2,66	2,49	0,15	0,92	
wrf.3.2_FNL	941,8	965,4	896,9	943,6	12,60	2,71	1,00	2,82	2,71	0,18	0,77	
obs80m	939,1	963,0	894,0	941,0	12,76	-	-	-	-	-	-	

Site E11:

Model results and observations for site E11 are shown in Figure 4-25 to Figure 4-26 for the winter seasons 2010/2011 and 2011/2012. Statistics is summarized in Table 4-15.

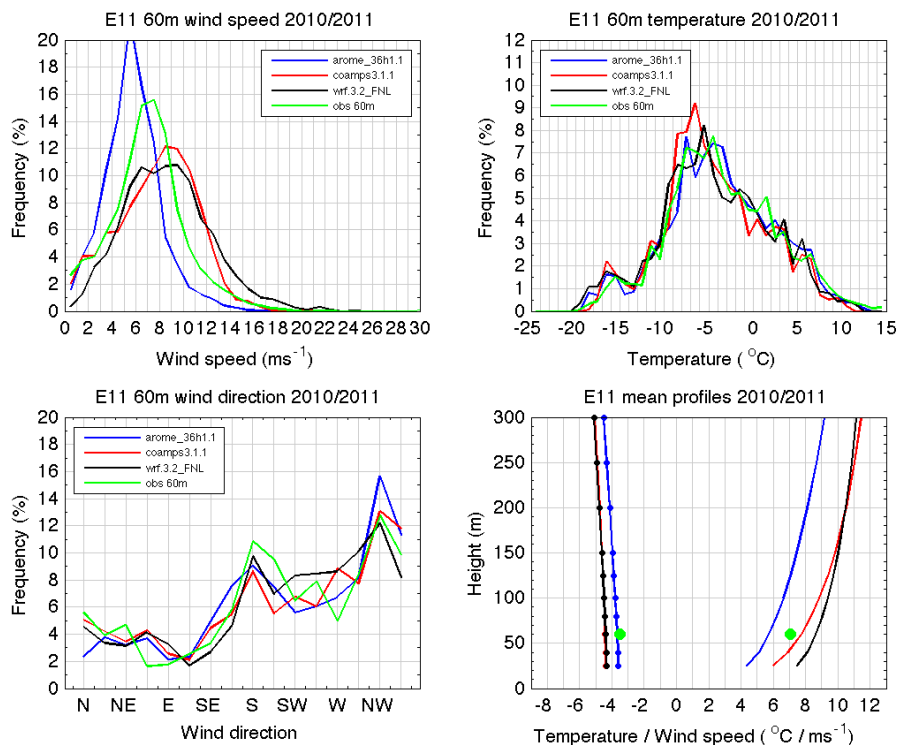


**Figure 4-25: Model results and observations for site E11, winter season 2010/2011. Upper left: wind speed distributions; Upper right: temperature distributions; Lower left: wind direction distributions; Lower right: profiles of mean temperature (solid/dotted) and mean wind speed (solid).**

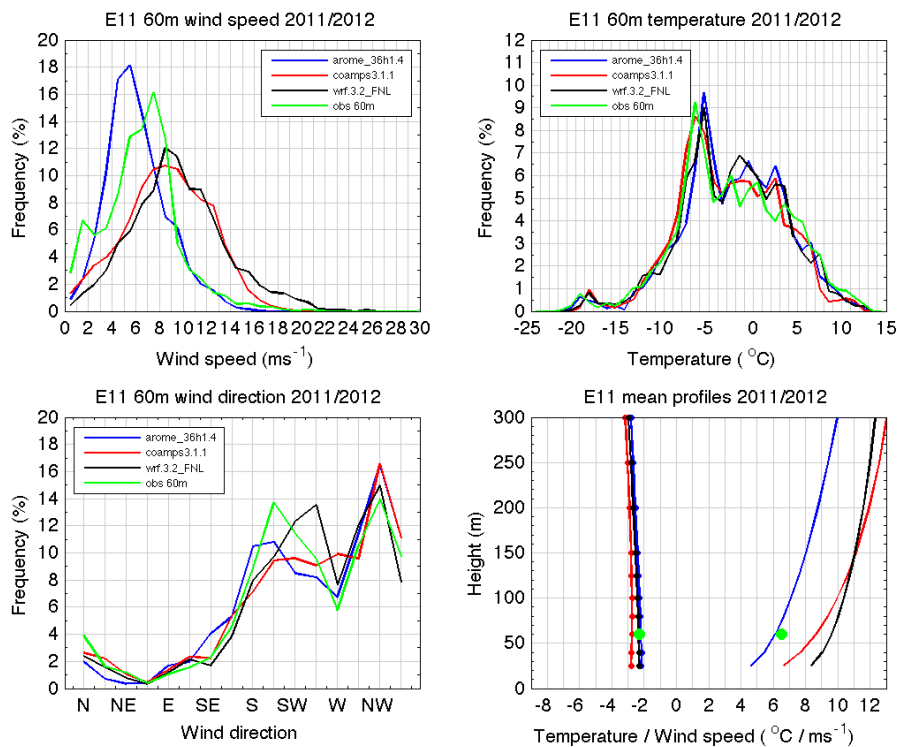


**Figure 4-26: Model results and observations for site E11, winter season 2011/2012. Upper left: wind speed distributions; Upper right: temperature distributions; Lower left: wind direction distributions; Lower right: profiles of mean temperature (solid/dotted) and mean wind speed (solid).**

**Table 4-15: Observation and model statistics and statistical scores for site 11.**

E11 2010/2011											
wind speed											
Data	Mean	Max	Min	Median	Std	MAE	r	RMSE	Bias	Bias Std	PhaseE
arome_36h1.1	5,74	17,92	0,05	5,62	2,38	1,81	0,81	2,27	-1,30	0,75	1,70
coamps3.1.1	7,75	20,39	0,11	8,07	3,34	2,08	0,70	2,60	0,70	0,21	2,50
wrf.3.2_FNL	8,65	24,36	0,25	8,44	3,64	2,14	0,78	2,80	1,60	0,51	2,23
obs60m	7,05	22,60	0,10	7,10	3,13	-	-	-	-	-	-
temperature											
Data	Mean	Max	Min	Median	Std	MAE	r	RMSE	Bias	Bias Std	PhaseE
arome_36h1.1	-3,66	12,73	-19,14	-3,97	6,07	1,13	0,97	1,47	-0,18	0,01	1,46
coamps3.1.1	-4,41	10,88	-18,30	-5,06	5,75	1,18	0,98	1,54	-0,76	0,28	1,31
wrf.3.2_FNL	-4,37	11,74	-19,64	-4,80	6,19	1,22	0,97	1,65	-0,88	0,12	1,39
obs60m	-3,48	16,40	-19,40	-4,10	6,06	-	-	-	-	-	-
pressure											
Data	Mean	Max	Min	Median	Std	MAE	r	RMSE	Bias	Bias Std	PhaseE
arome_36h1.1	892,4	916,7	862,2	892,3	11,41	5,19	1,00	5,27	5,19	0,33	0,82
coamps3.1.1	886,9	911,8	856,1	887,1	11,88	0,72	1,00	0,93	0,00	0,14	0,92
wrf.3.2_FNL	887,4	911,7	857,2	887,4	11,56	0,67	1,00	0,84	0,29	0,18	0,77
obs60m	887,2	912,0	857,0	887,0	11,74	-	-	-	-	-	-
E11 2011/2012											
wind speed											
Data	Mean	Max	Min	Median	Std	MAE	r	RMSE	Bias	Bias Std	PhaseE
arome_36h1.4	6,13	16,43	0,12	5,75	2,54	2,02	0,62	2,58	-0,38	0,61	2,47
coamps3.1.1	8,66	20,12	0,16	8,71	3,57	2,98	0,53	3,91	2,15	0,41	3,24
wrf.3.2_FNL	9,61	25,56	0,18	9,31	3,95	3,39	0,61	4,45	3,09	0,79	3,10
obs60m	6,51	22,00	0,10	6,60	3,15	-	-	-	-	-	-
temperature											
Data	Mean	Max	Min	Median	Std	MAE	r	RMSE	Bias	Bias Std	PhaseE
arome_36h1.4	-2,20	12,36	-20,67	-2,16	5,67	1,04	0,98	1,39	0,11	0,48	1,30
coamps3.1.1	-2,75	12,03	-19,26	-3,02	5,61	1,14	0,97	1,52	-0,45	0,55	1,35
wrf.3.2_FNL	-2,34	12,67	-20,46	-2,24	5,71	1,04	0,98	1,36	-0,02	0,44	1,29
obs60m	-2,30	12,60	-21,30	-2,70	6,15	-	-	-	-	-	-
pressure											
Data	Mean	Max	Min	Median	Std	MAE	r	RMSE	Bias	Bias Std	PhaseE
arome_36h1.4	892,4	924,8	853,7	893,6	14,51	4,83	1,00	4,92	4,83	0,28	0,87
coamps3.1.1	886,9	918,7	844,7	888,5	14,91	1,20	0,99	1,89	-0,74	0,12	1,74
wrf.3.2_FNL	887,5	919,1	846,2	888,6	14,68	0,62	1,00	0,80	-0,05	0,12	0,79
obs60m	887,6	920,0	848,0	889,0	14,79	-	-	-	-	-	-

Site E12:

Model results and observations for site E12 are shown in Figure 4-27 for the winter season 2011/2012. Statistics is summarized in Table 4-16.

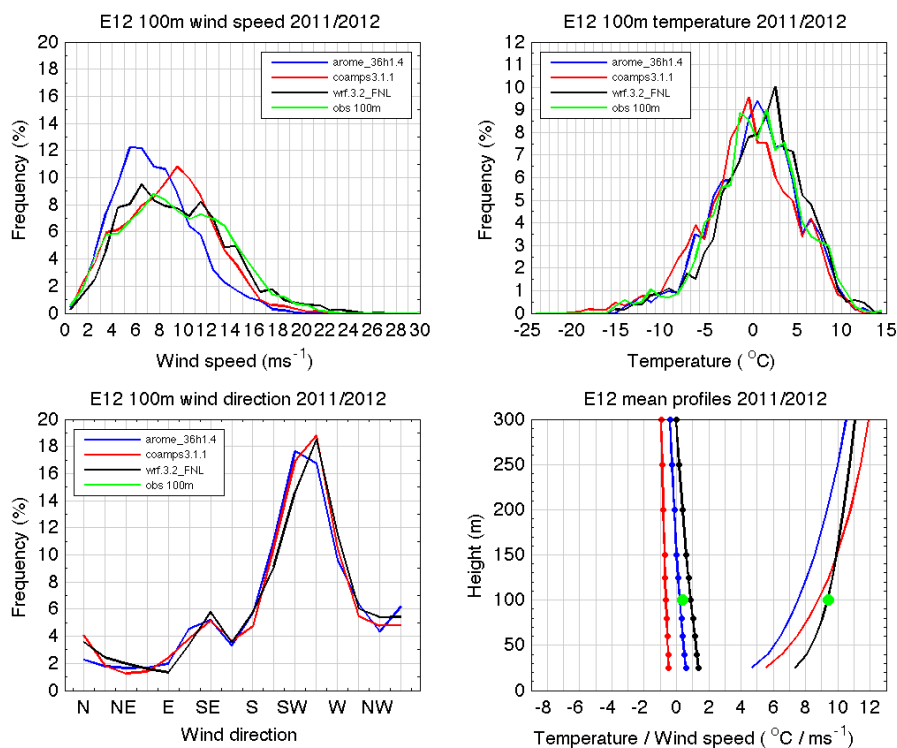


**Figure 4-27: Model results and observations for site E12, winter season 2011/2012. Upper left: wind speed distributions; Upper right: temperature distributions; Lower left: wind direction distributions; Lower right: profiles of mean temperature (solid/dotted) and mean wind speed (solid).**

**Table 4-16: Observation and model statistics and statistical scores for site E12.**

E12 2011/2012												
wind speed												
Data	Mean	Max	Min	Median	Std	MAE	r	RMSE	Bias	Bias Std	PhaseE	
arome_36h1.4	7,55	19,51	0,18	7,20	3,31	2,23	0,89	2,74	-1,84	1,00	1,77	
coamps3.1.1	8,79	21,68	0,26	8,86	3,76	1,99	0,82	2,56	-0,60	0,56	2,42	
wrf.3.2_FNL	9,37	26,06	0,25	8,97	4,31	1,62	0,88	2,09	-0,03	0,01	2,09	
obs100m	9,39	22,60	0,40	9,10	4,32	-	-	-	-	-	-	-
temperature												
Data	Mean	Max	Min	Median	Std	MAE	r	RMSE	Bias	Bias Std	PhaseE	
arome_36h1.4	0,22	12,92	-14,95	0,46	4,80	0,73	0,98	1,00	-0,18	0,15	0,98	
coamps3.1.1	-0,64	11,57	-20,77	-0,45	5,19	1,37	0,96	1,73	-1,04	0,24	1,37	
wrf.3.2_FNL	0,90	13,89	-15,93	1,33	4,82	1,01	0,97	1,31	0,50	0,13	1,20	
obs100m	0,40	15,20	-15,90	0,50	4,95	-	-	-	-	-	-	-
pressure												
Data	Mean	Max	Min	Median	Std	MAE	r	RMSE	Bias	Bias Std	PhaseE	
arome_36h1.4	966,0	997,0	921,5	967,2	14,50	1,32	1,00	1,62	-0,59	0,79	1,29	
coamps3.1.1	965,7	997,2	917,9	967,2	14,97	1,57	0,99	1,91	-0,94	0,32	1,63	
wrf.3.2_FNL	966,0	997,1	919,4	967,3	14,63	1,27	1,00	1,57	-0,62	0,66	1,28	
obs100m	966,6	1000,0	922,0	968,0	15,29	-	-	-	-	-	-	-

Site E13:

Model results and observations for site E13 are shown in Figure 4-28 for the winter season 2011/2012. Statistics is summarized in Table 4-17.

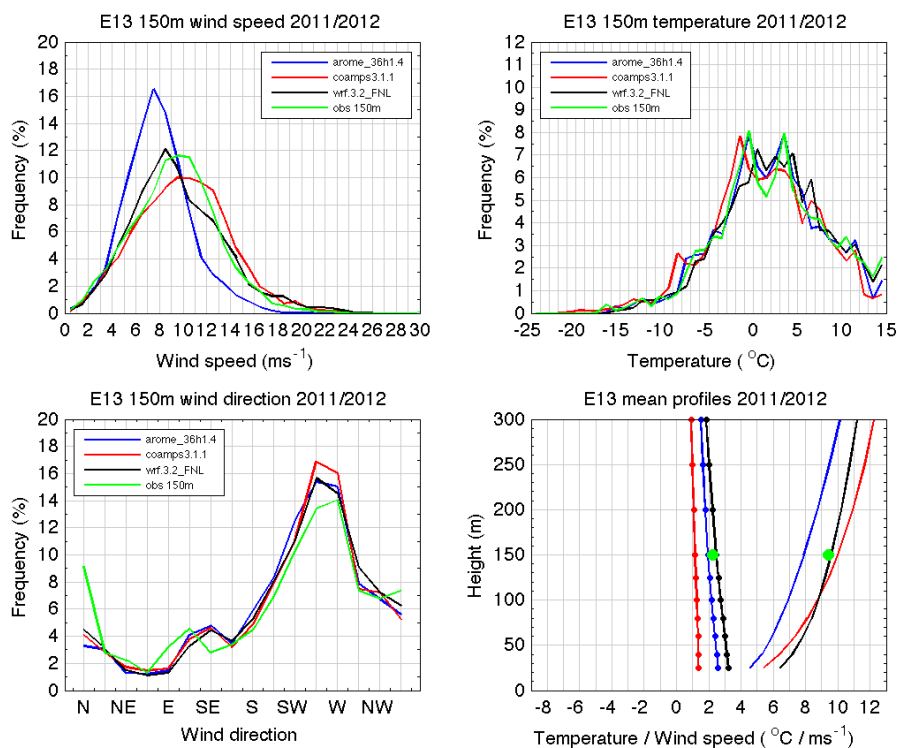


**Figure 4-28: Model results and observations for site E13, winter season 2011/2012. Upper left: wind speed distributions; Upper right: temperature distributions; Lower left: wind direction distributions; Lower right: profiles of mean temperature (solid/dotted) and mean wind speed (solid).**

**Table 4-17: Observation and model statistics and statistical scores for site E13.**

E13 2011/2012												
wind speed												
Data	Mean	Max	Min	Median	Std	MAE	r	RMSE	Bias	Bias Std	PhaseE	
arome_36h1.4	7,90	20,17	0,16	7,74	2,79	1,97	0,85	2,42	-1,53	0,79	1,71	
coamps3.1.1	9,99	24,28	0,03	9,96	3,85	1,72	0,84	2,22	0,56	0,27	2,13	
wrf.3.2_FNL	9,59	25,36	0,41	9,13	3,93	1,66	0,85	2,11	0,16	0,36	2,07	
obs150m	9,43	23,30	0,20	9,40	3,57	-	-	-	-	-	-	-
temperature												
Data	Mean	Max	Min	Median	Std	MAE	r	RMSE	Bias	Bias Std	PhaseE	
arome_36h1.4	1,97	18,78	-16,14	1,97	5,89	0,83	0,98	1,19	-0,28	0,34	1,11	
coamps3.1.1	1,18	15,93	-21,43	1,19	6,05	1,40	0,97	1,80	-1,07	0,18	1,43	
wrf.3.2_FNL	2,48	19,65	-15,94	2,46	5,92	0,95	0,98	1,24	0,23	0,31	1,18	
obs150m	2,25	20,80	-17,10	2,20	6,23	-	-	-	-	-	-	-
pressure												
Data	Mean	Max	Min	Median	Std	MAE	r	RMSE	Bias	Bias Std	PhaseE	
arome_36h1.4	955,6	977,0	915,7	956,9	10,61	2,51	0,99	2,76	-2,46	0,21	1,24	
coamps3.1.1	955,9	977,3	914,8	957,1	10,64	2,24	0,99	2,48	-2,14	0,19	1,24	
wrf.3.2_FNL	955,8	977,3	916,6	957,0	10,61	2,35	0,99	2,58	-2,30	0,21	1,14	
obs150m	958,1	981,0	918,0	959,0	10,83	-	-	-	-	-	-	-

Site E14:

Model results and observations for site E14 are shown in Figure 4-29 for the winter season 2011/2012. Statistics is summarized in Table 4-18.

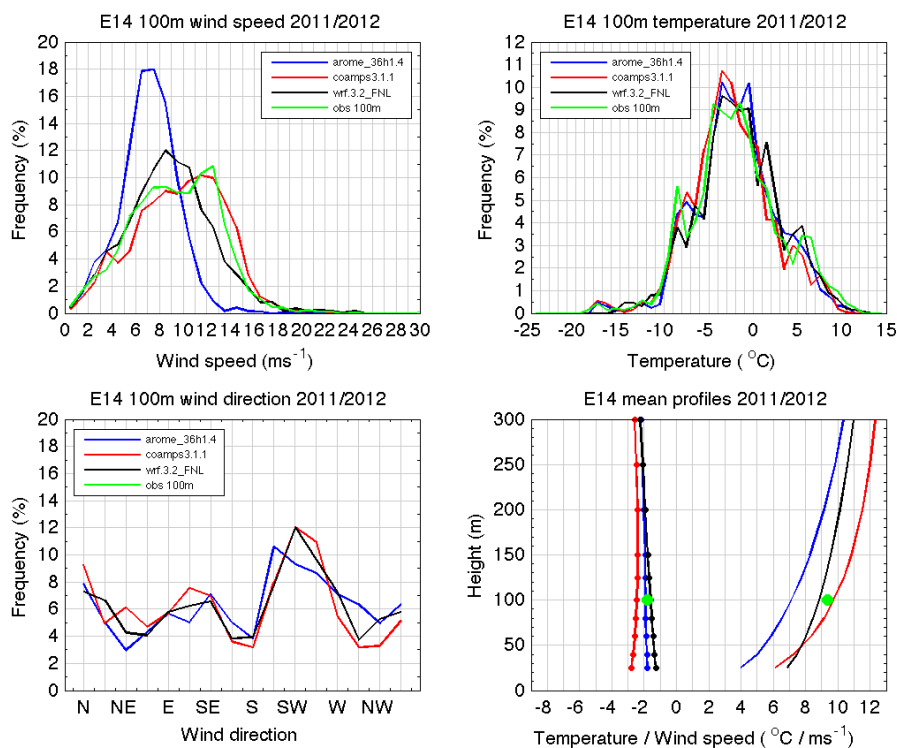


**Figure 4-29: Model results and observations for site E14, winter season 2011/2012. Upper left: wind speed distributions; Upper right: temperature distributions; Lower left: wind direction distributions; Lower right: profiles of mean temperature (solid/dotted) and mean wind speed (solid).**

**Table 4-18: Observation and model statistics and statistical scores for site E14.**

E14 2011/2012												
wind speed												
Data	Mean	Max	Min	Median	Std	MAE	r	RMSE	Bias	Bias Std	PhaseE	
arome_36h1.4	7,12	20,01	0,35	7,19	2,39	2,59	0,82	3,11	-2,22	1,26	1,77	
coamps3.1.1	9,74	22,70	0,15	9,99	3,67	1,74	0,82	2,23	0,40	0,02	2,19	
wrf.3.2_FNL	8,85	24,83	0,16	8,81	3,62	1,72	0,83	2,19	-0,49	0,03	2,13	
obs100m	9,34	24,10	0,10	9,50	3,65	-	-	-	-	-	-	-
temperature												
Data	Mean	Max	Min	Median	Std	MAE	r	RMSE	Bias	Bias Std	PhaseE	
arome_36h1.4	-1,90	10,70	-17,83	-1,97	4,55	0,90	0,97	1,18	-0,09	0,43	1,10	
coamps3.1.1	-2,44	10,48	-18,45	-2,65	4,57	1,25	0,95	1,61	-0,63	0,40	1,43	
wrf.3.2_FNL	-1,58	12,26	-15,87	-1,76	4,64	1,01	0,97	1,31	0,23	0,34	1,24	
obs100m	-1,82	11,60	-18,40	-2,10	4,98	-	-	-	-	-	-	-
pressure												
Data	Mean	Max	Min	Median	Std	MAE	r	RMSE	Bias	Bias Std	PhaseE	
arome_36h1.4	935,4	958,3	894,7	936,4	11,87	0,97	1,00	1,20	-0,22	0,48	1,07	
coamps3.1.1	933,8	956,2	891,2	934,7	12,32	2,00	0,99	2,26	-1,83	0,03	1,32	
wrf.3.2_FNL	935,7	958,6	893,1	936,7	12,01	0,98	1,00	1,23	0,08	0,34	1,18	
obs100m	935,6	960,0	894,0	937,0	12,35	-	-	-	-	-	-	-

#### 4.2.2 Ice load data

Ice load calculations have been performed using the Makkonen ice accretion equation for all three models on a monthly basis for all three seasons and the modelled ice load is compared to the observed ice load where available. There are no WRF-data available for the first season. The Makkonen equation is originally designed to only take liquid cloud water into account, however it has been seen during the project that only using the modelled cloud water the ice loads are much underestimated. Looking at the webcam images from the sites it is evident that there is often a mix of liquid and frozen particles that builds the ice formations on the instruments and masts. To take this effect into account the different species of water in the cloud are fed separately in to the equations using different concentrations. The equations for calculating number concentrations for cloud ice, rain, snow and graupel have been taken from the AROME microphysics scheme. A function to calculate median volume droplet diameter for cloud water from the Thompson microphysics scheme has been used. It is not clear how well the Makkonen model work for frozen particles so the results shown are a bit uncertain. Further research is needed on how the accretion behaves when there is a mixture of liquid and frozen particles in the air. Below, some examples of the modelled ice loads from all three models, compared to the observed loads, are shown. Three stations, one for each area defined in Section 3, are chosen to illustrate the models capacity to model ice load. The months chosen are from the season 2011/2012. There are two modelled ice load curves, one with only liquid cloud water and the other with all species included. In Appendix A summary tables of all the verification statistics are presented. In the tables the number of ice hours is referred to as hours with an ice growth rate larger than 10 grams/hour.

The first example is from the southernmost site E13 that experienced some icing events during February 2012. The observed ice loads comes from the smoothed time series described in chapter 3.

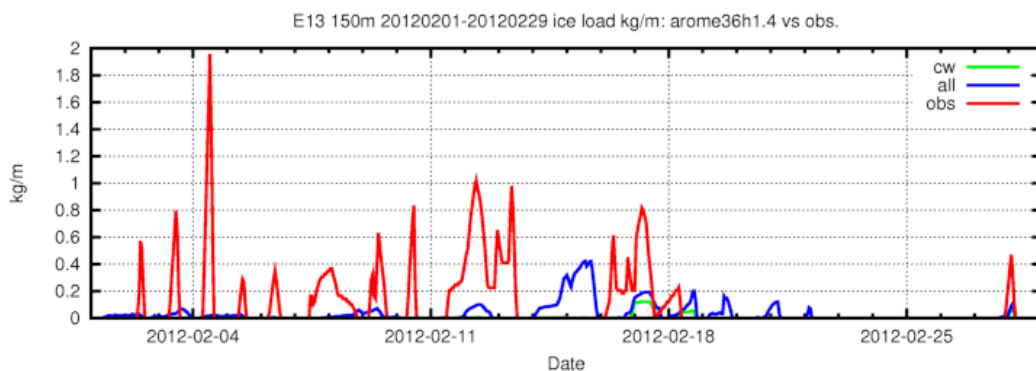


**Figure 4-30: Time series of observed (red) and AROME modelled (cloudwater only green, all condensates blue) ice load kg/m for site E13 February 2012.**

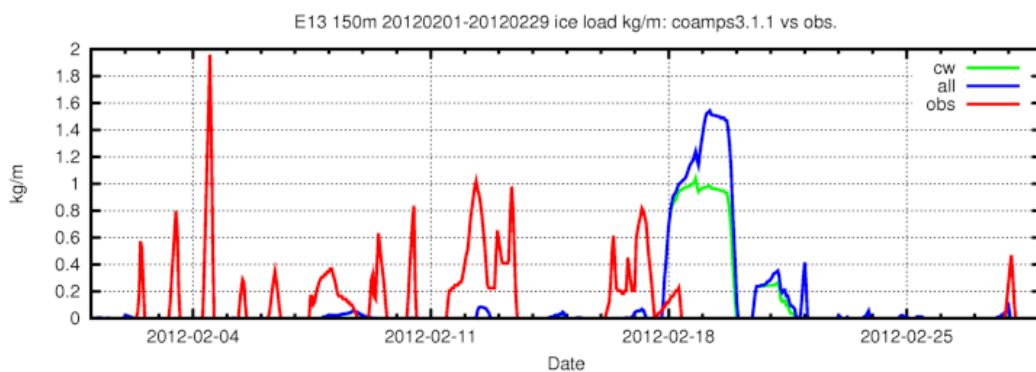


**Figure 4-31: Time series of observed (red) and COAMPS modelled (cloudwater only green, all condensates blue) ice load kg/m for site E13 February 2012.**

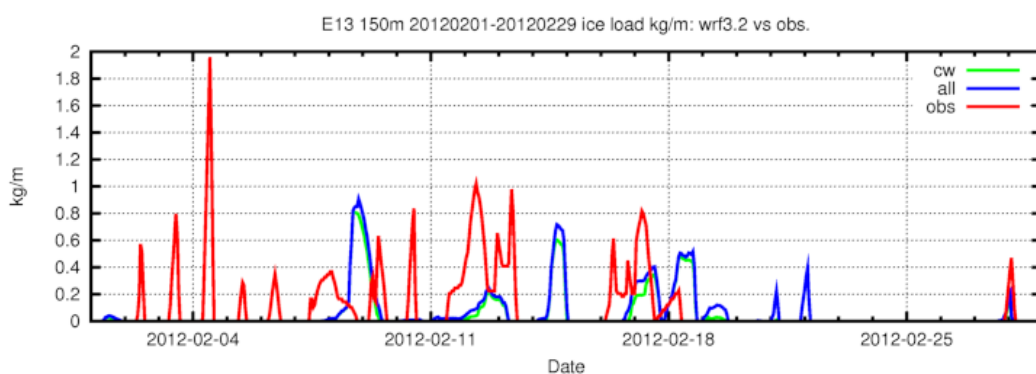


**Figure 4-32: Time series of observed (red) and WRF modelled (cloudwater only green, all condensates blue) ice load kg/m for site E13 February 2012.**

**Table 4-19: Monthly numbers February 2012 of rms (root mean square error), corr (correlation), number of icing hours and max ice load (kg/m) for site E13, all three models. First row using cloud water only in the icing calculation, second row with all condensates.**

	ARO				COA				WRF			
	rms	corr	ice hours	max load	rms	corr	ice hours	max load	rms	corr	ice hours	max load
201202												
cw	0,24	0,28	9	0,12	0,34	-0,09	34	1,04	0,26	0,05	55	0,81
all	0,24	0,09	50	0,42	0,41	-0,10	58	1,54	0,27	0,08	77	0,91

The observed curve show a lot of short-lived rather intense icing episodes. The models don't show any icing the first week, but they have some events later in the month. The timing of the model events are not that good in none of the models, WRF has some episodes that in magnitude is similar to the observed but the timing is off. COAMPS<sup>®</sup> has a rather long event around the 19:th that is not observed. The AROME model show too low ice loads all the time. In the statistics from Table 4-19 it is seen that WRF produces the highest number of ice hours and the COAMPS<sup>®</sup> has the highest ice load. The correlations are low for all three models. AROME has the biggest difference in ice hours for the two methods of ice calculation, only 9 hours using cloud water only.

The second example is from a northern site, E1. The observed curve start at a rather high ice load that decay slowly the first week. Since the model ice calculations starts at zero ice load the first every month it is not possible for the models to show this decay.

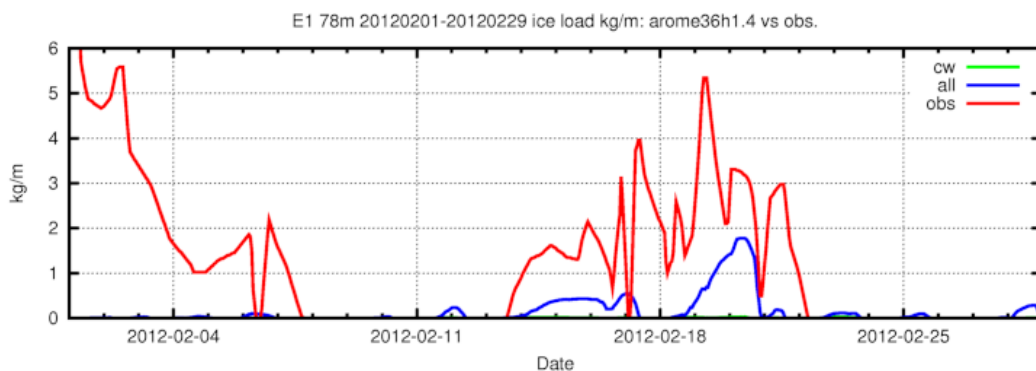


**Figure 4-33: Time series of observed (red) and AROME modelled (cloudwater only green, all condensates blue) ice load kg/m for site E1 February 2012.**

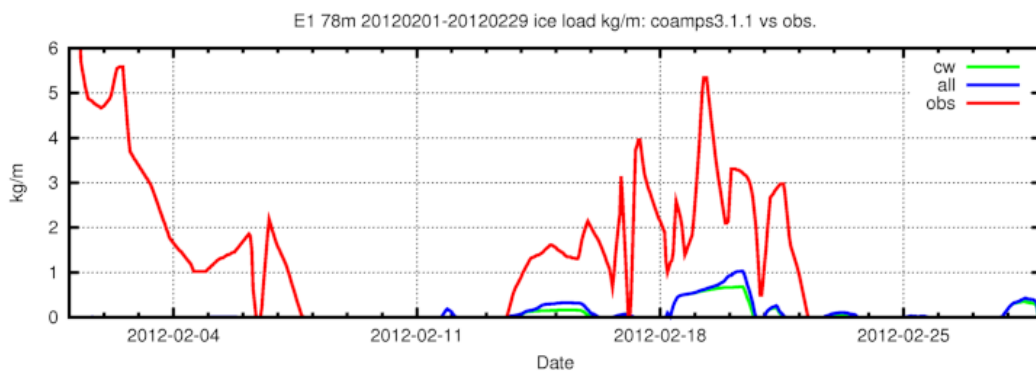


**Figure 4-34: Time series of observed (red) and COAMPS modelled (cloudwater only green, all condensates blue) ice load kg/m for site E1 February 2012.**

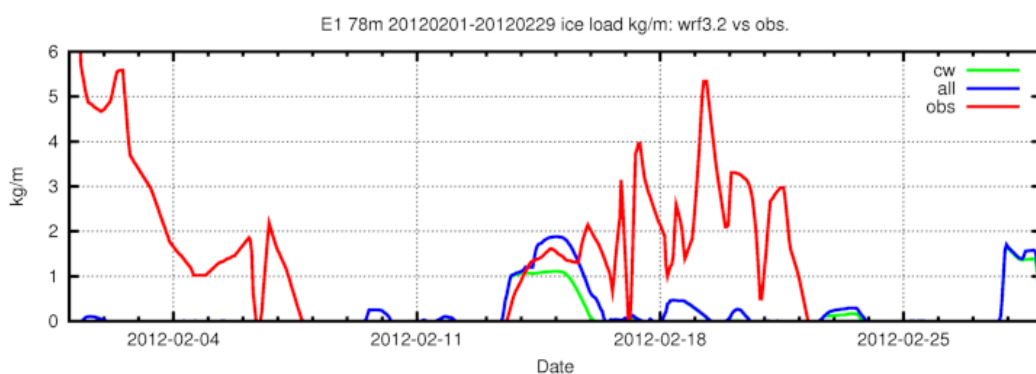


**Figure 4-35: Time series of observed (red) and WRF modelled (cloudwater only green, all condensates blue) ice load kg/m for site E1 February 2012.**

After the decay in observed ice load the first days there is an observed ice build-up around the 6:th that is not seen in the models. Then there is a rather long period of rather high observed ice loads during the third week. All models show ice during that period but most of the time the loads are lower than observed. The WRF model simulates the beginning of the period very well, but for the rest of the event has the lowest loads. All models have some ice the last day but none is observed. Again the correlations are low and there is a very big difference in ice hours and max ice load between the two AROME simulations. AROME with all condensates has the highest number of icing hours and WRF with all condensates has the highest ice load.

**Table 4-20: Monthly numbers February 2012 of rms (root mean square error), corr (correlation), number of icing hours and max ice load (kg/m) for site E1, all three models. First row using cloud water only in the icing calculation, second row with all condensates.**

	ARO				COA				WRF			
	rms	corr	ice hours	max load	rms	corr	ice hours	max load	rms	corr	ice hours	max load
201202												
cw	2,19	0,09	1	0,03	2,12	0,30	28	0,68	2,15	-0,03	36	1,67
all	2,06	0,27	93	1,78	2,10	0,29	66	1,03	2,13	-0,01	72	1,88

The final example is from site E5 for January 2012. The observed ice load curve show three well defined icing episodes, where the third one last for almost two weeks.

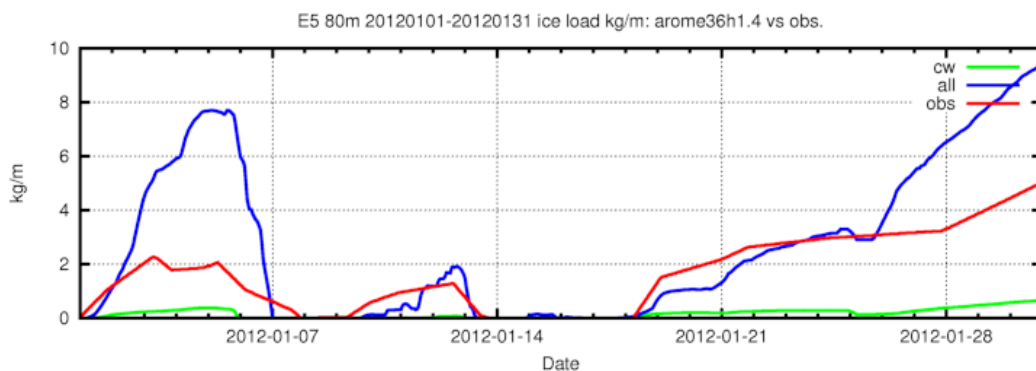


**Figure 4-36: Time series of observed (red) and AROME modelled (cloudwater only green, all condensates blue) ice load kg/m for site E5 January 2012.**

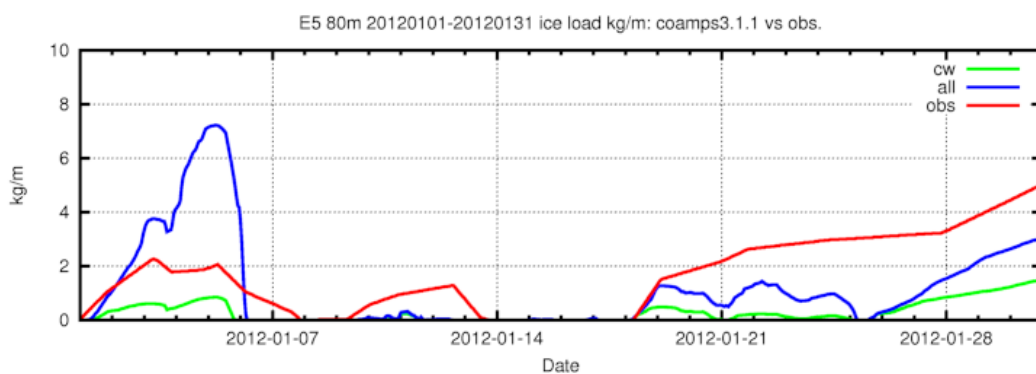


**Figure 4-37: Time series of observed (red) and COAMPS modelled (cloudwater only green, all condensates blue) ice load kg/m for site E5 January 2012.**

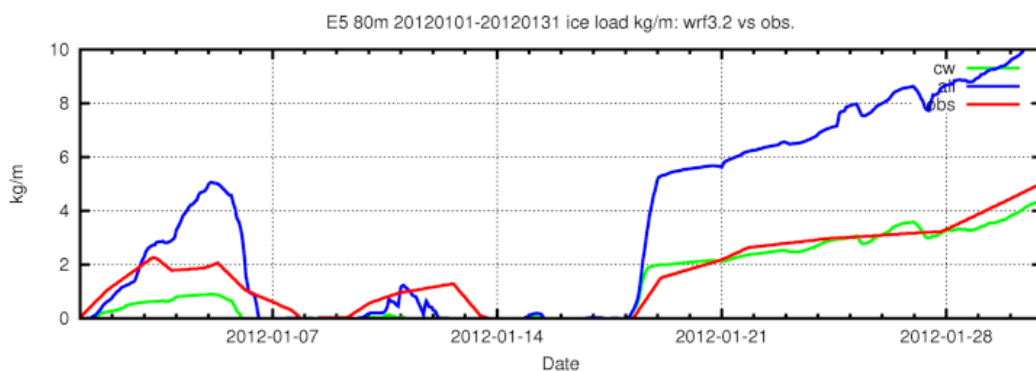


**Figure 4-38: Time series of observed (red) and WRF modelled (cloudwater only green, all condensates blue) ice load kg/m for site E5 January 2012.**

All three models have a good timing on the first episode but overestimate the loads with all condensates and underestimate it with cloud water only. The second period is hardly seen in COAMPS but is rather well predicted by AROME and WRF. The cloud water only curve from WRF agrees extremely well with the observed one for the last episode, whereas the load with all condensates from WRF is too high. Something goes wrong the first hours of the event, the rest of the time the build-up is similar to the observed. COAMPS underestimate the load for this event. The AROME curve (all condensates) agrees well with the observed during the first week but is too high for the last. Again very low loads for AROME cloud water only. In this case the correlations are better with WRF at the top of the table. WRF with all condensates show the highest ice load and AROME with all condensates has the highest number of icing hours.

**Table 4-21: Monthly numbers January 2012 of rms (root mean square error), corr (correlation), number of icing hours and max ice load (kg/m) for site E5, all three models. First row using cloud water only in the icing calculation, second row with all condensates.**

	ARO				COA				WRF			
	rms	corr	ice hours	max load	rms	corr	ice hours	max load	rms	corr	ice hours	max load
201201												
cw	1,91	0,91	17	0,65	1,76	0,74	127	1,47	0,63	0,93	197	4,34
all	2,15	0,81	348	9,38	1,73	0,42	277	7,22	2,96	0,95	312	10,35

To summarize these results it is clearly seen that it is difficult to model ice load. There are uncertainties in both the modelling and the observations. The last example shows that further research is needed on how the mix of liquid and frozen particles in the air interacts with each other to build the ice formations seen. For most of the cases the ice loads are underestimated using cloud water only but there are also many cases where the loads are exaggerated when all the condensates are used.

### 4.3 Sensitivity of results to model parameterizations and boundary condition

A modern numerical weather prediction model is a complex system built up by a considerable number of different parts and pieces all developed to take care of a specific task. For example, in a model system one will find routines that handle model terrain setup, interpolate forcing data (boundary conditions) to the model grid, integrate the equations in time and let the atmospheric state in neighbouring grid points interact through advection of the state variables. In fact, a model should not be viewed as "a model". It is more correct to view it as "a model system" which results depend on the model setup.

WRF is a model system that is widely used around the world and run by many modelling groups. Hence it seems appropriate to run a number of sensitivity tests using that modelling system. The WRF model, being a community model, has many researchers contributing to its development. This has led to an increasing number of physical schemes based on different assumptions and techniques for the user to choose from. This enables the testing of the most recent research in atmospheric modelling but it also makes it more challenging to evaluate the ability of the WRF model for a certain application. In order to assess the impact of different microphysical and planetary boundary layer schemes a number of sensitivity experiments have been carried out. In addition to testing different physical schemes the effect of using different datasets as initial and lateral boundary conditions has been investigated.

The base setup (FNL) used in this work is described in Section 4.1.3. The setup of each sensitivity experiment deviate from the FNL setup in only one of the following; the microphysics scheme used, the planetary boundary layer scheme (and consequentially the surface layer scheme) used or the dataset used for initial and lateral forcing. The different schemes and datasets used are briefly described in Table 4-22 and the experiment names and setups are summarized in Table 4-23.

**Table 4-22: Brief description of forcing data and schemes used in the sensitivity experiment. Description of the schemes is taken from the WRF users guide.**

	<b>Full name</b>	<b>Category</b>	<b>Description</b>
<b>FNL</b>	GFS Final analysis	Forcing	Final analysis of GFS operational forecast
<b>ERA</b>	ERA Interim	Forcing	Re-analysis produced by ECMWF
<b>NCAR</b>	NCEP/NCAR	Forcing	Re-analysis produced by NCEP/NCAR
<b>WSM3</b>	WRF Single-Moment 3-class	Microphysics	Simple, efficient scheme with ice and snow processes
<b>WSM6</b>	WRF Single-Moment 6-class	Microphysics	A scheme with ice, snow and graupel processes
<b>Morr</b>	Morrison 2-moment	Microphysics	Prognostic mixing ratio for 6 classes and double-moment ice, snow, rain and graupel
<b>MYJ</b>	Mellor-Yamada-Janjic	PBL	Eta operational scheme. Prognostic turbulent kinetic energy scheme with local vertical mixing
<b>QNSE</b>	Quasi-Normal Scale Elimination	PBL	A TKE-prediction option that uses a new theory for stably stratified regions
<b>MYNN2</b>	Mellor-Yamada Nakanishi and Niino Level 3	PBL	Predicts TKE and other second-moment terms.

**Table 4-23: Experiment names and setup. Deviations from FNL setup is marked in red.**

	<b>Microphysics</b>	<b>PBL</b>	<b>Surface layer</b>	<b>Radiation</b>	<b>Land surface</b>	<b>Cumulus</b>	<b>Forcing</b>
<b>FNL</b>	Thompson	YSU	Eta-MM5	RRTM+ Dudhia	Noah	Kain-Fritsch	FNL
<b>ERA</b>	-	-	-	-	-	-	ERA
<b>NCAR</b>	-	-	-	-	-	-	NCEP/ NCAR
<b>wsm3</b>	WSM3	-	-	-	-	-	-
<b>wsm6</b>	WSM6	-	-	-	-	-	-
<b>Morr</b>	Morrison	-	-	-	-	-	-
<b>myj</b>	-	MYJ	MO-ETA	-	-	-	-
<b>qnse</b>	-	QNSE	QNSE	-	-	-	-
<b>mynn2</b>	-	MYNN2	-	-	-	-	-

We will here first compare model output from the winter season 2010/2011 using different initial and lateral boundary conditions. The default setup is with FNL and its model output is compared to a setup with ERA-Interim and NCEP/NCAR reanalysis data.

Model results using different boundary conditions for sites E5, E6, E8, and E11 are shown in Figure 4-39 to Figure 4-42 for the winter season 2010/2011.

For all sites but one, E5, NCAR give a slightly cooler atmosphere with more cloud liquid water than FNL. NCAR also have slightly weaker vertical wind shear and thus slightly lower wind speeds at higher heights.

ERA give the coolest atmosphere of all three forcing data sets. For some sites ERA has a little more cloud liquid water than FNL while the opposite is true for other sites. Only small differences between ERA and FNL are found in the wind speed profiles.

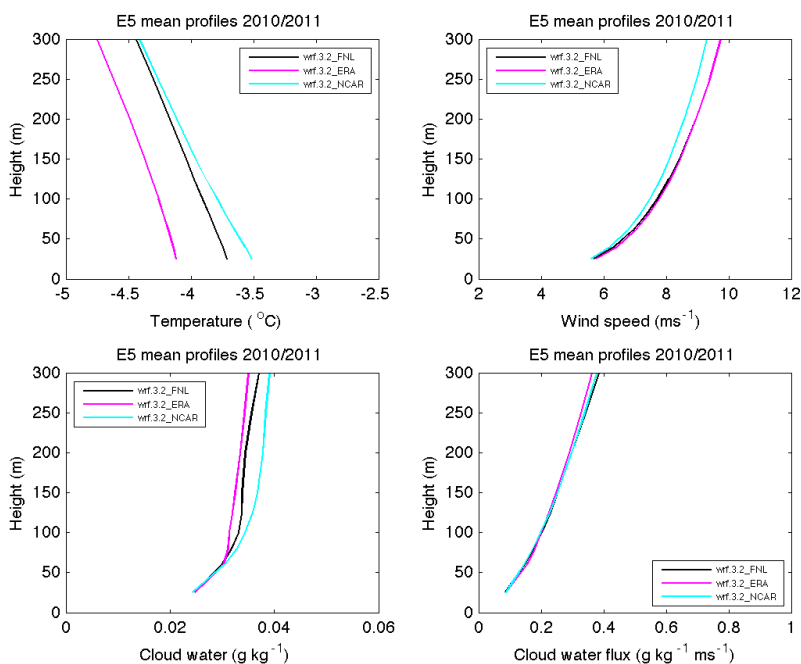


**Figure 4-39: Model results for site E5 winter season 2010/2011 using different boundary conditions, FNL, ERA, and NCAR.**

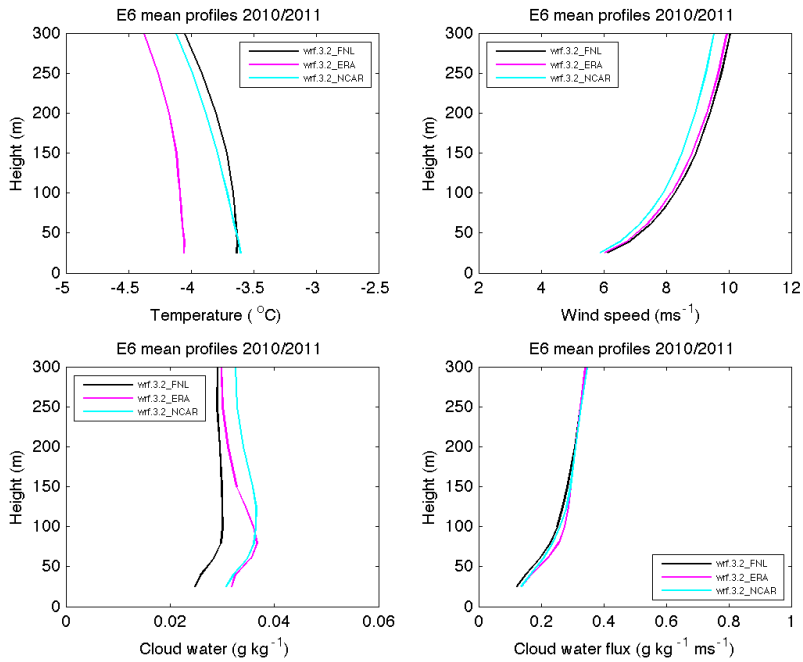


**Figure 4-40: Model results for site E6 winter season 2010/2011 using different boundary conditions, FNL, ERA, and NCAR.**

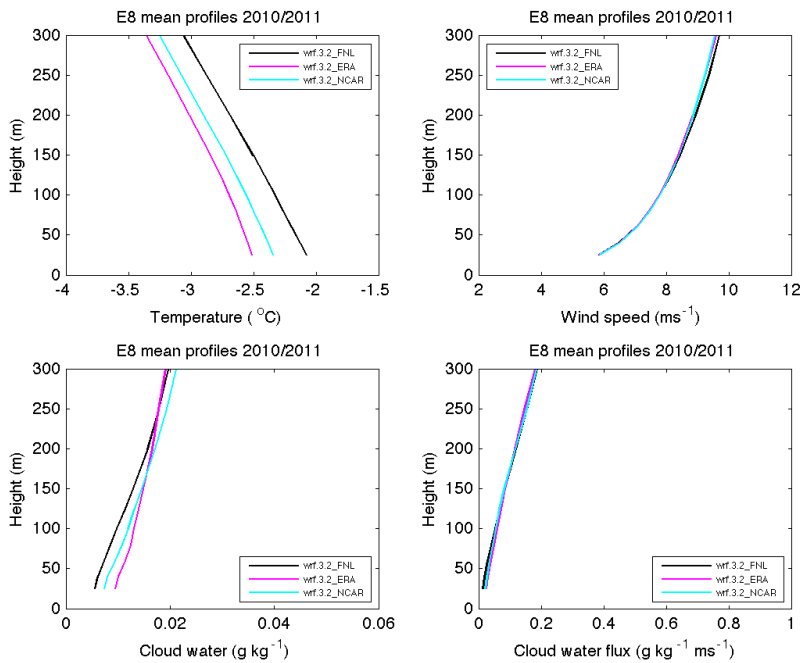


**Figure 4-41: Model results for site E8 winter season 2010/2011 using different boundary conditions, FNL, ERA, and NCAR.**

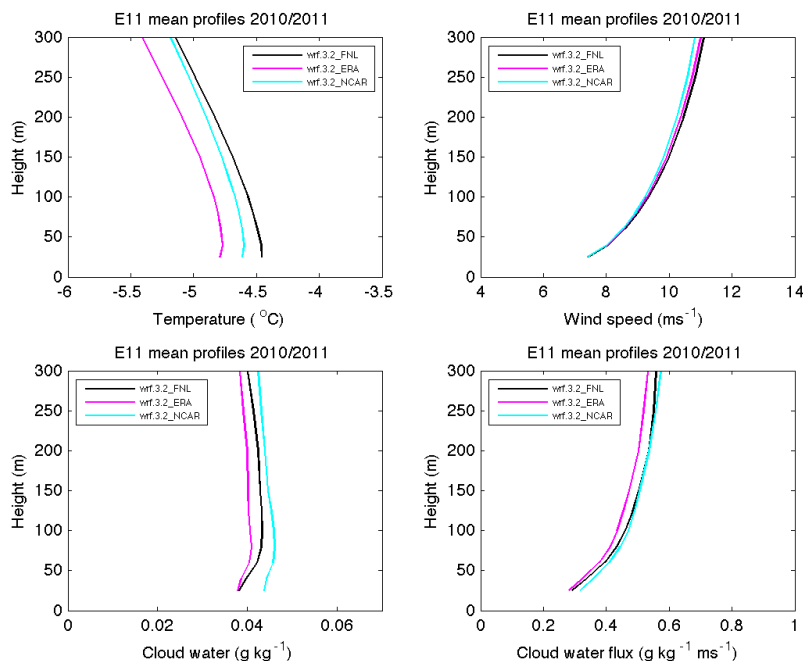


**Figure 4-42: Model results for site E11 winter season 2010/2011 using different boundary conditions, FNL, ERA, and NCAR.**

Model results from the experiments using different forcing have been compared to measurements and statistics have been calculated in the same way as in section 4.2.1. Using different boundary conditions reveal no major differences in wind speed, wind direction, and temperature distributions. Examples of statistics from site E6 is given in Table 4-24. Statistical scores for sites E4, E6, E7, E8, E9, and E11 are found in Appendix B.

For temperature, correlation is equally good for all three forcings. NCAR has somewhat lower correlation for wind speed than ERA and FNL, which have almost similar scores for the sites investigated. The cooler atmosphere given by ERA is seen in the larger negative temperature bias compared to FNL and NCAR. Worth to continue investigating are underlying reasons to why ERA give a cooler atmosphere than FNL and NCAR.

In general, the differences in the statistics between FNL, ERA, and NCAR are small. Hence, it is hard to say from the statistics which forcing that will give the best results. In particular it is hard to find significant differences in the statistical scores between FNL and ERA. This suggests that FNL, ERA, and NCAR are all describing the large-scale weather patterns in a similar way. It is here of importance to underline that extracting e.g., wind data directly from the forcing databases in single points will most likely give a spread in wind speed and wind directions. This is not unexpected since the forcing data have different horizontal resolutions and e.g., have differences in terrain height and land/sea areas. However, when the mesoscale model is set up the atmospheric state is given by the forcing. The mesoscale model adjusts the coarse data in a physical sound way to a higher model grid resolution. Hence,

as long as the large-scale atmospheric state does not vary a lot between different forcing data, the resulting state of the mesoscale model will not differ a lot.

But, one difference found in the scores is a slightly larger phase errors in NCAR than in FNL and ERA. One possible reason for this could be the much coarser resolution in the NCAR forcing data. A higher resolution in the forcing data allow for a better representation of e.g., intense small-scale low-pressure systems. This can in turn influence the initial state and time evolution of the mesoscale model in a way so that the timing and magnitude of changes in the atmospheric state can vary in certain weather situations. Relatively small differences in the time evolution can, as mentioned in section 4.2.1, give rise to a “double penalty” in the point wise statistical scores, even though the weather patterns on a larger scale are well captured.

**Table 4-24: Observation and model statistics and statistical scores for site E6 from the forcing experiments.**

E6 2010/2011											
wind speed											
Data	mean	max	min	median	std	abse	corr	rmse	bias	bias std	dispe
wrf.3.2_FNL	8,24	21,97	0,18	7,94	3,53	2,18	0,70	2,92	1,26	0,28	2,62
wrf.3.2_ERA	8,07	22,43	0,20	7,87	3,52	2,10	0,71	2,81	1,10	0,27	2,57
wrf.3.2_NCAR	7,85	21,07	0,09	7,65	3,47	2,34	0,63	3,02	0,87	0,22	2,88
obs100m	6,97	19,70	0,10	7,10	3,24	-	-	-	-	-	-
temperature											
Data	mean	max	min	median	std	abse	corr	rmse	bias	bias std	dispe
wrf.3.2_FNL	-4,28	13,39	-20,84	-4,69	6,84	1,29	0,98	1,72	-0,87	0,31	1,46
wrf.3.2_ERA	-4,70	13,45	-21,97	-5,09	7,10	1,58	0,97	2,13	-1,29	0,56	1,60
wrf.3.2_NCAR	-4,23	14,39	-20,42	-4,65	6,86	1,44	0,97	1,89	-0,82	0,33	1,67
obs100m	-3,41	15,70	-19,50	-4,10	6,53	-	-	-	-	-	-
pressure											
Data	mean	max	min	median	std	abse	corr	rmse	bias	bias std	dispe
wrf.3.2_FNL	922,2	945,3	893,6	922,6	12,18	0,82	1,00	1,04	-0,45	0,05	0,93
wrf.3.2_ERA	922,5	945,9	893,9	923,0	12,07	0,75	1,00	0,97	-0,20	0,16	0,94
wrf.3.2_NCAR	923,3	946,6	893,8	923,6	12,15	1,09	0,99	1,43	0,66	0,08	1,26
obs100m	922,7	947,0	895,0	923,0	12,23	-	-	-	-	-	-

Varying the physical parameterizations used in the model setup reveal more interesting results than varying the boundary conditions. Results from a sensitivity study in which several microphysics and boundary layer schemes are presented here. The default setup microphysics scheme is Thompson Microphysics v3.1; the default PBL scheme is Yonn State University (YSU).

Model results using 4 different microphysics schemes and 4 different PBL schemes for site E5 are shown in Figure 4-43 to Figure 4-44.

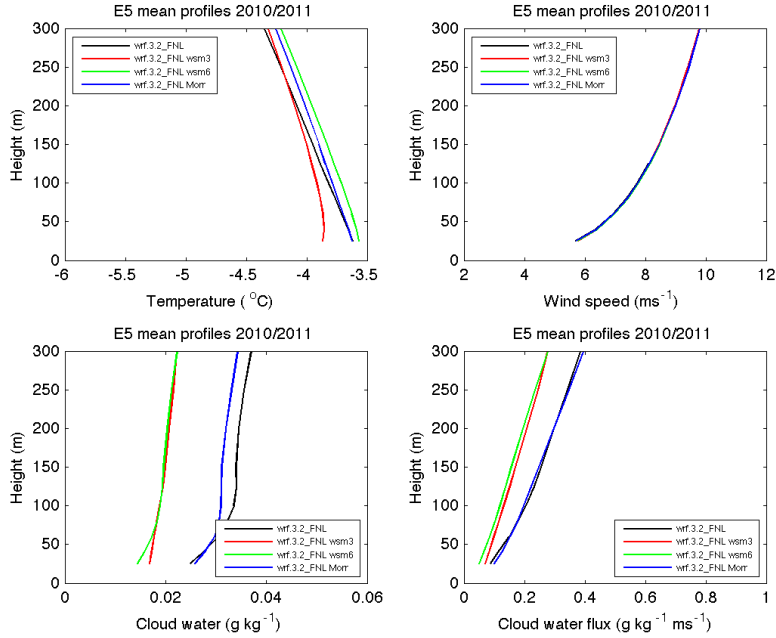


**Figure 4-43: Model results for site E5 winter season 2010/2011 using different microphysics schemes, Thompson, WSM3, WSM6, and Morrison.**

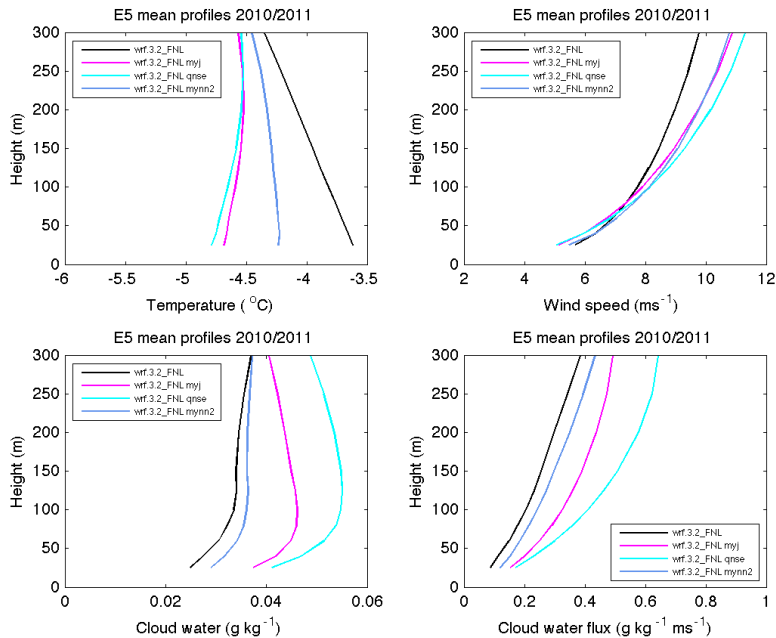


**Figure 4-44: Model results for site E5 winter season 2010/2011 using different PBL schemes, YSU, MYJ, QNSE, and MYNN2.**

Model results using 4 different microphysics schemes and 4 different PBL schemes for site E6 are shown in Figure 4-45 to Figure 4-46.

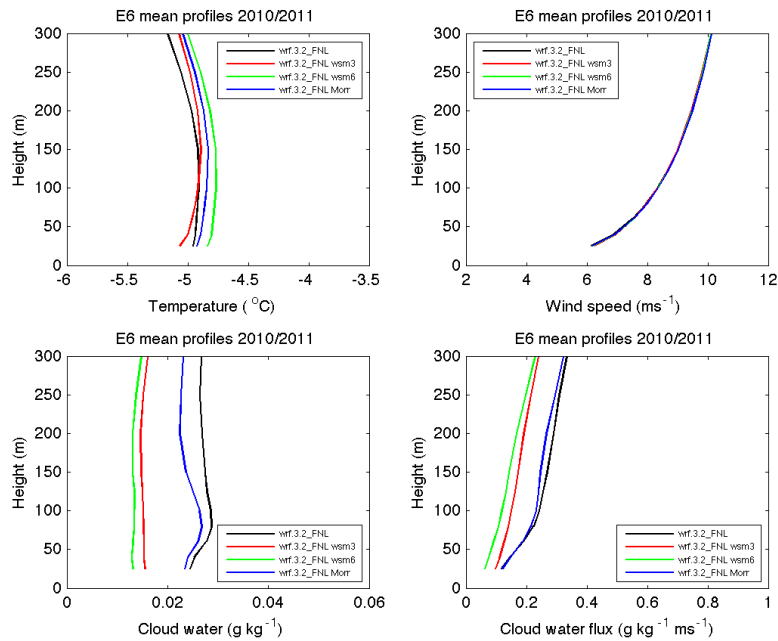


**Figure 4-45: Model results for site E6 winter season 2010/2011 using different microphysics schemes, Thompson, WSM3, WSM6, and Morrison.**

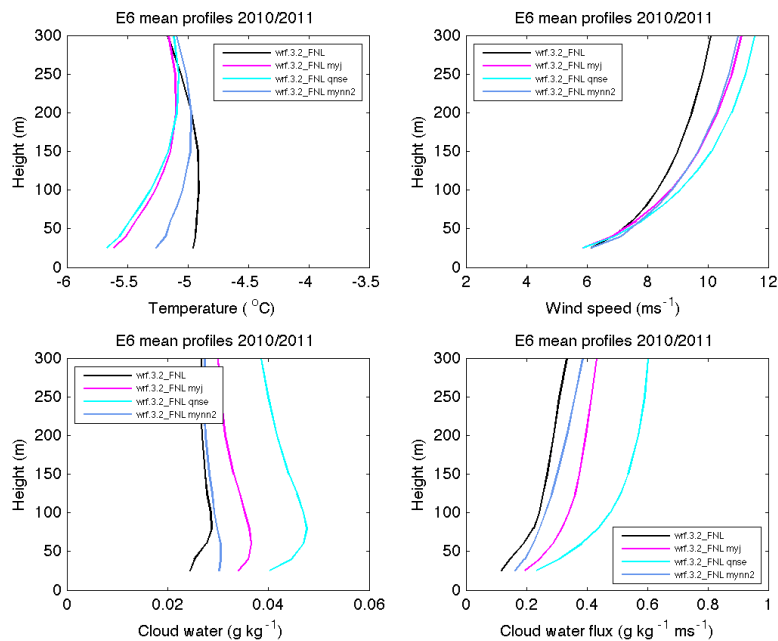


**Figure 4-46: Model results for site E6 winter season 2010/2011 using different PBL schemes, YSU, MYJ, QNSE, and MYNN2.**

Model results using 4 different microphysics schemes and 4 different PBL schemes for site E8 are shown in Figure 4-47 to Figure 4-48.

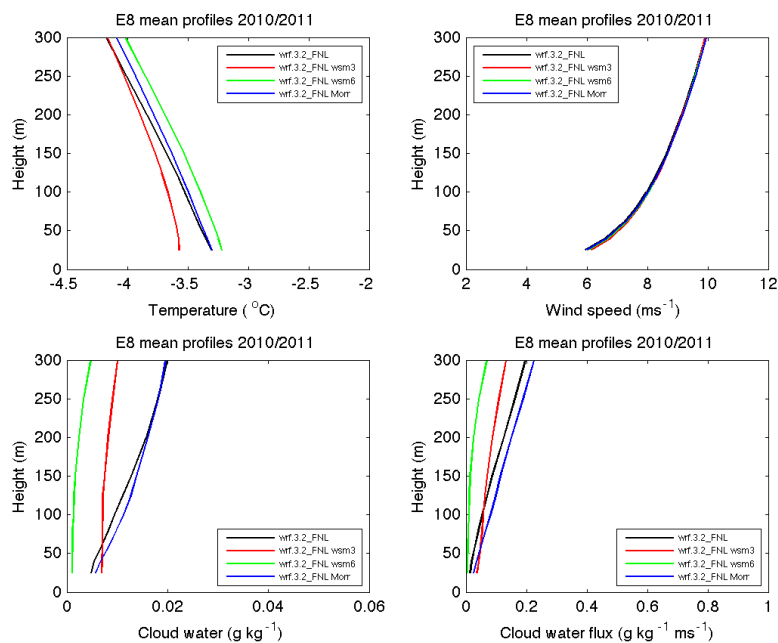


**Figure 4-47: Model results for site E8 winter season 2010/2011 using different microphysics schemes, Thompson, WSM3, WSM6, and Morrison.**

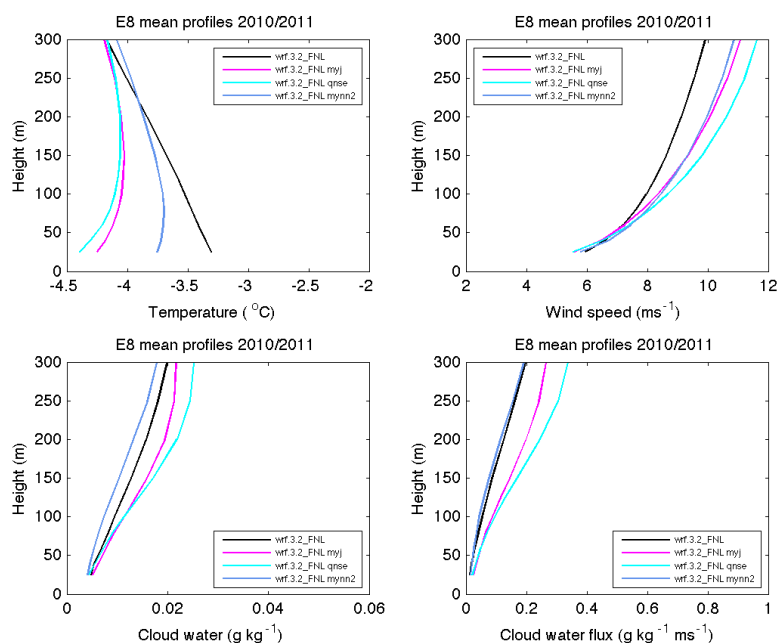


**Figure 4-48: Model results for site E8 winter season 2010/2011 using different PBL schemes, YSU, MYJ, QNSE, and MYNN2.**

Model results using 4 different microphysics schemes and 4 different PBL schemes for site E11 are shown in Figure 4-49 to Figure 4-50.

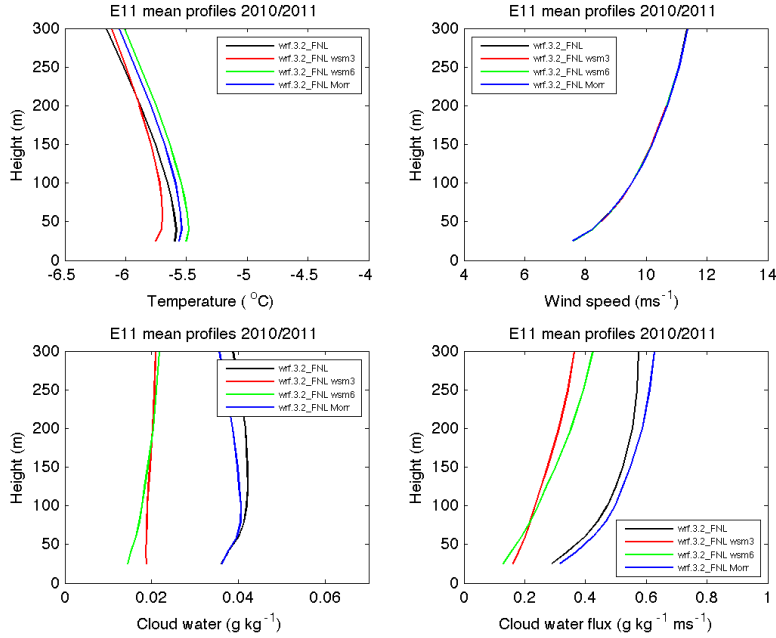


**Figure 4-49: Model results for site E11 winter season 2010/2011 using different microphysics schemes, Thompson, WSM3, WSM6, and Morrison.**

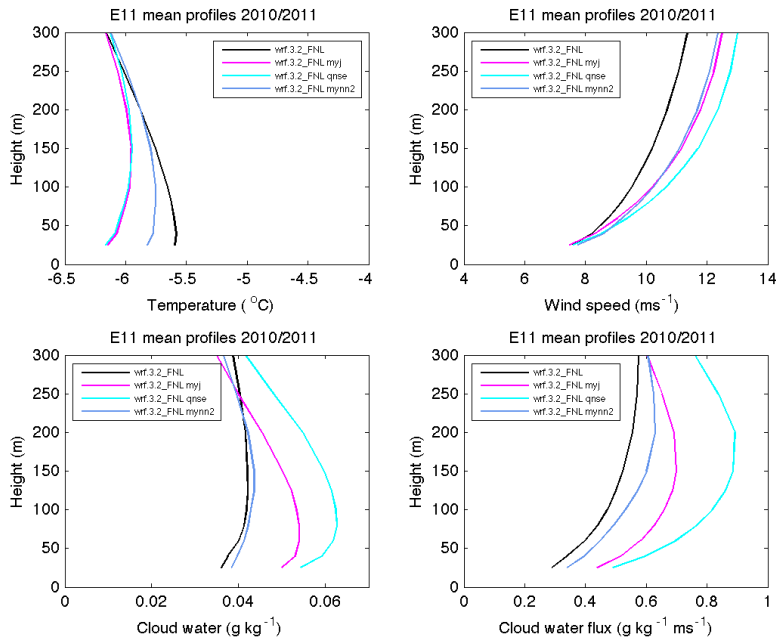


**Figure 4-50: Model results for site E11 winter season 2010/2011 using different PBL schemes, YSU, MYJ, QNSE, and MYNN2.**

All but the Morrison scheme give less mean cloud water than the Thompson scheme. The Morrison and Thompson schemes give relatively similar mean cloud water profiles. However, altering the microphysics scheme will not only influence the mean profiles of cloud water, it will also affect the mean temperature profiles. Using the WSM3 scheme instead of the Thompson scheme results in an increased stability in the lowest 150-200 m above ground. Using the WSM5 scheme instead of the Thompson scheme results in a somewhat warmer boundary layer. One should not be surprised that changing the microphysics scheme also have an effect on the temperature. When moisture in the atmosphere changes phase there will be a latent heat exchange. It is all connected through the thermodynamics of the atmosphere.

Altering the PBL scheme give rise to more drastic changes to the mean vertical profiles than altering the microphysics scheme. All tested schemes increase the stability in the boundary layer, MYJ and QNSE by a lot. The increased stability also give rise to an increased wind shear and higher wind speeds from ~50m height. Of great importance for ice accretion estimations is the cloud liquid water. Here it is evident that altering the PBL-scheme also has an impact on the mean liquid cloud water profiles. In fact, changing the PBL scheme results in a larger change in the mean liquid cloud water profile than changing the microphysics scheme. The combined effect of an increased wind speed and increased liquid water content in the boundary layer has a significant effect on the mean cloud water flux.

Statistical scores for each PBL and MP test for sites E4, E6, E7, E8, E9, and E11 are found in Appendix B.

The differences found in cloud water flux and temperature profiles have a direct effect on the ice accretion. Examples to this are illustrated in Figure 4-51 in which 8 days of sensitivity simulations for site E5 during January 2011 are presented in more detail. In the figure, WRF FNL runs are displayed as reference together with the observed loads. The modelled ice load is estimated using only cloud water. During these days there is a slow rather light ice build-up during the first three days, then another more severe event during the last three days. There is a slow decay in observed ice load between the 12:th and the 14:th, probably due to sublimation.

In Figure 4-52, modelled time series of cloud water is shown. It is evident that the simulated cloud water content varies a lot between the different model versions for this time period, which of course largely explains the differences in modelled ice load shown. But, the ice load is not only a function of cloud water it also depend on the wind speed. Varying the PBL-scheme can alter the modelled wind speed considerably which can be seen in Figure 4-53. For instance, during the morning hours on the 11:th mynn2 has a much lower wind speed than any other PBL scheme while mynn2 has a higher wind speed than the other schemes around the 16:th. Note that the observed wind speed is probably affected by icing during the first two days and also from the 15:th to the 17:th. This points to the fact that measuring wind in icing climates is a tricky task and that evaluations of model results and observations must be carefully undertaken. During some events the models are not performing well enough while during other events, the measurements are not trustworthy.

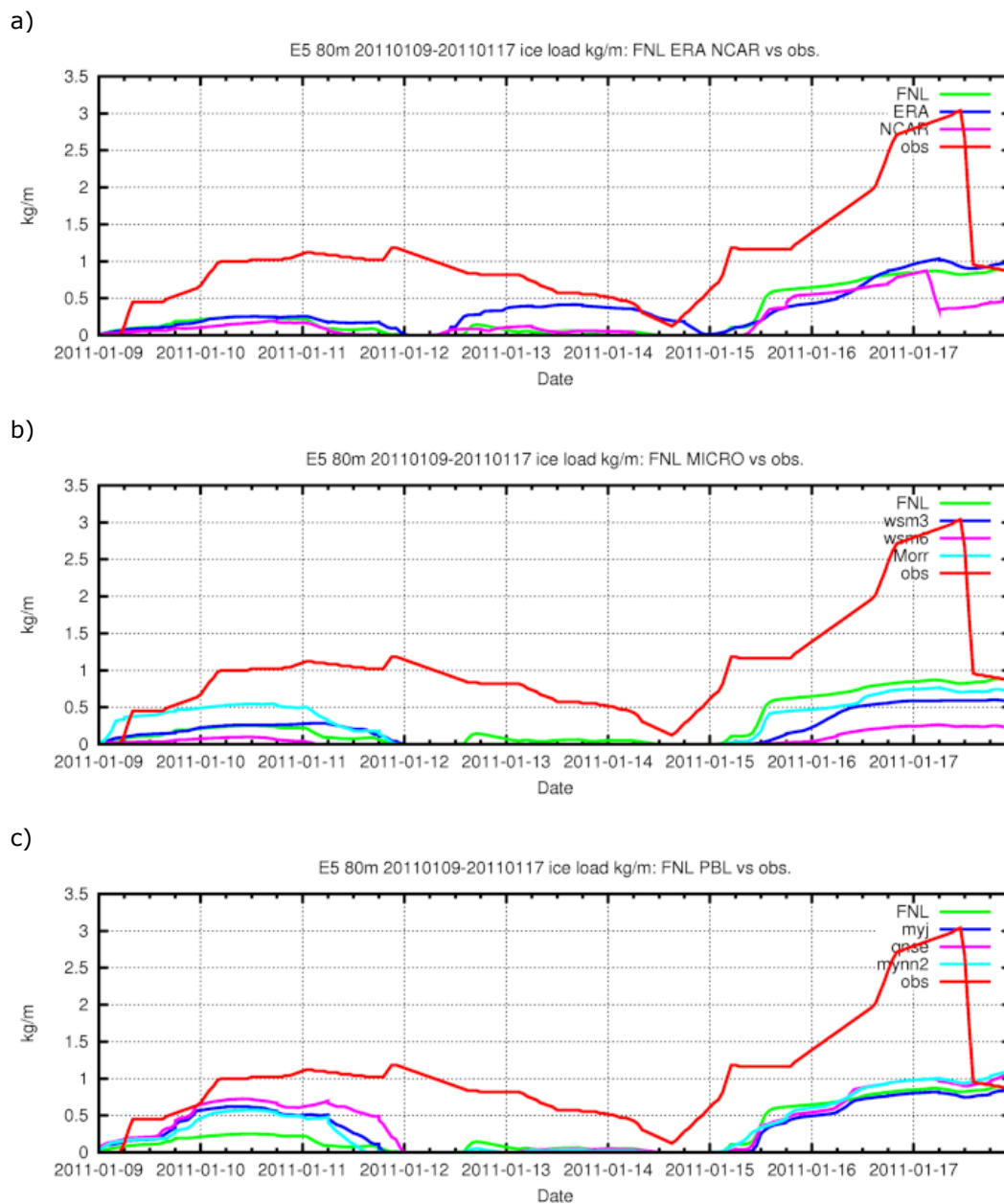


**Figure 4-51: Time series of observed and modelled ice load (kg/m) for site E5 January 2011. Sensitivity experiment: a) Forcing; b) Microphysics; c) PBL.**

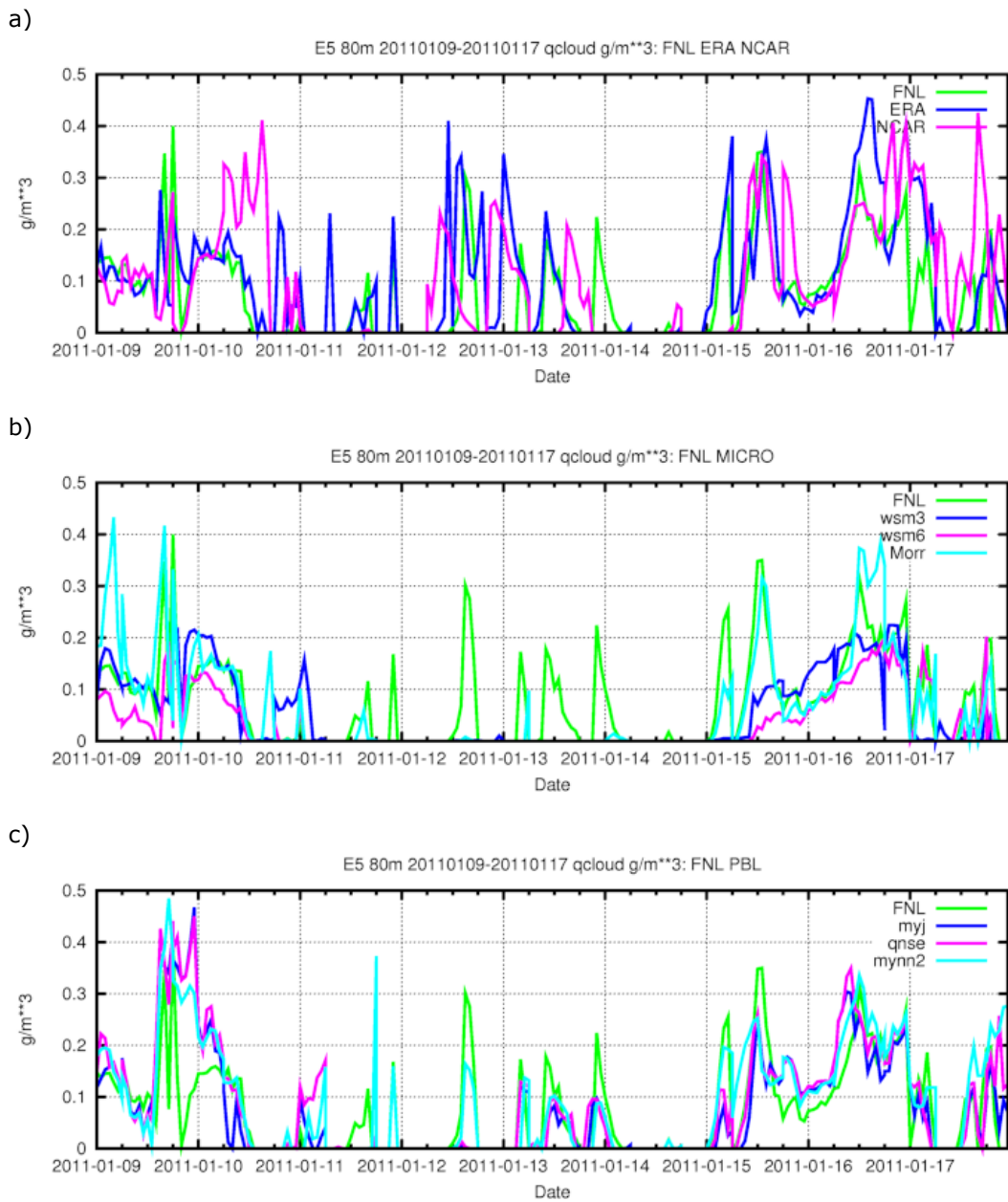


**Figure 4-52: Time series of modelled cloud water ( $\text{g}/\text{m}^3$ ) for site E5 January 2011. Sensitivity experiment: a) Forcing; b) Microphysics; c) PBL.**

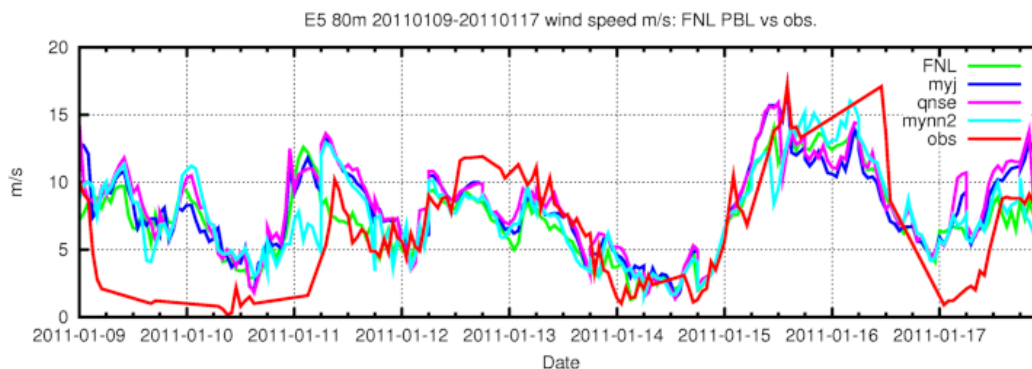


**Figure 4-53: Time series of observed and modelled wind speed (m/s) for site E5 January 2011. Sensitivity experiment PBL.**

Using only the cloud liquid water in the ice accretion calculations the number of hours with active icing was estimated for site E5, E6, E8, and E11. The results are summarized in Table 4-25 to Table 4-28. Note in particular how sensitive WRF is to the choice of PBL scheme. The QNSE-scheme gives the largest number of hours with active icing by far. Of all WRF sensitivity runs, the WSM3 and WSM6 schemes give the lowest number of hours with active icing. In WSM3, only ice processes are active below 0 °C. This is illustrated in Figure 4-54, a scatter plot of modelled temperature and cloud water for WSM3 and FNL, the base setup with the Thompson microphysics scheme. The threshold for cloud liquid water below the freezing point in the WSM3-scheme is evident. The WSM3 scheme is not suitable in studies of atmospheric icing since supercooled liquid cloud water is not properly handled.

Further research is needed to better address which combination of schemes in WRF that is best suited. The observations currently available are not sufficient for this. In particular measurements of cloud liquid water and droplet number concentrations would help finding out more about the uncertainties in the ice load model. A site with measurement on several heights is also needed in order to evaluate how well the models are able to model the boundary layer structure.

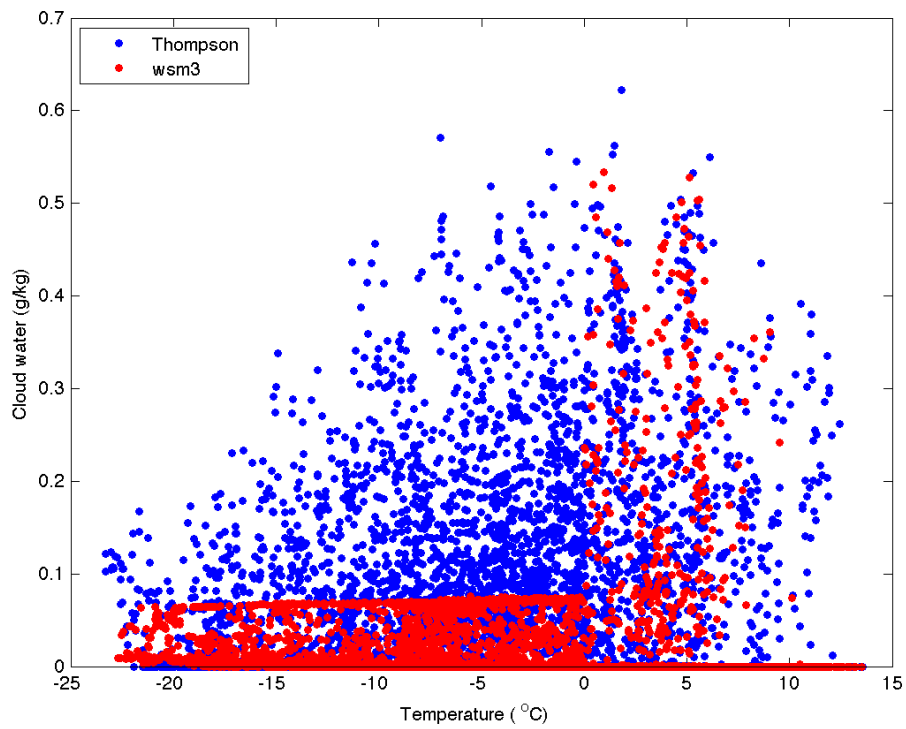


**Figure 4-54: Scatter plot of modelled temperature and cloud water from site E5 with the Thompson scheme in the base setup (blue) and the WSM3 scheme (red).**

**Table 4-25: Estimated number of hours with active icing winter season 2010/2011 for site E5 using cloud liquid water only from AROME, COAMPS®, and WRF and the sensitivity study using different microphysics and PBL schemes in WRF.**

	AROME	COAMPS	WRF FNL	WRF ERA	WRF NCAR	WRF WSM3	WRF WSM6	WRF Morr	WRF MYJ	WRF QNSE	WRF MYNN2
201010	51	58	55	48	31	59	55	58	88	115	67
201011	13	36	60	108	63	17	28	56	85	108	72
201012	5	16	29	65	93	22	17	27	41	71	49
201101	12	35	46	99	48	36	14	51	94	160	105
201102	13	26	59	61	61	16	43	55	74	110	46
201103	23	67	77	55	75	55	51	57	139	199	101
201104	17	50	58	65	64	31	51	62	103	188	85
	134	288	384	501	435	236	259	366	624	951	525

**Table 4-26: Estimated number of hours with active icing winter season 2010/2011 for site E6 using cloud liquid water only from AROME, COAMPS®, and WRF and the sensitivity study using different microphysics and PBL schemes in WRF.**

	AROME	COAMPS	WRF FNL	WRF ERA	WRF NCAR	WRF WSM3	WRF WSM6	WRF Morr	WRF MYJ	WRF QNSE	WRF MYNN2
201010	40	26	28	33	12	16	26	34	43	65	40
201011	23	29	74	117	119	6	20	64	94	115	59
201012	7	16	34	66	69	16	14	27	44	73	44
201101	16	37	66	94	52	43	19	61	127	165	79
201102	13	17	86	59	46	15	12	39	53	69	44
201103	26	42	56	45	40	9	18	40	82	116	52
201104	18	22	48	57	38	0	37	50	51	68	49
	143	189	392	471	376	105	146	315	494	671	367

**Table 4-27: Estimated number of hours with active icing winter season 2010/2011 for site E8 using cloud liquid water only from AROME, COAMPS®, and WRF and the sensitivity study using different microphysics and PBL schemes in WRF.**

	AROME	COAMPS	WRF FNL	WRF ERA	WRF NCAR	WRF WSM3	WRF WSM6	WRF Morr	WRF MYJ	WRF QNSE	WRF MYNN2
201010	1	13	9	12	15	3	6	7	27	26	15
201011	0	39	71	80	69	30	27	70	133	169	76
201012	0	3	3	3	16	14	6	3	16	22	22
201101	0	17	14	18	8	9	7	30	33	46	34
201102	1	9	45	40	44	9	3	43	37	34	30
201103	0	8	7	5	11	0	0	1	15	24	0
201104	3	23	18	16	21	1	15	10	23	36	19
	5	112	167	174	184	66	64	164	284	357	196

**Table 4-28 Estimated number of hours with active icing winter season 2010/2011 for site E11 using cloud liquid water only from AROME, COAMPS®, and WRF and the sensitivity study using different microphysics and PBL schemes in WRF.**

	AROME	COAMPS	WRF FNL	WRF ERA	WRF NCAR	WRF WSM3	WRF WSM6	WRF Morr	WRF MYJ	WRF QNSE	WRF MYNN2
201010	42	51	36	51	50	16	47	41	66	88	43
201011	20	62	274	255	216	23	27	193	298	316	211
201012	0	4	48	38	75	20	5	35	68	83	58
201101	23	85	65	75	57	12	18	65	129	205	104
201102	5	19	154	126	92	12	8	110	139	136	86
201103	8	48	66	37	48	1	11	35	60	81	53
201104	18	32	38	32	47	4	28	32	62	109	44
	116	301	681	614	585	88	144	511	822	1018	599

## 4.4 Summary of Chapter 4

In the project, three meso-scale models have been employed: AROME, COAMPS<sup>®</sup>, and WRF. The term meso-scale here refers to a scale in space and time that the models can resolve. Typical meso-scale phenomena are thunderstorms and sea breezes with scales of the order of 1-20 km in space and ½-6 hours in time. Processes on smaller scales than can be resolved on the model grid are parameterized. In a parameterization the sub-grid scale processes are described as a function of the resolved scale variables, and the mean effect of the sub-grid tendency (such as heating, cooling, moistening, drying) is added to the time-derivative of the resolved state variable such as wind and temperature for instance. All three models rest on the same physical foundation. But, there are differences in the way the equations for the resolved state variables are solved and how the parameterizations of the unresolved scales are formulated. One of the questions that this project addresses is how sensitive the estimated ice load is to model and model setup.

The ice load is modelled on a 1 m tall cylinder with a constant diameter of 30 mm using an ice accretion model often referred to as "the Makkonen model". Input to the model is wind speed, pressure, liquid water content, temperature, and droplet concentration. All input parameters but droplet concentration  $N$  is taken from the mesoscale model. The mesoscale models applied here do not model  $N$ , instead a constant droplet concentration of  $100 \text{ cm}^{-3}$  is assumed and used in the estimation of median volume diameter (MVD). The droplet diameter is in turn used to give an estimate how many of the droplets that hit the obstacle. In this study melting and sublimation of ice has been added to the ice accretion model. The ice accretion model was further extended by including rain, snow, and ice cloud condensates in the calculations, motivated by including wet snow in the ice growth.

A comprehensive verification of the three mesoscale models was carried out against the meteorological observations at the 12 sites. The results are given in terms of distribution curves and in tables. In general all three models perform quite well. Some specific comments are that all models have a cold bias; WRF has in the mean a slightly less stable temperature profile and less near-surface vertical wind shear. The latter could in part be due to a recently found bug in the boundary layer scheme but will have to be further investigated before a firm conclusion can be drawn. For wind speed, the main contribution to the root mean square error is the phase error, i.e., error in timing the change in wind speed. Modelling the ice load is, however, not a trivial task. The start and end of the icing events are in many cases quite well captured by the models while the magnitude of the ice load is often underestimated. Including all cloud condensates in the ice load estimate did improve the results for some events but overestimated the ice load quite significantly in other cases.

It was pointed out that a modern numerical weather prediction model is a complex system and should be viewed as "a model system" rather than as "a model". The sensitivities to lateral boundary forcing as well as the initial conditions (analysis) have been investigated using WRF. It was found that the sensitivity to boundary forcing is relatively small while the choice of different physical parameterisations has a large impact on the model results. The cloud

scheme affects the cloud water content itself, but the turbulence scheme has a more profound impact on wind and temperature profiles as well as the cloud water. In terms of icing hours the variations are large, between models and particularly physics schemes.

In summary, these results clearly illustrate that even though the mesoscale models perform well in capturing "standard meteorological parameters" such as wind speed and temperature it is difficult to model the ice load. There are uncertainties in both the modelling and the observations. Further research is needed on how the mix of liquid and frozen particles in the air interacts with each other to build the ice formations on the instruments. The observations currently available are not sufficient for determining which model or model setup that is the most appropriate for using in a mapping of the icing climate. In particular measurements of cloud liquid water and droplet number concentrations would help finding out more about the uncertainties in the ice load model. A site with measurement on several heights is also needed in order to evaluate how well the models are able to model the boundary layer structure.

## 5 Results from modelling of ice load during three winter seasons

In this section, maps with number of icing hours for the three modelled icing seasons September-April 2009/2010, 2010/2011, and 2011/2012 are presented. The ice accretion model has been used to calculate icing rate in every model gridpoint and every hour. One icing hour is counted if the icing rate is larger than 10 g/hour on a 30 mm cylinder. The icing rate has been calculated using the method described in section 4.1 taking all cloud condensates into account. The cylinder diameter is reset to 30 mm every hour. No lifting has been applied to adjust the model results for differences between model terrain and real topography.

To facilitate a comparison between the different model results AROME 2.5km, COAMPS<sup>®</sup> 3km, and WRF 3km maps are shown sections 5.1 and 5.2. In section 5.3 COAMPS<sup>®</sup> and WRF 1km model results are compared for one domain.

### 5.1 AROME 2.5km

The AROME model has been run with 2.5 km horizontal resolution on two different areas during the three winter seasons. For the first season the area was chosen to cover the northern part of Sweden since all the observations were located there. For the two last seasons there were observations also in the southern part of the country and the model area were increased to cover almost all of southern Sweden as well.

The maps in Figure 5-1 to Figure 5-3 show that as expected the highest number of icing hours is counted at the highest mountains. There is a high correlation between icing hours and topographic height. The maps also show rather high inter-seasonal variations, e.g., over southern Sweden there is more ice during 2010/2011 than during 2011/2012. In the northern part on the contrary there is more ice 2011/2012 than 2010/2011.

To illustrate the effect of including all cloud condensates in the ice load estimate, a map for the 2011/2012 winter season in which only cloud water is used is shown in Figure 5-4. It is apparent that including all cloud condensates in the ice load estimates have a profound effect on the AROME results.

If the model results are interpolated to a finer mesh and adjusted for differences in model terrain and real terrain height in each new grid point the number of icing hours will certainly be higher than here. However, in doing this and creating icing maps introduce new uncertainties that are not quantified.

The results for 2009/2010 appear to show higher local variability than for the other seasons. The reason for this is not clear. Could to some part be "true" differences, but could also be due to that different model versions were used.

SMHI Arome 2.5km  
Ice hours 100m amgl season 2009/2010

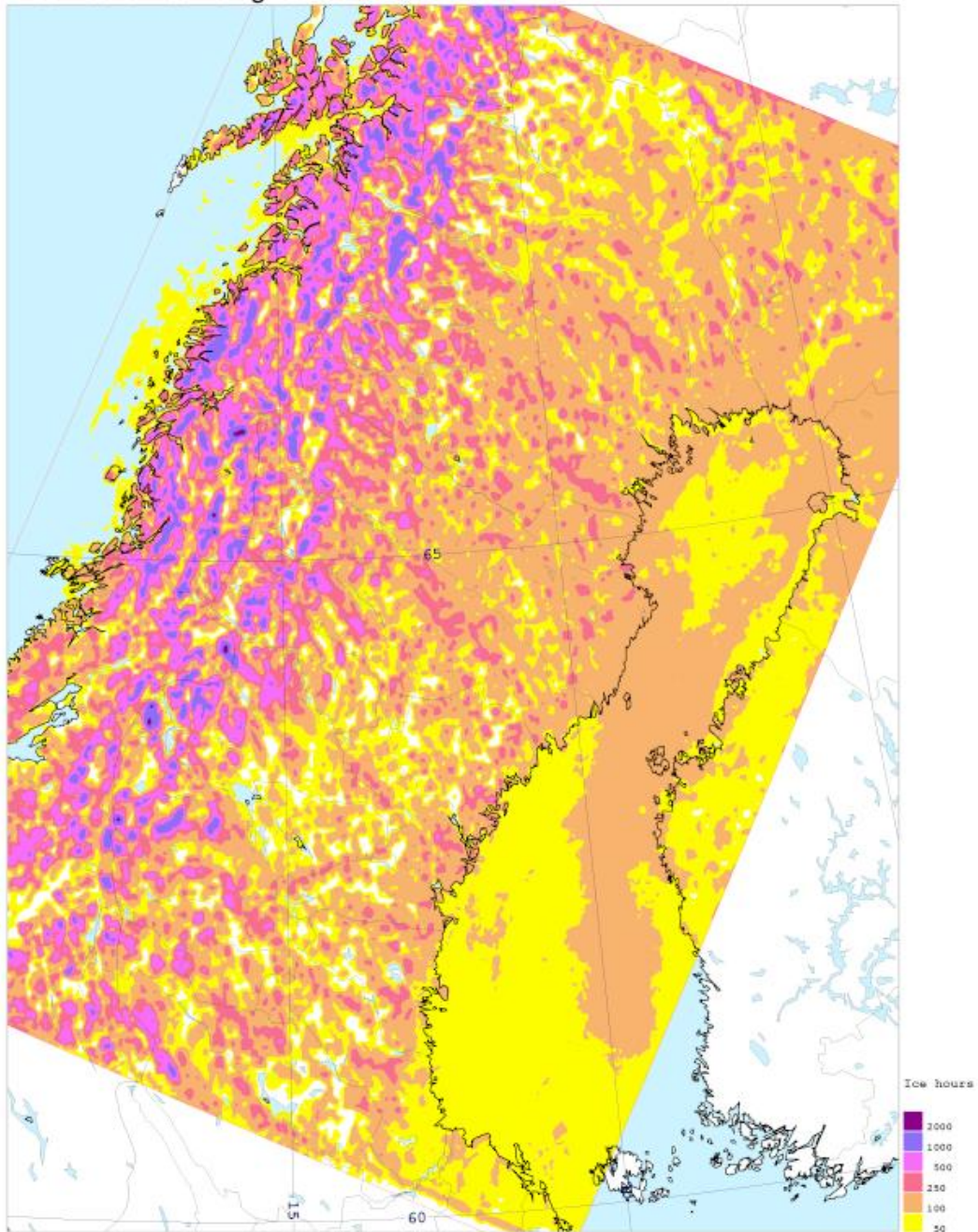


**Figure 5-1: SMHI AROME 2.5 km 2009/2010: Numbers of hours with an ice growth > 10g/hour 100 meters above the model terrain using all condensates.**

SMHI Arome 2.5km  
Ice hours 100m amgl Season 2010/2011

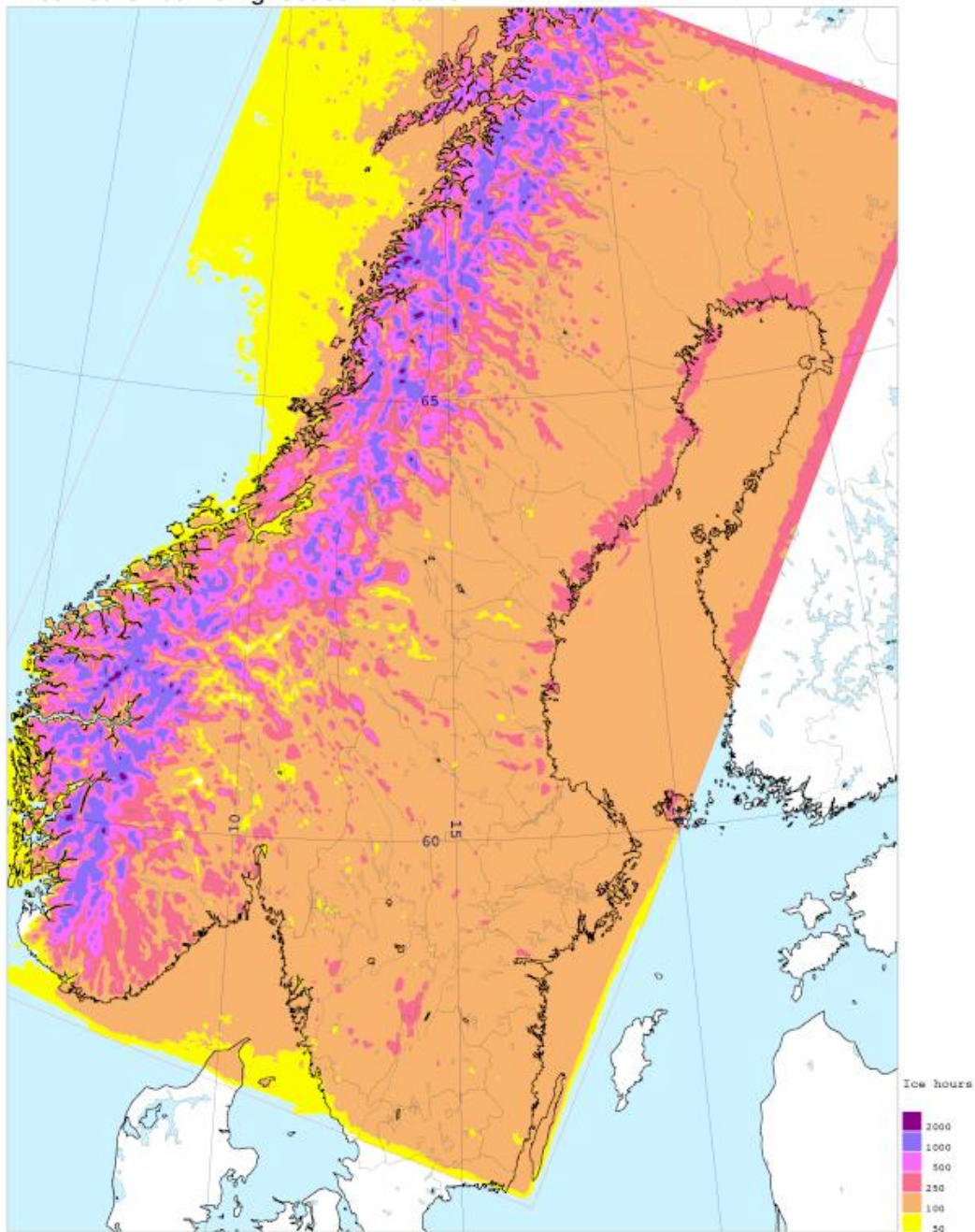


**Figure 5-2: SMHI AROME 2.5 km 2010/2011: Numbers of hours with an ice growth > 10g/hour 100 meters above the model terrain using all condensates.**

SMHI Arome 2.5km  
Ice hours 100m amgl Season 2011/2012

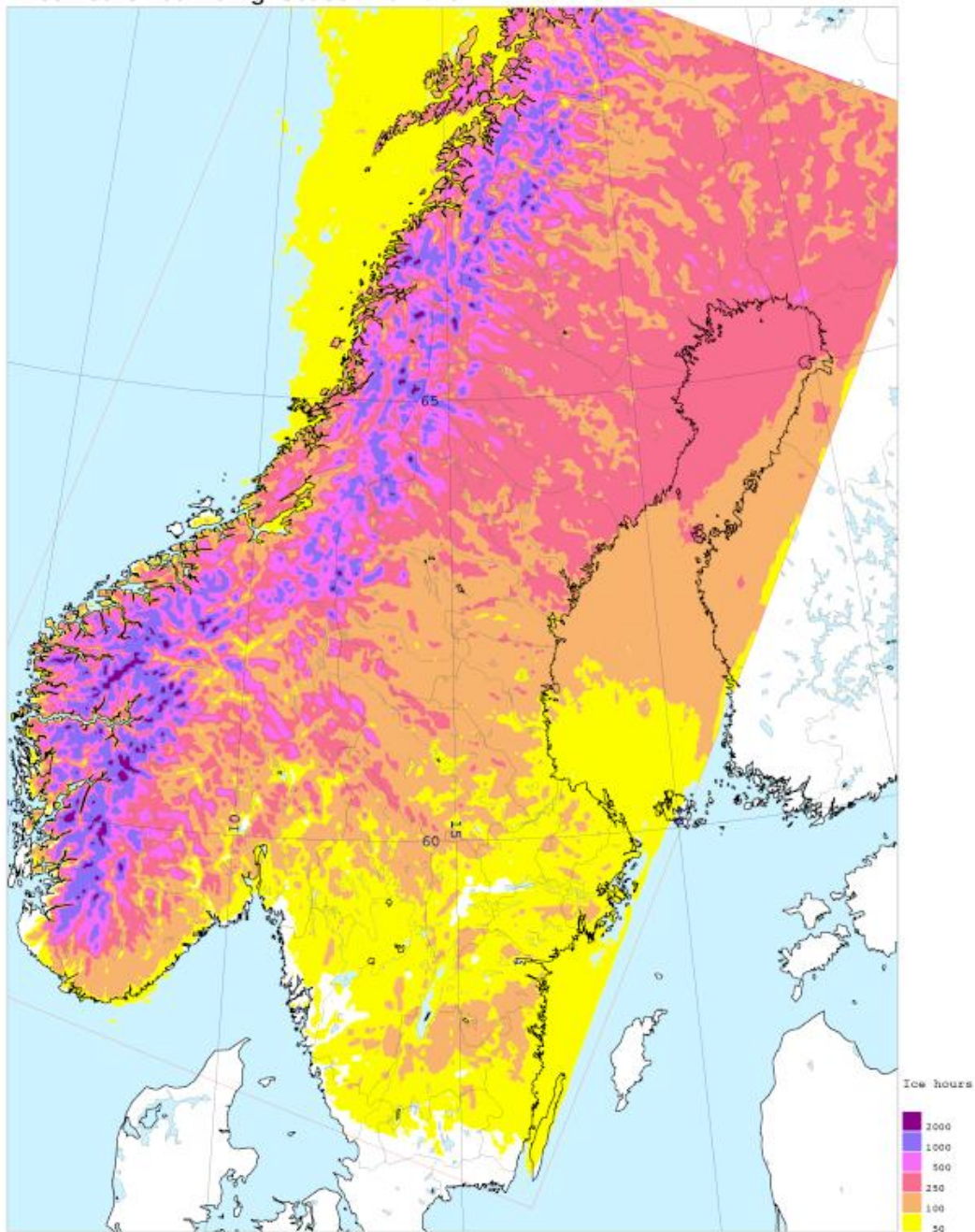


**Figure 5-3: SMHI AROME 2.5 km 2011/2012: Numbers of hours with an ice growth > 10g/hour 100 meters above the model terrain using all condensates.**

SMHI Arome 2.5km  
Ice hours 100m amgl cwonly Season 2011/2012

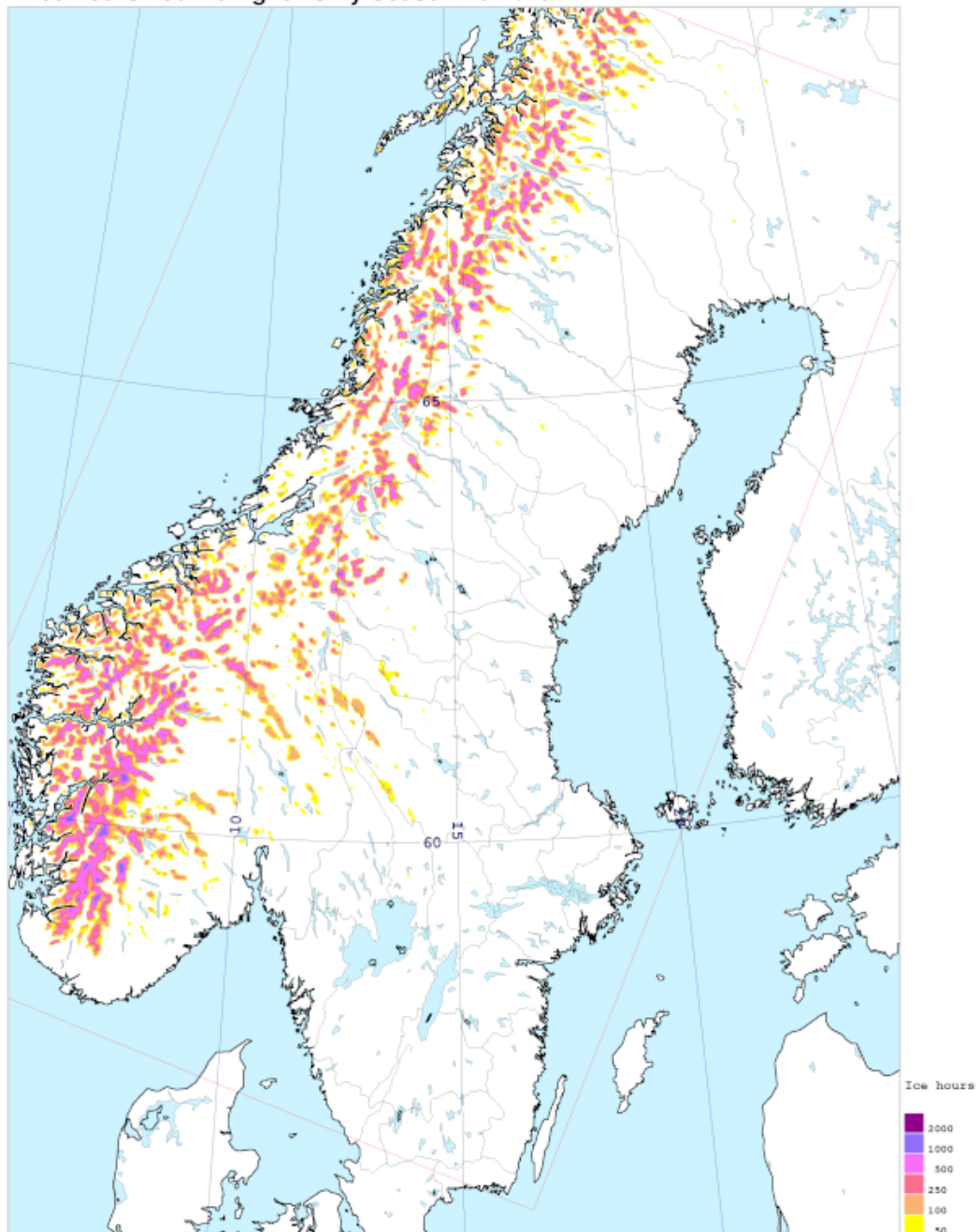


Figure 5-4: As Figure 5-3 but ice load calculated using cloud water only.

## 5.2 COAMPS<sup>®</sup> and WRF 3km

To cover the geographical areas of the observations COAMPS<sup>®</sup> and WRF were set up with different nest configurations over the 3 seasons. The total area covered with the 3km model grid domains are much smaller than for AROME. Nevertheless, similarities and differences can still be found between the model results. Maps from COAMPS<sup>®</sup> model results are shown in Figure 5-5 to Figure 5-7 and from WRF model results in Figure 5-8 and Figure 5-9.

First of all, the number of icing hours is much smaller in COAMPS<sup>®</sup> and WRF than in AROME. In section 4.2.2 it was found that the number of icing hours increased much more for AROME than for COAMPS<sup>®</sup> and WRF when using all cloud condensates instead of only cloud water.

Similar to AROME, a inter-seasonal variation is found with more icing in southern Sweden in 2010/2011 than in 2011/2012 and more icing in northern Sweden in 2011/2012 than in 2010/2011. The highest number of icing hours is counted at the highest mountains and a high correlation between icing hours and topographic height is found.

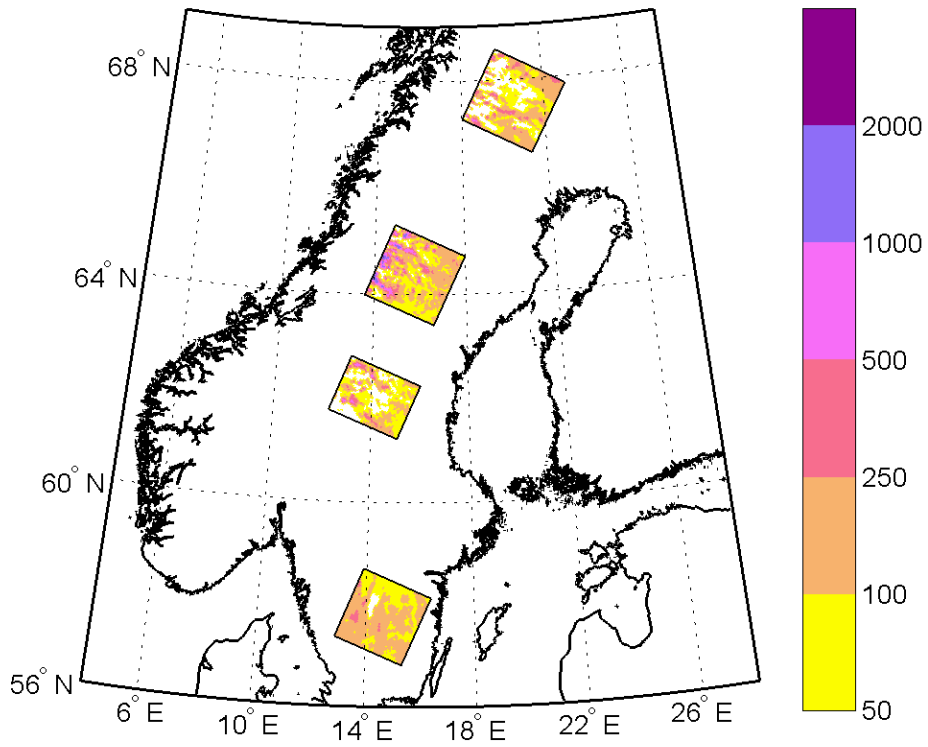


**Figure 5-5: COAMPS® 3 km 2009/2010: Numbers of hours with an ice growth > 10g/hour 100 meters above the model terrain using all condensates.**

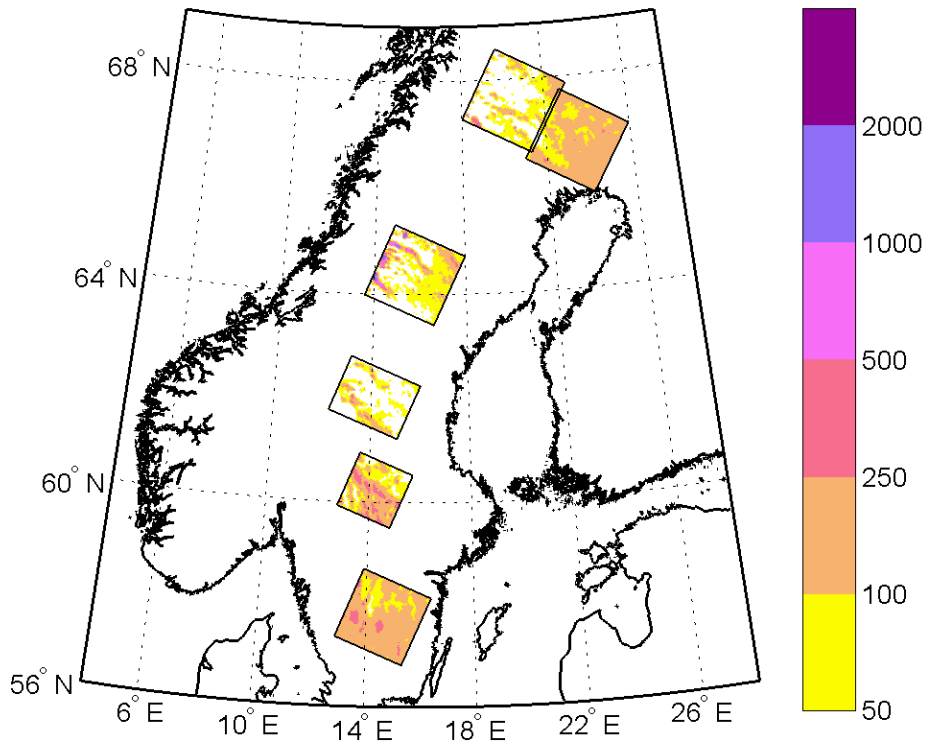


**Figure 5-6: COAMPS® 3 km 2010/2011: Numbers of hours with an ice growth > 10g/hour 100 meters above the model terrain using all condensates.**

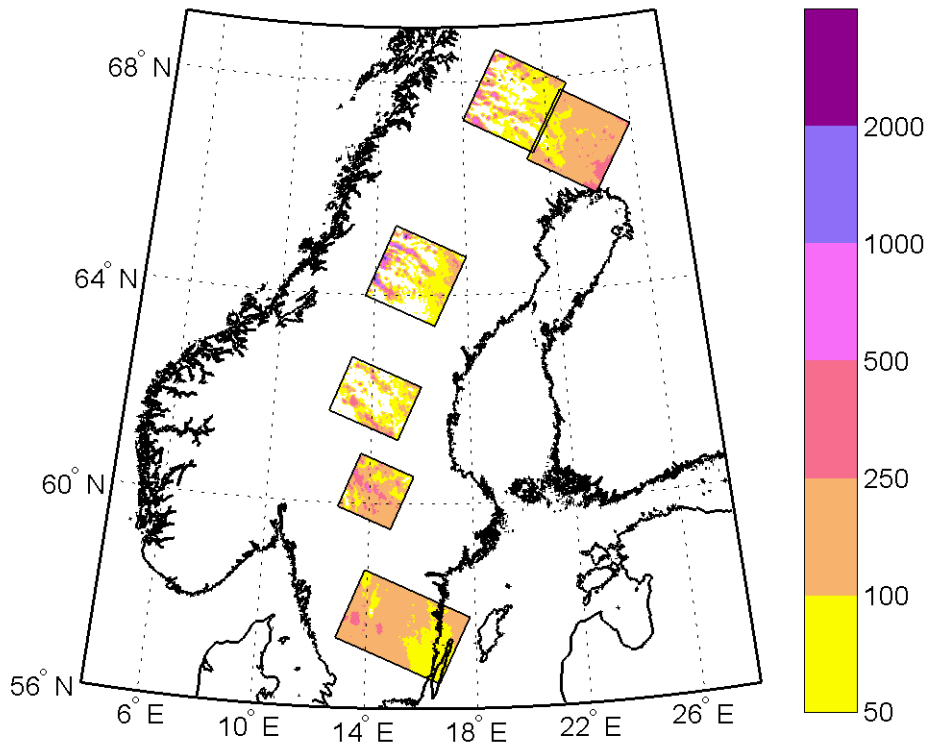


**Figure 5-7 COAMPS® 3 km 2011/2012: Numbers of hours with an ice growth > 10g/hour 100 meters above the model terrain using all condensates.**

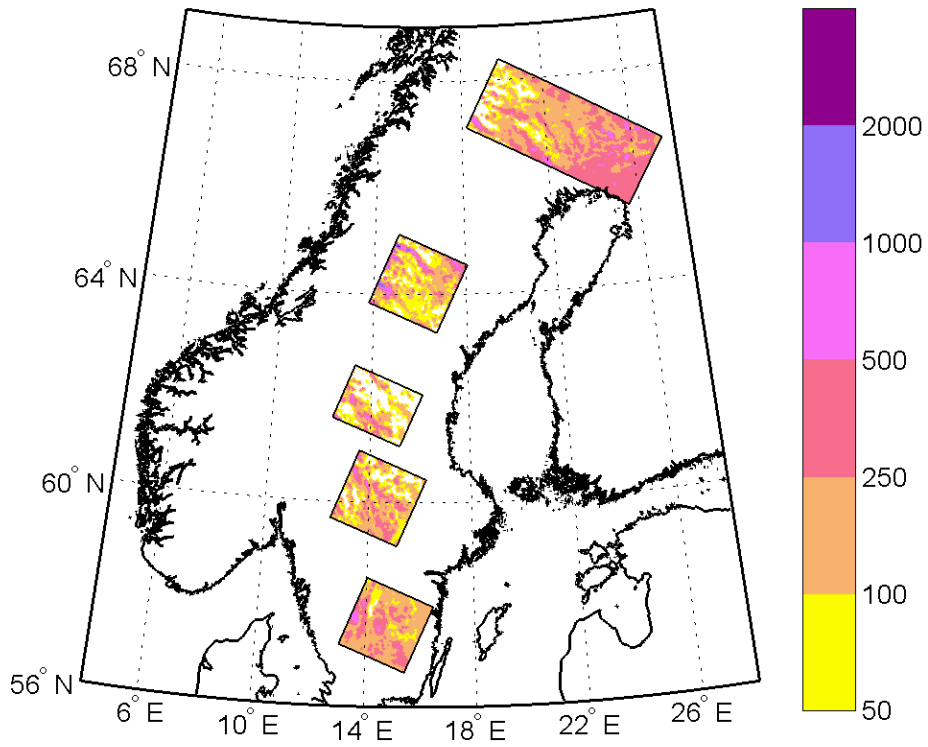


**Figure 5-8: WRF 3 km 2010/2011: Numbers of hours with an ice growth > 10g/hour 100 meters above the model terrain using all condensates.**

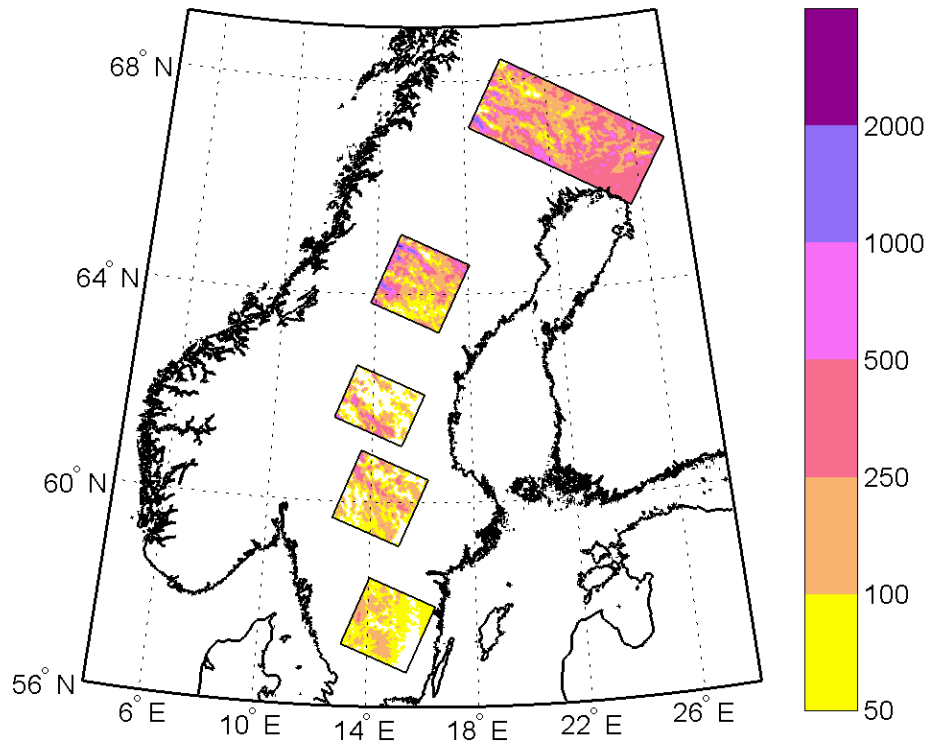


**Figure 5-9: WRF 3 km 2011/2012: Numbers of hours with an ice growth > 10g/hour 100 meters above the model terrain using all condensates.**

### 5.3 COAMPS<sup>®</sup> and WRF 1km

To study differences in the modelled number of icing hours between COAMPS<sup>®</sup> and WRF, one of the 1km nests is studied in more detail.

From Figure 5-3 and Figure 5-4 in section 5.1 we could conclude that AROME is sensitive to if all cloud condensates or only cloud water is used in the ice load estimation. In Figure 5-10 estimations of numbers or icing hours from COAMPS<sup>®</sup> and WRF with all cloud condensates and with cloud water only is illustrated. It is here evident that even though the number of icing hours increase when using all cloud condensates the difference in the maps between the two methods are considerable smaller for COAMPS<sup>®</sup> and WRF than for AROME. The icing is still concentrated to areas with the highest terrain features.

In Figure 5-11 maps of numbers of icing hours and wind speed at 100 m height above model terrain from the WRF forcing sensitivity test are shown. In general the results do not diverge very much other than that NCAR indicate somewhat lighter icing conditions than FNL and WRF; the mean wind speed is also slightly lower.

Using the WSM3 and WSM6 microphysics schemes however alters the results to a large degree. These sensitivity tests produce maps indicating no or only light icing in the studied area. The Morrison scheme produces an ice map similar to the base setup (FNL) with the Thompson scheme. In the mean wind speed maps there are only minor differences.

In section 4.3 it was found that the choice of PBL scheme has a quite substantial impact on the mean wind speed, temperature, and cloud water profiles. In Figure 5-13 we note that using different PBL schemes does not alter the geographical distribution of icing notably compared to FNL. What is changed, however, is the number of hours with active icing in areas with icing conditions.

The sensitivity maps were all presenting icing hours estimated with cloud water only. Figure 5-14 show a map for WSM3 using all condensates in the ice estimates. For this scheme "all condensates" is cloud water and cloud rain, the two mass variables in the scheme. Ice and snow are treated by WSM3 at temperatures below 0 °C but are stored in the cloud rain mass variable. There is a tremendous difference in the estimated icing climate using the WSM3 scheme and all condensates compared to FNL and all condensates, see Figure 5-10, and further emphasises the need for further research on using all condensates in estimations of ice accretion.

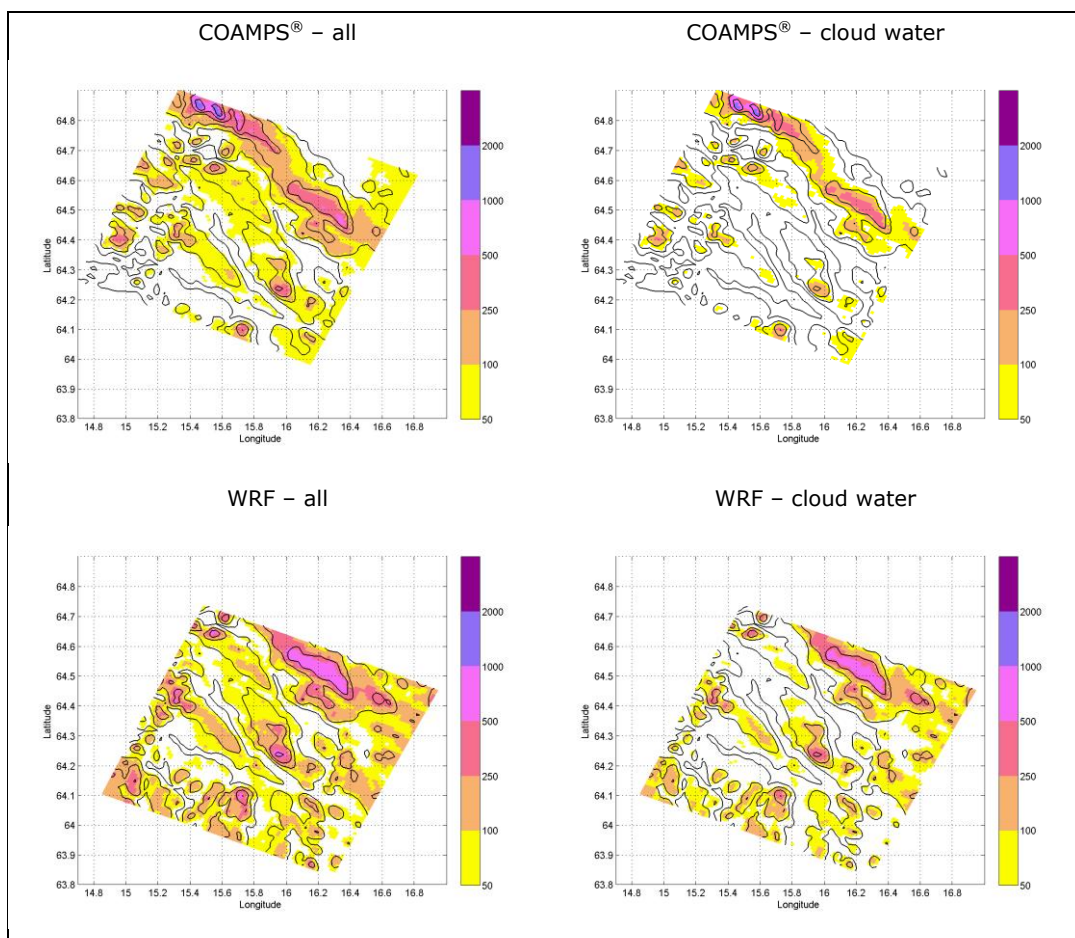


**Figure 5-10: COAMPS® and WRF 1 km 2010/2011: Numbers of hours with an ice growth > 10g/hour 100 meters above the model terrain with all cloud condensates to the left and with cloud water only to the right. Terrain height contours every 100 m in black. Note the differences in geographical extent of COAMPS® and WRF model domains.**

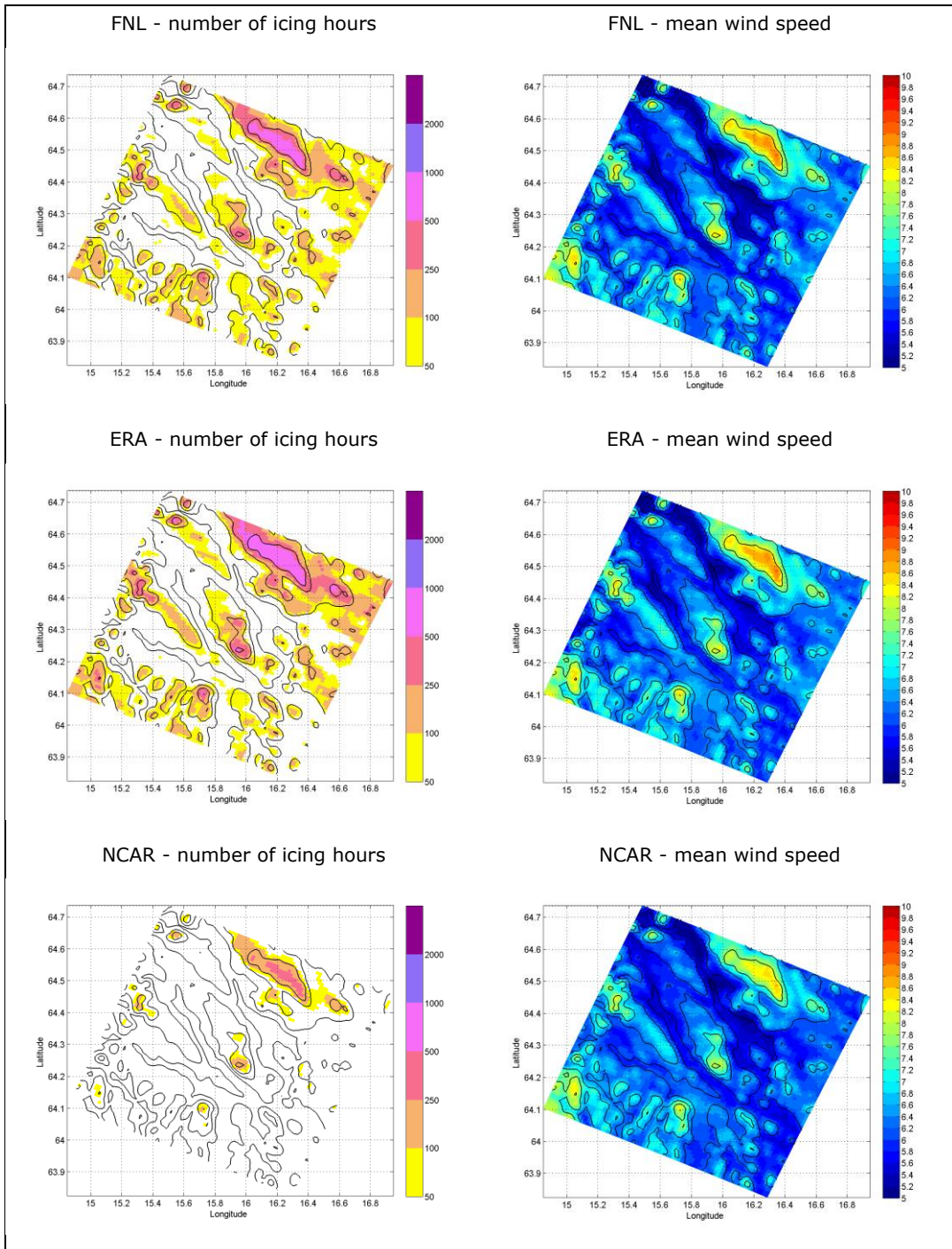


**Figure 5-11: WRF 1 km forcing tests 2010/2011: Numbers of hours with an ice growth > 10g/hour 100 meters above the model terrain with cloud water only to the left and mean wind speed 100 m above model terrain. Terrain height contours every 100 m in black.**

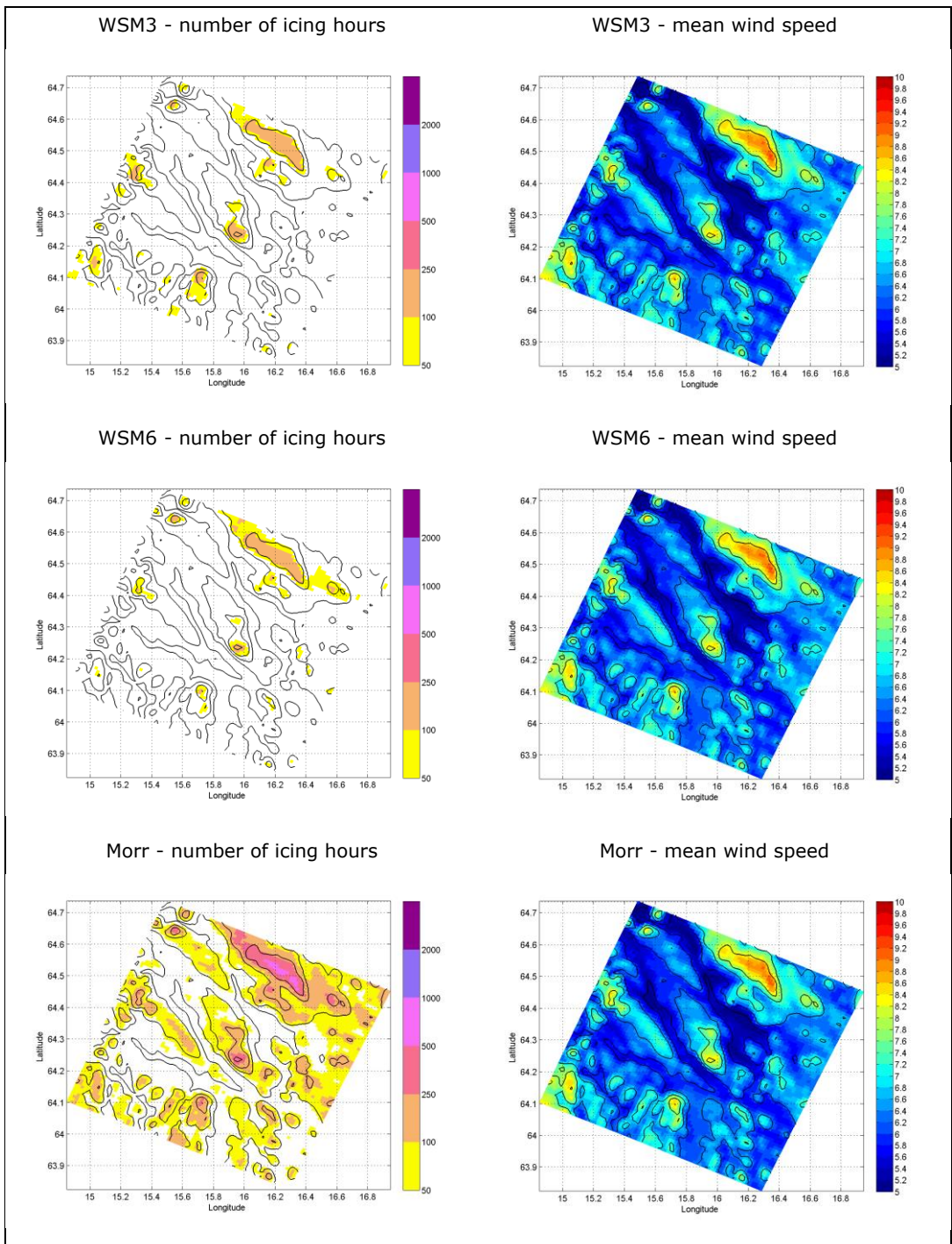


**Figure 5-12: WRF 1 km microphysics tests 2010/2011: Numbers of hours with an ice growth > 10g/hour 100 meters above the model terrain with cloud water only to the left and mean wind speed 100 m above model terrain. Terrain height contours every 100 m in black.**

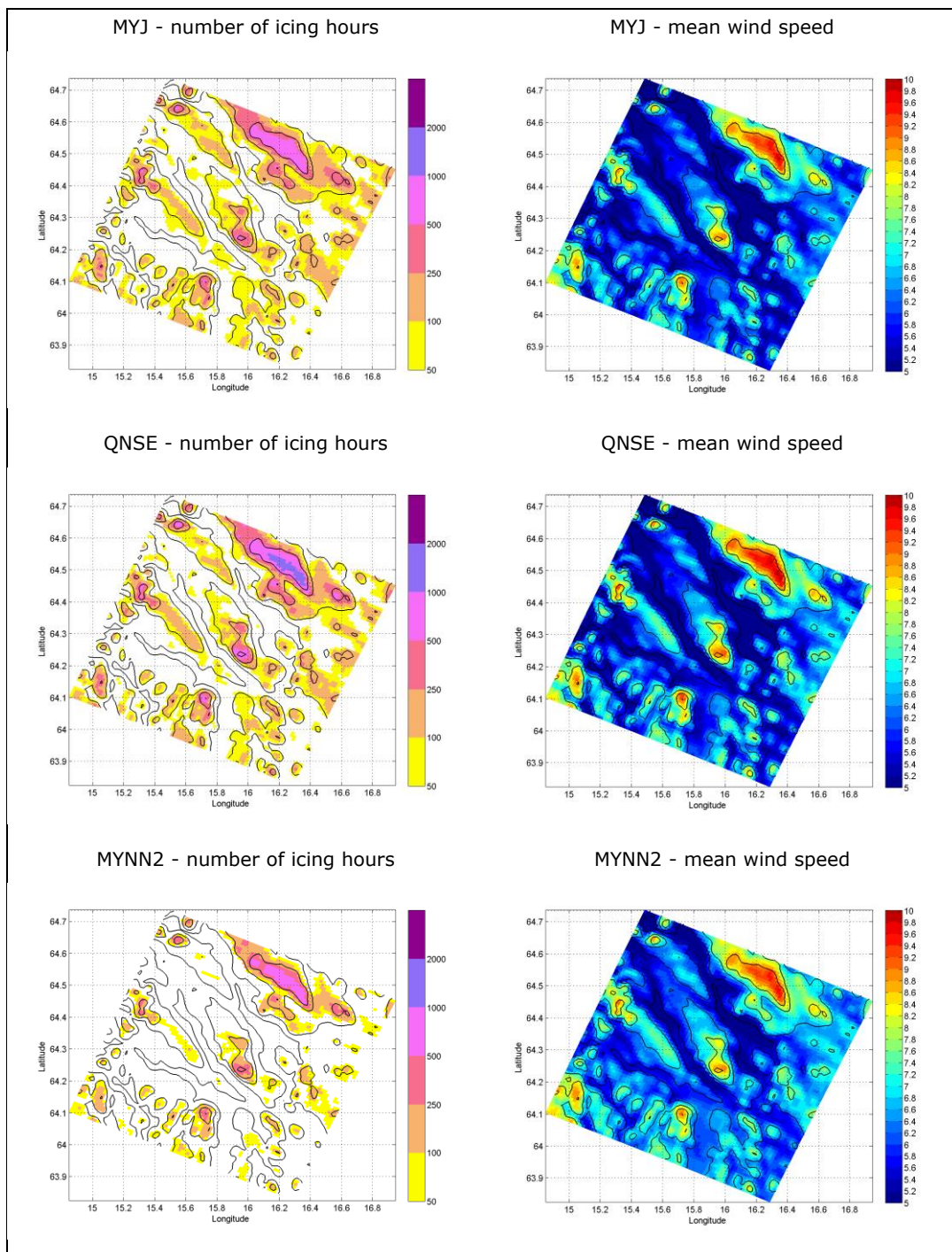


**Figure 5-13: WRF 1 km PBL tests 2010/2011: Numbers of hours with an ice growth > 10g/hour 100 meters above the model terrain with cloud water only to the left and mean wind speed 100 m above model terrain. Terrain height contours every 100 m in black.**

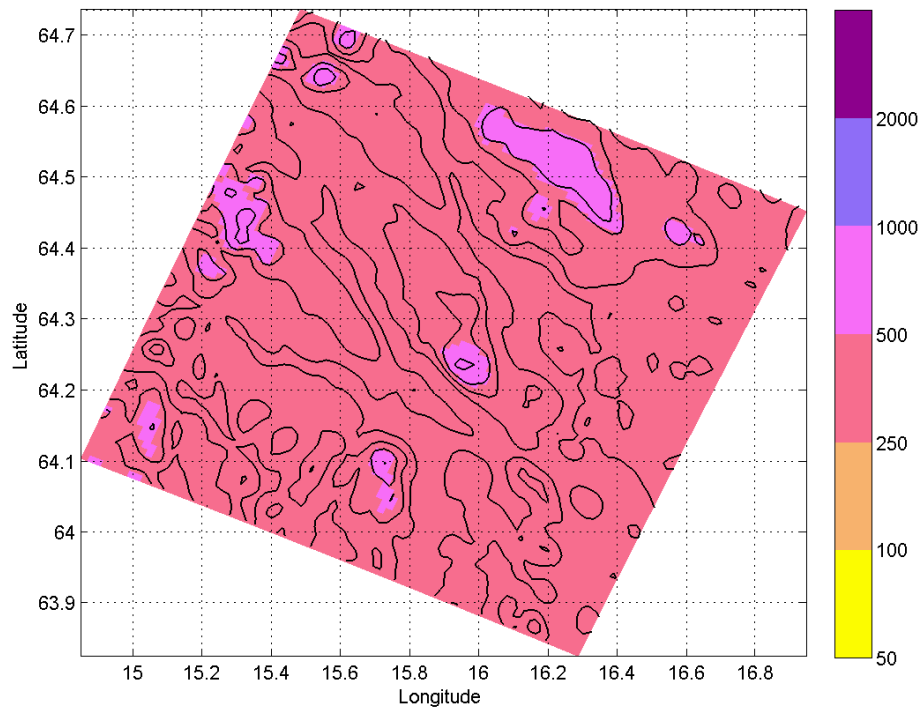


**Figure 5-14: WRF 1 km microphysics test, WSM3, 2010/2011: Numbers of hours with an ice growth > 10g/hour 100 meters above the model terrain with cloud water and cloud rain. Terrain height contours every 100 m in black.**

## 5.4 Summary of Chapter 5

The high resolution model runs for three winter seasons has been summarized on maps showing number of hours with active icing from September to April. Also here the Makkonen ice accretion model has been used with liquid cloud water only and also using all cloud condensates. All calculations are done at 100 m height above the model topography; no lifting was applied to adjust for differences between model terrain and the real topography. When the icing rate exceeds 10 g/h on a 1 m tall cylinder with 30 mm diameter this is counted as an icing hour.

The maps show a relation between topographic height and icing hours. In particular it is the local differences in terrain height that are of importance, more icing is found on hilltops than in valleys. It is found that the maps show a high inter-seasonal variation in the numbers of icing hours. Not only in the number of icing hours in a single point but also in which part of the country that most icing is found. This understanding is of importance for choosing a method to create an icing climatology.

As with the site-specific calculations there is a big difference in the AROME results between cloud water only and using all species. The model runs for COAMPS<sup>®</sup> and WRF cover smaller areas than AROME but the results show similar features concerning height dependence and inter-seasonal variations. On one of the 1km areas the differences in icing hours between COAMPS<sup>®</sup> and WRF has been studied in more detail. Also in these runs the number of icing hours is greater using all condensates in the icing calculation but the difference is not as big as for the AROME model. Sensitivity tests with different WRF microphysics and PBL schemes shows big differences in number of icing hours in agreement with the findings in section 4.

## 6 Modelling the icing climate

The term climatology in meteorology usually means statistics over 30 years of data and usually in the form of direct or indirect measurements, as discussed in Section 2. This length of period is for standard meteorological variables and agreed internationally with the context of the World Meteorological Organisation (WMO). Modelling 30 years of icing using  $1 \times 1 \text{ km}^2$  resolutions would need huge computer resources why alternative methods are investigated.

As an icing climatology is a derived quantity from several variables. The required length of the climatological period is basically unknown. It depends to a large degree on the user requirements, how important the extreme events are. In the end, it is the worst possible production loss scenario, which is of interest, and that is an even more complex function of days of icing and ice accumulation as well as ice shedding, variables that can be computed albeit with uncertainties described in the previous sections.

Since there will never be any complete or comprehensive measurements of these variables, they have to be model generated from sophisticated meteorological prediction models. This has been discussed in Section 2.

The concept of climatology is further complicated by the fact that the climate itself drifts and is accentuated by the current observed and predicted changes. One may thus also decide to use future climate scenarios that have been derived by many modelling groups in the world. So far we are however mostly interested in the "current" climate.

In this section we illustrate the effect of using shorter time periods than 30 years and a few different methods of deriving climatologies based on coarser resolution models for which long time periods are possible.

## 6.1 Using representative months or periods

One alternative to overcome the limited time period of simulation is to sample the climate from certain "representative" periods during the 30 years. The assumption is that by sampling from sub-periods during the full 30 year data records (observations or re-analysis) the full statistics can be represented accurately enough by carefully chosen sub-periods.

For the FMI wind atlas some 19 years of wind data from 9 stations have been used to find the best years for each month that can describe the wind distribution for the full period. The commonly used Weibull distribution has been used and the fitting has been done on the two parameters in that distribution and the wind direction. It is thus not the average wind that was aimed for, but the mean distribution, i.e. the right mixture of weak, average and strong winds. For each month the four best years were chosen in order to arrive at the four years to be simulated with the high-resolution meteorological model.

FMI has also made an icing atlas but due to perhaps lack of strong alternatives and resources to run the model for many other years, the same years as for the wind atlas have been used. The underlying assumption and hope is that the wind climate distribution and the wind direction climatology and the calendar month are adequate to estimate the icing climate. This approach does not take account of temperature and especially liquid water content. Only the wind has determined the choice of months.

Since the icing climate to a large degree depends on three variables, wind, temperature and cloud water, it is not enough to choose the distribution of only one of them to represent the complex combination. As will be shown in this section, the representative months are different for ice versus the ones for temperature or wind. Some suitable methods will be demonstrated here and in 6.2.

Another way of deriving an approximate icing climatology has been made by Kjeller Vindteknikk. A high resolution (1 km) run has been made for one year and the results indicate occurrences of icing, much depending on that year, of course. A normal year correction has been applied with respect to the 10 year low resolution (5 km) climate, analogous to what has been applied for wind climate. The method is however more uncertain for the more complex icing variable, but it may be improved in the future.

In the V-313 project we want to do a bit more than this. We do not have the constraint of any simultaneous wind climatology so the distribution of wind speeds is not the only criterion. Wind speed is important in the Makkonen formula, but the cloud water has been crucial for the amounts of icing modelled in this project. It has been shown that icing diagnostics from the 80 km gridded ECMWF ERA-Interim re-analysis are quite realistic in terms of episodes of icing. The large-scale circulation is what is very well described in the re-analyses whereas the local orographic effects on the flow and height differences are not accounted for. That is where the meso-scale models come in.

In the climatological literature various flow patterns or flow regimes are frequently used. The long time series of also a spatial extension can be decomposed into the different flow regimes. In Northern Europe the winter

weather is very different in the case of cyclonic westerly flow (mild and rainy) as opposed to anti-cyclonic and easterly flow (cold and dry). Such flow patterns and several more classes in between can be determined from sea level pressures in a relatively coarse grid. Over larger areas like the Europe-Atlantic or Northern Hemisphere EOF based methods are often employed, but the outcome is similar but less detailed than the regional method (like for Scandinavia).

In the V-313 project we have tried to find the most representative years for each month, in some way analogous to what FMI did for the wind distributions. Here we have looked at 30 years of number of days in each flow pattern class and then found for each month the year that is most similar in its distribution over classes as the full 30 years. Note that for different months quite different years are usually found. Like in the FMI case we do not propose to run any complete year but rather compose a typical year from individual months from various years. Also here the sampling can be improved by choosing additional samples for a month from other years that improve the sampling.

A disadvantage with representative years, as explored in V-313 and utilized by FMI, is that it to a high degree leads towards mean conditions and not the extremes. Ways of extrapolating extremes from a relatively short period data set may be employed but introduces new uncertainties.

#### 6.1.1 Comparison between different representative period methods

There are several existing methods in which a shorter time period can be extended to represent the long-term climate. In the present study, some of these methods are examined, such as using the random day method or five consecutive years to represent 30 years. These two methods have been tested together with a new method, which tries to find the best fit to the long term mean with a low resolution data set in two different ways. Altogether there are four different approaches to create a climatology compared in this study.

All the methods have been tested on the long term means of temperature, wind speed and ice (icing rate and ice load) in two data sets, one low and one higher resolution. All the methods are first tested on the ERA Interim data set. The methods that show a good agreement with the long term mean are then tested on a 9x9 km<sup>2</sup> WRF data set. WeatherTech Scandinavia has used the WRF model to downscale 30 years of NCEP/NCAR reanalysis data on a 9km model grid covering Sweden, Finland, Norway, Denmark and the rest of the Baltic Sea shorelines. This downscaled dataset consists of hourly values of all common meteorological parameters including temperature, pressure, wind, humidity, cloud water etc., making it a suitable data source for studying the climate.

All of the comparisons are done on a monthly basis; longer time periods will not be presented here.

#### **Presentation of the different methods**

As previously stated a total of four different approaches to construct a climatology have been tested: the random days method, the five consecutive

years method and two best fit approaches. The best fit method is a new method using the best fit of monthly means to the long term means. This method is adaptable, it can be used with different parameters and has been tested with both one parameter and two parameters. One approach uses the best fit of Lamb classification and one using the best fit of temperature and wind speed. To differentiate between these two methods the best fit of Lamb classification will be called the Lamb class method or Lamb classification method and the best fit of temperature and wind speed will be called the best fit method. All of the methods tested will be described in further detail in the following sections.

#### *Random days*

The random days approach is commonly used for creating estimates of the wind for wind power purposes. A random month is created by choosing from the complete data set a random day to represent that day in the data set. To create a random January month, a random 1st of January is chosen from the complete data set, then a random 2nd of January and so on until there is a complete random January. This method has been slightly modified from a method previously used to assess the wind climate of potential wind power sites.

#### *Five consecutive years*

The five consecutive years method has previously been suggested as a possible method to create an icing climatology. Using five consecutive years to estimate the climate is an interesting approach since modelling only five years would save time and resources.

To study this method, five consecutive years have been modelled with both data sets, in ERA Interim and for WRF five 5 year climatologies were created (1985-1989 to 2005-2009). Here only two such periods will be presented, 1990-1994 and 1995-1999.

#### *Best fit approach: temperature and wind speed*

The best fit method is a novel approach to create a climatology. The monthly means for each year and month are compared with the corresponding long term mean in a low resolution data set (here the ERA Interim). For each latitudinal band the years that have the best fits are saved, creating five representative months where the best fit for a latitudinal band is saved. The first month contains the bands with the best fit, the second with the second best and so on. As one year can be the best fit for a number of bands the five most common bands/years are chosen as the years which are the most representative of the long term mean. This method can work for a single or several parameters. Here the method have been tested on the best fit of both temperature and wind speed. The difference between the long term mean temperature and the monthly mean temperature is added to the difference between the long term mean wind speed and the monthly mean wind speed. The years chosen by the method can be seen in Table 6-1. The chosen years will be used in a higher resolution data set for further comparison.

**Table 6-1: The years chosen as best fit to the long term mean in regards to wind speed and temperature.**

Month	Best year	2nd best	3rd best	4th best	5th best
January	1988	1994	1995	1999	2002
February	1992	1987	2009	1981	1999
March	1982	2004	2002	1999	1983
October	1989	1996	2004	1990	1999
November	1985	2004	2008	2007	1994
December	1990	2005	1987	1989	1993

In the approach presented here five years are chosen, however one can choose more or fewer years depending on preferences. The main reason why five years are chosen is to be comparable to the five consecutive years method. Another aspect is that the more years chosen, the more accurate is the method. However chose too many years and the benefit of only having to model a few years is lost, see Figure 6-1. For each additional year used there is an improvement, though the gain is smaller as the number of years used increases. This will be discussed further in section 6.1.5.

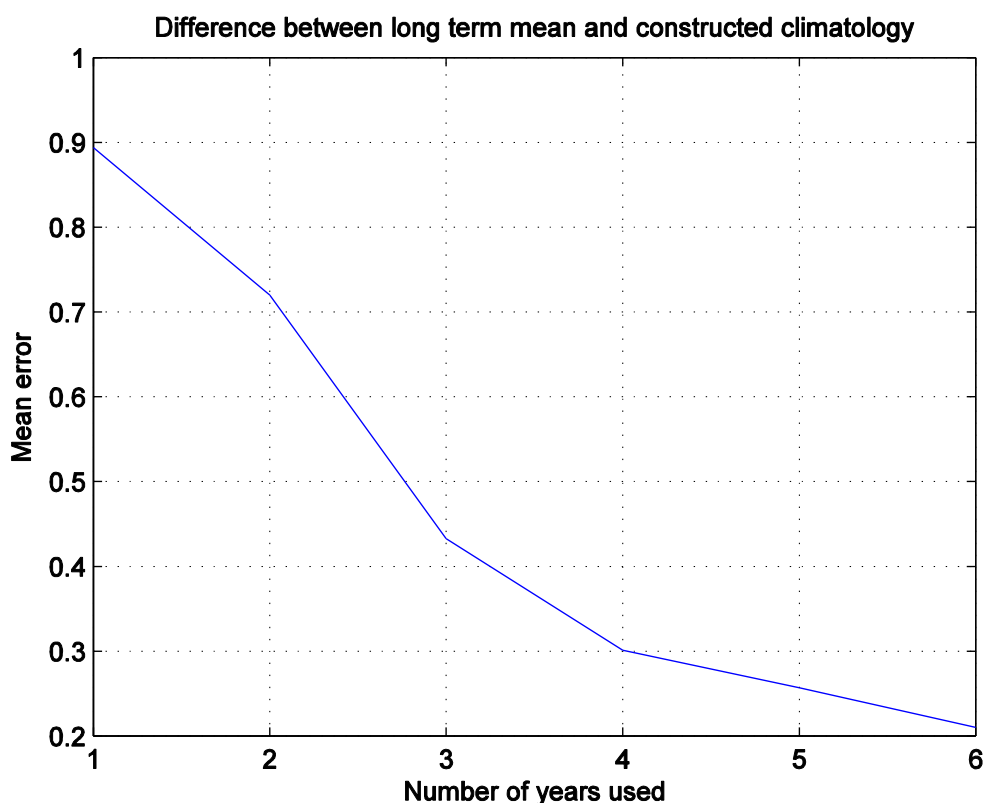


**Figure 6-1: Example of the "improvement of error" (absolute value) for the reconstructed wind climate with the number of years used, here for March. Difference between long term mean wind speed and constructed mean wind speed. Note that the method used here uses the best fit of both wind speed and temperature.**

*Best fit approach: Lamb classes*

The Lamb classification is a commonly used weather classification based on the pressure and circulation type. To test this approach Sweden has been divided into three parts, northern Norrland, southern Norrland and Götaland/Svealand. In this study the southern Norrland area have been used, which in theory should mean that the best match to the long term climate is in this area. The Lamb classification scheme divides the circulation into one of 27 different classes. Two are pressure classes (cyclonic, anti-cyclonic), eight are circulation types (northerly flow, north-westerly flow, westerly flow), 16 are hybrid classes (i.e. anti-cyclone with westerly flow) and one unclassified.

The Lamb class approach is similar to the best fit approach for temperature and wind speed, but it uses Lamb classification instead. Each day in the ERA Interim data set have been classified in accordance with Lamb. From this a long term distribution for each month has been calculated as well as a monthly distribution. The five years that have the smallest differences between the long term distribution and the monthly are chosen to represent the whole period. The chosen years for each month can be found in Table 6-2.

**Table 6-2: The years chosen as best fit to the long term mean in regards to the Lamb classification.**

Month	Best year	2nd best	3rd best	4th best	5th best
January	1998	2010	1988	1991	2004
February	1983	1986	1991	1997	1998
March	1981	1983	1996	2004	2009
October	2008	1982	2002	2004	2006
November	1994	1990	2003	1989	2007
December	1986	1988	2001	2002	2005

### 6.1.2 Modelling the icing

The icing modelling is done with Makkonen equation described in section 4.1. Here the liquid water content that is needed in the Makkonen equation is calculated using an equation from Mazin (1995) for the median cloud water content:

$$\log_{10} w_m = -1.03739 + 0.03130T \quad (14)$$

where  $T$  is the temperature in °C and  $w_m$  is in g/kg. This is used for both the data sets for consistency as the ERA Interim data set used here lacks cloud water.

For both the data sets the icing rate is calculated and classified for light, medium, heavy and very little to no icing. Areas where there is light, medium and heavy icing are areas where the icing exceeds 10 g/6h (light), 15 g/6h (medium) and 20 g/6h (heavy) for the ERA Interim data set 10 times during a month. For WRF the limits are kept the same as for ERA, but since the temporal resolution is higher the limit for icing is 20 times per month instead.

It should be noted that the areas where there is heavy icing might not always be the same as where the greatest ice loads are found. An area can suffer from one heavy icing event that then melts away, so that the ice loads in that

area are small. Likewise, an area with large ice loads might be subject to small icing events that are persistent and due to low temperatures the ice can accrete for a long time. To get a correct grasp of atmospheric icing it is important to understand this difference and consider the implications of both.

### 6.1.3 Comparison between the different methods

#### **ERA Interim data set**

All of the methods will first be tested on temperature and wind speed. If the method can reconstruct the long term climate for these two variables the icing rate and ice load will be modelled and the method tested on a data set with higher resolution. The results for the ERA Interim data set can be seen in Figure 6-2 to Figure 6-5. Due to practicality only the results from November will be shown in the maps, but all of the results will be described.

The long term means of temperature and wind speed can be seen in Figure 6-2 and Figure 6-3, top left corner. All of the long term mean temperatures exhibits a similar pattern. The colder air is mostly located in the eastern area (Finland and the Baltic countries) and the warmer air is mostly over the sea. For some months there is colder air over inland Sweden (e.g. February, November and December). For the wind speed there is a clear pattern that is present for most months. The lower wind speeds are centred over the Bay of Bothnia, with a local minimum located in southern Norway and western Sweden in some of the months, as can be seen in Figure 6-3 (long term wind speed - top left corner) for November.

The ice load can be seen in Figure 6-4 and the icing rate in Figure 6-5. All of the months are subjected to icing, but some months less than others. For October the mean ice load is very small, at most about 60 grams, and for the icing rate there is only the "very little" ice class present (not shown here). For the other months the icing amounts and ice load patterns are similar to that in November.

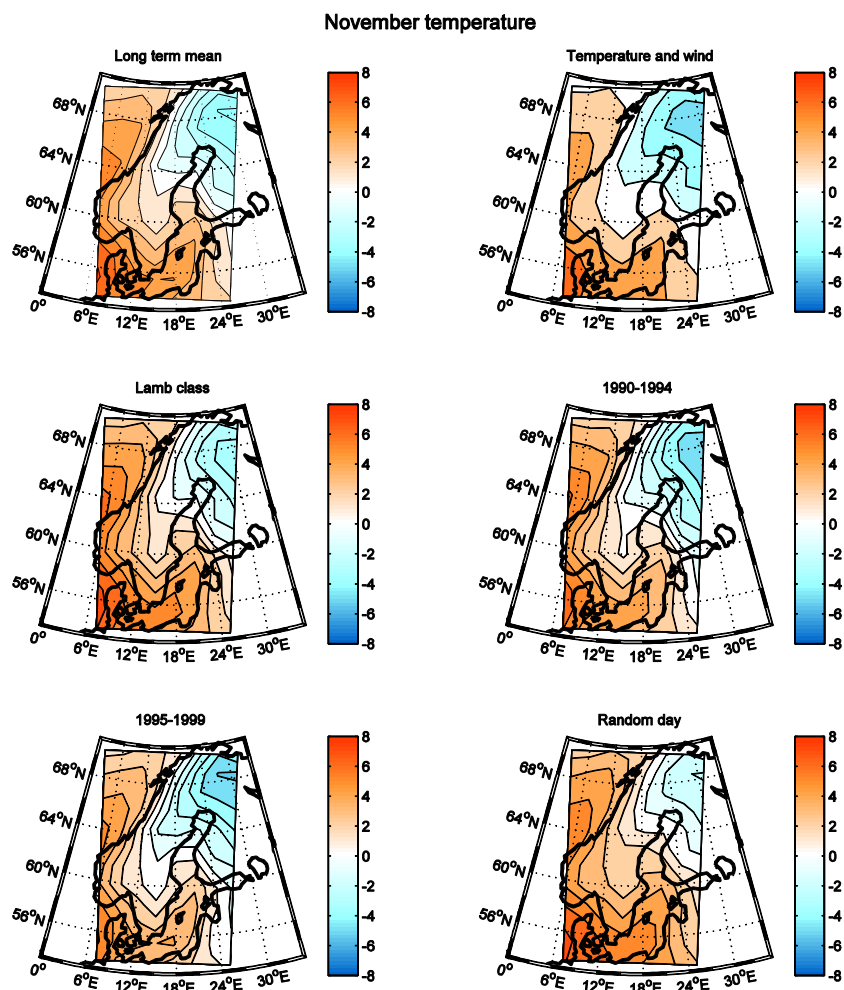


**Figure 6-2: Temperature from the ERA data set, November. Long term mean temperature - top left. Best fit method - top right. Lamb class method - middle left. Five consecutive years 1990-1994 - middle right. Five consecutive years 1995-1999 - bottom left. Random day method - bottom right.**

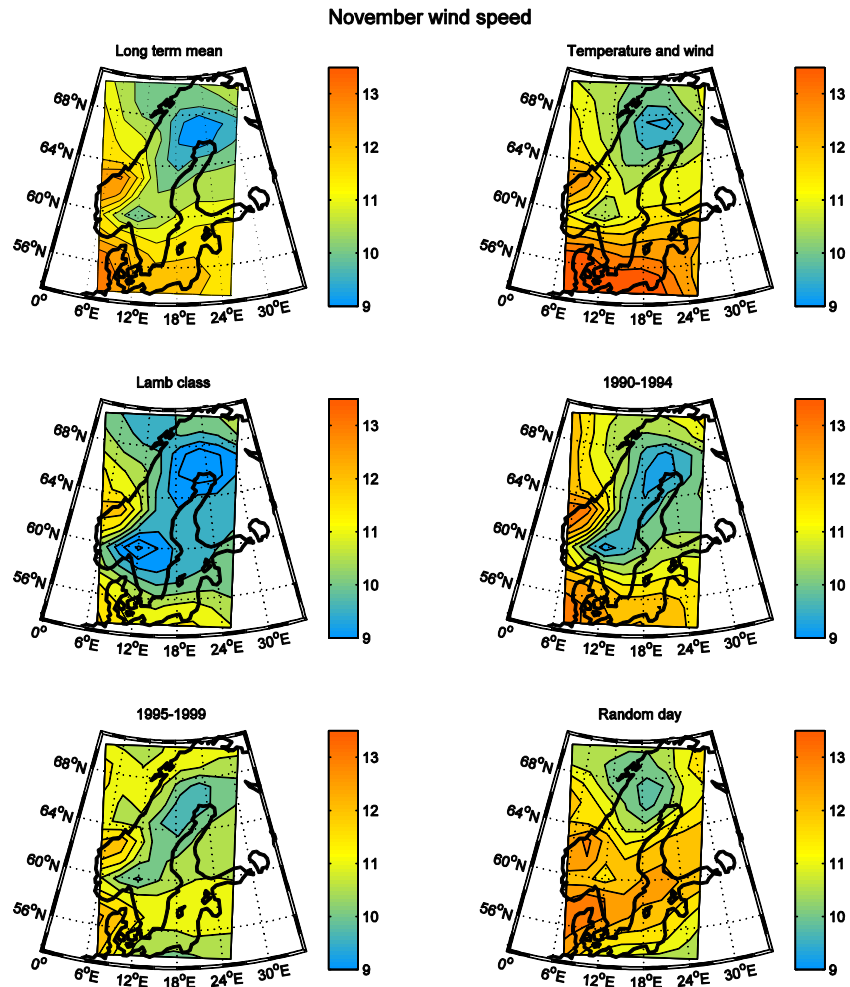


**Figure 6-3: Wind speed from the ERA Interim data set, November. Temperature from the ERA data set. Long term mean temperature - top left. Best fit method - top right. Lamb class method - middle left. Five consecutive years 1990-1994 - middle right. Five consecutive years 1995-1999 - bottom left. Random day method - bottom right.**

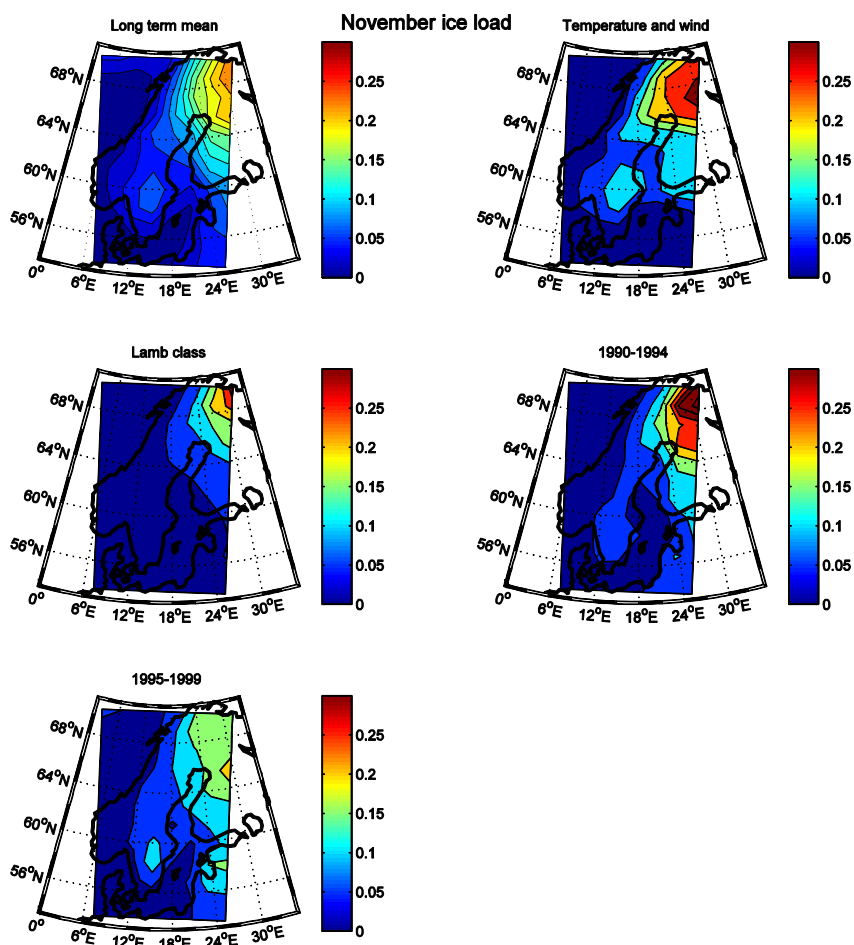


**Figure 6-4: Ice load from ERA Interim data set, November. Temperature from the ERA data set. Long term mean temperature - top left. Best fit method - top right. Lamb class method - middle left. Five consecutive years 1990-1994 - middle right. Five consecutive years 1995-1999 - bottom left.**

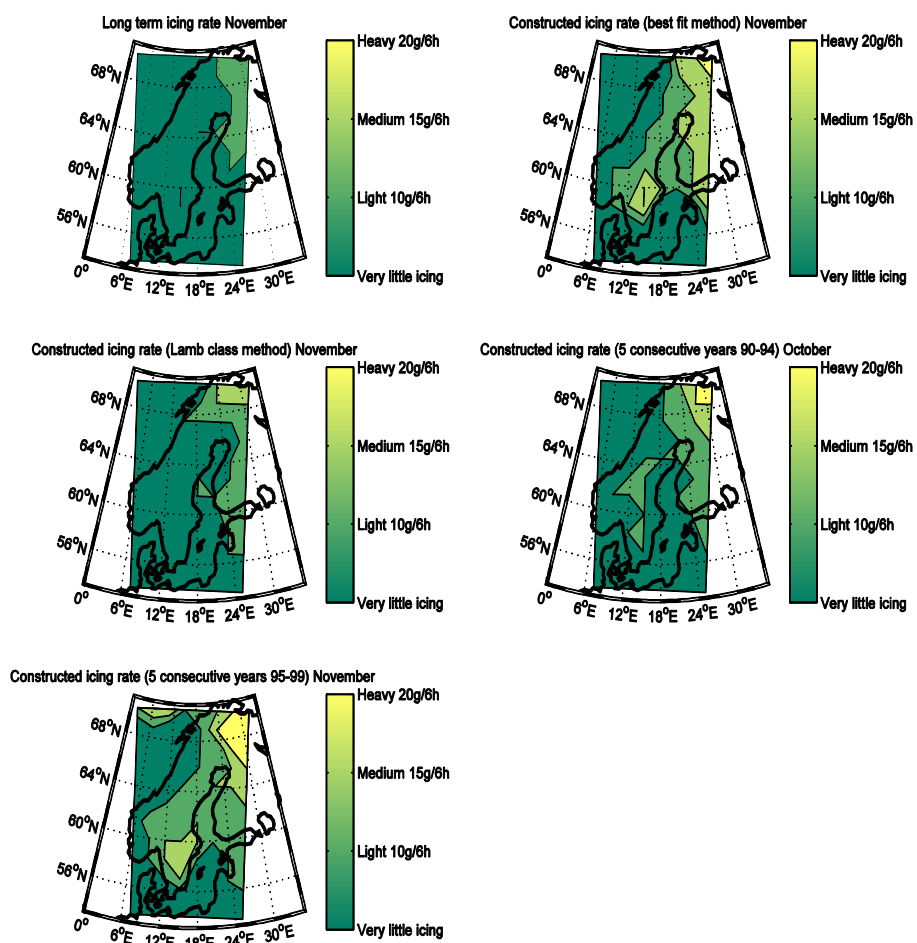


**Figure 6-5: Icing rate from ERA Interim data set. Temperature from the ERA data set. Long term mean temperature - top left. Best fit method - top right. Lamb class method - middle left. Five consecutive years 1990-1994 - middle right. Five consecutive years 1995-1999 - bottom left.**

*Best fit of temperature and wind speed*

The method using the best fit of temperature and wind speed shows a good agreement with both long term means, better with temperature than with wind speed. There is good agreement between the constructed temperature mean and the long term mean for most of the winter months. The temperature pattern is captured very well for all months. In some regions there can be some slight over- or underestimations of the temperature, but this method captures the temperature quite well. In Figure 6-2 the constructed mean temperature for November can be seen in the top right corner. For November there is a good agreement between the long term mean and the constructed mean with this method, but a slight underestimation of the temperature in the northern areas.

The constructed mean wind speed has a good agreement with the long term mean, and captures most of the features in the pattern well. The constructed mean wind speed misses the local minimum over southern Norway and western Sweden for January and October, but in general the pattern features the maxima and minima correctly. For November there is a good agreement between the long term wind speed and the constructed wind speed for this method, see Figure 6-3. The pattern is captured very well and both the global and local minima are captured, though the constructed mean overestimated the wind speed in the southern Baltic Sea with this method.

Compared to the long term mean ice load the constructed ice load is comparable for some months in pattern and for some in amount. Overall this method can capture where the icing is occurring and gives some information on the amount. During some months are captured relatively well, for March this method captures in what area there is ice and the amounts. For November, Figure 6-4, there is a good agreement between the long term ice load and the constructed ice load. The method can capture in which area the largest ice loads are, but slightly overestimate the loads.

The icing rate is overestimated compared with the long term mean, though it is interesting to notice that there are consistencies in some of the patterns for the months. For January the long term icing is mostly located over the Fennoscandian land areas and the Baltic, as is the constructed icing rate even though it's overestimated. The constructed icing rate for November is overestimated (Figure 6-5 top right).

### *Best fit Lamb classes*

For the Lamb classes the temperature is captured well in pattern, but with a slight under- or overestimation for some of the months. October is captured very well with this method, though there is a slight overestimation over the southern Baltic Sea. For November, seen in Figure 6-2, the temperature pattern is captured very well for November with this method.

For most of Sweden the wind speed is severely underestimated compared with the long term mean wind speed. The pattern of the wind speed is captured poorly with this method. For November the wind speed is much underestimated, the two minima are captured, but covering almost all of Sweden (Figure 6-3, middle left).

The corresponding ice load is comparable to the long term mean ice load for some of the months, March especially. For some of the months, January and February, the constructed climatology shows icing in the southern part of the domain, which isn't there in the long term climatology. The November ice load (Figure 6-4) overestimates the largest ice loads and underestimates the extent of the area.

The icing rate for the Lamb class method doesn't match the long term icing rate very well for some months. The icing rates are overestimated for most months, the only month captured well is October, but since there is virtually no icing in this month that isn't a surprise. Though the constructed icing rate can capture the areas where the icing is occurring for November.

One reason that could explain why the Lamb classification method doesn't capture the wind speeds well could be that the Lamb classifications for a month in the data set tend to be very similar. A quick overview of 30 years of Lamb classification has shown that few types dominate the circulation and all the other types are rare. This homogeneity makes the months very difficult to distinguish from each other and thus some months that are chosen might not give a good result for the climatology in regards to temperature, wind speed and ice. A simple study showed that two months from different years with very similar circulation patterns have very different mean temperatures. Thus finding the best fit for the circulation might not ensure a good fit for other meteorological parameters. So while the Lamb classification might not be a good option for creating an icing climatology the classification can be very useful for other applications.

### *Five consecutive years*

The use of five consecutive years gives results, that vary depending on which five year period is chosen. In this study two five year periods are compared, 1990-1994 and 1995-1999. These two periods have very different constructed climatologies for wind speed and temperature; the temperature can be overestimated for one month in the 1990-1994 period and underestimated the same month in the 1995-1999 period.

The temperature pattern that the long-term mean temperature climate exhibits can to a certain degree be seen for the constructed temperature climate as well. Though for some months the temperature is over- or underestimated and some months don't have the cold air stretching out from

the northern part to the inland of Sweden. For the 1990-1994 period the temperature is overestimated for four months, slightly underestimated for October and captured well for November (Figure 6-2, middle right). This five year period captures the pattern that the long term means exhibits well. For the following period 1995-1999 the temperature is captured very well for January, March and October, the other months are not captured as well. February is overestimated and December is underestimated. November (Figure 6-2, bottom left) is underestimated with the 1995-1999 five year period.

The wind speed pattern for both of the periods is not constructed well for all months (Figure 6-3, middle right and bottom left). For some of the months the local minimum over southern Norway and western Sweden is missing. The values are often over- or underestimated with this method. For the 1990-1994 period the wind speeds are overestimated in three months (January, March and December), the other three months have a better agreement with the long term mean. The constructed mean wind speed for November has a good agreement with the long term mean for this five year period. For the second period 1995-1999 the wind speed is underestimated for January, November and December. There is also an overestimation of the wind speed for February and October compared with the long term mean. When using the 1995-1999 the constructed mean wind speed pattern is captured poorly for November.

For the first period 1990-1994 the ice loads are not captured well by this method, some of the months show an overestimation of the ice load, e.g. October and November (Figure 6-4 top left corner and middle right). For the second period (1995-1999) the ice load is better captured for most of the months, November is captured very well during this period (Figure 6-4 bottom left).

The icing rates for this method can be seen in (1990-1994) and (1995-1999). During the first period, 1990-1994, the method captures the icing rate adequately for some of the months, though the icing rate is overestimated for most months. November is captured rather well in pattern this period, but the icing rate is overestimated. During the 1995-1999 period this method overestimates the icing rate for all months. The pattern is captured no better or worse than the previous period.

### *Random day*

The random day approach to constructing a climate is not a recommended method to use for creating an icing climatology on a monthly scale. The temperature climate constructed with this method can be seen in Figure 6-2, bottom right corner. For November the temperature is overestimated, though the pattern is captured well.

As can be seen the wind speed is relatively poorly reconstructed by the random days method compared with the other methods, Figure 6-3, bottom right corner. The wind speed is overestimated in most areas over Sweden and Finland. Several tries were made, however very few of these tries could reproduce the wind speed climate in an adequate way. Since the results for the constructed climatology were not as good as expected, this method will not be used further to model icing or tested with a higher resolution data set.

Though the method failed to construct a good monthly climatology it is our belief that this method is more useful for longer time periods for temperature and wind speed. When the method is tested for a six month period a better agreement between the long term climate and the constructed climate is found (results not shown here), and to use it for an even longer time period might give good results. But for a shorter time period this method is not recommended.

### **WRF data set**

Only November will be presented with climatological maps in this section. Note that for the sake of clarity and to get a good understanding of the ice load, ice loads smaller than 0.05 kg have been removed and that the colour scaling of all ice load figures will be kept constant so that ice loads larger than 0.3 kg will be shown in a dark red/maroon colour.

In an effort to avoid repetition only some of the climatological maps will be presented here, those that are of most interest and will be most illustrative, the focus will be on the ice load and icing maps. All results discussed here will be for November only, though all months will be presented with statistics in a following chapter.

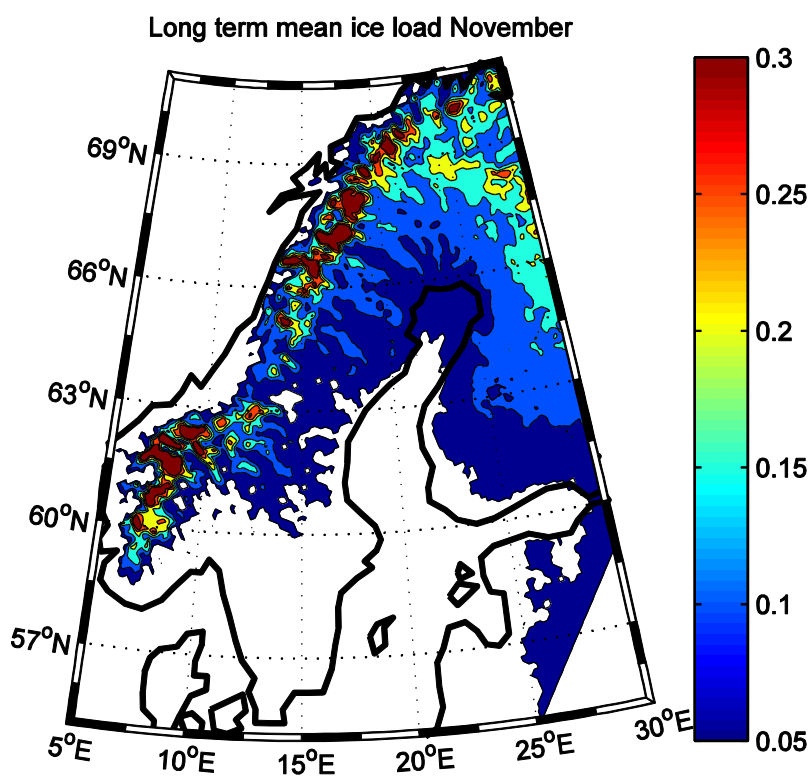
The long term temperature for November for the WRF data set has some features in common with the long term November temperature for the ERA Interim data set. The colder air is located over northern Norway, Sweden and Finland. The warmer air is located over the oceans and Denmark. There is colder air extending down over Sweden and Norway as well as over the three Baltic countries. There are some very fine details visible in the maps, such as the highland of Småland in southern Sweden and the mountain pass of Jämtland.

The long term wind speed shows lower wind speeds over land with higher wind speeds over the sea. The highest wind speeds are over the North Sea outside southern Norway, over the Baltic the wind speeds are slightly lower than over the North Sea. Over land there are greatly detailed features, such as the large Swedish lakes, Vänern and Vättern, and the islands of Åland and Öland.

The long term mean ice load can be seen in Figure 6-6. The mountainous areas have most of the icing, the largest ice loads are mostly in the

Norwegian and Swedish mountains (maroon colour). Most of the icing affects the land areas north of 60°. Some of the Baltic countries also have some ice, but the loads are very small. The most substantial ice loads outside the Swedish-Norwegian mountain range is in northern Finland.

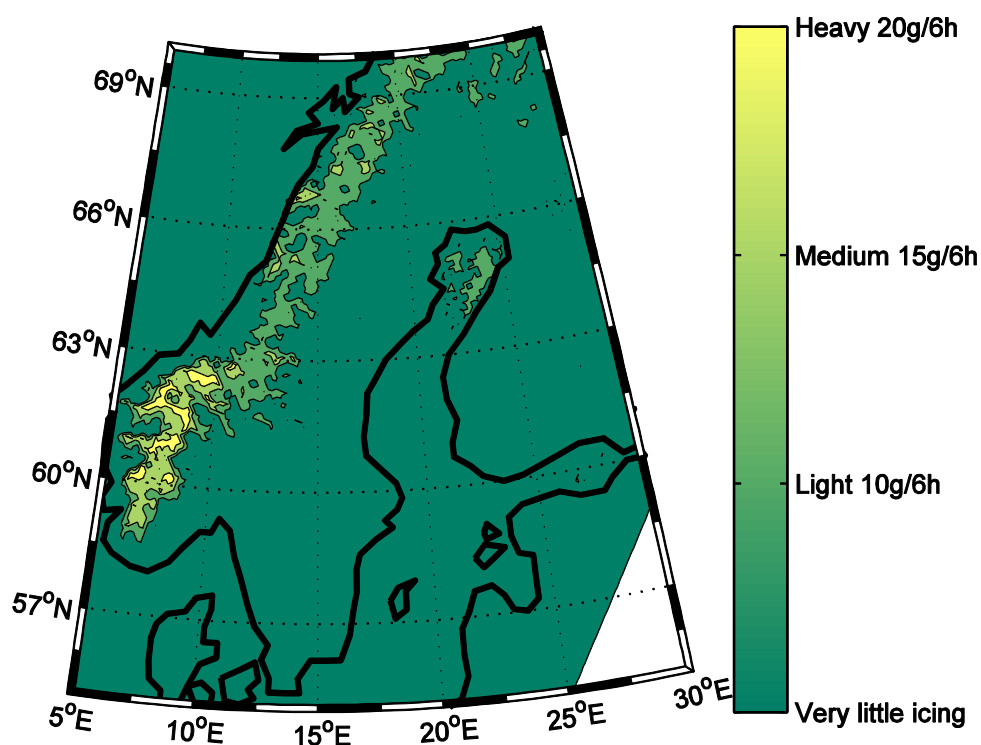
The icing rate for November can be seen in Figure 6-7. Most areas have very little icing or no icing at all. The most noticeable feature is the Norwegian and Swedish mountains, which are subjected to some icing. There is also some light icing over the Bay of Bothnia. The constructed icing rates are very similar, all of the constructed icing rates share that they overestimate the icing. Because of this only one constructed icing rate will be shown as a comparison to the long term icing rate.



**Figure 6-6: Long term ice load for November. All ice loads less than 0.05 kg/m have been removed and all ice load more than 0.3 kg/m are dark red to improve resolution.**

*Best fit: temperature and wind speed*

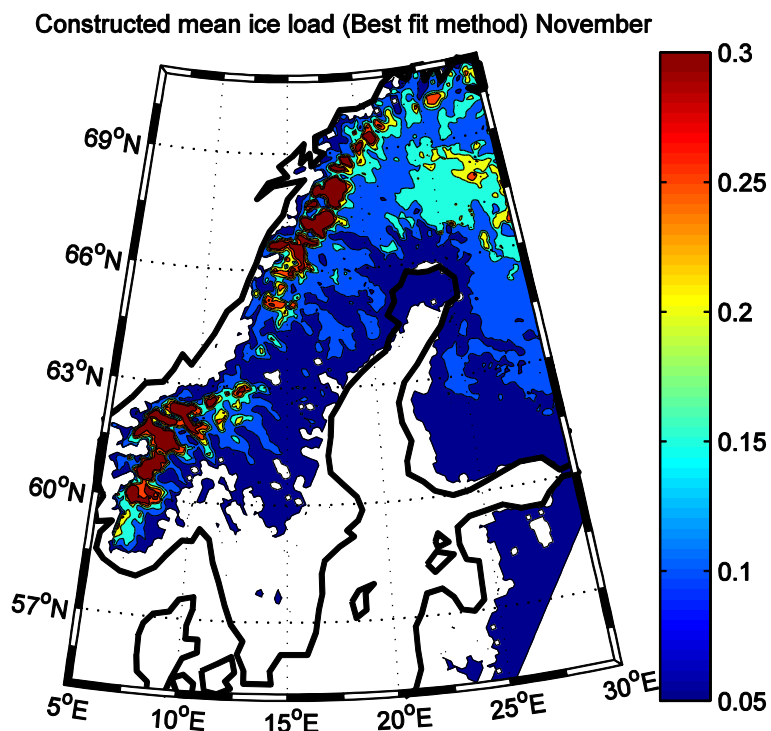
For the best fit method temperature is captured very well, some very fine scale details are captured very accurately. One example would be the mountain pass of Jämtland. The temperature is captured very well over the Baltic sea and the Baltic countries. The extent of the coldest air on the map is also captured very well. There are areas which aren't captured as well also; the temperature is underestimated over southern Norway.



**Figure 6-7: Long term icing rate November.**

The wind speed is captured well with this method. The fine scale details of the wind speed are captured very well over Finland. A feature over south-eastern Finland, near Lake Ladoga is captured with very accurate precision. There are areas which are less well captured, over the sea the method have some trouble in capturing the wind speed. Overall the method does capture many of the features that can be seen in the long term mean wind speed. The large lakes in Sweden, Vänern and Vättern, can be seen in the constructed mean wind speed, as well as in the long term mean wind speed.

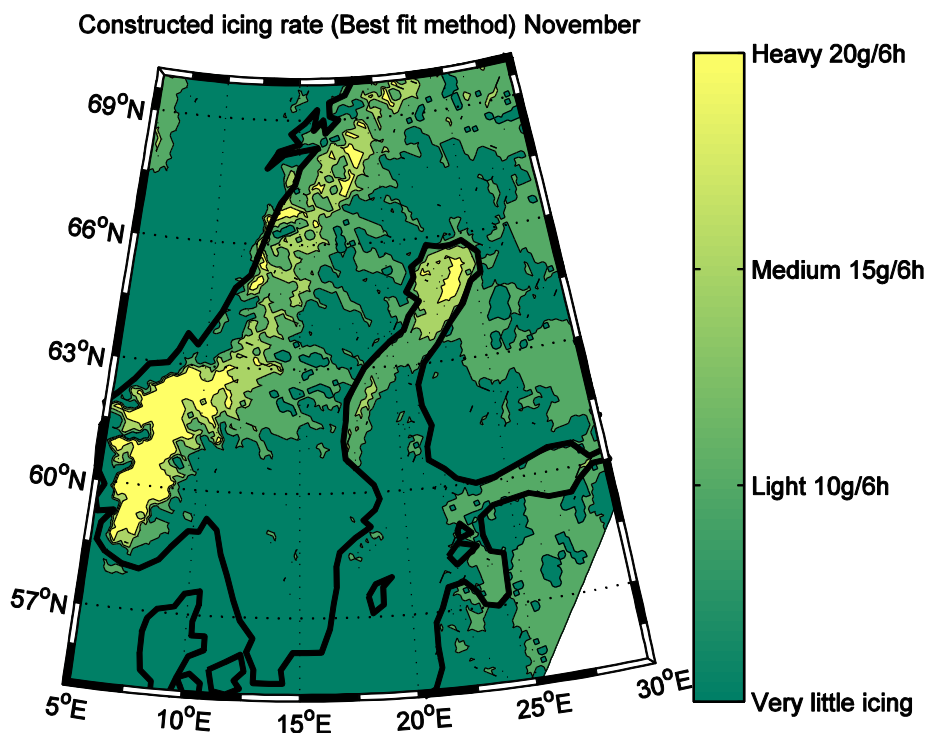
The constructed mean ice load (Figure 6-8) underestimates the ice load slightly for November. For some areas, like in the Norwegian mountains, the method misses some of the severe ice accretions compared with the long term means, though the extent of the ice load is captured well with this method. The icing rate, Figure 6-9, is overestimated compared with the long term mean. The method captures more icing and also in more areas than the long term mean.



**Figure 6-8: Constructed ice load using best fit method for November.**

*Best fit: Lamb classes*

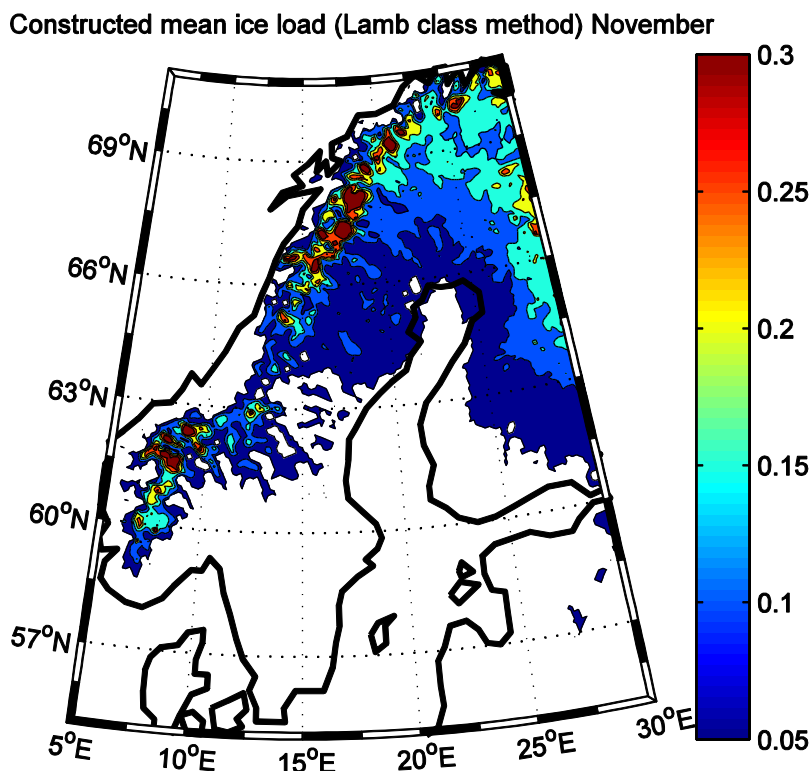
There is a good agreement with the long term temperature. The highland area in southern Sweden is captured, as are details in the temperature in the east Svealand area. In Finland and the three Baltic countries the temperature is also captured well. But in the mountains of Sweden and Norway the temperatures are overestimated compared with the long term mean, e.g. the Jämtland mountain pass can be seen in the constructed temperature, but the temperature is overestimated there.



**Figure 6-9: Constructed icing rate for November using the best fit method.**

The mean constructed wind speed is underestimated compared to the long term mean. Over the Baltic Sea the wind speed is much underestimated. And while the constructed wind speed does capture some of the details (islands of Åland and Öland and some of the Swedish lakes); the wind speed is underestimated for all land areas. This is consistent with the results from the ERA Interim data set, in which the wind speed for this method is severely underestimated compared with the long term mean.

From Figure 6-10 one can see that the constructed mean ice load is underestimated in the Norwegian and Swedish mountain range and in southern Finland and the Baltic countries. The constructed mean icing rate is overestimated compared to the long term mean. The constructed icing rate captures the area in the Norwegian-Swedish mountain range where the icing occurs, but overestimates the area subjected to heavy and medium icing.

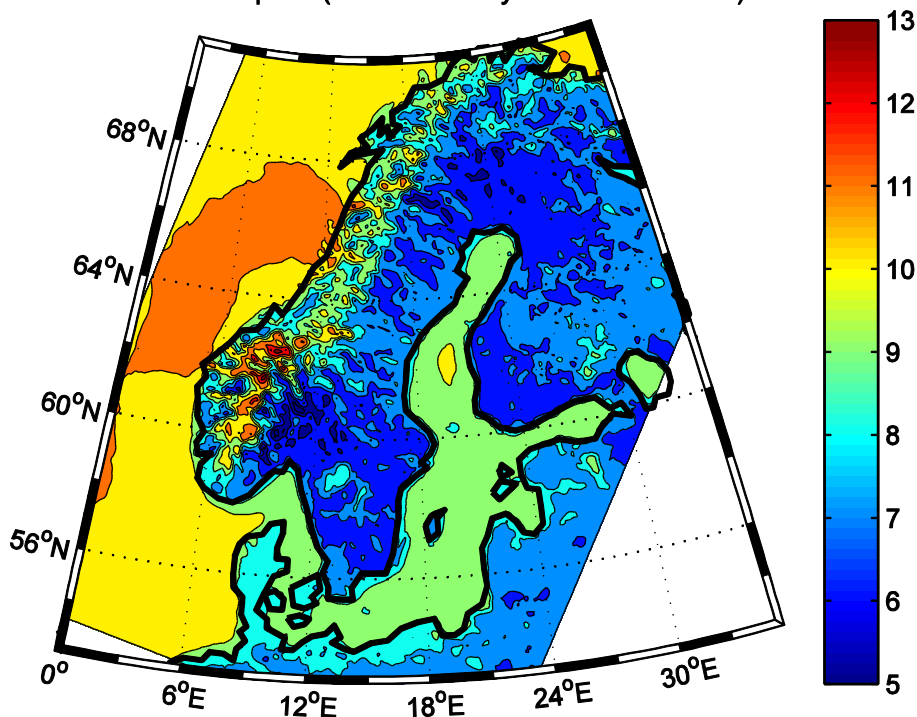


**Figure 6-10: Constructed mean ice load using the Lamb classes method for November.**

*Five consecutive years*

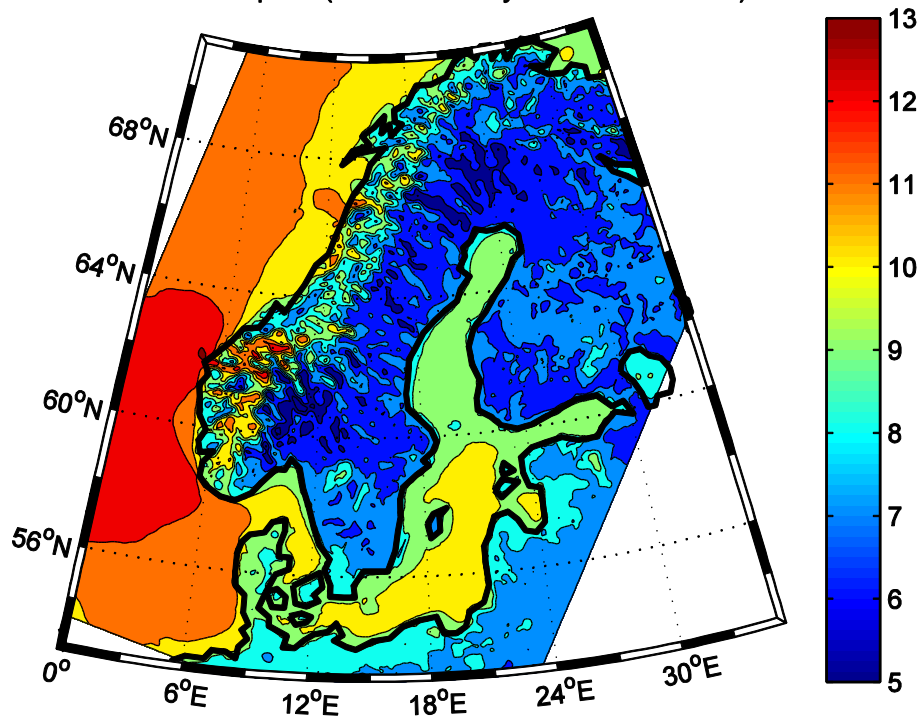
The constructed mean temperature for 1990-1994 for November generally has a good agreement between the long term temperature and the constructed one for this period. Over the Götaland region of Sweden the temperatures are lower than compared with the long term mean and in the northern Svealand/southern Norrland area the temperature is overestimated. But there are also some very fine features that are captured by this method, the temperature is captured very well over the Baltic Sea and the Baltic countries.

For the following five year period (1995-1999) the constructed mean temperature doesn't capture the long term mean as well as the previous period. There are several areas in which the temperatures are underestimated, such as in the Baltic countries and over northern Finland. This is in agreement with the results from the ERA Interim data set, in which the constructed mean temperature for this period also was underestimated.

**Constructed mean wind speed (5 consecutive years method 90-94) November****Figure 6-11: Constructed mean wind speed using the five consecutive years method (November, 1990-1994).**

The constructed mean wind speed for the 1990-1994 period is underestimated for most of the areas (Figure 6-11). There are areas where the wind speed is captured well. For the 1995-1999 period the wind speed is captured very well compared with the long term mean (Figure 6-12). What should be noticed is that the method produces results that are different from each other and this could have large impacts on the modelled ice load. As an example the wind speed patterns over the North Sea and the Baltic is very different from each other.

The ice load for this method can be seen in Figure 6-13 for 1990-1994 and in Figure 6-14 for 1995-1999. For the first period some features of the ice load is captured well in the middle of Sweden, but not so well in other areas. Over Finland the ice loads are overestimated in this period and for the southern Baltic area the areas afflicted with icing are farther south than the long term mean. This period also misses some of the mountainous areas, which have very severe icing over southern Norway. The second period 1995-1999 captures the ice better than the first period, but the ice loads are slightly underestimated in some areas, e.g., Finland and in some mountain areas. But as for the 1990-1994 period this method indicates icing over the southern Baltic countries that is not seen in the long term mean.

**Constructed mean wind speed (5 consecutive years method 95-99) November****Figure 6-12: Constructed mean wind speed (November), using the five consecutive years method (1995-1999)**

The icing rate for the first period 1990-1994 captures more icing events than the long term icing rate. In southern Norway there is more heavy icing than the long term mean and in the east there are more icing events than in the long term mean. When using the second period, 1995-1999, the icing rate shows similarities with the previous five year period and the icing rate is overestimated.

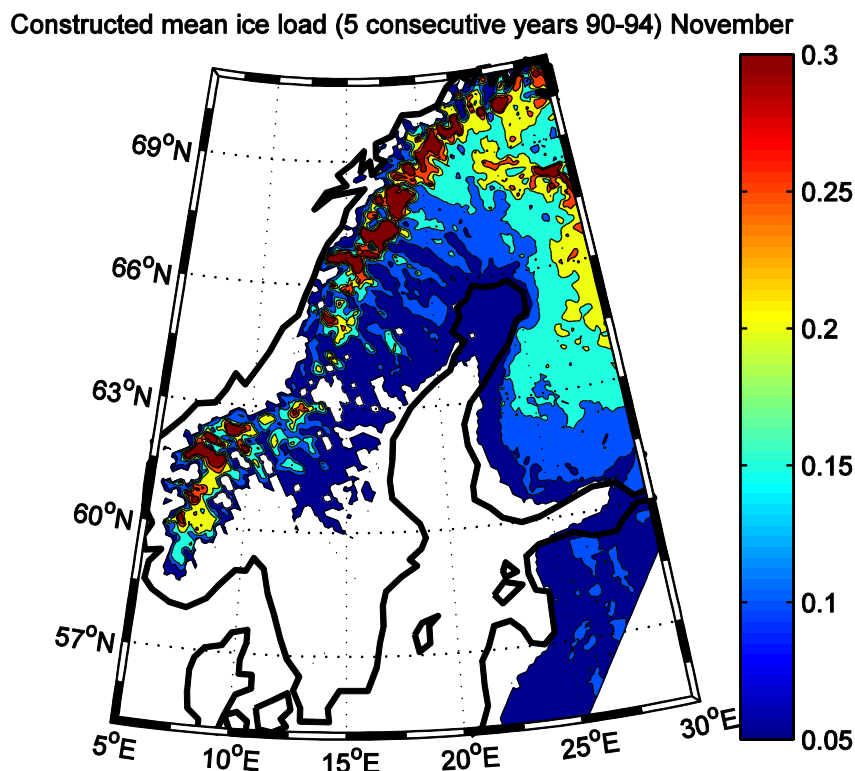


**Figure 6-13: Constructed mean ice load five consecutive years method, 1990-1994, November.**

#### **Presentation of all winter months and further information on November**

For all of the months the mean and standard deviation of the parameters (temperature, wind speed and ice load) have been calculated over the entire domain (this is a spatial measure, rather than a temporal one). The means and the standard deviation for each of the approaches are presented in Figure 6-15 (temperature), Figure 6-16 (wind speed) and Figure 6-17 (ice load). Compared with the long term mean all of the methods show a good result. Some of the methods give a consistently better result than other. Temperature and wind speed will be dealt with in the following section, while icing will have a separate section. For all three figures the long term means are black with circles at the mean. The constructed means are all in red. The square is the best fit method; diamonds are the five consecutive years method and the Lamb class method in triangles.

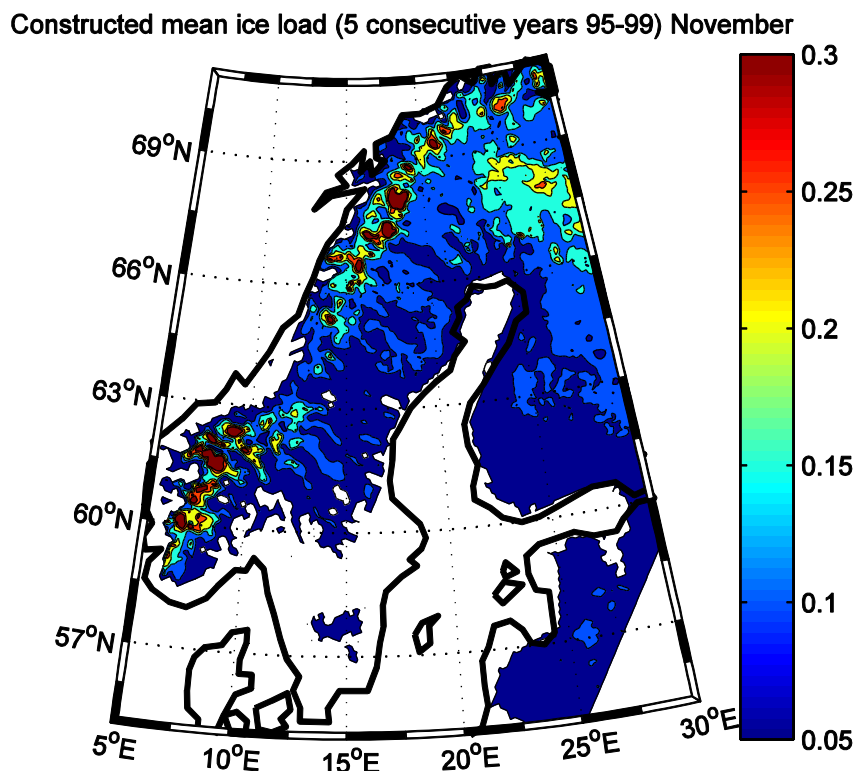


**Figure 6-14: Constructed mean ice load five consecutive years method, 1995-1999, November.**

#### *Temperature and wind speed*

The first period 1990-1994 captures the temperature very well for three months (October, November and December) and the other three months are not captured as well. The means are within the standard deviations of the long term mean temperatures for all months except January. On the other hand the constructed mean temperature using the 1995-1999 period is doing a very poor job at capturing the temperature. Half of the means from the constructed climatology fall outside the long term standard deviation. With wind speed one can see that both periods don't always capture the wind speed well. As before half of the constructed means of are outside the long term means error bars for the second period, 1995-1999. It is therefore concluded that this method should be used with extreme caution since one five year period can perform well while the following could be very off. And even if the method captures one parameter it might not capture another well with the same five year period.

For temperature the Lamb class method captures January and October very well. The other months are also within the standard deviation of the long term mean, except for December where the constructed Lamb temperature is much underestimated. For the wind speed the Lamb class method is on par with the five consecutive years method, three of the constructed mean wind speeds are outside the long term mean's standard deviation. Consistent with the

results from the ERA Interim data set the wind speed is generally underestimated when using this method.

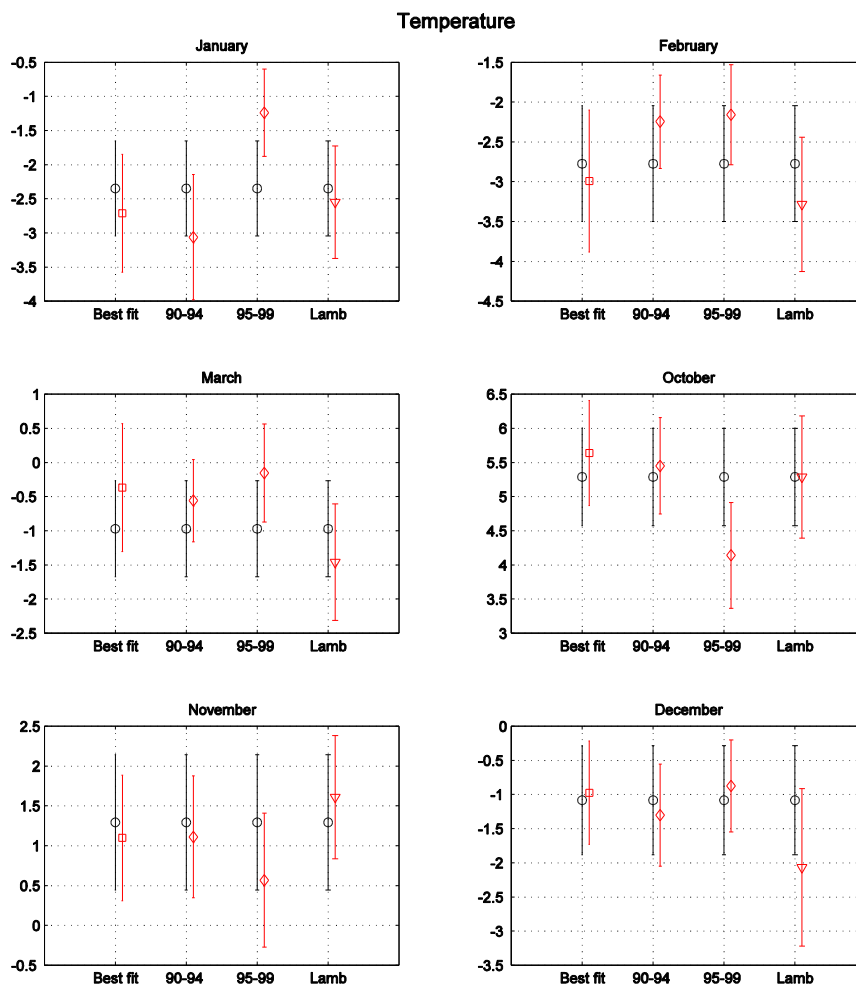


**Figure 6-15: The mean temperature of the long term temperature field (in black) compared with the mean temperature field of each method (in red). Both with standard deviation. Squares - best fit method, diamonds - five consecutive years and triangle - Lamb class method.**

The best fit method captures the temperature very well for all months; it can easily be regarded as the method which gives the best results for temperature. The five consecutive years method for the period 1990-1994 also does a good job, but since the method also gives bad results for the following five year period the best fit method must be considered as the method which gives the best results. For wind speed the best fit method mean is outside the long term standard deviation only once, in February. For all the other months the best fit method captures the long term mean well.

*Ice load*

It is important here to issue a warning about this comparison. Not only is the tool used a very blunt one, here it will be applied to a parameter that in itself is difficult to get a grip on. Icing is difficult to model correctly and when this method is applied it might not give a true overview of the ice load. What needs to be considered is also that there are large areas and regions that have very small ice loads (i.e. ice loads under 0.05 g/m).

Unlike temperature and wind speed most almost all of the method seems to capture the ice load well. This is most likely due to the fact that most of the ice loads are very small and close to zero, and very few areas where there is large ice loads that can change the mean.

No method gives a better result than any other, and all of the constructed means are within the standard deviations (with the exception of the October five consecutive years method for 1990-1994).

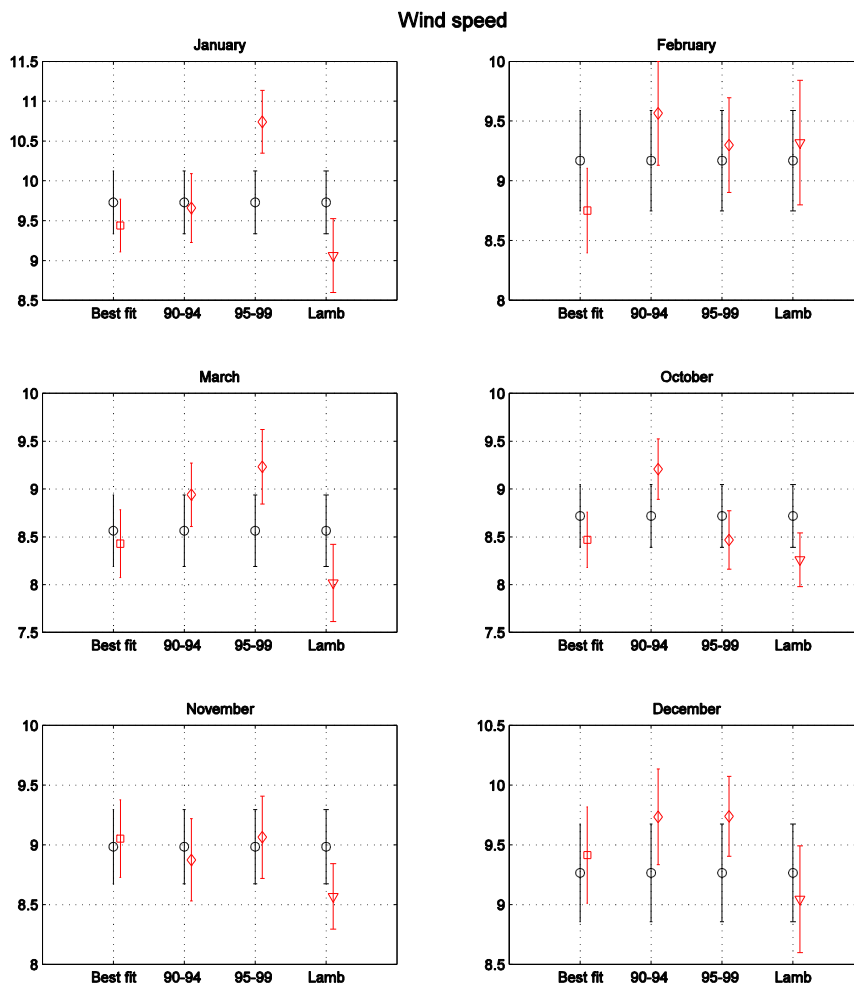


**Figure 6-16: The mean wind speed of the long term wind field (in black) compared with the mean wind field of each method (in red). Both with the standard deviation. Squares - best fit method, diamonds - five consecutive years and triangle - Lamb class method.**

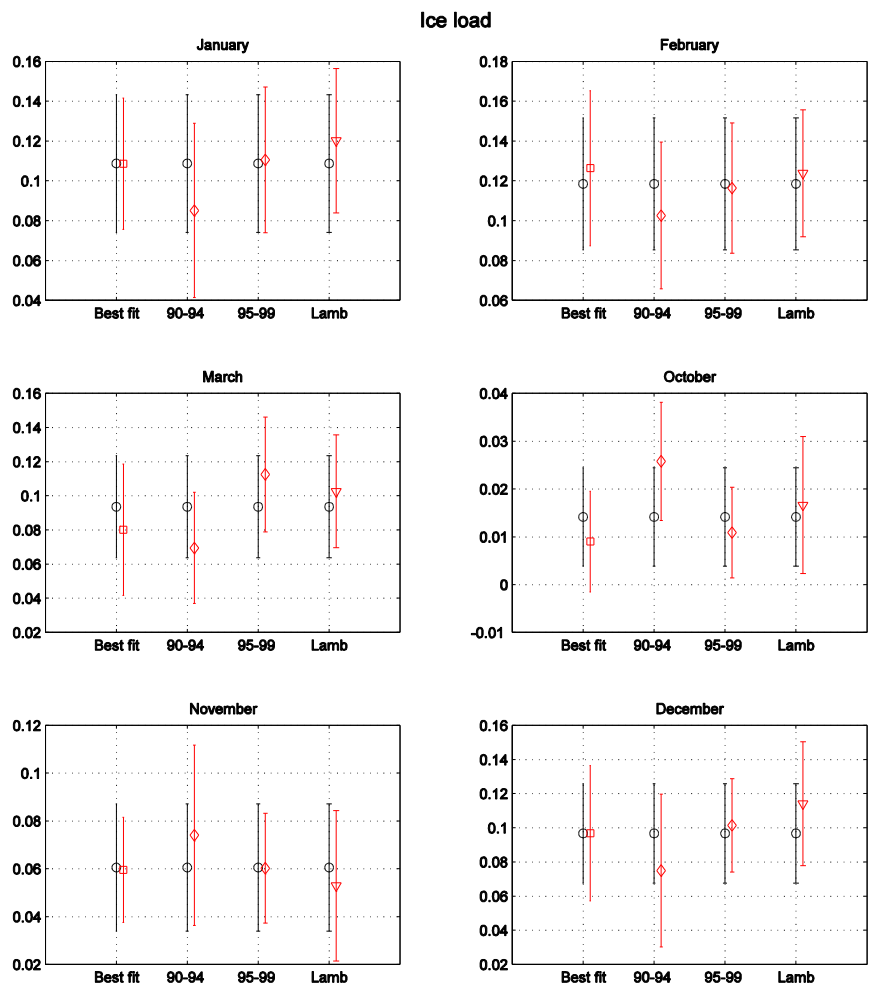


**Figure 6-17: The mean ice load of the long term ice load (in black) compared with the mean wind field of each method (in red). Both with the standard deviation. Squares - best fit method, diamonds - five consecutive years and triangle - Lamb class method.**

### *Statistics for November*

The mean, standard deviation, bias, MAE and RMSE have been calculated for five locations during November, equation 6-10 in section 4.2.1. The locations were randomly selected, with the constraint that they have to be land sites. The results are presented in Table 6-3 to Table 6-7, see map in Figure 6-18 for locations of sites.

With this section additional information is provided about the ice load conditions in November. The values in the following tables should be a guide to understanding ice loads and icing. To further validate these methods using an area might be of more interest rather than using only one point.

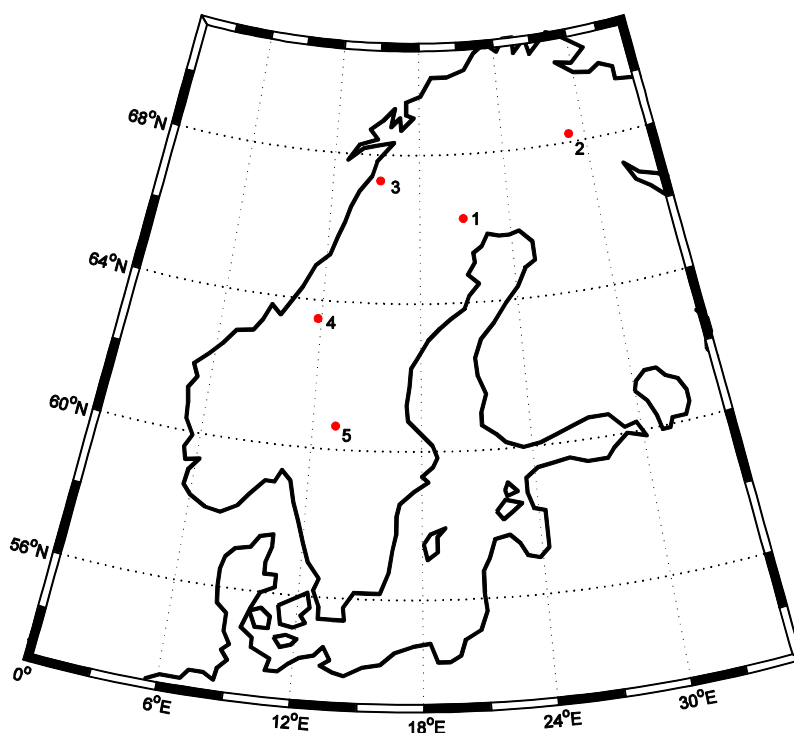


**Figure 6-18: Locations of sites used to calculate mean, standard deviation, bias, MAE and RMSE for November. Locations indicated with numbered red dots.**

**Table 6-3: : The mean, standard deviation, bias, MAE and RMSE for ice load for all methods. Location 1. In kg/m on cylinder.**

Location		Method	Mean	Standard deviation	Bias
Lat:	66.3	Long term	0.0735	0.0375	-
		Best fit	0.0599	0.0427	-0.0176
		Lamb class	0.0634	0.0429	-0.0101
Lon:	20.9	90-94	0.0726	0.0451	-0.0009
		95-99	0.0824	0.0515	0.0089

**Table 6-4: The mean, standard deviation, bias, MAE and RMSE for ice load for all methods, as above. Location 2.**

Location		Method	Mean	Standard deviation	Bias
Lat:	68.2	Long term	0.2475	0.1404	-
		Best fit	0.1720	0.0928	0.0755
		Lamb class	0.2027	0.1055	-0.0448
Lon:	28.6	90-94	0.3166	0.1600	0.0690
		95-99	0.2050	0.0847	-0.0425

**Table 6-5: The mean, standard deviation, bias, MAE and RMSE for ice load for all methods, as above. Location 3.**

Location		Method	Mean	Standard deviation	Bias
Lat:	67.3	Long term	0.0409	0.0193	-
		Best fit	0.0322	0.0208	-0.0087
		Lamb class	0.0395	0.0342	-0.0014
Lon:	15.3	90-94	0.0410	0.0294	0.0690
		95-99	0.0462	0.0263	0.0053

**Table 6-6: The mean, standard deviation, bias, MAE and RMSE for ice load for all methods, as above. Location 4.**

Location		Method	Mean	Standard deviation	Bias
Lat:	63.5	Long term	0.0759	4.6992e-4	-
		Best fit	0.0746	0.0463	-0.0013
		Lamb class	0.0398	0.0343	-0.0361
Lon:	11.8	90-94	0.0728	0.0689	-0.0031
		95-99	0.0669	0.0371	-0.0090

**Table 6-7: : The mean, standard deviation, bias, MAE and RMSE for ice load for all methods, as above. Location 5.**

Location		Method	Mean	Standard deviation	Bias
Lat:	60.6	Long term	0.0712	0.0397	-
		Best fit	0.0716	0.0488	0.0004
		Lamb class	0.0412	0.0316	-0.0301
Lon:	13.3	90-94	0.0741	0.0461	0.0029
		95-99	0.0974	0.0500	0.0261

#### 6.1.4 Comments on the results

Several methods to create and icing climatology have been tested in this section. The random day method is not recommended for time periods shorter than six months, the method works better for longer time periods of at least six months. The Lamb class method is also not recommended to create an icing climatology, as this method had troubles to correctly capture standard meteorological parameters.

The two methods which are slightly better at capturing the temperature and wind speed climate is the best fit method and the five consecutive years method. These two methods have some skill in reproducing the climate. But as has been shown these methods are not without problems. When using the five consecutive years method one should be aware of that one five year period might represent the long term climate well, but the next five years might have large errors. There is no guarantee that a five year period is a good match for the long term climate. The best fit method gives a good result for most parameters. More research is needed before any of the tested methods can be recommended for creating an icing climatology.

#### ERA Interim dataset

For the ERA Interim dataset all of the methods used indicate that the temperature is easier to catch than wind speed and icing. The temperature patterns differ very little from each other from year to year and all of the tested methods get the pattern for the temperature correctly. Some of the methods do get the pattern correct but under- or overestimates the temperature in the entire domain or in a smaller area.

The wind speed is harder to catch for all methods. While there is a pattern it is less stable than the temperature pattern and varies between days and months. The lack of variability would explain why the temperature pattern is captured better by all methods.

All of the methods were more or less skilful in reproducing the climate for temperature, wind speed and icing, except the random day method. The five consecutive years method can for some months and five year periods reproduce the climate, though there are examples of when the method fails to reconstruct the climate well. The ice loads are modelled well for some months and periods with this method, but the method can for the next period construct a climatology that don't agree well with the long term mean. The

best fit of temperature and wind speed captures the temperature and wind speed climate very good for the ERA dataset and also the ice load is captured well with this method. The best fit of Lamb classes method does not work very well at all times for the ERA dataset. As has been discussed there is a homogeneity in the distribution of the Lamb classes between the years. Since the circulation pattern is very similar between the years it will be hard to have the circulation represent the temperature and wind speed in a good way.

For the ERA Interim data set all of the methods could represent the climate very well for some months. However for some of the method it is at times depending on luck. As have been shown the random days method should be used with extreme caution for short time periods. The five years consecutive method is dependent on which five year period that is selected, if comparing the wind speeds for November 1990-1994 and 1995-1999 there are some similarities, but also some large differences between the two periods (Figure 6-3).

### **WRF dataset**

Using the methods on the WRF dataset have shown that some of the method can be used on a higher resolution dataset with good results for at least temperature and wind speed. With these two standard meteorological parameters at least two methods performed well, the best fit method and the five consecutive years method, the former better than the latter. There are some troubles with the wind speed for the five consecutive years methods. On this basis the recommended method is the best fit approach. The Lamb class method has problems with capturing the wind speed well, but can capture the temperature in an adequate fashion. But since there are some troubles with capturing the wind speed, this method is not recommended for creating a climatology.

Nevertheless the icing climatology will have to be taken into account. All the methods do a seemingly good job at capturing the ice load (see Figure 6-17). It can't be stressed enough that this comparison is done with a very blunt tool and that the ice load used here is largely made up of very small ice loads close to zero.

It is interesting to note is that there are consistencies between the low resolution ERA dataset and the high resolution WRF dataset. This can most clearly be seen for the Lamb class method. The wind speed is underestimated in the ERA data set and as can be seen in Figure 6-16 the wind speed is also underestimated in the WRF data set.

#### **6.1.5 A discussion on the length of the representative period**

When comparing the length of the number of years used to create icing climatologies previous methods in this section use 5 years. The reasoning behind using five years is to model as few years as possible while still capturing some of the variability of the atmosphere. It could be argued that four years also have a good enough agreement between long term and constructed , at least for wind speed (see Figure 6-1). Five years were chosen so that there could be a good comparison between the best fit and Lamb class method with the five consecutive years method.

In Figure 6-19 the long term mean ice load for southern Norway and the three 10 year periods have been plotted. As can be seen there is a rather good agreement between the three periods and the long term mean. The ten year period captures the ice load better than the methods using five years - which is expected. Of course for each year added there is a cost of increased computational time.

The number of years used to construct a climatology will of course have an impact on the results. The more years that are used the better will the constructed climatology represent the 30 year mean. But as previously stated, each extra year used will increase the computational time. If a high resolution climatology is needed, say  $1 \times 1 \text{ km}^2$ , each extra year is very costly.

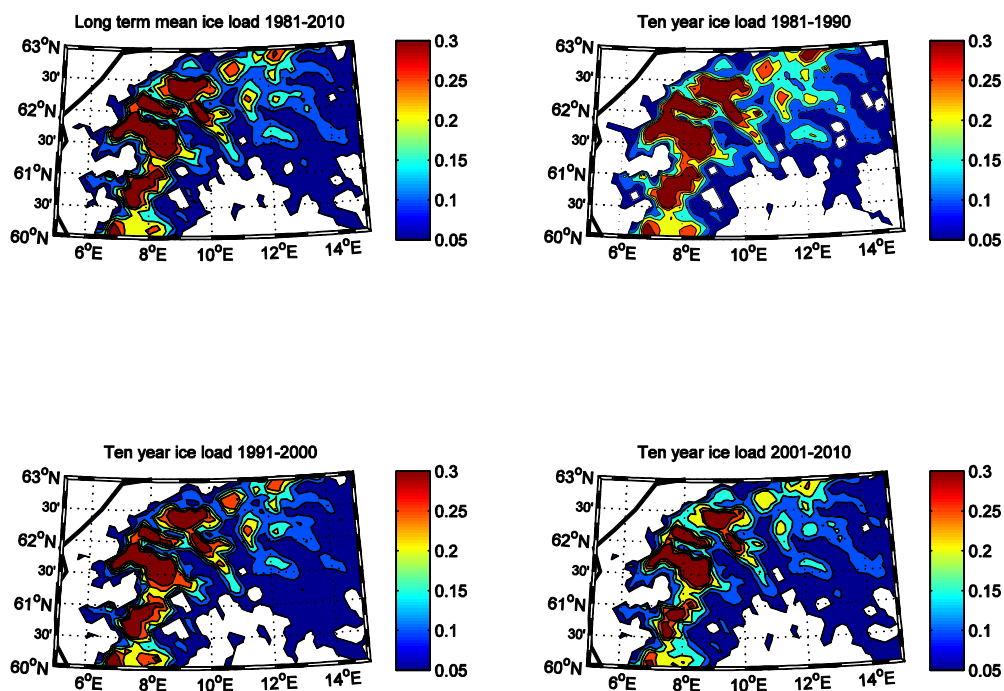


**Figure 6-19: Long term ice load (top left) compared with mean ice loads for three ten year periods (1981-1990 top right, 1991-2000 bottom left, 2001-2010 bottom right). Parts of southern Norway shown here.**

## 6.2 Using downscaling techniques

A second method to overcome the limited time period of simulation feasible with a  $1 \times 1 \text{ km}^2$  resolution is to use a downscaling technique. First the climatology is made using a coarse enough resolution to make a modelling of a 30-year period possible. After that these results are downscaled to the final results of  $1 \times 1 \text{ km}^2$  resolution. The downscaling may be made using different techniques. Dynamical downscaling has been used to increase the resolution of wind using detailed information about the topography, and a simple adiabatic cooling may be used for temperature, but regarding such a complex phenomenon as icing it is not obvious that this type of approach may be used.

Here instead pure statistical techniques have been used. As described in Section 4.1.2, model simulations using different resolutions have been made for several areas using the COAMPS<sup>®</sup> model. Similar results are available using the WRF model, see Section 4.1.3. As modelling a 30-year period using a 9 km resolution would be the most computer time efficient to do, results from these model results were chosen as primary results. As the final goal is to downscale the icing climatology, which depends on three parameters; wind speed, temperature, and liquid water content, all three parameters must be downscaled separately to reach the goal.

The downscaling was made in three steps. First the 9 km results regarding wind speed were statistically analysed. The modelled average wind speed was plotted as a function of height above sea level using the 9 km resolution of topography. In this way using a high-resolution topography these analyses could be used to derive a new high resolution wind speed climatology by using the difference in height above sea level between the 9 km model results and the 1 km resolution topography. Two typical examples of the wind speed dependence on terrain height are shown in Figure 6-20. The regression coefficient for these relations were of the order 0.6 to 0.8. The lines show the result from a linear regression giving the wind speed versus height above sea level as an average for a 9 km resolution model area around the centre of the 1 km model domain.

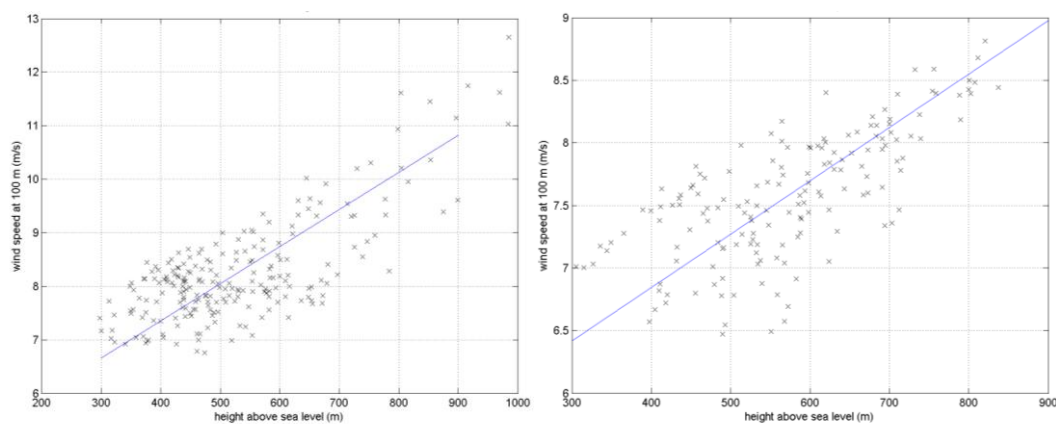


**Figure 6-20: Two of examples showing average wind speed dependence upon terrain heights. Left: November 2011 for model domain N3B. Right: January 2012 for model domain N3D.**

Next a similar statistical analysis was made regarding temperature from which also a high-resolution temperature field could be estimated, again using the difference in height above sea level between the 9 km and 1 km resolutions. As an alternative to this an adiabatic lifting of the 9 km model temperature using also the difference in height between 9 km and 1 km resolution could have been used. But as the adiabatic cooling with height might not necessarily be a good approximation to the actual average vertical temperature gradient it was judged better to use the modelled gradient statistics arrived at with the coarse resolution. Two examples of the relation between temperature and terrain height are given in Figure 6-21. Not surprisingly the correlation is better for temperature than for wind speed. The correlation coefficient for temperature against height was typically -0.9 to -0.95.

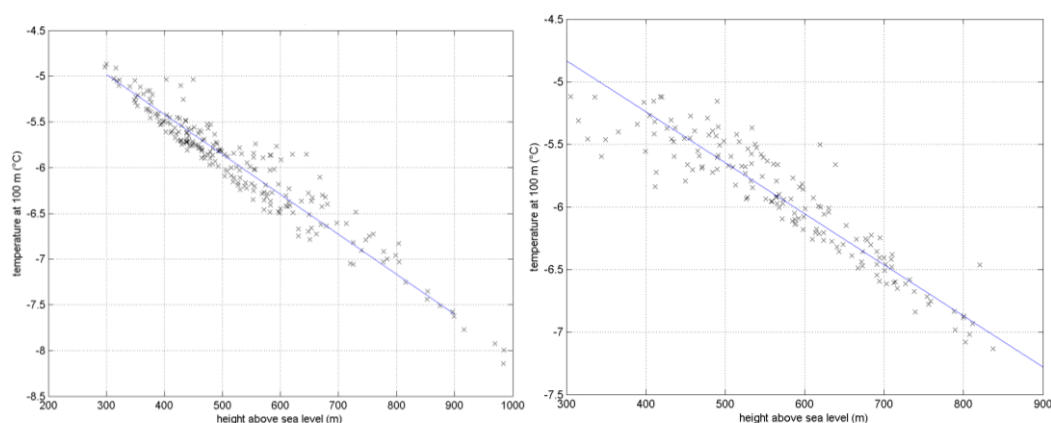


**Figure 6-21: Two of examples showing average temperature dependence upon terrain heights. Left: December 2011 for model domain N3B. Right: January 2012 for model domain N3D.**

In the third step the liquid water content from the 9 km model results was used together with modelled specific humidity. The saturation vapour pressure was estimated for the new temperature using the high resolution terrain and assuming that the specific humidity is approximately kept constant, the 9 km resolution value was then compared to the 1 km resolution results. In the case of super saturation a part of the water vapour content was transferred to liquid water until the saturation level was reached. Of course in the condensation process some latent heat would be released, but this was not taken account of here.

A regression technique was also tested for the liquid water content, but as seen in Figure 6-22 the relation with terrain height was poor. For some months and sites a correlations was found, but typically the correlation was not significant, why instead the above described method was used.

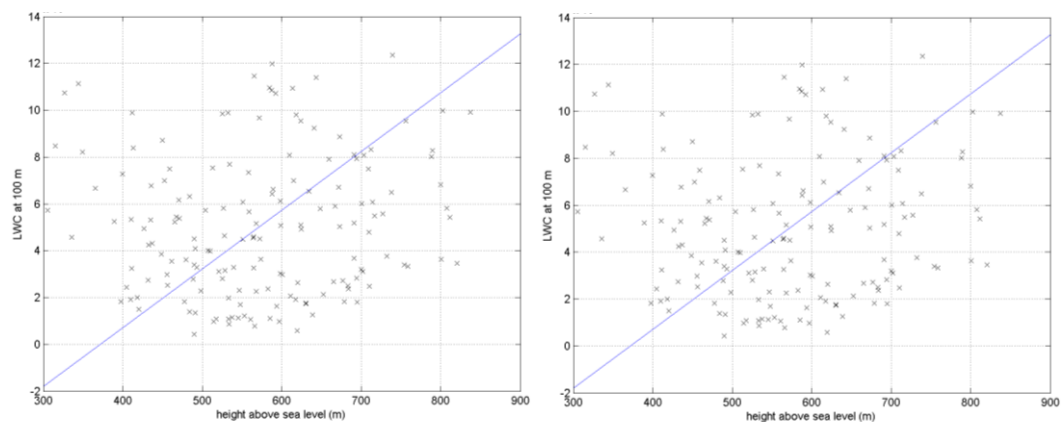


**Figure 6-22: Two of examples showing liquid water content dependence upon terrain heights. Left: December 2011 for model domain N3B. Right: January 2012 for model domain N3D.**

Finally the downscaled 1 km resolution liquid water content was used for ice accretion and the number of icing hours was estimated at each model grid point. These results could then be compared to the number of icing hours arrived at directly using the 1 km resolution model results.

The statistical downscaling technique have been tested and evaluated for the six  $1 \times 1 \text{ km}^2$  model domains shown in Sections 4.1.2 and 4.1.3. These six domains are all located around the ice measurement sites described in Section 3. All results refer to 100 m above local ground level. The statistical relations used for the downscaling were estimated monthly using 9 km resolution model results for an area about twice the size of the 1 km model domains, centred at the centre of the 1 km domains. By using monthly average statistics account was taken for differences in large scale weather conditions, which might affect the results. In this way also seasonal differences could be accounted for.

### 6.2.1 Results using statistical downscaling

Examples showing that the downscaled temperature and wind speed agrees quite well with the results of the 1 km resolution modelling are given in Figure 6-23 to Figure 6-24 for temperature, and in Figure 6-25 to Figure 6-26 for wind speed. Each figure shows results using COAMPS<sup>®</sup> (left hand graphs) and WRF (right hand graphs), and results using the 9 km resolution model outputs directly (top row graphs), results using output from the 9 km resolution downscaled to 1 km resolution (middle row graphs), and results using the 1 km model outputs directly (bottom row graphs). Results are given as seasonal averages for the winter seasons 2010-2011 and 2011-2012. It should be noted comparing results using the two models that the COAMPS<sup>®</sup> and the WRF model domains do not exactly overlap.

Looking at the average temperature fields, it is obvious that the 9 km resolution model results do not capture more than the large scale topographic variability. Comparing the downscaled results with the 1 km model resolution results the temperature fields agrees well. Typically the difference is less than 0.5 °C.

Also regarding wind speed the downscaling technique works well as can be seen in Figure 6-25 and Figure 6-26, although some differences may be notes regarding the exacts magnitude of the wind speed. But mostly the difference is within 1 m/s comparing the downscaled wind speed to the 1 km model resolution wind speed. The results thus show that both the downscaled temperature and wind speed may be expected to be accurate enough to be used as the base for downscaling the time of active icing from 9 km to 1 km resolution.

The results concerning seasonal numbers of hours with active icing (>10 g ice accretion per hour) are shown in Figure 6-27 to Figure 6-38 for the winter seasons 2010-2011 and 2011-2012 and for the two models, COAMPS<sup>®</sup> and WRF. Similar results as for temperature and wind speed are shown in the graphs for hours with active icing.

Also as regards number of active icing hours the downscaling technique is capable of catching the 1 km scale terrain variability well. From the results using the 9 km model resolution results directly (two top row graphs in each figure) after downscaling the geographical variability turn up principally as they also appear in the graphs showing results using the 1 km model results directly. But the agreement between them is not as good as for temperature and wind speed. Similar patterns are seen in both results, but the actual number of icing hours may differ somewhat, as e.g. comparing the COAMPS<sup>®</sup> results shown in Figure 6-27. The higher number of icing hours are found at the same locations, corresponding to higher elevation terrain, but the actual numbers may differ. At some locations the downscaled numbers are larger while at other locations the directly modelled results using 1 km resolution are larger. But we do not have measurements to confirm which result, which is the most accurate one. Typically the downscaled COAMPS<sup>®</sup> results however show somewhat smaller numbers of icing hours than those given by the 1 km resolution model results directly.

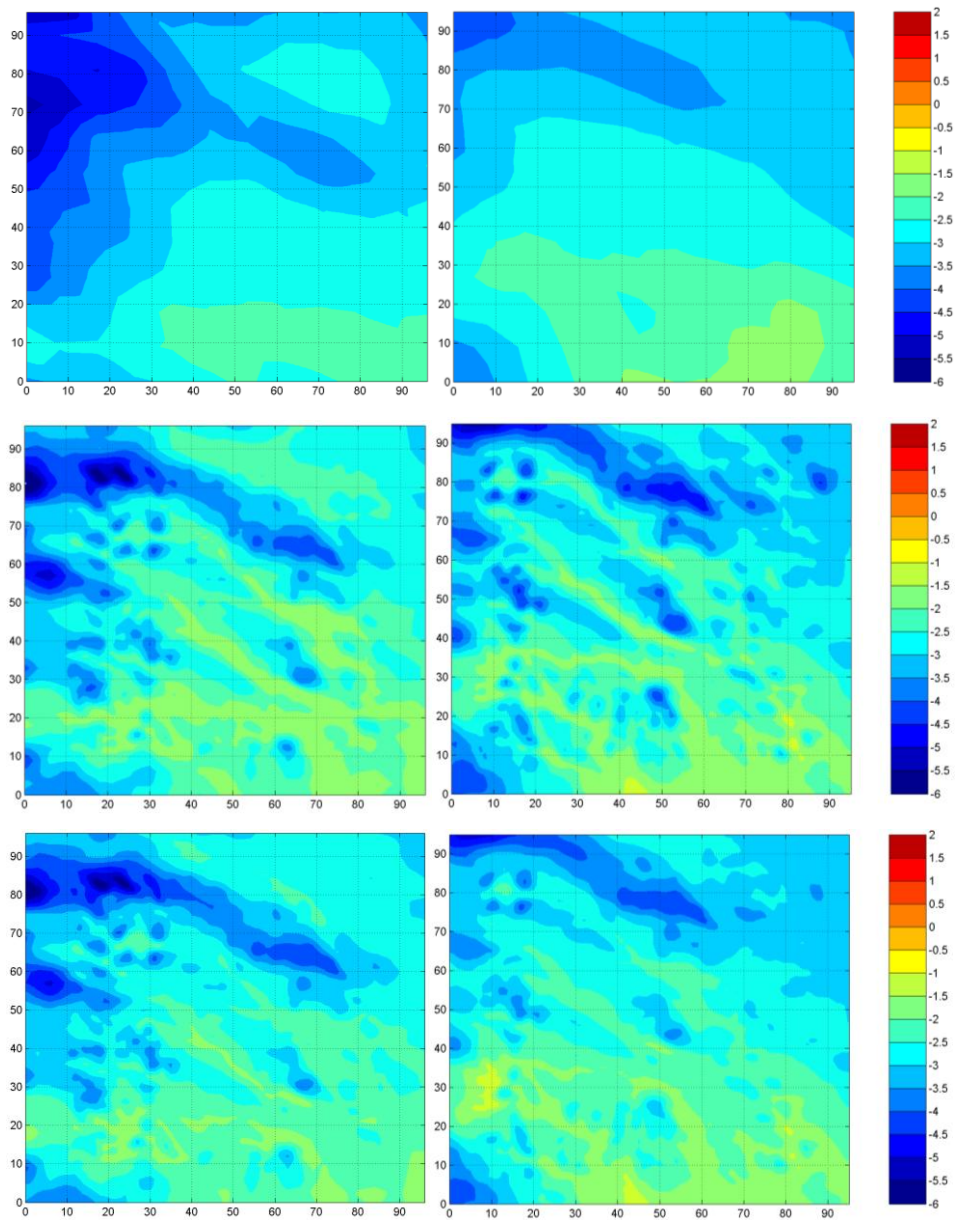


**Figure 6-23: Modelled seasonal average temperature (°C) Sep 2010-Apr 2011 for model domain N3C. Left hand plots results from COAMPS®, right hand plots from WRF. Top row plot results using 9 km model resolution. Second row results after downscaling from 9 km to 1 km resolution. Bottom row results using 1 km resolution. Horizontal scales given in km.**

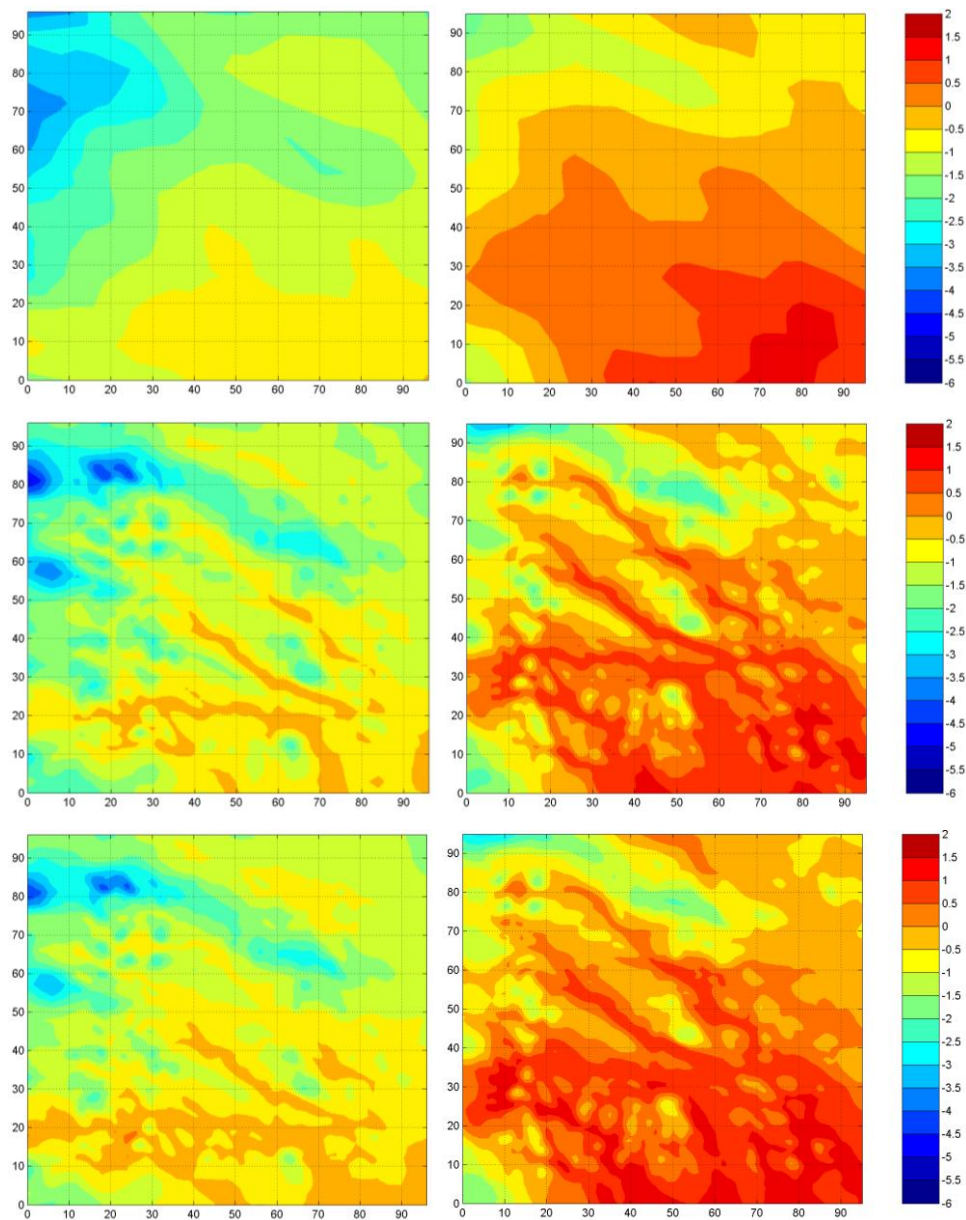


**Figure 6-24: Modelled seasonal average temperature (°C) Sep 2011-Apr 2012 for model domain N3C. Left hand plots results from COAMPS®, right hand plots from WRF. Top row plot results using 9 km model resolution. Second row results after downscaling from 9 km to 1 km resolution. Bottom row results using 1 km resolution. Horizontal scales given in km.**

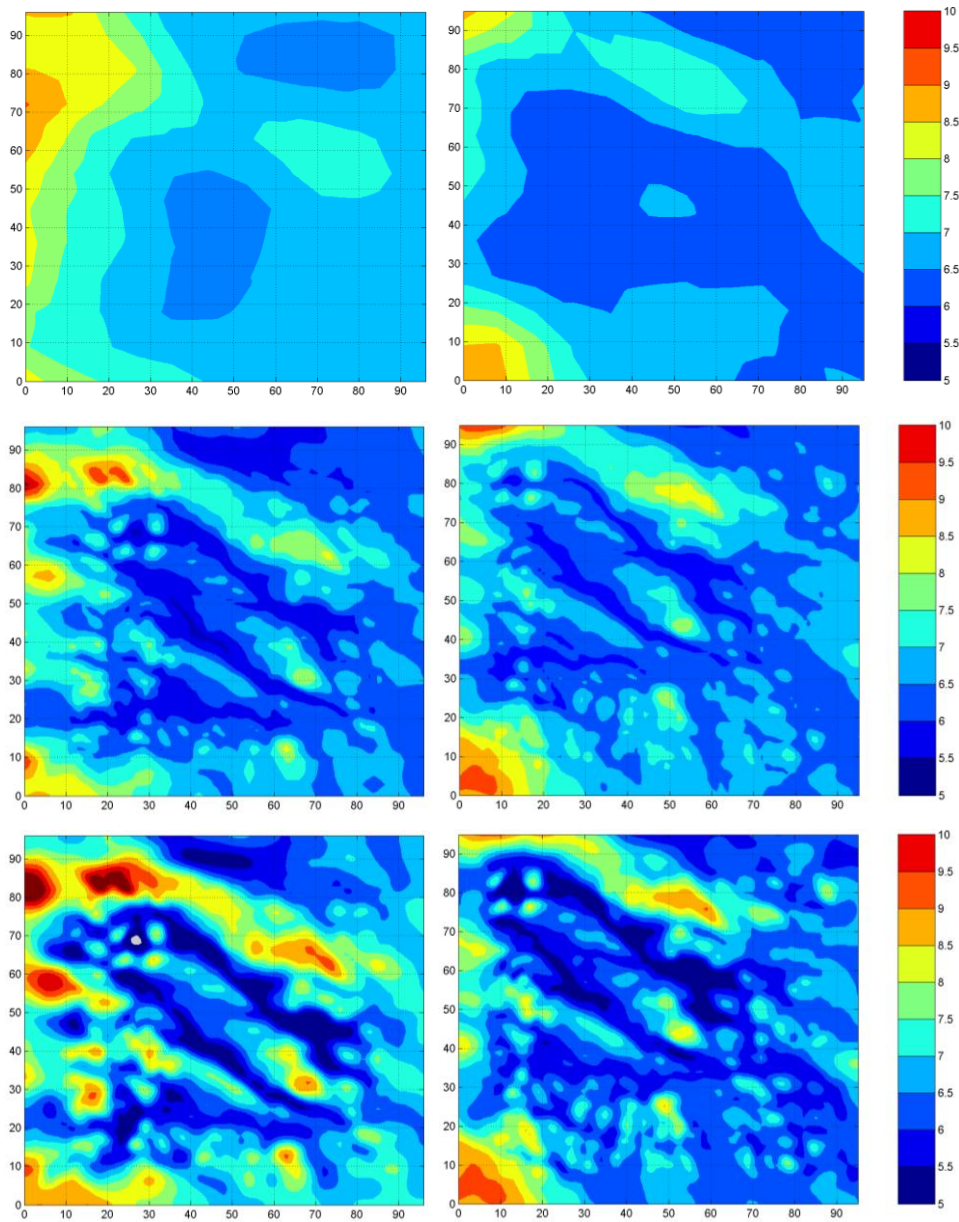


**Figure 6-25: Modelled seasonal average wind speed (m/s) Sep 2010-Apr 2011 for model domain N3C. Left hand plots results from COAMPS®, right hand plots from WRF. Top row plot results using 9 km model resolution. Second row results after downscaling from 9 km to 1 km resolution. Bottom row results using 1 km resolution. Horizontal scales given in km.**

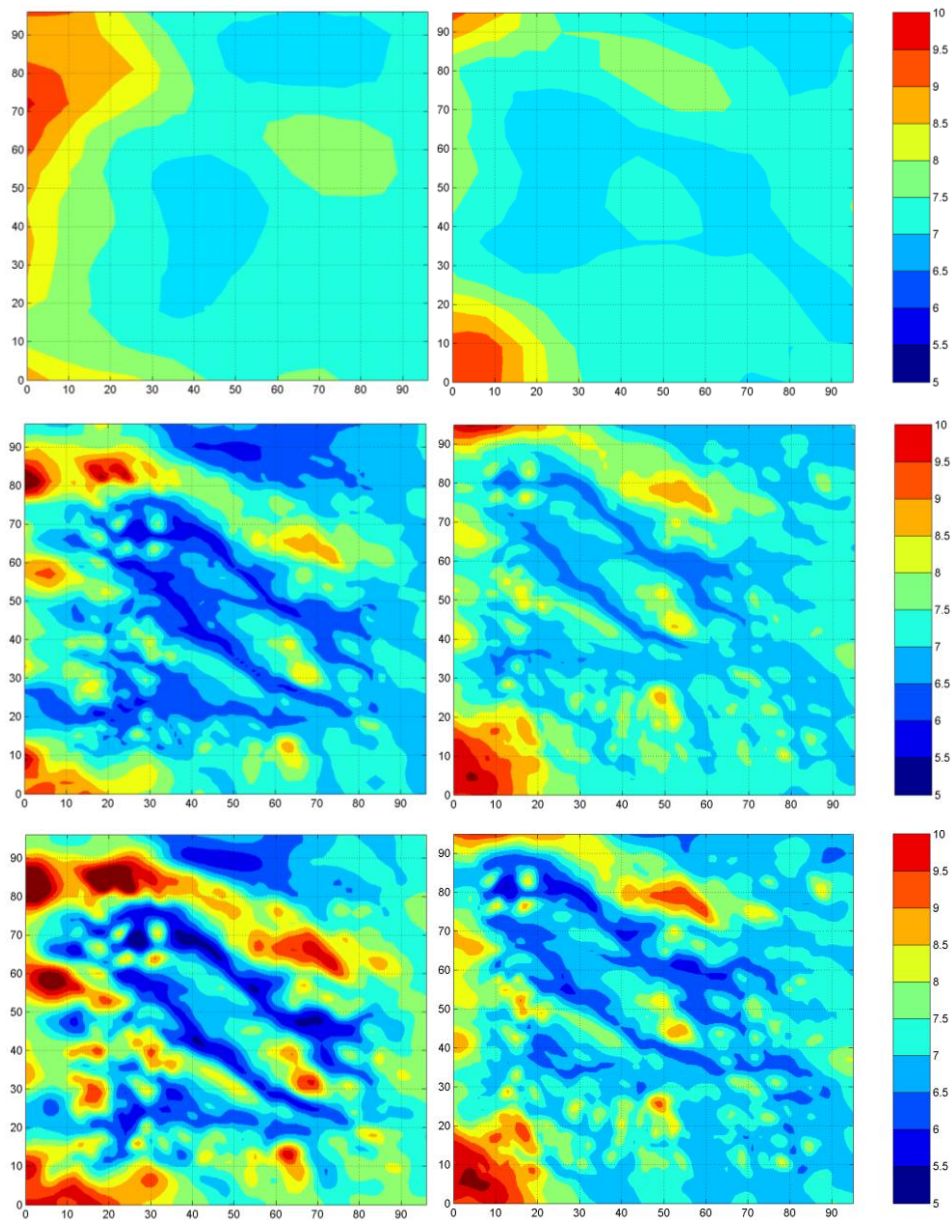


**Figure 6-26: Modelled seasonal average wind speed (m/s) Sep 2011-Apr 2012 for model domain N3C. Left hand plots results from COAMPS®, right hand plots from WRF. Top row plot results using 9 km model resolution. Second row results after downscaling from 9 km to 1 km resolution. Bottom row results using 1 km resolution. Horizontal scales given in km.**

The differences between results using the COAMPS<sup>®</sup> and the WRF model are however the largest ones. The WRF results show larger numbers of icing hours than the COAMPS<sup>®</sup> model. This result was also shown above in section 5. Another difference between using COAMPS<sup>®</sup> and WRF results is that, as we saw above, downscaling using COAMPS<sup>®</sup> 9 km model runs typically gave a smaller number of icing hours than using the 1 km resolution model results directly. Using WRF 9 km model runs for downscaling, the opposite results were obtained. The downscaled results gave a larger number of icing hours compared to what was estimated using the WRF 1 km resolution model results directly. This can be seen for all six model domains shown in Figure 6-27 to Figure 6-38. As using COAMPS<sup>®</sup> model results, the high elevation terrain induced maxima in number of icing hours are found at the same locations using both downscaled data and 1 km resolution model data, but comparing the magnitudes the downscaled number of icing hours were here found to be the largest ones.

Although the above described differences are typical, there are exceptions as e.g. regarding the results that the WRF model typically gives a larger number of icing hours than the COAMPS<sup>®</sup> model. For model domains N3E and N3F, and for the winter season 2011-2012, the COAMPS<sup>®</sup> results show larger numbers of icing hours. These are the two southernmost model domains, but the same results were not obtained for the winter season 2010-2011. The results is thus not of a general nature and the reason for this is not obvious. Further investigations are needed to find an explanation.

Some numerical results are presented in Table 6-8. Seasonal numbers of hours of active icing are given for both COAMPS<sup>®</sup> and WRF results. The average numbers of icing hours for the whole model domains are presented together with maximum and minimum number of icing hours found within each domain. Icing hours are given using the 1 km model results directly, using the downscaled 9 km model results, and using the 9 km model results directly.

As already described above the WRF model using the 1 km resolution model results gives larger numbers of icing hours than given by the COAMPS<sup>®</sup> model. As an average for all model domains the ratio between number of active icing hours using WRF and using COAMPS<sup>®</sup> was 1.47. But as said above for the southern model domains, especially for the winter season 2011-2012, the opposite results were found. For these two domains the average ratio was estimated to 0.59, while the average ratio for the four northern model domains alone was 1.91. The average number of icing hours for all domains using the COAMPS<sup>®</sup> 1 km model runs was 260, while the corresponding number was 323 using the WRF model.

Comparing with results using just the 9 km model results for the same area as the 1 km model domain we get the average number of icing hours 184 and 351 from the COAMPS<sup>®</sup> and the WRF model respectively. That is the average for the WRF model is somewhat larger than using the 1 km domain results, while the COAMPS<sup>®</sup> results were found to give about 30 % less number of icing hours. The average ratio between the number of icing hours using WRF and COAMPS<sup>®</sup> was here 2.32. The tendency towards a smaller ratio for the southern model domains was still found. The average for the four northern domains was 2.91 while the average for the two southern domains was 1.12.

Downscaling the 9 km model results to 1 km we find that the number of icing hours using the COAMPS® model was smaller than given by the 1 km results. The average was here 186 hours as compared to 260 hours using the 1 km resolution runs directly. The corresponding numbers using the WRF model were 455 hours and 323 hours respectively. Using the WRF model results the downscaling thus increase the average over the whole model domain while the COAMPS® model results give a smaller number of icing hours.

Turning to the maximum found in each of the model domains we find that the average maximum using the COAMPS® model 1 km results was 1316 hours with no clear trend from north to south. The corresponding number using the WRF model 1 km results was 1123 hours, here with some tendency towards smaller numbers for the southern domains.

The maximum icing hours using the 9 km model results directly gave smaller numbers. 512 hours using COAMPS® results and 715 hours using WRF results. This could be expected as the maxima are found in the higher elevation terrain and with a smaller resolution the topography is smoothed out and lack the high elevation parts.

The results for downscaled data using the COAMPS® model data gave the maximum 1272 hours as an average for all model domains, about the same as the results using the 1 km model resolution data directly. Using WRF model data the average maximum using downscaled data was 1459 hours, somewhat larger than the 1123 hours using the 1 km model results directly.

The minimum number of icing hours for the whole model domains was estimated to 50 hours on the average using the COAMPS® 1 km model results and to 60 hours using the WRF model results. The corresponding results using the 9 km resolution model results directly were 48 hours and 140 hours respectively. About the same results were found using the COAMPS® model results but larger using the WRF model results.

Also using the downscaled results the minimum using the COAMPS® model results gave about the same number of icing hours, 45 hours as an average for all model domains, while the average minimum was 109 hours using the WRF model results.

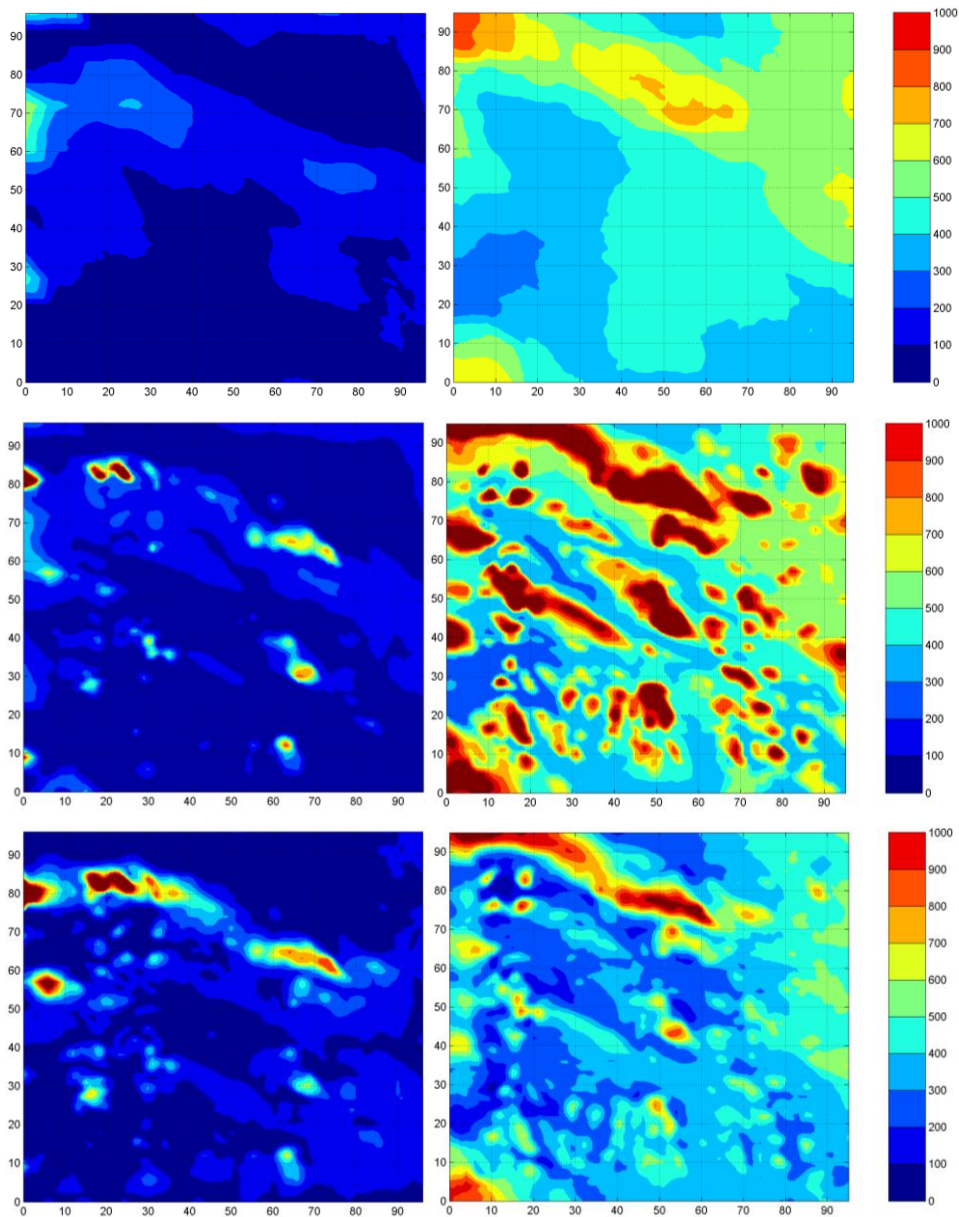


**Figure 6-27: Modelled seasonal number of hours with active icing Sep 2010-Apr 2011 for model domain N3C. Left hand plots results from COAMPS®, right hand plots from WRF. Top row plot results using 9 km model resolution. Second row results after downscaling from 9 km to 1 km resolution. Bottom row results using 1 km resolution. Horizontal scales given in km.**

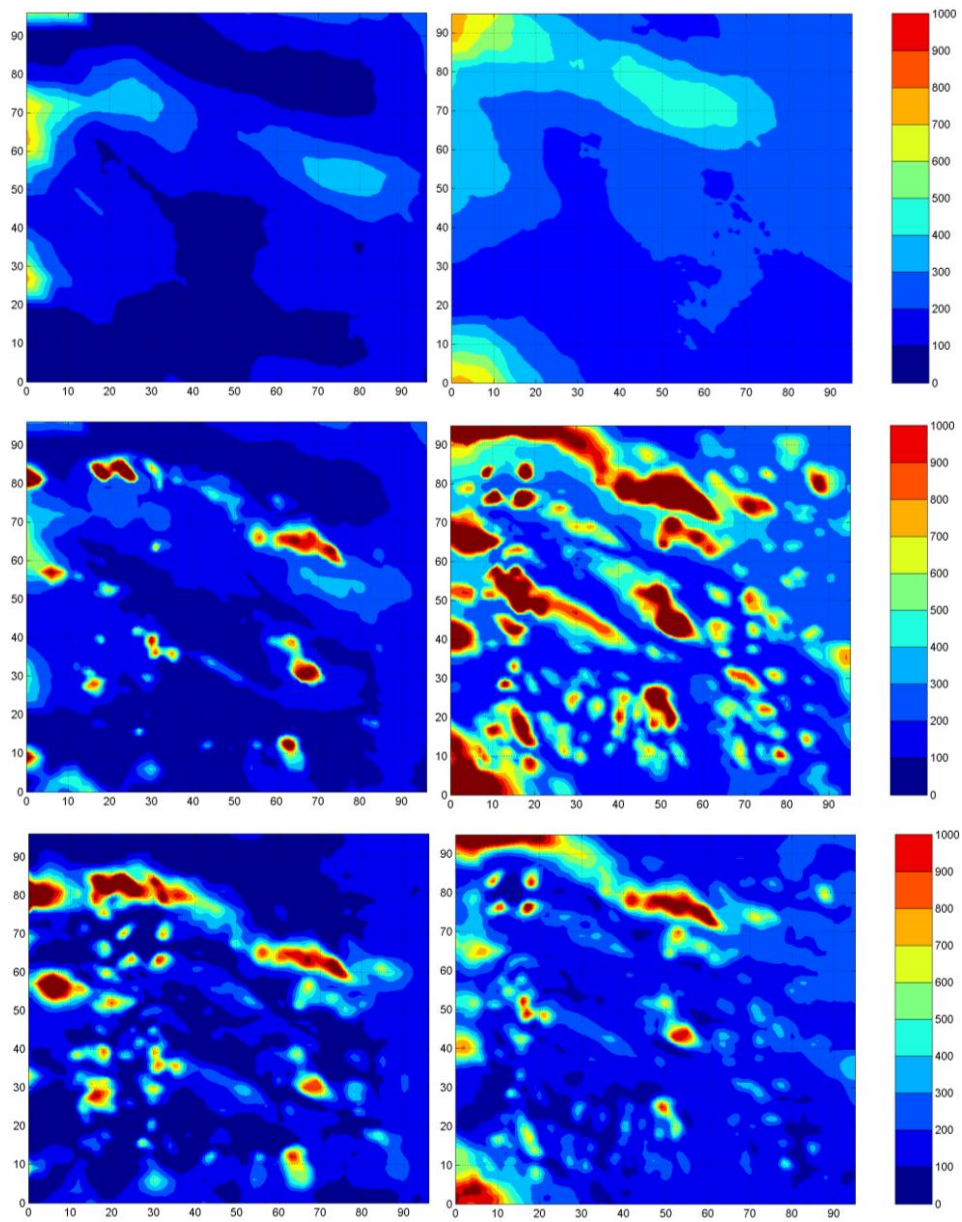


**Figure 6-28: Modelled seasonal number of hours with active icing Sep 2011-Apr 2012 for model domain N3C. Left hand plots results from COAMPS®, right hand plots from WRF. Top row plot results using 9 km model resolution. Second row results after downscaling from 9 km to 1 km resolution. Bottom row results using 1 km resolution. Horizontal scales given in km.**

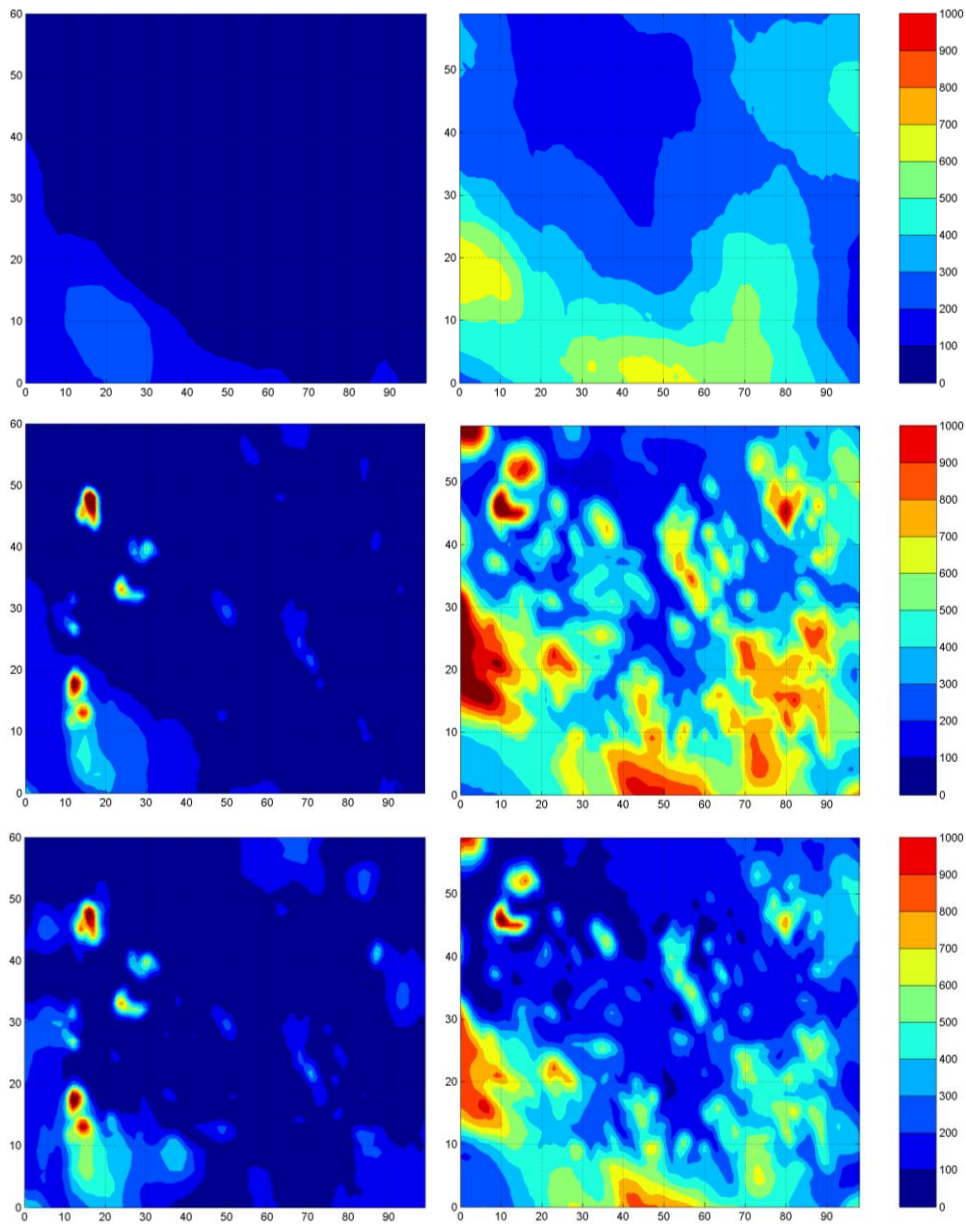


**Figure 6-29: Modelled seasonal number of hours with active icing Sep 2010-Apr 2011 for model domain N3D. Left hand plots results from COAMPS®, right hand plots from WRF. Top row plot results using 9 km model resolution. Second row results after downscaling from 9 km to 1 km resolution. Bottom row results using 1 km resolution. Horizontal scales given in km.**

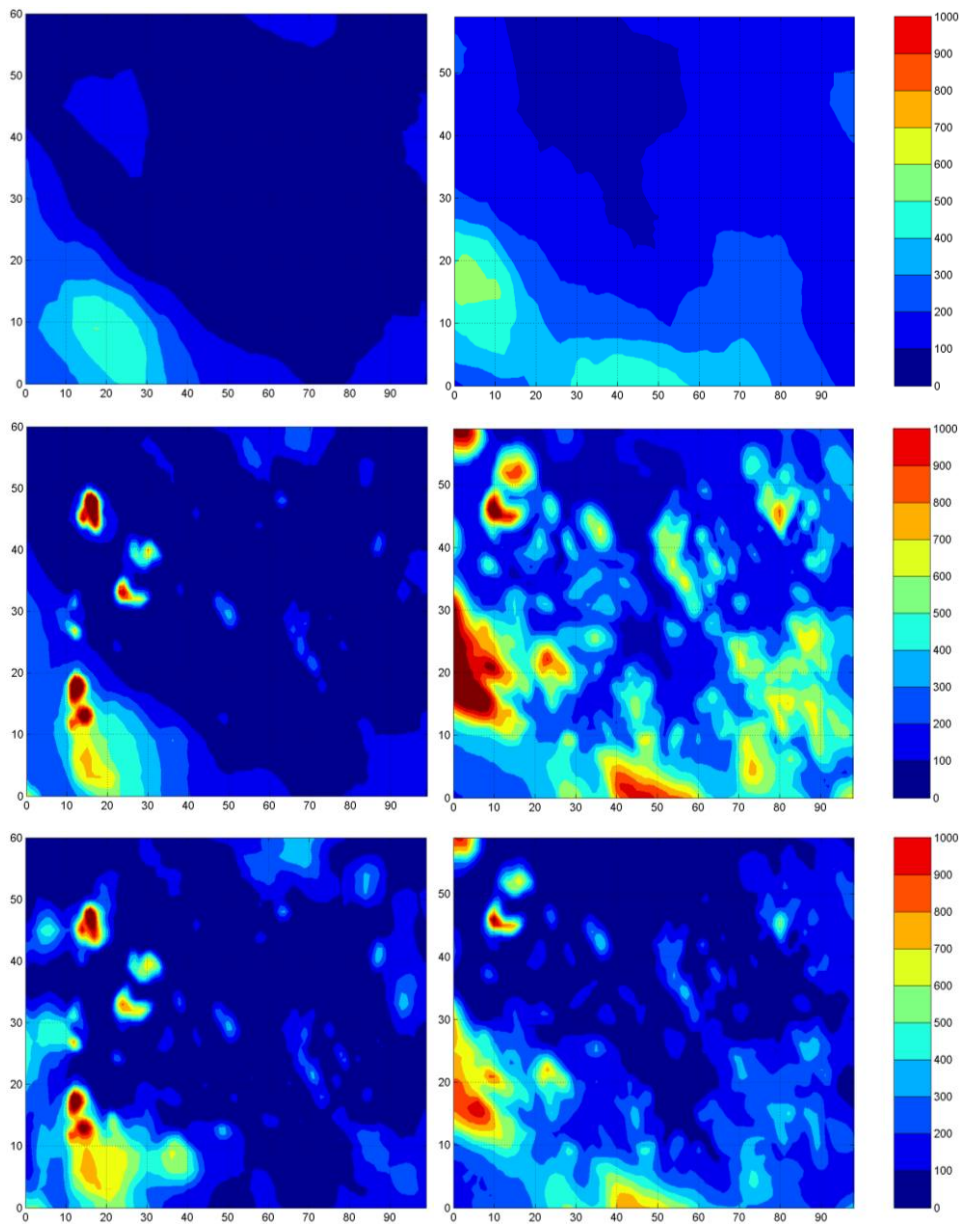


**Figure 6-30: Modelled seasonal number of hours with active icing Sep 2011-Apr 2012 for model domain N3D. Left hand plots results from COAMPS®, right hand plots from WRF. Top row plot results using 9 km model resolution. Second row results after downscaling from 9 km to 1 km resolution. Bottom row results using 1 km resolution. Horizontal scales given in km.**

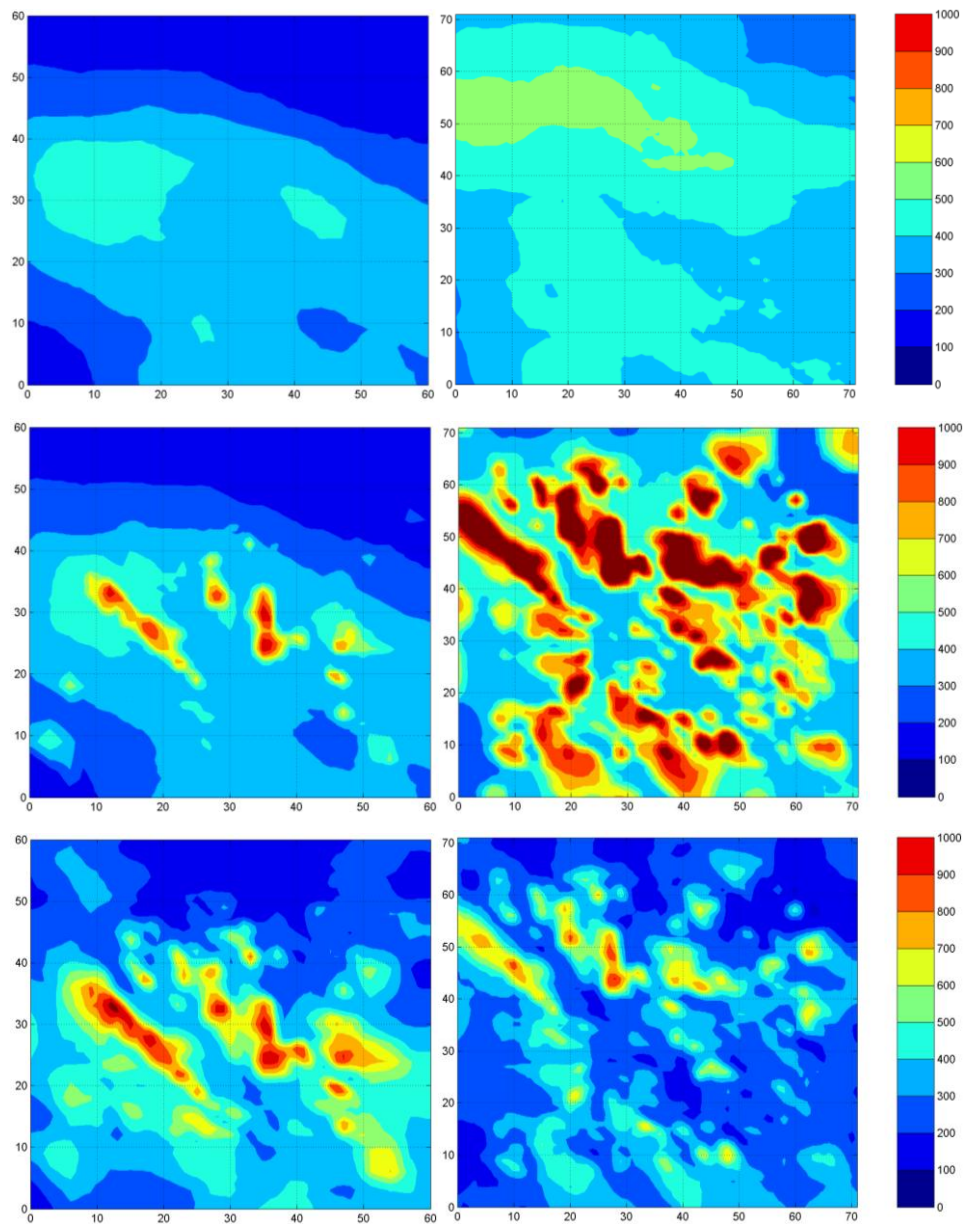


**Figure 6-31: Modelled seasonal number of hours with active icing Sep 2010-Apr 2011 for model domain N3E. Left hand plots results from COAMPS®, right hand plots from WRF. Top row plot results using 9 km model resolution. Second row results after downscaling from 9 km to 1 km resolution. Bottom row results using 1 km resolution. Horizontal scales given in km.**

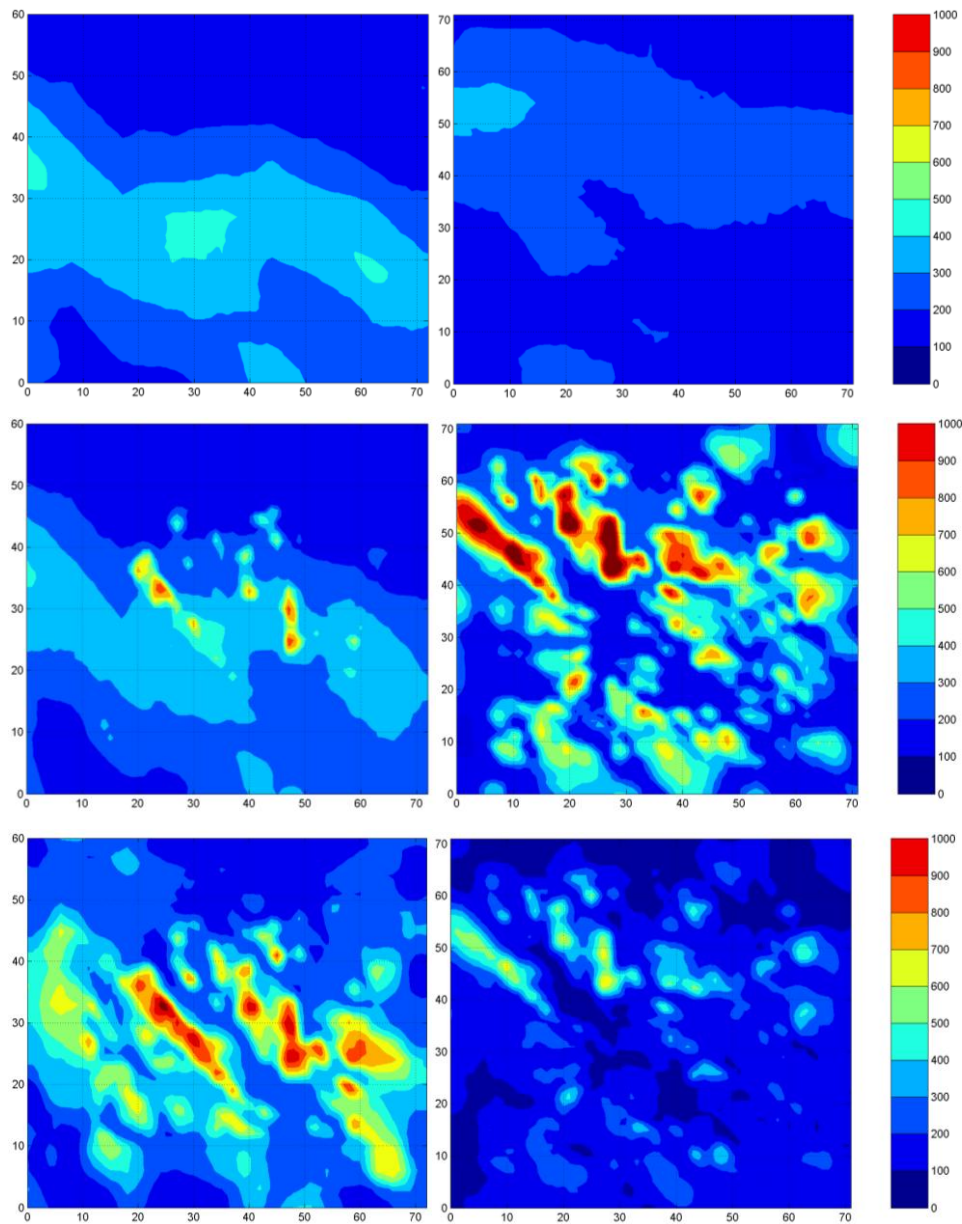


**Figure 6-32: Modelled seasonal number of hours with active icing Sep 2011-Apr 2012 for model domain N3E. Left hand plots results from COAMPS®, right hand plots from WRF. Top row plot results using 9 km model resolution. Second row results after downscaling from 9 km to 1 km resolution. Bottom row results using 1 km resolution. Horizontal scales given in km.**

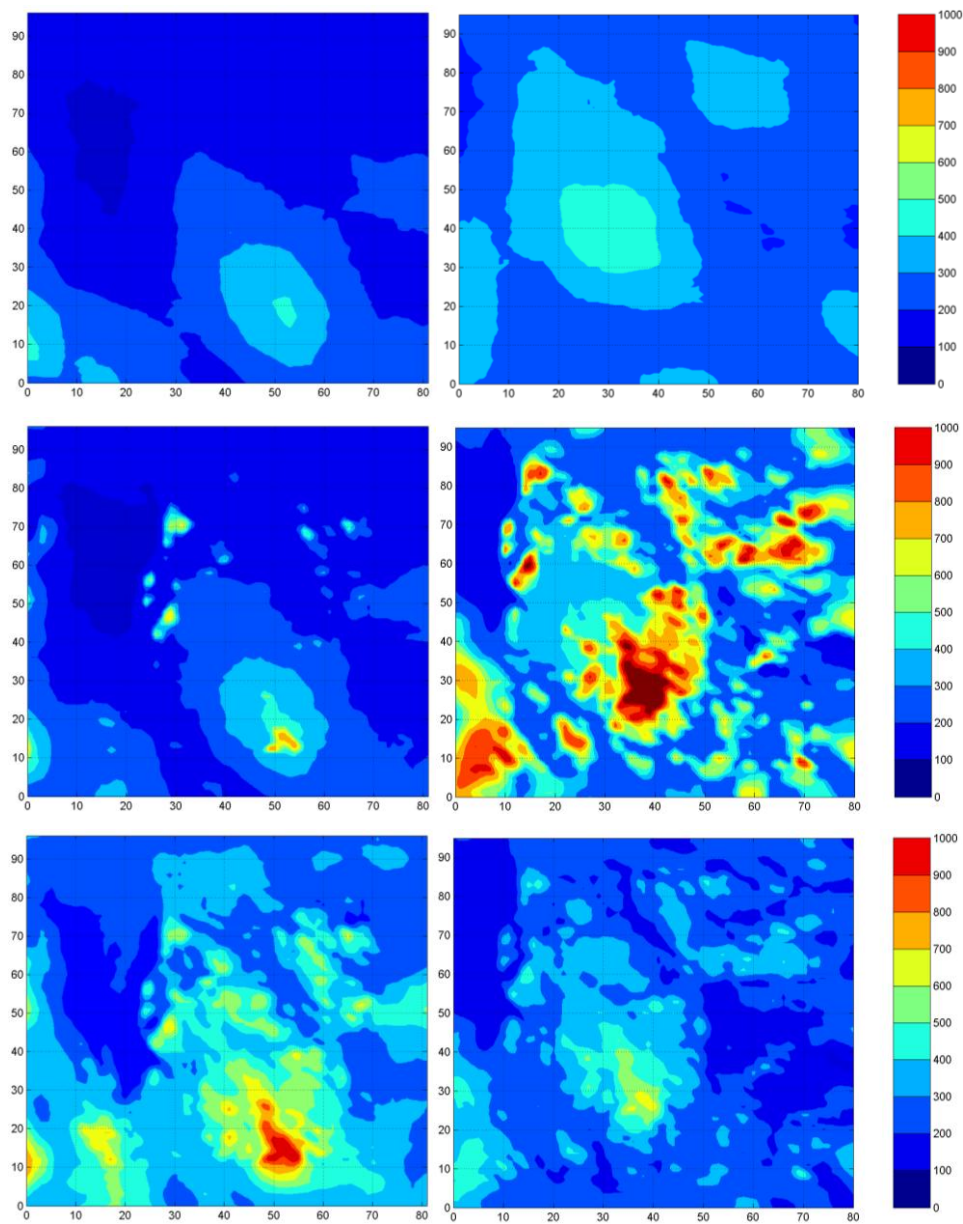


**Figure 6-33: Modelled seasonal number of hours with active icing Sep 2010-Apr 2011 for model domain N3F. Left hand plots results from COAMPS®, right hand plots from WRF. Top row plot results using 9 km model resolution. Second row results after downscaling from 9 km to 1 km resolution. Bottom row results using 1 km resolution. Horizontal scales given in km.**

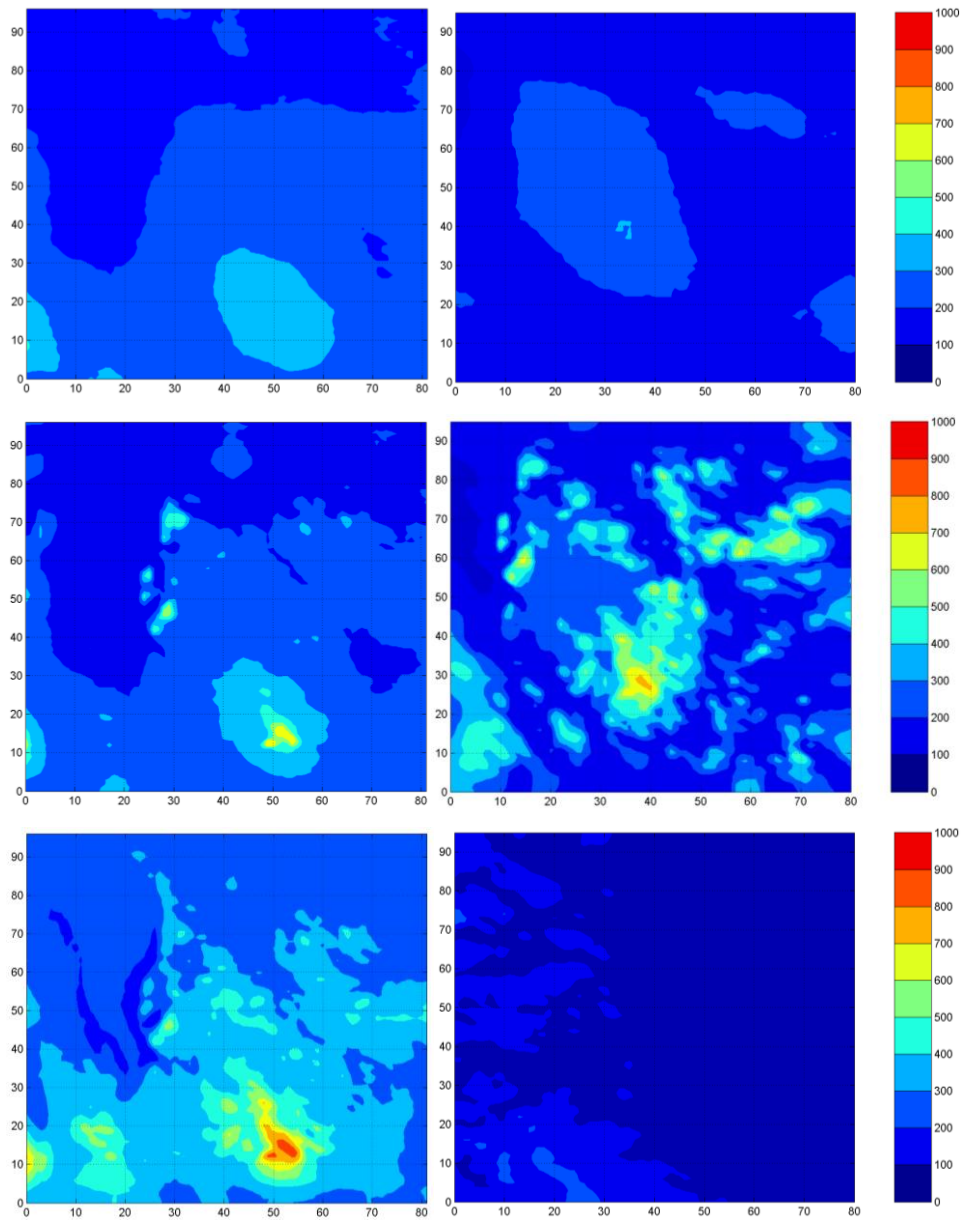


**Figure 6-34: Modelled seasonal number of hours with active icing Sep 2011-Apr 2012 for model domain N3F. Left hand plots results from COAMPS®, right hand plots from WRF. Top row plot results using 9 km model resolution. Second row results after downscaling from 9 km to 1 km resolution. Bottom row results using 1 km resolution. Horizontal scales given in km.**

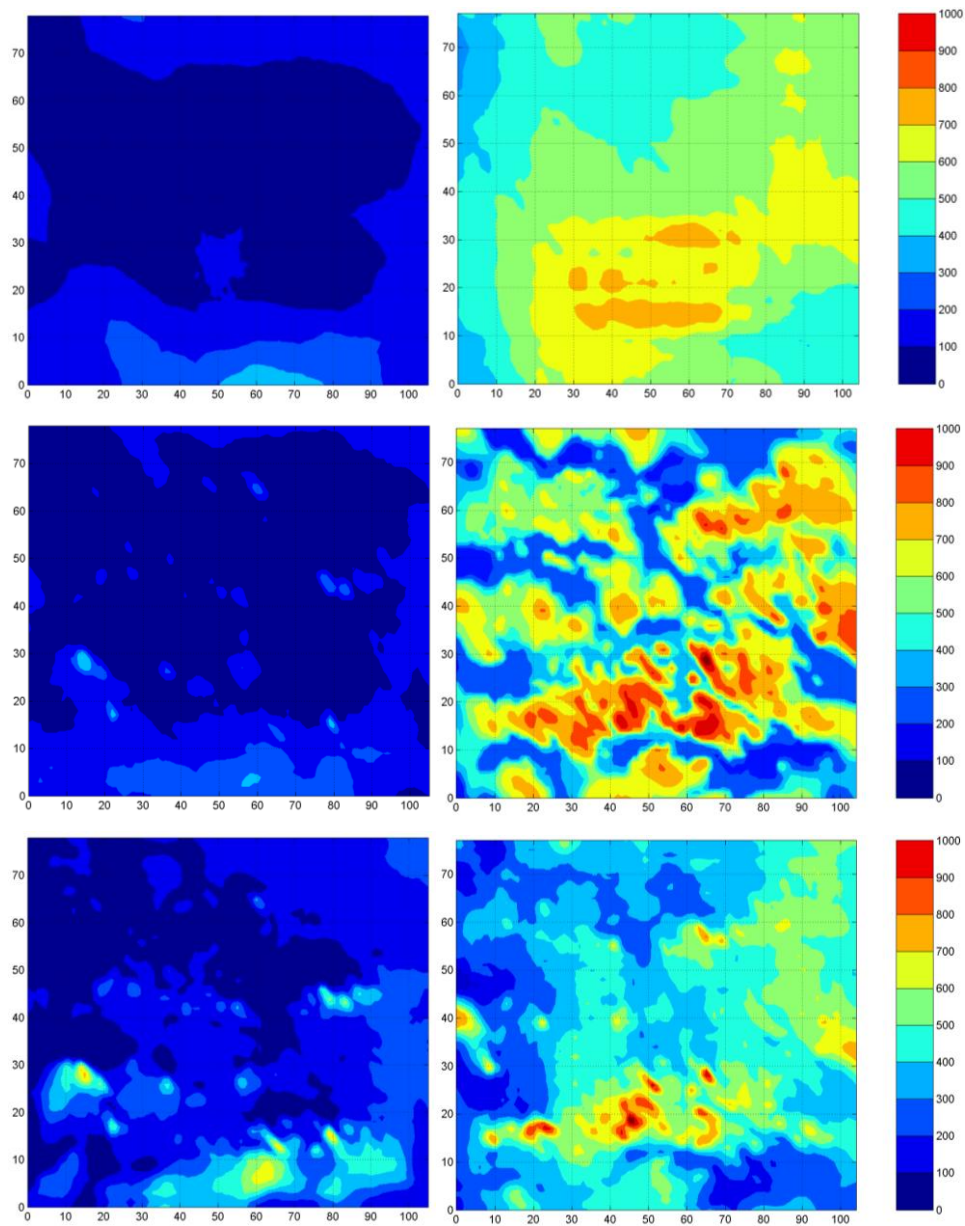


**Figure 6-35: Modelled seasonal number of hours with active icing Sep 2010-Apr 2011 for model domain N3B. Left hand plots results from COAMPS®, right hand plots from WRF. Top row plot results using 9 km model resolution. Second row results after downscaling from 9 km to 1 km resolution. Bottom row results using 1 km resolution. Horizontal scales given in km.**

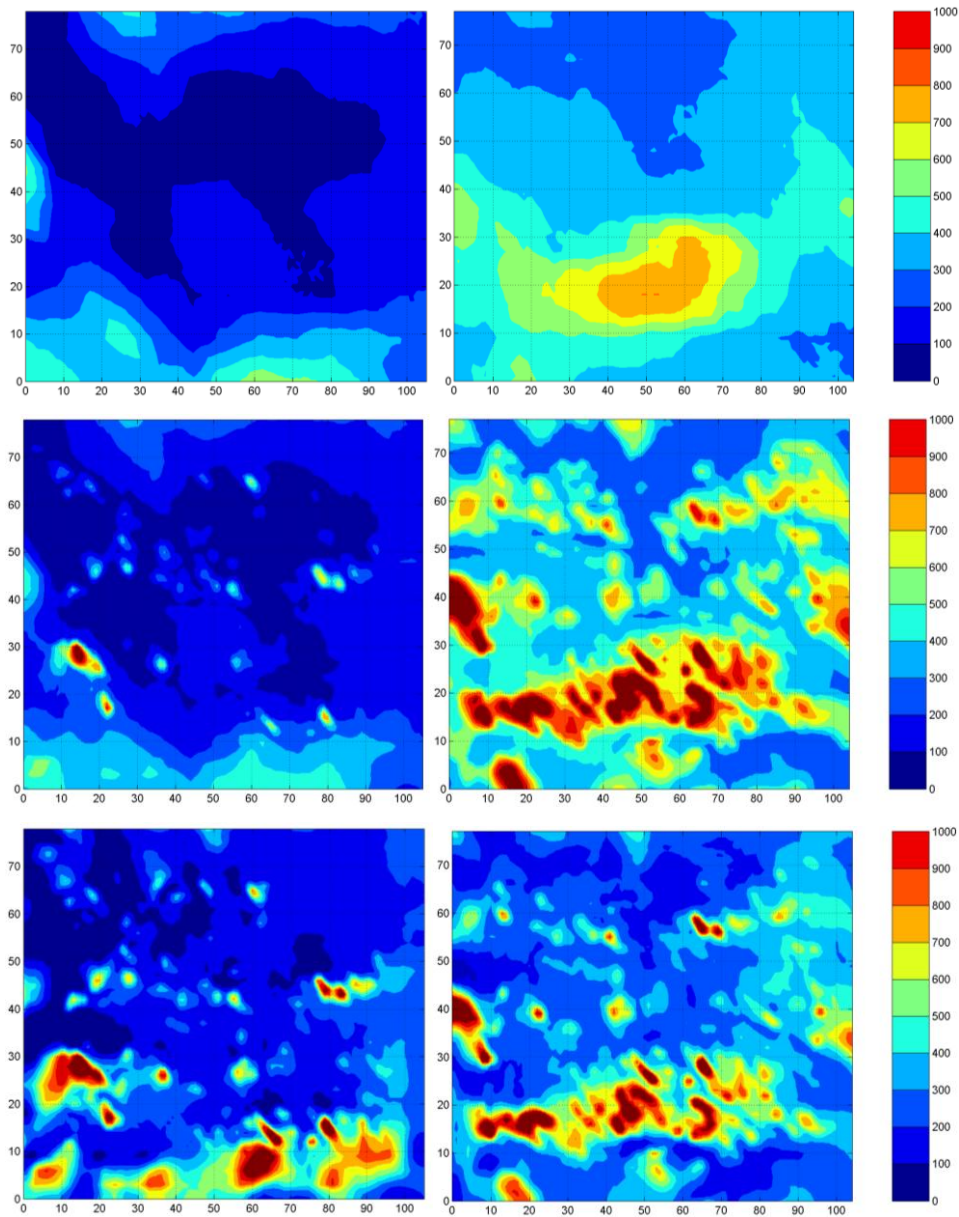


**Figure 6-36: Modelled seasonal number of hours with active icing Sep 2011-Apr 2012 for model domain N3B. Left hand plots results from COAMPS®, right hand plots from WRF. Top row plot results using 9 km model resolution. Second row results after downscaling from 9 km to 1 km resolution. Bottom row results using 1 km resolution. Horizontal scales given in km.**

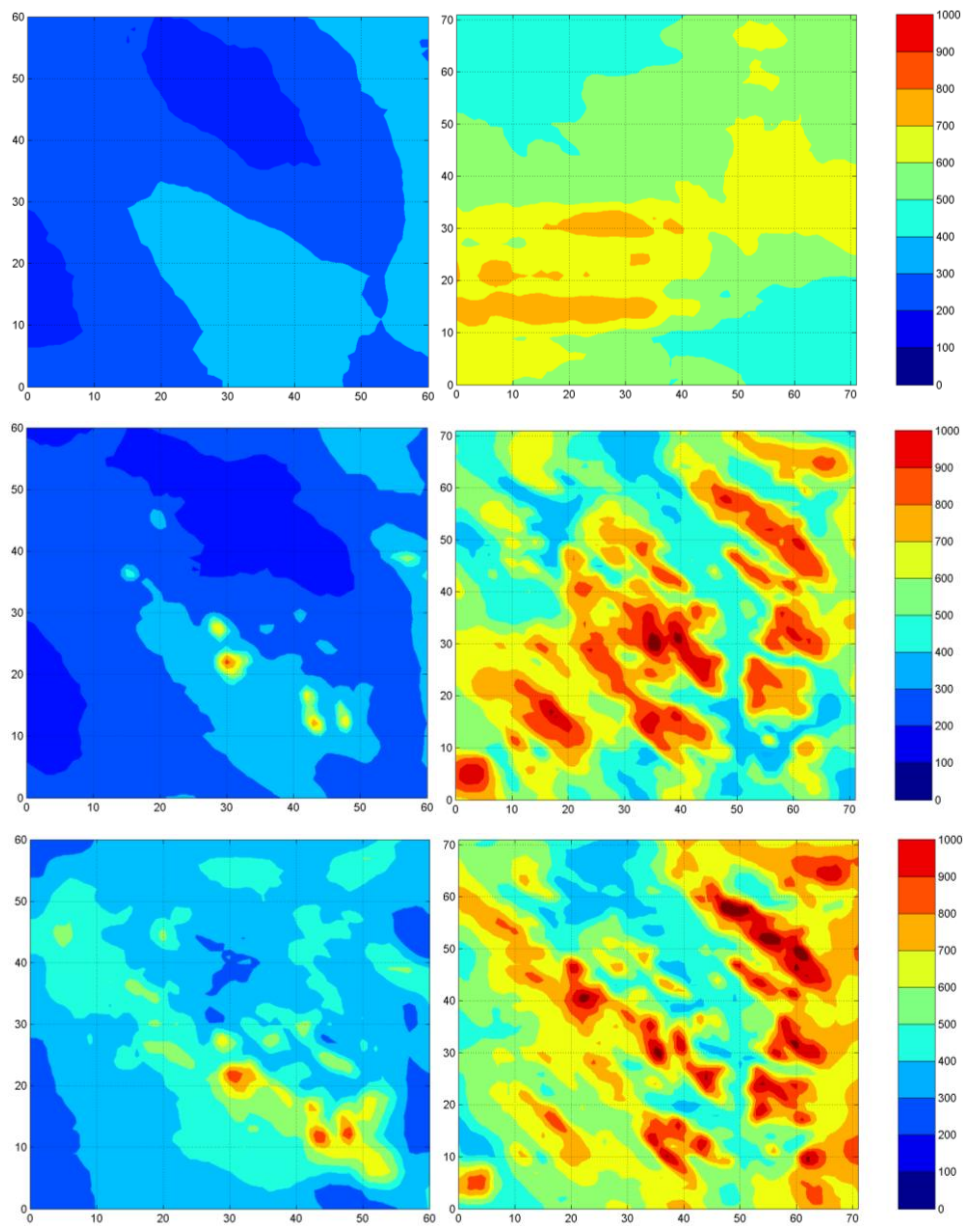


**Figure 6-37: Modelled seasonal number of hours with active icing Sep 2010-Apr 2011 for model domain N3A. Left hand plots results from COAMPS®, right hand plots from WRF. Top row plot results using 9 km model resolution. Second row results after downscaling from 9 km to 1 km resolution. Bottom row results using 1 km resolution. Horizontal scales given in km.**

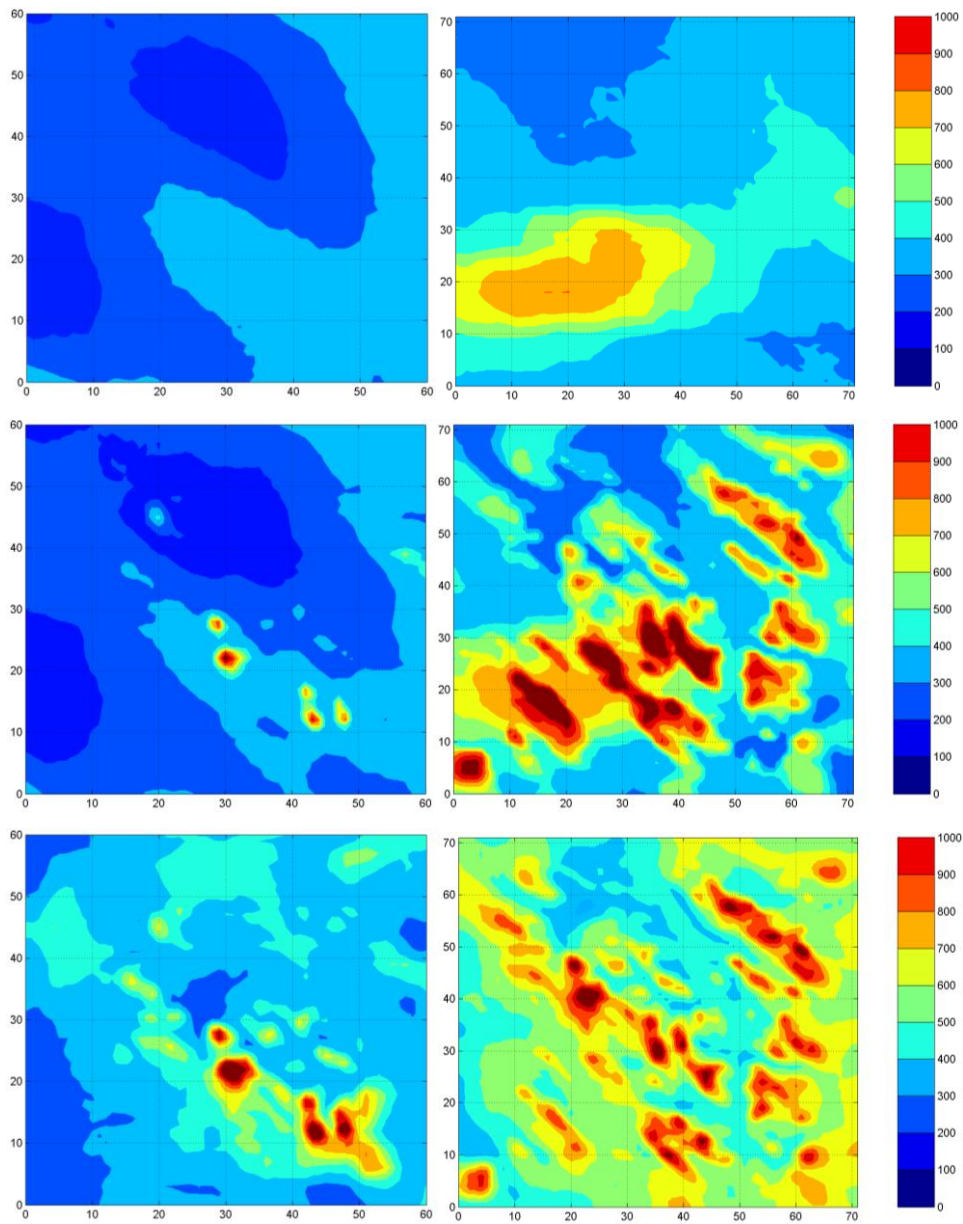


**Figure 6-38: Modelled seasonal number of hours with active icing Sep 2011-Apr 2012 for model domain N3A. Left hand plots results from COAMPS®, right hand plots from WRF. Top row plot results using 9 km model resolution. Second row results after downscaling from 9 km to 1 km resolution. Bottom row results using 1 km resolution. Horizontal scales given in km.**

**Table 6-8: Model estimated seasonal numbers of hours with active icing for the 1 km resolution model domains. Column "1 km": Results using 1 km resolution. Column "9 km to 1 km": Results using 9 km resolution downscaled to 1 km resolution. Column "9 km": Results using 9 km resolution.**

Model domain	Season	Model	Average 9km to 1 km			Maximum 9km to 1 km			Minimum 9km to 1 km		
			1 km	9km	9km	1 km	9km	1 km	9km	1 km	9km
N3A	2010/2011	COAMPS	388	259	264	963	864	430	153	100	114
		WRF	622	600	566	1192	1154	884	234	241	321
	2011/2012	COAMPS	388	267	271	1347	1093	483	134	107	114
		WRF	579	512	406	1352	1592	865	221	170	184
N3B	2010/2011	COAMPS	157	96	108	903	458	378	0	1	1
		WRF	401	502	541	1115	1172	911	46	99	233
	2011/2012	COAMPS	246	171	170	1525	1247	660	1	8	10
		WRF	355	489	400	1685	1611	873	38	141	155
N3C	2010/2011	COAMPS	140	113	110	1789	2465	611	2	9	3
		WRF	391	611	461	1338	2030	972	13	145	167
	2011/2012	COAMPS	187	160	147	2072	2392	845	0	11	7
		WRF	234	415	254	1660	2245	878	10	60	66
N3D	2010/2011	COAMPS	102	77	69	1438	1574	330	0	0	1
		WRF	291	448	317	1269	1416	775	6	58	66
	2011/2012	COAMPS	143	117	103	1542	1634	517	0	2	6
		WRF	184	321	185	1165	1369	592	2	34	30
N3E	2010/2011	COAMPS	369	304	290	1102	1024	492	67	77	80
		WRF	310	574	410	982	1594	605	61	162	203
	2011/2012	COAMPS	337	249	251	1074	914	467	71	89	87
		WRF	163	335	201	722	1242	360	17	67	83
N3F	2010/2011	COAMPS	345	194	194	1125	886	491	85	53	60
		WRF	260	406	287	719	1348	524	43	67	98
	2011/2012	COAMPS	315	224	225	914	719	446	90	83	95
		WRF	84	243	180	279	738	330	24	63	69

### 6.3 Summary of Chapter 6

Creating an icing climatology using representative months could be a viable option to modelling 30 years. The methods have a varying degree of success with the parameters on which they were tested. All the methods consistently work best on temperature, then wind speed and the least well on icing/ice load. How successful the methods are at capturing a parameter seems largely dependent on the complexity of the parameter, temperature being a relatively simple parameter and icing being more complex.

The method using the best fit of temperature and wind speed monthly means to the long term means gives the best results for the tested parameters. The other tested methods have either problems catching the parameters correctly (random day method and Lamb class method) or were highly variable in the results (the five consecutive years method). There are issues with all the tested methods, it cannot be stressed enough that they are just estimations of the means and should not be taken as truth.

The statistical downscaling technique gives quite reasonable results. Although the exact numbers sometimes may be questioned, the geographical variation in response to topography seems to be well captured. The uncertainty obtained regarding the quantitative number of active icing hours should also be judged in relation to the differences in icing hours arrived at using different models. There are today no measurements having sufficient quality to judge which numbers to believe in.

Aiming for an icing climatology, one may argue that a long enough period should be given a high priority. Our results using statistical downscaling show that this technique gives the opportunity to include enough number of years in the analysis (30 years or so) by which the statistical representativeness of the results used for the climatology will be sufficient for a high accuracy.

The uncertainty in this method mainly is in the downscaling itself. In the other alternative tested here, using representative months, the reduction in period length needed to catch the climatology from 30 years to about 5 years, makes it more feasible to actually use a 1 km resolution modelling directly. But instead of having an uncertainty in the downscaling, we here will have the uncertainty in the choice of the representative periods. Still the differences remain concerning the choice of model used for the high resolution climatology. An interesting alternative would be to make the 30 year coarse resolution climatology using all available models. Then make an ensemble climatology out of this and finally downscale this result to 1 km resolution. This has, however, been outside the scope of the present study.

Based on today's knowledge the best method to recommend making an icing climatology might be to run the models on a 1 km x 1 km resolution for 1-2 years, and then run the models for 30 years using a 3-9 km model grid. Finally making a statistical downscaling based on the contemporary data.

## 7 Meso-scale modelling of production losses

### 7.1 Method

Since we do not know the relationship between the observed ice loads and ice loads on wind turbine blades it is difficult to estimate the production loss due to ice based on the observed ice loads. The estimation has to be based on a comparison between the observed ice load and observed production loss. The observed production loss is estimated by using wind speed data, an "ice free" power curve and actual production data. The "ice free" power curve is calculated from all available data from site E5 for temperatures above +5 degrees to be certain that the blades are ice free. Examination of time series of ice load, estimated power production using wind speed together with the power curve and actual power production reveals that the losses primary happen during ice load build-up. The production picks up again when the ice build-up stops and the measured ice load stays at a constant level. This might indicate that the blades while moving loose the ice faster than the measuring device. Production losses also seem to be dependent on the wind speed, the losses are greater at low wind speeds. Empirical functions, matrices that relate power loss to ice build-up, ice load and wind speed have been constructed and tuned against data from E5 and these functions have then been used for all the production loss estimations. The tuning has been done on two months of E5 data where there is a reasonably good agreement between the observed and modelled ice load. Table 7-1 shows the matrix for production loss in per cent as a function of wind speed and icing rate. The determinations of very high production losses, and in particular total stand-still (100 %), are a bit uncertain since there are few data and the matrices are mainly based on extrapolations. The conditions that can cause complete production loss would be very interesting to establish better, but they are probably also very model and site dependent. In this study the type of ice has not been considered, i.e. all types of ice are treated in the same way. In reality quite different production efficiency is expected with clear ice and rime ice.

**Table 7-1: Production loss matrix one. Production loss in per cent as a function of wind speed and icing rate**

	Wind speed m/s	3	4	5	6	7	8	9	10	11	12	>=13
Icing rate kg/hour												
0.001		10	9	8	7	6	5	4	3	2	1	0
0.005		30	27	24	21	18	15	12	9	6	3	0
0.010		50	45	40	36	31	26	21	16	12	7	2
0.015		70	63	57	50	44	37	30	24	17	11	4
0.020		85	77	69	62	54	46	38	30	23	15	7
0.025		100	91	82	73	64	55	46	37	28	19	10
0.030		100	95	86	77	67	58	49	40	30	21	12
0.035		100	100	91	81	72	62	53	43	34	24	15
0.040		100	100	91	82	73	64	54	45	36	27	18
0.045		100	100	92	84	77	69	61	53	46	38	30
0.050		100	100	93	86	78	71	64	57	49	42	35
0.055		100	100	93	87	80	73	67	60	53	47	40
0.060		100	100	94	88	82	76	69	63	57	51	45
0.065		100	100	100	94	88	81	75	69	63	56	50
0.070		100	100	100	96	93	89	85	81	78	74	70
0.075		100	100	100	100	96	93	89	86	82	79	75
0.080		100	100	100	100	97	94	91	89	86	83	80
0.085		100	100	100	100	100	98	95	93	90	88	85
0.090		100	100	100	100	100	100	98	96	94	92	90
0.095		100	100	100	100	100	100	100	100	98	97	95
>= 0.100		100	100	100	100	100	100	100	100	100	100	100

Production loss table derivation in detail:

1. Take production data and wind data from E5 when T > +5.
2. Fit an ice-free production curve by sampling wind data in ranges and average production data for each range.
3. Smooth the resulting curve manually by visual inspection.

Production loss as a function of ice build up and wind speed:

1. Use observed wind and production data from E5 for a 2 month period when there is a good agreement between modelled and observed ice load.
2. Build a table like in Table 7-1.
3. For each hour during the period, take the modelled ice build up
4. Use the available production data and compare with the above computed ice-free curve and calculate production loss.
5. Accumulate loss figures for the ice build class AND observed wind speed class in question.

6. Calculate average value in each table box in Table 7-1.
7. Smooth manually by inspection, interpolate and extrapolate to boxes without data.

A similar matrix, Table 7-2, relates production loss to wind speed and ice load.

**Table 7-2: Production loss matrix two. Production loss in per cent as a function of wind speed and ice load.**

	Wind speed m/s	3	4	5	6	7	8	9	10	11	12	>=13
Ice load kg/m												
0.0		0	0	0	0	0	0	0	0	0	0	0
1.0		80	75	70	65	60	55	50	45	40	35	30
2.0		100	100	90	85	80	75	70	65	60	55	50
3.0		100	100	100	88	84	80	76	72	68	64	60
4.0		100	100	100	100	88	85	82	79	76	73	70
>=5.0		100	100	100	100	100	90	88	86	84	82	80

In the production loss calculation it is first checked whether the icing rate is greater than zero, if so, the production loss is interpolated from Table 7-1. If no active icing is going on the production loss estimate is interpolated from Table 7-2.

## 7.2 Results from winter season 2011/2012

Power production data from five sites are available for the last season. The sites are E1, E5, E10, E12 and E14. To compare the model estimated production loss to the observed production loss, power curves for these sites are calculated using "ice free" (temperature > +5 deg) observations of wind speed and production. These power curves are then used to calculate the observed loss for each turbine at the site. A mean value for each site is then produced using all the turbines. The model estimated power production loss is calculated for all three models AROME, COAMPS<sup>®</sup> and WRF, using both ice load calculations with all condensates and cloud water only as described in section 4.1. Monthly values are summarized in Table 7-3 to Table 7-7.

**Table 7-3: Model estimated and observed monthly power production loss in percent for site E1.**

	aro cw	coa cw	wrf cw	aro all	coa all	wrf all	obs
201110	2	3	2	2	4	3	0
201111	3	4	3	6	5	6	3
201112	6	17	10	39	42	52	22
201201	1	9	17	16	21	46	53
201202	0	3	9	8	5	12	12
201203	1	4	8	9	5	13	1
201204	3	11	13	17	23	52	1

**Table 7-4: Model estimated and observed monthly power production loss in percent for site E5.**

	aro cw	coa cw	wrf cw	aro all	coa all	wrf all	obs
201110	5	6	5	6	9	6	5
201111	6	5	5	13	8	7	6
201112	13	19	19	57	34	55	28
201201	5	10	21	46	32	41	47
201202	4	7	12	14	13	28	29
201203	3	8	6	11	13	11	4
201204	6	14	13	15	29	32	12

**Table 7-5: Model estimated and observed monthly power production loss in percent for site E10.**

	aro cw	coa cw	wrf cw	aro all	coa all	wrf all	obs
201110	1	0	0	1	0	0	0
201111	1	5	1	2	5	1	18
201112	4	13	4	28	29	17	5
201201	2	10	8	17	17	18	13
201202	3	8	10	14	13	17	9
201203	3	4	2	4	4	2	0
201204	0	4	1	7	10	8	3

**Table 7-6: Model estimated and observed monthly power production loss in percent for site E12.**

	aro cw	coa cw	wrf cw	aro all	coa all	wrf all	obs
201111	0	0	0	1	0	0	7
201112	1	3	2	12	5	4	3
201201	0	3	2	6	5	3	0
201202	1	3	3	5	4	4	6
201203	0	1	0	1	1	0	3
201204	0	1	0	3	2	2	2

**Table 7-7: Model estimated and observed monthly power production loss in percent for site E14.**

	aro cw	coa cw	wrf cw	aro all	coa all	wrf all	obs
201201	3	10	10	22	23	33	11
201202	4	10	15	14	15	28	7
201203	5	5	3	6	5	4	0
201204	1	4	2	9	12	11	0

For site E1 there are rather high observed production losses for December-February. The modelled losses are higher using all condensates as expected. They are close to the observed values for some months, a bit further away for some of the others. It's only WRF with all condensates that is close to the observed high value in January. All models predict rather high production losses for April but the observed value is low.

Also for site E5 the observed losses are high, especially for December-February and a rather high value also for April. The model (all condensates) estimated losses are too high in December, fairly close in January and for February WRF is almost spot on but the other two are a bit low. All models are a bit on the high side in March and April.

Mixed results also for site E10, the high observed value in November is a bit suspicious. For the rest of the months the model estimations (all condensates) are a little pessimistic, especially for December and February.

Suspiciously high observed value in November for site E12, it's only one turbine that contributes, the others are around 100% production. Small observed losses for the rest of the winter. The AROME (all condensates) value for December sticks out a bit, all model predicts some losses in January but none is observed.

Only four months of production data available for site E14. Here all the model estimates using all condensates are too high, whereas the estimates using cloud water only are closer to the observations.

### 7.3 Summary of Chapter 7

Empirical functions that relate power production losses to icing rate, ice load and wind speed have been constructed using simultaneous observations of ice load and power production at one of the sites. In order to do this, an "ice free" power curve has been calculated utilizing time series of wind speed and power production at above +5 degrees conditions. The data shows that the production losses primarily occur during ice build-up. The production picks up again rather quickly when the build-up stops while the measured ice load stays at a constant level. The losses also seem to be greater at lower wind speeds.

Time series of modelled icing rate, ice load and wind speed together with the empirical functions have been used to estimate the monthly power production loss at five sites during the 2011/2012 winter season. The ice calculations have been made with liquid cloud water only and also using all condensates. The monthly observed losses are calculated as mean values of all wind turbines at each site. Of course all predicted losses are lower using cloud water only in the icing calculations and again the biggest difference is seen in the AROME production losses. Sometimes the cloud water only losses agree well with the observed and other times it is the losses with all condensates that are closest to the observations.

## 8 Discussion and future work

### **Observations**

Observations of ice load and icing that have been established in Sweden the last few years are unique and of great value for monitoring and model validation. They can however not be taken directly into use but need quality control involving manual intervention. One has to look at the data curves and take some decisions in the smoothing or zero level adjustment process.

Experiences from the O2 Pilot Project have furthermore showed very clearly that comparison of model data with observations add more and an independent value. The meteorological parameters can readily be checked since the modelled pressure and temperature are very accurate and the wind and humidity are quite good but not as easily modelled as the first two. The models often capture icing events while differences are found in the modelled and observed ice load. Most often the models underestimate the ice load. Nevertheless, some errors in the ice load measurements can be detected and confirmed with the model at hand. (Or in fact more than one model, since for the ice loads the models do not agree as close as for meteorological parameters.)

A more or less routine monitoring of the data and quality control with corrections is crucial for the use of data, for any purpose, also in the future. For conventional meteorological data, National Meteorological Services, like SMHI in Sweden, are responsible for doing this on their national data before it is archived and made available for climate monitoring and model validation etc. For the special observations in the O2 Pilot Project, this has been carried out mainly in this project (aided by the validation against models in the O2 project). A process to handle future data from the Pilot Project needs to be established.

The existing network should be maintained and continued and if possible extended somewhat. Mast measurements at different heights add a lot of values for conventional meteorological parameters. With future very large rotor diameters the blades will sweep through different wind and icing conditions below and above the nacelle. Icing measurements at several heights would add value to icing studies if instruments at the different levels are equally well calibrated and ways in the analysis process were developed to ensure that differences in measured ice load/icing intensity between the levels is due to differences in icing conditions only.

### **Modelling, precision and uncertainties**

The meso-scale modelling at the km scale is still an evolving area and there have been a lot of model development including sub-grid parameterisation during the last decade in particular. For instance, the surface modelling schemes and databases of surface conditions have been improved to better represent the spatial and temporal variability as one gets down to km scales. It is driven by many applications of meso-scale models for operational

weather forecasting and what were once research applications have been transferred to operational more demanding environments and requirements. It is only fairly recently that computers have developed that far to make it possible to reach this high resolution (of a few km down to 1 km in some cases) in operational weather forecasting.

As models evolve and the schemes improve, it is expected that improved results also for the icing computations will be obtained in the near future, and in fact every few years as developments continue. When significantly improved versions have become established, one should re-run past periods as well, much the same way as re-analyses are made over again.

There are of course uncertainties in the model results, and particularly for the derived quantity of icing, depending on at least three model variables. The availability of several models is helpful for understanding these, as is the possibility of applying different physical parameterisations. The differences have been shown in the project, but one can probably make more use of such differences in the context of ensemble forecasting methodology. It is well established for global models and baroclinic developments (frontal systems that are connected with weather systems at several 100 km to 1000 km scales). Meso-scale ensemble systems are in their infancy, but a lot of effort is going into this area. Even though the influence of the different boundary conditions has been shown to be relatively small compared to e.g. the different parameterisations, both sorts of perturbations are used for meso-scale ensemble prediction. The interpretation of ensembles of forecasts is also important when estimating uncertainties. It is e.g. not as useful to employ one scheme, which is inferior to other ones, and assign the same weight or probability to an inferior member.

The initial conditions of the forecasts have been interpolated from larger scale models and their analyses, using conventional meteorological observations including also some satellite data over surrounding oceans. The more immediate local data for cloudiness (cloud base measurements) or cloud analyses from satellite have not been used at all. Stations with lidar cloud measurements are available in the normal networks and at some of the O2 Pilot project stations. Satellite data are only available a few times per day since polar orbiting satellites is the only alternative at these high latitudes and the short daylight period imposes some limitation too. Visibility instruments are also available and the values are related to liquid water content but it is a fairly rough relationship. In all, it should be possible, with admittedly large efforts, to use more local data to initialise models. Particularly for short forecasting times (less than 12 hours) it is possible to see effects of satellite, cloud and radar information in modelling systems in other countries. An effort into at least mapping the cloudiness better will hopefully improve model performance. There is also a value of better knowledge of low clouds when validating the models against ice measurements.

**Icing modelling and icing climate**

The icing calculations depend on not only the amount of liquid cloud water but also on droplet size distribution. Advancements in this area are likely to be possible and in particular as the cloud microphysics is something that will be developed further. Including other cloud condensates such as snow in the icing calculation results in a much higher modelled ice load than if using liquid cloud water only. To improve the models, measurements of liquid cloud water and droplet size distributions are most likely necessary. It would also be good to monitor the amount of the different cloud species.

Ice shedding is very uncertain and needs both more consideration how to model this and how to verify this. There is probably a lot of manual work involved, from analysing camera images to checking production losses against modelled or measured ideal production. The current estimates are very uncertain and for many turbines during rime ice events, shedding may in reality be quite rapid. (As opposed to the case with clear ice, but there is little experience in the project of its occurrence.)

Icing climate in terms of number of hours with ice accretion exceeding e.g., 10 g/m per hour is a practically achievable computation from model simulation over long seasons and years. There are quite large variations between the three seasons shown in this report, and these calculations should be extended to a longer period for an estimate of an icing climate.

With the relatively realistic estimates over long periods of the statistical downscaling, this method could be extended, both for 30 years (or more in fact, 30 years is not a holy number) and to many sites or as a complete map of Sweden. The statistical downscaling has the potential to be able to extend over more than 30 years, so further understanding of the length of period needed can be obtained.

In Table 8-1 a summary of Pro's and Con's for the different climatology methodologies investigated here are given.

**Table 8-1: Summary of Pro’s and Con’s for different climatology methodologies and specific comments for each methodology.**

Methology	Pro’s	Con’s	Rating and comments
Direct 1x1 km model simulation (Ch 5)	Best description of local scales and variability in time	Very computationally demanding for large areas and many years. Model uncertainties are still large and should be quantified, possibly by running different models over one or a few years.	Preferable since it gives a good estimate of both spatial and temporal variability.  Needs substantial financing for supercomputers.
Representative months with best fit method (Ch 6.1)	Cost effective way to sample climate. This is the best representative method tested.	Does not cover the full distribution and some features may be missed. Difficult to extend beyond mean conditions.	Might be applicable. If only limited computer resources available it is a cost effective method. But, the icing climate is not fully satisfactory sampled.
5 consecutive years (or 10) Ch 6.1)	Possible to run at high resolution.	Sensitive to which 5/10 years period that is sampled.	No, not recommendable at least not for time periods of the order of 5 years.
Statistical downscaling (Ch 6.2)	Cost effective way of reproducing most of the high-resolution features.	Relies on regression and is not perfect for local icing conditions.	A promising method that can serve as an alternative before long high-resolution runs are available.

Finally, production losses due to icing needs to be further investigated. One interesting path is for example to find ways to include different types of ice, glaze and rime ice, in the production loss model. This would then make it possible to include the different effects glaze and rime ice have on production losses, both in magnitude and duration due to differences in shape and ice shedding. To develop and validate such model, more detailed observations is however needed. Another possible approach has been tested in a newly developed production loss model (see Baltscheffsky, M., 2013, and Söderberg, S., M. Baltscheffsky, and H. Bergström, 2012, in section “Publications and conference proceedings”). Instead of modelling ice load on a rotating cylinder and use this as an input to a production loss model, the new approach is to model the potential icing over the entire rotor disc. The “potential icing” and several weather parameters such as wind speed, wind direction, temperature from the mesoscale model output are then used in a statistical model, which is trained against wind farm data. The model has been applied to single wind farms with some success, even for individual turbines within the farm but more work on making the production loss model more general is needed.

Acknowledgements: The NCEP/NCAR reanalysis data for this study are from the Research Data Archive (RDA) which is maintained by the Computational and Information Systems Laboratory (CISL) at the National Center for Atmospheric Research (NCAR). NCAR is sponsored by the National Science Foundation (NSF). The original data are available from the RDA (<http://dss.ucar.edu>) in dataset number ds090.0.



## References

- Brooks I. M., Söderberg S. and Tjernström M., 2003: The Turbulence Structure of the Stable Atmospheric Boundary Layer Around a Coastal Headland: Aircraft Observations and Modelling Results. *Bound.-Layer Meteor.*, **107**, 531-559.
- Burk, S. D., and W. T. Thompson, 1996: The summertime low-level jet and marine boundary-layer structure along the California coast. *Mon. Wea. Rev.*, **124**, 668-686.
- Burk, S. D., T. Haack, and R. M. Samelson, 1999: Mesoscale simulation of supercritical, subcritical and transcritical flow along coastal topography. *J. Atmos. Sci.*, **56**, 2780-2795.
- Caniaux, G., J.-L. Redelsperger and J.-P. Lafore, 1994: A numerical study of the stratiform region of a fast-moving squall line. Part I. General description, and water and heat budgets. *J. Atmos. Sci.*, **51**, 2046-2074.
- Chaboureau J.-P., and P. Bechtold, 2005: Statistical representation of clouds in a regional model and the impact on the diurnal cycle of convection during Tropical Convection, Cirrus and Nitrogen Oxides (TROCCINOX). *J. Geophys. Res.*, **110**, D17103, doi:10.1029/2004JD005645.
- Chen, S., J. Cummings, J. Doyle, R. Hodur, T. Holt, C.S. Liou, M. Liu, J. Ridout, J. Schmidt, W. Thompson, A. Mirin, and G. Sugiyama, 2003: COAMPS™ version 3 model description - general theory and equations. Naval Research Laboratory Technical Report, NRL/ PU7500-04-448. 141 pp.
- De Rooy, W. C., and P. Siebesma, 2008: A simple parameterization for detrainment in shallow cumulus. *Mon. Wea. Rev.*, **136**, 560-576.
- Finstad, K., E. P. Lozowski, and L. Makkonen, 1988: On the Median Volume Diameter Approximation for Droplet Collision Efficiency, *J. Atmos. Sci.*, **45**, 4008-4012.
- Häggmark, Lars, Ivarsson, K-I, Gollvik, S, and Olofsson, P-O, 2000: MESAN, an operational mesoscale analysis system. *Tellus A*, **52**, no 1, pp 2-20.
- Hodur, R. M., 1997: The Naval Research Laboratory's Coupled Ocean/Atmosphere Mesoscale Prediction System (COAMPS). *Mon. Wea. Rev.*, **125**, 1414-1430.
- Horvath, K, D. Koracin, R. Vellore, J. Jiang, and R. Belu, 2012: Sub-kilometer dynamical downscaling of near-surface winds in complex terrain using WRF and MM5 mesoscale models, *J. Geophys. Res.*, **111**, D11111-11130, doi:10.1029/2012JD017432

ISO 12494. Atmospheric Icing of Structures. ISO/TC 98/SC3 200.

Kalnay, E., M. Kanamitsu, R. Kistler, W. Collins, D. Deaven, L. Gandin, M. Iredell, S. Saha, G. White, J. Woollen, Y. Zhu, M. Chelliah, W. Ebisuzaki, W. Higgins, J. Janowiak, K.C. Mo, C. Ropelewski, J. Wang, A. Leetmaa, R. Reynolds, R. Jenne, and D. Joseph, 1996: The NCEP/NCAR 40-year reanalysis project. *Bull. Amer. Meteor. Soc.*, **77**, 437-471.

Kessler, E., 1969: On the distribution and continuity of water substance in atmospheric circulations. *Meteor. Monog.*, 10, No 32, 84pp.

Le Moigne, P. 2012: SURFEX SCIENTIFIC DOCUMENTATION [www.cnrm.meteo.fr/surfex/IMG/pdf/surfex\\_scidoc\\_v2.pdf](http://www.cnrm.meteo.fr/surfex/IMG/pdf/surfex_scidoc_v2.pdf)

Makkonen, L., 2000: Models for the growth of rime, glaze, icicles and wet snow on structures. *Phil. Trans. R. Soc. Lond. A*, **358**, 2913-2939.

Masson V., J.-L. Champeaux, F. Chauvin, C. Meriguet and R. Lacaze, 2003 : A global database of land surface parameters at 1km resolution in meteorological and climate models. *J. Climate*, **16**, 1261-1282.

Mazin, I. P., Korolev, A. V., Heymsfield, A., Isaac, G. A., Cober, S. G., 2001: Thermodynamics of Icing Cylinder for Measurements of Liquid Water Content in Supercooled Clouds. *Journal of Atmospheric and Oceanic Technology* , Volume 18 (4).

Mazin, I.P., 1995: Cloud water content in continental clouds of middle latitudes, *Atmospheric Research*, **35**, 283-297.

Mellor, G. L., and Yamada, T., 1974: A hierarchy of turbulence closure models for planetary boundary layers, *J. Atmos. Sci.*, **31**, 1791-1806.

Monin, A.S., and A.M. Obukhov (1954): Basic laws of turbulent mixing in the surface layer of the atmosphere. *Contrib. Geophys. Inst. Acad. Sci., USSR*, **151(1)**:163-187.

Murphy, A. H., 1988: Skill scores based on the mean square error and their relationships to the correlation coefficient, *Mon. Weather Rev.*, **116**, 2417-2424, doi:10.1175/1520-0493(1988)116<2417:SSBOTM>2.0.CO;2.

Pielke, R. A., 1984: *Mesoscale Meteorological Modelling*. Academic Press, 612 pp.

Pinty, J.-P. and P. Jabouille, 1998: A mixed-phase cloud parameterization for use in mesoscale non-hydrostatic model: simulations of a squall line and of orographic precipitations. *Proc. Conf. of Cloud Physics*, Everett, WA, USA, *Amer. Meteor. Soc.*, Aug. 1999, 217 - 220.

Seity, Y. and Brousseau, P. and Malardel, S. and Hello, G. and Bénard, P. and Bouttier, F and Lac, C. and Masson, V., 2012: The AROME-France convective scale operational model, *Monthly Weather Review*, **139**, 976-991.

Siebesma, P., P. M. M. Soares, and J. Teixeira, 2007: A combined Eddy-Diffusivity Mass-Flux approach for the convective boundary layer. *J. Atmos. Sci.*, **64**, 1230-1248.

Skamarock, W. C., J. B. Klemp, J. Dudhia, D. M. Gill, M. Duda, X.-Y. Huang, W. Wang, and J. G. Powers, 2008: A Description of the Advanced Research WRF Version 3. NCAR Technical Note.

- Söderberg, S., and O. Parmhed, 2006: Numerical modelling of katabatic flow over a melting outflow glacier. *Bound.-Layer Meteor.*, **120**, 509-534.
- Söderberg, S., and Tjernström M., 2001: Supercritical Channel Flow in the Coastal Atmospheric Boundary Layer: Idealized Numerical Simulations, *J. Geophys. Res.*, **106**, 17811-17829.
- Söderberg, S., and Tjernström M., 2002: Diurnal Cycle of Supercritical Along-Coast Flows, *J. Atmos. Sci.*, **59**, 2615-2624.
- Thompson, G., B. E. Nygaard, L. Makkonen and S. Dierer, 2009: "Using the Weather Research and Forecasting (WRF) Model to Predict Ground/Structural Icing", Conference proceeding from IWAIIS XIII in Andermatt, 2009.
- Thompson, G., P. R. Field, R. M. Rasmussen, and W. D. Hall, 2008: Explicit forecasts of winter precipitation using an improved bulk microphysics scheme. Part II: Implementation of a new snow parameterization. *Mon. Wea. Rev.*, **136**, 5095-5115.
- Thompson, G., R. M. Rasmussen, and K. Manning, 2004: Explicit forecasts of winter precipitation using an improved bulk microphysics scheme. Part I: Description and sensitivity analysis. *Mon. Wea. Rev.*, **132**, 519-542.
- Thorsson, P., 2010: Modelling of Atmospheric Icing. An introduction essay. Uppsala University, pp 57.
- Trewin, Blair C., 2011. The role of climatological normals in a changing climate. WCDMP-No. 61. WMO-TD No. 1377. World Meteorological Organisation, Geneva.  
<http://www.wmo.int/pages/prog/wcp/wcdmp/documents/WCDMPNo61.pdf>
- U.S. National Centers for Environmental Prediction, updated daily: NCEP FNL Operational Model Global Tropospheric Analyses, continuing from July 1999. Dataset ds083.2 published by the CISL Data Support Section at the National Center for Atmospheric Research, Boulder, CO, available online at <http://dss.ucar.edu/datasets/ds083.2/>.
- Undén, Per, L. Rontu, H. Järvinen, P. Lynch, J. Calvo, G. Cats, J. Cuxart, K. Eerola, C. Fortelius, J. Antonio Garcia-Moya, C. Jones, G. Lenderlink, A. McDonald, R. McGrath, B. Navascues, N. Woetman Nielsen, V. Ødegaard, E. Rodriguez, M. Rummukainen, R. Rööm, K. Sattler, B. Hansen Sass, H. Savijärvi, B. Wichers Schreur, R. Sigg, H. The, A. Tijn, 2002: HIRLAM-5 Scientific Documentation, HIRLAM-5 Project, c/o Per Undén SMHI, S-601 76 Norrköping, SWEDEN.

## Publications and conference proceedings in the project

### **Journal publications**

- Thorsson, P., S. Söderberg, and H. Bergström, 2013: Modelling ice loads using measured meteorological parameters, manuscript to Cold Regions Science and Technology.
- Thorsson, P., S. Söderberg, H. Bergström, and E. Olsson, 2012: Using representative periods to create icing climatologies, manuscript.

### **Conference presentations**

- Andrae, U., Thorsson, P., S. Söderberg, H. Bergström, E. Olsson, and P. Undén, 2010: En kommande svensk iskartering, lägesrapport från Vindforsk III projekt V-313 'Vindkraft i kallt klimat'. Vintervind 2010, Piteå, Sweden, oral presentation.
- Baltscheffsky, M., 2013: Modelling of production losses due to icing for individual turbines in a wind farm – development of techniques for forecasting and site assessment. Winterwind 2013, Östersund, Sweden, oral presentation.
- Bergström H., Thorsson P., Olsson E., Undén P., and Söderberg S., 2012: Wind power in cold climates – Vindforsk project V-313. Konferensbidrag Winterwind 2012.
- Bergström, H., U., Andrae, P., Thorsson, S. Söderberg, E. Olsson, and P. Undén, 2011: Windpower in cold climates - Vindforsk project V313. Winterwind 2011, Umeå, Sweden, oral presentation.
- Olsson, E., P., Thorsson, H., Bergström, U., Andrae, S. Söderberg, and P. Undén, 2011: Towards a high-resolution icing climatology in Sweden. IWAIS Chongqing, China, oral presentation.
- Söderberg, S., 2013: Mesoscale modelling of icing climate: Sensitivity to model and model setup, Winterwind 2013, Östersund, Sweden, oral presentation.
- Söderberg, S., and M. Baltscheffsky, 2012: Long-term estimates and variability of production losses in icing climates. Winterwind 2012, Skellefteå, Sweden, poster presentation.
- Söderberg, S., M. Baltscheffsky, and H. Bergström, 2012: Estimation of production losses due to icing - a combined field experiment and numerical modelling effort: EWEA 2013, Wien, Austria, oral presentation.
- Thorsson, P., and E. Olsson, 2012: Creating an icing climatology. EMS Łódź Poland, oral presentation.
- Thorsson, P., S. Söderberg, and H. Bergström, 2011: Validation of icing measurements - Vindforsk project V - 313. IWAIS Chongqing, China, oral presentation.
- Thorsson, P., S. Söderberg, H. Bergström, E. Olsson, and P. Undén, 2013: Creating an icing climatology using typical months. WinterWind 2013, Östersund, Sweden, oral presentation.

### **Other presentations**

- Bergström H., 2010: Meteorologiska prediktioner av nedisning. Konferensbidrag Energitinget 2010.

- Bergström H., 2011: Vindkraft i skog och kallt klimat. Konferensbidrag Nationella Vindkraftskonferensen, Kalmar 2011-05-12.
- Bergström H., 2011: Iskartering - möjligheter och frågeställningar. Konferensbidrag Nolia Vind 2011.
- Bergström H., 2012: Vindkraft och nedisning - iskartering, möjligheter och frågeställningar. Konferensbidrag Vindkraftforskning i fokus, Göteborg, januari 2012.
- Bergström H., 2012: Windpower in forests and wind power in cold climates. Conference contribution, STandUP for Energy, KTH 30 May 2012.
- Thorsson, P., and E. Olsson, 2012: Creating an icing climatology. Vindkraftsforskning i fokus, Göteborg, poster presentation.

**Reports**

- Carlsson V., 2009: Measuring routines of ice accretion for wind turbine applications. Master thesis, Engineering Physics, Umeå University, 2009.
- Rindeskär E., 2010: Modelling of icing for wind farms in cold climate. Master thesis, Inst. F. geovetenskaper, Uppsala universitet, 2010.
- Söderberg S., 2011: Wind power in cold climates - Vindoforsk project V-313. Konferensbidrag VindkraftNet - cold climates 2011-04-04.
- Thorsson, P., 2010: Modelling of atmospheric icing. Introductory essay, Department of Earth Sciences, Uppsala University, 57 pp.
- Thorsson P., 2012: Wind power in cold climates. Conference contribution, STandUP for Energy, KTH 30 May 2012.

## Appendix A

Tables A-1 to A-20, summary tables of all the verification statistics in section 4.2.2.

**Table A-1: Monthly numbers season 2009/2010 of rms (root mean square error), corr (correlation), number of icing hours and max ice load (kg/m) for site E1, all three models. First row using cloud water only in the icing calculation, second row with all condensates.**

	ARO				COA				WRF			
	rms	corr	ice hours	max load	rms	corr	ice hours	max load	rms	corr	ice hours	max load
200910												
Cw	2,18	0,96	21	0,25								
All	1,92	0,94	87	0,94								
200911												
Cw	1,68	-0,18	119	0,79								
All	2,19	-0,18	271	6,72								
200912												
Cw	0,77	0,45	0	0,40								
All	0,89	0,01	126	2,16								
201001												
Cw	2,27	0,20	0	0,04								
All	2,27	-0,18	24	0,20								
201002												
Cw	0,54	0,31	0	0,01								
All	0,50	0,28	45	0,44								
201003												
Cw	0,03	0,00	1	0,14								
All	0,55	0,00	93	1,88								
201004												
Cw	0,01	0,00	14	0,11								
All	0,01	0,00	39	0,40								

**Table A-2: Monthly numbers season 2010/2011 of rms (root mean square error), corr (correlation), number of icing hours and max ice load (kg/m) for site E1, all three models. First row using cloud water only in the icing calculation, second row with all condensates.**

	ARO				COA				WRF			
	rms	corr	ice hours	max load	rms	corr	ice hours	max load	rms	corr	ice hours	max load
201009												
Cw	0,00	0,00	0	0,00	0,00	0,00	0	0,00	0,00	0,00	0	0,00
All	0,00	0,00	0	0,00	0,00	0,00	0	0,00	0,00	0,00	0	0,00
201010												
Cw	0,10	0,59	21	0,13	0,10	0,66	63	0,76	0,08	0,76	35	0,31
All	0,19	0,60	71	1,94	0,14	0,62	78	1,05	0,13	0,76	55	1,42
201011												
Cw	0,46	0,23	8	0,14	0,44	0,08	32	0,52	0,44	0,06	51	0,46
All	0,27	0,74	74	0,73	0,40	0,31	63	0,70	0,28	0,72	101	1,18
201012												
Cw	0,71	0,40	0	0,04	0,69	0,13	10	0,30	0,65	0,20	20	0,55
All	0,56	0,78	120	3,04	0,65	0,22	52	0,66	0,55	0,48	54	0,74
201101												
Cw	0,77	0,01	0	0,03	0,77	-0,17	16	0,15	0,70	0,23	49	0,42
All	0,81	0,18	104	2,59	0,76	-0,12	21	0,24	0,65	0,27	99	0,72
201103												
Cw	0,02	-0,01	6	0,18	0,36	0,35	82	1,30	0,10	0,13	38	1,74
All	0,13	0,23	49	0,73	0,40	0,36	107	1,50	0,21	0,14	70	1,78
201104												
Cw	0,31	0,77	17	0,18	0,31	0,39	43	0,74	0,30	0,60	77	1,38
All	0,25	0,88	43	0,71	0,35	0,37	71	1,17	0,49	0,80	125	4,70

**Table A-3: Monthly numbers season 2011/2012 of rms (root mean square error), corr (correlation), number of icing hours and max ice load (kg/m) for site E1, all three models. First row using cloud water only in the icing calculation, second row with all condensates.**

	ARO				COA				WRF			
	rms	corr	Ice hours	Max load	rms	corr	Ice hours	Max load	rms	corr	Ice hours	Max load
201201												
Cw	5,36	-0,28	0	0,12	5,28	-0,26	36	1,00	4,72	0,67	149	1,97
All	5,19	-0,38	164	4,24	5,24	-0,33	161	4,77	4,57	-0,22	337	7,59
201202												
Cw	2,19	0,09	1	0,03	2,12	0,30	28	0,68	2,15	-0,03	36	1,67
All	2,06	0,27	93	1,78	2,10	0,29	66	1,03	2,13	-0,01	72	1,88
201203												
Cw	0,53	0,22	10	0,10	0,49	0,37	56	0,77	0,46	0,40	68	1,42
All	0,51	0,20	94	1,65	0,48	0,34	82	0,93	0,47	0,39	126	3,09
201204												
Cw	0,31	0,57	19	0,21	0,30	0,33	69	0,50	0,30	0,50	108	0,98
All	0,47	0,51	153	1,78	0,70	0,10	187	2,63	3,34	0,24	226	8,52

**Table A-4: Monthly numbers season 2011/2012 of rms (root mean square error), corr (correlation), number of icing hours and max ice load (kg/m) for site E2, all three models. First row using cloud water only in the icing calculation, second row with all condensates.**

	ARO				COA				WRF			
	rms	corr	ice hours	max load	rms	corr	ice hours	max load	rms	corr	ice hours	max load
201109												
Cw	2,65	0,42	14	0,24	2,63	0,34	11	0,46	2,61	0,37	16	0,67
All	2,62	0,31	33	1,05	2,56	0,27	35	1,56	2,53	0,31	38	1,92
201110												
Cw	2,08	0,53	97	0,47	2,05	0,66	87	0,70	2,02	0,60	74	1,24
All	2,03	0,31	117	1,86	1,97	0,39	105	3,43	1,92	0,50	94	3,69
201111												
Cw	1,31	0,67	46	0,82	1,33	0,47	43	0,45	1,27	0,58	37	1,01
All	1,28	0,64	78	1,24	1,32	0,51	53	0,78	1,23	0,56	48	2,23
201112												
Cw	2,11	0,00	44	0,55	2,04	0,07	93	1,03	1,94	0,33	79	0,77
All	2,01	-0,01	210	2,00	1,86	0,27	212	1,43	1,43	0,66	245	6,24
201201												
Cw	3,81	0,74	0	0,06	3,72	0,53	32	0,57	3,24	0,36	157	2,44
All	2,71	0,82	125	4,99	3,17	0,75	107	2,41	1,93	0,82	241	8,36
201202												
Cw	0,26	0,11	0	0,07	0,26	0,18	21	0,39	0,27	-0,04	11	0,33
All	0,30	0,04	62	1,01	0,27	0,15	35	0,60	0,27	0,07	16	0,33
201203												
Cw	0,40	0,11	14	0,09	0,38	0,38	33	0,33	0,40	0,43	51	1,36
all	0,39	0,14	52	0,49	0,37	0,40	42	0,39	0,42	0,42	73	1,41
201204												
cw	0,76	0,25	16	0,29	0,64	0,65	58	0,67	0,64	0,55	55	0,88
all	0,71	0,32	121	2,03	1,28	0,61	150	4,69	1,56	0,53	126	6,07

**Table A-5: Monthly numbers season 2009/2010 of rms (root mean square error), corr (correlation), number of icing hours and max ice load (kg/m) for site E5, AROME and COAMPS. First row using cloud water only in the icing calculation, second row with all condensates.**

	ARO				COA				WRF			
	rms	corr	ice hours	max load	rms	corr	ice hours	max load	rms	corr	ice hours	max load
200909												
cw	0,43	0,11	8	0,20	0,44	0,16	1	0,02				
all	0,43	0,11	10	0,25	0,44	0,16	1	0,02				
200910												
cw	3,23	0,66	19	0,49	3,08	0,67	76	1,07				
all	2,90	0,81	84	2,34	2,72	0,78	135	2,98				
200911												
cw	9,90	0,08	131	1,38	9,33	0,04	339	4,24				
all	8,01	0,18	409	11,08	9,45	-0,11	464	23,18				
200912												
cw	13,65	0,44	20	1,04	13,04	0,40	155	3,36				
all	13,05	0,23	252	4,59	12,24	0,31	248	7,71				
201001												
cw	0,76	0,15	3	0,10	0,76	0,21	147	1,70				
all	0,49	0,73	125	1,81	0,86	0,53	179	2,60				
201002												
cw	0,06	0,25	0	0,00	0,04	0,71	3	0,12				
all	0,23	0,82	61	0,91	0,20	0,73	68	0,93				
201003												
cw	0,40	0,41	2	0,09	0,32	0,84	24	0,31				
all	0,45	0,31	74	1,44	0,86	0,95	102	3,28				
201004												
cw	0,86	0,63	25	0,25	0,98	0,16	92	2,25				
all	0,72	0,71	88	1,17	1,58	0,10	144	4,86				

**Table A-6: Monthly numbers season 2010/2011 of rms (root mean square error), corr (correlation), number of icing hours and max ice load (kg/m) for site E5, all three models. First row using cloud water only in the icing calculation, second row with all condensates.**

	ARO				COA				WRF			
	rms	corr	Ice hours	Max load	rms	corr	Ice hours	Max load	rms	corr	Ice hours	Max load
201009												
cw	0,00	0,00	0	0,00	0,00	0,00	0	0,00	0,00	0,00	0	0,00
all	0,00	0,00	0	0,00	0,00	0,00	0	0,00	0,00	0,00	0	0,00
201010												
cw	0,32	0,70	51	0,37	0,27	0,70	58	1,17	0,27	0,72	55	1,13
all	0,24	0,77	78	1,31	0,22	0,79	64	2,18	0,23	0,82	60	3,28
201011												
cw	0,90	0,21	13	0,36	0,90	0,05	36	1,11	0,84	0,25	60	0,91
all	0,56	0,84	60	0,81	0,85	0,18	68	1,72	0,53	0,72	96	2,06
201012												
cw	1,10	0,48	5	0,13	1,10	0,00	16	0,40	1,07	-0,46	29	0,63
all	0,40	0,73	71	1,64	0,97	-0,59	35	1,74	1,63	-0,28	67	4,22
201101												
cw	0,72	0,68	12	0,16	0,67	0,71	35	0,47	0,57	0,70	46	0,88
all	4,67	0,45	193	8,35	0,75	0,41	120	2,74	1,56	0,60	189	5,92
201102												
cw	0,21	0,69	13	0,23	0,26	0,12	26	0,48	0,26	0,32	59	0,91
all	2,55	0,28	271	6,45	0,34	0,30	126	1,16	0,80	0,44	168	2,58
201103												
cw	0,09	0,39	23	0,34	0,30	-0,09	67	1,18	0,17	0,13	77	0,64
all	0,16	0,09	76	0,59	0,37	-0,09	87	1,68	0,46	0,28	117	3,51
201104												
cw	0,10	0,83	17	0,23	0,10	0,66	50	0,84	0,17	0,84	58	1,74
all	0,08	0,74	49	0,48	0,17	0,51	79	1,06	0,31	0,87	85	3,01

**Table A-7: Monthly numbers season 2011/2012 of rms (root mean square error), corr (correlation), number of icing hours and max ice load (kg/m) for site E5, all three models. First row using cloud water only in the icing calculation, second row with all condensates.**

	ARO				COA				WRF			
	rms	corr	ice hours	max load	rms	corr	ice hours	max load	rms	corr	ice hours	max load
201109												
cw	0,00	0,00	0	0,00	0,00	0,00	0	0,00	0,00	0,00	0	0,00
all	0,00	0,00	0	0,00	0,00	0,00	0	0,00	0,00	0,00	0	0,00
201110												
cw	0,12	0,45	50	0,62	0,21	0,54	51	0,98	0,08	0,88	40	1,17
all	0,15	0,50	59	1,14	0,48	0,41	58	2,32	0,17	0,83	45	1,79
201111												
cw	0,37	0,55	56	0,49	0,35	0,44	39	1,31	0,41	0,11	52	1,01
all	0,30	0,64	98	1,25	0,36	0,44	64	1,41	0,43	0,15	61	2,42
201112												
cw	8,72	0,52	93	0,96	8,15	0,55	183	2,52	8,41	0,55	214	1,96
all	6,34	0,78	321	6,25	7,23	0,61	242	5,23	5,20	0,65	289	29,55
201201												
cw	1,91	0,91	17	0,65	1,76	0,74	127	1,47	0,63	0,93	197	4,34
all	2,15	0,81	348	9,38	1,73	0,42	277	7,22	2,96	0,95	312	10,35
201202												
cw	3,10	0,16	27	0,24	3,08	0,05	54	0,67	3,30	0,18	84	0,56
all	3,07	0,11	113	1,02	3,09	0,12	80	2,23	3,06	0,17	134	2,55
201203												
cw	0,06	0,00	28	0,39	0,56	0,00	122	1,89	0,30	0,00	95	1,40
all	0,38	0,00	86	1,99	1,08	0,00	131	3,76	0,63	0,00	121	4,36
201204												
cw	0,15	0,89	26	0,50	0,32	0,42	117	1,28	0,22	0,56	86	1,25
all	0,14	0,82	94	1,64	1,59	0,18	189	4,54	2,06	0,31	163	6,76

**Table A-8: Monthly numbers season 2010/2011 of rms (root mean square error), corr (correlation), number of icing hours and max ice load (kg/m) for site E6, all three models. First row using cloud water only in the icing calculation, second row with all condensates.**

	ARO				COA				WRF			
	rms	corr	ice hours	max load	rms	corr	ice hours	max load	rms	corr	ice hours	max load
201009												
cw	0,00	0,00	0	0,00	0,00	0,00	0	0,00	0,00	0,00	0	0,00
all	0,00	0,00	0	0,00	0,00	0,00	0	0,00	0,00	0,00	0	0,00
201010												
cw	0,14	0,67	40	0,50	0,14	0,65	26	1,16	0,17	0,34	28	0,63
all	0,15	0,54	61	1,03	0,16	0,63	42	1,40	0,34	0,37	43	3,68
201011												
cw	0,27	0,38	23	0,54	0,25	0,47	29	0,95	0,38	0,39	74	1,70
all	0,24	0,72	78	1,02	0,26	0,48	31	1,20	0,54	0,53	98	2,15
201012												
cw	0,17	0,81	7	0,81	0,20	0,22	16	0,30	0,22	0,08	34	0,56
all	0,84	0,85	94	2,28	0,30	0,39	35	1,38	0,65	0,49	51	2,70
201101												
cw	1,03	0,32	16	0,22	0,98	0,59	37	0,55	0,90	0,56	66	1,11
all	1,18	0,62	170	4,06	0,86	0,68	94	1,31	0,54	0,81	147	3,52
201102												
cw	0,19	0,18	13	0,16	0,20	-0,07	17	0,29	0,22	0,56	86	0,93
all	0,29	0,56	85	1,06	0,21	-0,08	33	0,44	0,33	0,57	133	1,17
201103												
cw	0,04	0,59	26	0,17	0,19	0,63	42	0,89	0,09	0,82	56	0,57
all	0,29	0,18	80	1,45	0,30	0,71	76	1,54	0,21	0,78	86	1,29
201104												
cw	0,07	0,80	18	0,25	0,06	0,79	22	0,65	0,24	0,88	48	2,05
all	0,07	0,75	34	0,42	0,10	0,77	47	1,08	0,39	0,91	66	3,68

**Table A-9: Monthly numbers season 2011/2012 of rms (root mean square error), corr (correlation), number of icing hours and max ice load (kg/m) for site E6, all three models. First row using cloud water only in the icing calculation, second row with all condensates.**

	ARO				COA				WRF			
	rms	corr	Ice hours	Max load	rms	corr	Ice hours	Max load	rms	corr	Ice hours	Max load
201109												
cw	0,00	0,00	0	0,00	0,00	0,00	0	0,00	0,00	0,00	0	0,00
all	0,00	0,00	0	0,00	0,00	0,00	0	0,00	0,00	0,00	0	0,00
201110												
cw	0,04	0,70	15	0,35	0,07	0,62	19	0,62	0,09	0,45	13	0,93
all	0,08	0,71	20	0,78	0,15	0,58	35	1,10	0,14	0,57	15	1,74
201111												
cw	0,19	0,64	63	0,60	0,17	0,76	36	0,56	0,19	0,56	31	0,83
all	0,17	0,71	77	0,67	0,16	0,75	50	0,81	0,20	0,56	42	1,44
201112												
cw	6,38	-0,06	107	0,94	6,22	-0,09	137	1,90	6,33	0,05	122	0,96
all	5,27	0,18	284	11,96	5,89	0,02	196	3,49	6,47	0,45	211	47,23
201201												
cw	1,66	0,46	36	0,38	1,57	0,61	84	0,99	2,02	-0,36	174	3,35
all	1,43	0,82	273	8,63	1,13	0,73	198	4,29	3,87	0,11	239	8,50
201202												
cw	2,12	-0,18	30	0,30	2,12	-0,12	31	0,63	2,06	0,43	58	0,46
all	2,10	-0,11	94	1,11	2,13	-0,17	62	1,38	2,07	-0,01	96	1,48
201203												
cw	0,04	0,00	34	0,22	0,13	0,00	47	0,58	0,21	0,00	75	0,73
all	0,09	0,00	70	0,46	0,25	0,00	94	1,21	0,46	0,00	91	2,30
201204												
cw	0,18	0,88	38	0,62	0,17	0,74	52	1,46	0,17	0,77	46	1,69
all	0,20	0,65	89	1,30	0,24	0,70	100	1,85	1,28	0,47	114	6,33

**Table A-10: Monthly numbers season 2010/2011 of rms (root mean square error), corr (correlation), number of icing hours and max ice load (kg/m) for site E7, all three models. First row using cloud water only in the icing calculation, second row with all condensates.**

	ARO				COA				WRF			
	rms	corr	ice hours	max load	rms	corr	ice hours	max load	rms	corr	ice hours	max load
201009												
cw	0,00	0,00	0	0,00	0,01	0,00	2	0,05	0,00	0,00	2	0,05
all	0,00	0,00	0	0,00	0,05	0,00	14	0,41	0,01	0,00	4	0,15
201010												
cw	0,13	0,71	69	0,89	0,11	0,91	31	1,92	0,09	0,95	35	1,17
all	0,18	0,64	83	1,47	0,14	0,91	47	2,21	0,26	0,54	44	3,70
201011												
cw	0,35	0,23	34	0,91	0,33	0,48	23	1,46	0,38	0,26	58	1,26
all	0,34	0,61	99	1,26	0,33	0,49	27	1,71	0,38	0,47	78	1,43
201012												
cw	0,35	0,86	9	0,29	0,43	0,29	22	0,38	0,38	0,52	64	1,41
all	0,68	0,97	95	2,70	0,43	0,44	43	1,75	1,79	0,80	93	6,26
201101												
cw	3,94	0,32	34	0,37	3,89	0,52	52	0,72	3,75	0,57	95	1,44
all	3,48	0,35	174	2,50	3,81	0,58	99	1,42	3,23	0,72	167	3,26
201102												
cw	0,19	0,37	23	0,25	0,21	-0,05	13	0,19	0,29	0,05	105	0,62
all	0,31	0,72	104	1,27	0,21	-0,02	22	0,34	0,43	-0,02	131	1,93
201103												
cw	0,22	0,31	57	0,42	0,24	0,24	41	0,57	0,25	0,29	74	0,82
all	0,71	-0,02	103	3,04	0,26	0,30	68	1,11	0,31	0,35	97	1,62
201104												
cw	0,13	0,84	31	0,55	0,15	0,58	22	0,64	0,18	0,68	45	1,43
all	0,15	0,63	45	0,68	0,14	0,67	43	1,08	0,30	0,73	64	2,96

**Table A-11: Monthly numbers season 2011/2012 of rms (root mean square error), corr (correlation), number of icing hours and max ice load (kg/m) for site E7, all three models. First row using cloud water only in the icing calculation, second row with all condensates.**

	ARO				COA				WRF			
	rms	corr	Ice hours	Max load	rms	corr	Ice hours	Max load	rms	corr	Ice hours	Max load
201109												
cw	0,00	0,00	0	0,00	0,00	0,00	0	0,00	0,00	0,00	0	0,00
all	0,00	0,00	0	0,00	0,00	0,00	0	0,00	0,00	0,00	0	0,00
201110												
cw	0,12	0,78	37	1,31	0,17	0,54	22	0,84	0,18	0,42	18	1,00
all	0,18	0,70	40	2,00	0,23	0,40	36	1,34	0,20	0,42	23	1,78
201111												
cw	0,44	0,34	74	1,20	0,47	0,11	33	0,86	0,46	0,17	36	0,86
all	0,41	0,44	84	1,28	0,46	0,16	47	0,86	0,47	0,20	42	1,50
201112												
cw	5,85	0,41	150	1,50	5,80	0,12	144	2,46	5,79	0,45	154	1,59
all	3,11	0,83	303	16,59	5,38	0,34	183	4,04	2,57	0,88	225	15,62
201201												
cw	3,03	0,04	69	0,61	3,02	-0,10	114	1,17	2,97	-0,20	194	4,02
all	2,11	0,62	257	9,17	2,74	0,27	185	3,88	3,46	0,18	259	8,73
201202												
cw	0,70	0,09	55	0,59	0,71	0,06	36	1,07	0,70	-0,18	62	0,79
all	0,65	0,17	120	1,43	0,70	0,13	62	1,75	0,66	0,02	95	1,77
201203												
cw	0,20	-0,12	69	0,40	0,27	-0,12	68	0,87	0,24	0,09	77	0,78
all	0,23	-0,15	107	0,69	0,46	-0,15	107	2,38	0,30	0,02	103	1,19
201204												
cw	0,29	0,90	54	1,06	0,26	0,80	69	2,20	0,24	0,83	71	2,44
all	0,32	0,65	109	1,75	0,35	0,76	103	2,58	1,10	0,68	110	6,82

**Table A-12: Monthly numbers season 2010/2011 of rms (root mean square error), corr (correlation), number of icing hours and max ice load (kg/m) for site E8, all three models. First row using cloud water only in the icing calculation, second row with all condensates.**

	ARO				COA				WRF			
	rms	corr	ice hours	max load	rms	corr	ice hours	max load	rms	corr	ice hours	max load
201009												
cw	0,08	0,53	2	0,10	0,09	0,24	11	0,29	0,09	0,31	11	0,39
all	0,25	0,33	23	2,18	0,21	0,21	18	1,75	0,31	0,27	19	2,49
201010												
cw	0,00	0,00	1	0,03	0,03	0,00	13	0,24	0,01	0,00	9	0,12
all	0,06	0,00	10	0,40	0,05	0,00	18	0,40	0,05	0,00	15	0,39
201011												
cw	1,67	0,21	0	0,05	1,58	0,52	39	0,39	1,46	0,40	71	1,17
all	1,31	0,42	110	1,99	1,25	0,81	141	1,43	0,82	0,83	160	2,20
201012												
cw	1,01	0,05	0	0,01	1,03	0,09	3	0,06	1,00	-0,04	3	0,21
all	1,85	0,64	166	6,09	0,91	0,22	71	1,12	0,91	0,18	68	1,40
201101												
cw	0,24	-0,02	0	0,05	0,22	0,45	17	0,31	0,22	0,47	14	0,22
all	0,34	0,16	89	1,22	0,21	0,41	48	0,54	0,27	0,37	87	1,36
201102												
cw	0,00	0,00	1	0,02	0,04	0,00	9	0,13	0,39	0,00	45	1,54
all	0,22	0,00	46	0,81	0,11	0,00	29	0,64	0,45	0,00	79	1,65
201103												
cw	0,00	0,00	0	0,01	0,02	0,00	8	0,14	0,03	0,00	7	0,16
all	0,04	0,00	29	0,21	0,04	0,00	20	0,35	0,06	0,00	37	0,32
201104												
cw	0,00	0,00	3	0,03	0,03	0,00	23	0,24	0,02	0,00	18	0,15
all	0,02	0,00	7	0,17	0,11	0,00	26	0,84	0,11	0,00	27	0,90

**Table A-13: Monthly numbers season 2011/2012 of rms (root mean square error), corr (correlation), number of icing hours and max ice load (kg/m) for site E8, all three models. First row using cloud water only in the icing calculation, second row with all condensates.**

	ARO				COA				WRF			
	rms	corr	Ice hours	Max load	rms	corr	Ice hours	Max load	rms	corr	Ice hours	Max load
201109												
cw	0,00	0,00	0	0,00	0,00	0,00	0	0,00	0,00	0,00	0	0,00
all	0,00	0,00	0	0,00	0,00	0,00	0	0,00	0,00	0,00	0	0,00
201110												
cw	0,00	0,00	4	0,05	0,02	0,00	12	0,17	0,01	0,00	8	0,22
all	0,02	0,00	10	0,14	0,02	0,00	14	0,18	0,03	0,00	9	0,51
201111												
cw	0,06	0,57	4	0,06	0,08	0,31	17	0,48	0,06	0,63	19	0,48
all	0,07	0,36	17	0,58	0,11	0,42	26	0,89	0,10	0,62	35	1,01
201112												
cw	0,76	0,75	1	0,10	0,70	0,37	47	0,53	0,71	0,48	22	0,58
all	0,51	0,70	120	1,57	0,59	0,57	111	1,38	0,56	0,67	119	3,17
201201												
cw	1,21	0,22	0	0,06	1,14	0,50	36	0,45	1,13	0,61	32	0,43
all	1,21	0,02	72	2,38	1,10	0,55	64	0,64	1,08	0,45	79	0,72
201202												
cw	0,98	-0,07	1	0,03	0,98	-0,05	15	0,19	0,98	-0,07	13	0,37
all	0,95	0,57	21	0,23	0,97	-0,04	29	0,26	0,96	0,26	25	0,48
201203												
cw	0,01	0,00	3	0,07	0,03	0,00	20	0,29	0,00	0,00	4	0,04
all	0,01	0,00	4	0,09	0,03	0,00	27	0,29	0,01	0,00	11	0,13
201204												
cw	0,01	0,00	5	0,06	0,14	0,00	51	0,48	0,05	0,00	32	0,19
all	0,10	0,00	55	0,55	1,79	0,00	154	5,48	0,59	0,00	97	2,01

**Table A-14: Monthly numbers season 2010/2011 of rms (root mean square error), corr (correlation), number of icing hours and max ice load (kg/m) for site E9, all three models. First row using cloud water only in the icing calculation, second row with all condensates.**

	ARO				COA				WRF			
	rms	corr	ice hours	max load	rms	corr	ice hours	max load	rms	corr	ice hours	max load
201009												
cw	0,12	0,95	17	0,32	0,11	0,78	15	0,59	0,06	0,96	20	0,76
all	0,24	0,89	25	2,73	0,25	0,68	22	2,28	0,43	0,94	23	3,93
201010												
cw	0,02	0,00	7	0,12	0,07	0,00	24	0,65	0,04	0,00	16	0,31
all	0,13	0,00	18	0,48	0,10	0,00	29	0,66	0,08	0,00	19	0,62
201011												
cw	1,79	0,33	10	0,16	1,56	0,43	118	1,23	1,15	0,63	209	2,54
all	1,43	0,38	172	2,77	1,44	0,40	194	2,43	1,96	0,56	259	6,01
201012												
cw	1,30	0,07	0	0,05	1,31	0,30	13	0,20	1,25	0,04	47	0,89
all	1,89	0,84	177	7,70	1,05	0,53	104	1,25	1,10	0,40	147	2,98
201101												
cw	0,19	0,27	5	0,19	0,17	0,48	39	0,52	0,15	0,60	53	0,61
all	0,26	0,41	97	0,96	0,18	0,50	66	0,84	0,37	0,60	137	1,87
201102												
cw	0,17	0,12	4	0,05	0,18	-0,02	35	0,43	0,56	0,20	117	2,72
all	0,50	-0,26	88	1,22	0,20	0,00	51	0,74	0,62	0,17	152	2,79
201103												
cw	0,01	0,00	1	0,04	0,09	0,00	24	0,44	0,12	0,00	24	0,56
all	0,10	0,00	37	0,53	0,10	0,00	39	0,44	0,20	0,00	65	1,11
201104												
cw	0,01	0,00	7	0,12	0,05	0,00	25	0,35	0,06	0,00	21	0,49
all	0,04	0,00	12	0,32	0,13	0,00	27	0,94	0,15	0,00	27	1,01

**Table A-15: Monthly numbers season 2011/2012 of rms (root mean square error), corr (correlation), number of icing hours and max ice load (kg/m) for site E9, all three models. First row using cloud water only in the icing calculation, second row with all condensates.**

	ARO				COA				WRF			
	rms	corr	Ice hours	Max load	rms	corr	Ice hours	Max load	rms	corr	Ice hours	Max load
201109												
cw	0,00	0,00	0	0,00	0,00	0,00	0	0,00	0,00	0,00	0	0,00
all	0,00	0,00	0	0,00	0,00	0,00	0	0,00	0,00	0,00	0	0,00
201110												
cw	0,09	0,00	35	0,56	0,08	0,00	35	0,47	0,10	0,00	16	0,94
all	0,11	0,00	36	0,89	0,10	0,00	36	0,75	0,14	0,00	19	1,22
201111												
cw	0,04	0,00	25	0,22	0,16	0,00	34	1,08	0,12	0,00	34	0,75
all	0,10	0,00	36	0,85	0,20	0,00	40	1,15	0,16	0,00	42	1,14
201112												
cw	1,22	0,74	16	0,50	1,20	0,20	116	1,01	1,12	0,56	99	1,14
all	1,46	0,90	202	9,29	1,08	0,42	170	1,94	1,55	0,83	205	9,26
201201												
cw	0,81	0,16	7	0,30	0,74	0,35	55	0,91	0,65	0,52	100	1,02
all	0,94	0,12	87	2,84	0,68	0,50	95	1,16	0,66	0,53	161	2,58
201202												
cw	0,02	0,00	7	0,11	0,09	0,00	34	0,39	0,10	0,00	35	0,93
all	0,06	0,00	37	0,40	0,10	0,00	45	0,50	0,12	0,00	47	1,10
201203												
cw	0,01	0,00	7	0,10	0,06	0,00	19	0,56	0,03	0,00	21	0,20
all	0,01	0,00	9	0,16	0,06	0,00	28	0,56	0,03	0,00	32	0,28
201204												
cw	0,04	0,00	29	0,21	0,27	0,00	121	0,80	0,16	0,00	77	0,60
all	0,16	0,00	97	0,70	2,72	0,00	190	8,40	1,05	0,00	137	3,19

**Table A-16: Monthly numbers season 2011/2012 of rms (root mean square error), corr (correlation), number of icing hours and max ice load (kg/m) for site E10, all three models. First row using cloud water only in the icing calculation, second row with all condensates.**

	ARO				COA				WRF			
	rms	corr	ice hours	max load	rms	corr	ice hours	max load	rms	corr	ice hours	max load
201101												
cw	0,39	0,24	5	0,11	0,55	0,03	88	1,63	0,35	0,40	55	0,68
all	0,22	0,84	145	4,75	1,55	-0,02	145	5,01	0,28	0,74	120	2,66
201102												
cw	0,19	0,02	14	0,41	0,32	0,31	65	1,88	0,22	-0,01	61	0,79
all	0,23	0,51	116	1,81	0,51	0,53	134	1,99	0,30	0,69	125	1,86
201103												
cw	0,08	-0,02	7	0,13	0,65	-0,03	114	2,20	0,17	0,36	67	1,00
all	0,34	-0,07	63	1,67	1,28	-0,08	165	5,67	0,51	0,07	115	3,22
201104												
cw	0,20	0,03	13	0,27	0,20	-0,02	23	0,43	0,20	0,05	21	0,34
all	0,19	0,04	13	0,29	0,20	-0,02	31	0,56	0,20	0,05	21	0,34

**Table A-17: Monthly numbers season 2010/2011 of rms (root mean square error), corr (correlation), number of icing hours and max ice load (kg/m) for site E11, all three models. First row using cloud water only in the icing calculation, second row with all condensates.**

	ARO				COA				WRF			
	rms	corr	ice hours	max load	rms	corr	ice hours	max load	rms	corr	ice hours	max load
201009												
cw	0,04	0,95	12	0,35	0,08	0,56	12	0,29	0,07	0,73	19	0,75
all	0,54	0,75	35	3,41	0,61	0,67	26	3,67	0,47	0,87	31	3,40
201010												
cw	0,13	0,87	42	0,61	0,21	0,70	51	1,86	0,15	0,62	36	1,30
all	0,20	0,40	56	0,81	0,22	0,69	59	1,88	0,16	0,72	46	1,97
201011												
cw	0,98	-0,09	20	0,62	0,96	0,16	62	2,09	0,52	0,79	274	3,59
all	0,83	0,39	128	1,49	0,82	0,43	132	2,21	1,95	0,83	303	6,86
201012												
cw	0,89	0,77	0	0,05	0,92	0,07	4	0,09	0,62	0,78	48	1,17
all	2,72	0,11	167	7,05	0,75	0,82	44	0,53	0,55	0,85	121	3,05
201101												
cw	2,28	0,35	23	0,25	2,12	0,70	85	1,04	2,17	0,67	65	0,89
all	2,06	0,31	147	1,21	2,02	0,70	148	1,24	1,93	0,51	184	2,38
201102												
cw	0,66	0,01	5	0,07	0,64	0,83	19	0,30	0,46	0,88	154	2,26
all	0,56	0,14	92	0,89	0,61	0,18	70	0,92	0,46	0,65	205	4,42
201103												
cw	0,39	0,11	8	0,08	0,44	-0,01	48	1,05	0,38	0,29	66	1,32
all	0,37	0,29	38	0,28	0,45	0,00	59	1,15	0,41	0,33	84	1,99
201104												
cw	0,02	0,00	18	0,12	0,03	0,00	32	0,35	0,15	0,00	38	0,90
all	0,14	0,00	24	0,81	0,14	0,00	44	0,92	0,19	0,00	45	0,98

**Table A-18: Monthly numbers season 2011/2012 of rms (root mean square error), corr (correlation), number of icing hours and max ice load (kg/m) for site E11, all three models. First row using cloud water only in the icing calculation, second row with all condensates.**

	ARO				COA				WRF			
	rms	corr	Ice hours	Max load	rms	corr	Ice hours	Max load	rms	corr	Ice hours	Max load
201201												
cw	0,66	0,21	9	0,34	0,59	0,44	84	1,34	0,67	0,62	142	2,48
all	1,16	0,03	162	4,06	0,63	0,45	133	1,73	1,69	0,22	211	6,13
201202												
cw	6,71	0,54	22	0,40	6,62	0,61	34	1,72	6,69	0,33	43	0,54
all	6,68	0,70	51	1,07	6,59	0,67	43	2,23	6,66	0,57	71	1,16
201203												
cw	2,58	-0,12	24	0,20	2,56	0,03	66	1,95	2,54	0,07	65	1,68
all	2,58	-0,12	42	0,42	2,56	0,02	69	2,03	2,56	0,01	85	2,26
201204												
cw	0,34	0,80	46	0,56	0,31	0,71	108	1,48	0,34	0,65	92	1,39
all	0,28	0,74	135	1,24	4,02	-0,05	225	9,92	1,73	0,25	185	5,18

**Table A-19: Monthly numbers season 2011/2012 of rms (root mean square error), corr (correlation), number of icing hours and max ice load (kg/m) for site E13, all three models. First row using cloud water only in the icing calculation, second row with all condensates.**

	ARO				COA				WRF			
	rms	corr	ice hours	max load	rms	corr	ice hours	max load	rms	corr	ice hours	max load
201109												
cw	0,00	0,00	0	0,00	0,00	0,00	0	0,00	0,00	0,00	0	0,00
all	0,00	0,00	0	0,00	0,00	0,00	0	0,00	0,00	0,00	0	0,00
201110												
cw	0,00	0,00	1	0,02	0,00	0,00	1	0,02	0,00	0,00	0	0,00
all	0,00	0,00	1	0,03	0,00	0,00	1	0,02	0,00	0,00	0	0,00
201111												
cw	0,01	0,00	9	0,07	0,01	0,00	8	0,14	0,01	0,00	7	0,15
all	0,01	0,00	12	0,08	0,01	0,00	9	0,14	0,01	0,00	9	0,15
201112												
cw	1,84	-0,20	2	0,07	1,82	-0,03	50	0,74	1,84	-0,10	17	0,16
all	2,04	-0,26	193	3,69	1,82	-0,20	138	0,82	1,84	-0,15	56	0,67
201201												
cw	2,54	0,19	2	0,04	2,48	-0,19	84	0,65	2,51	0,17	46	0,44
all	2,53	-0,21	145	2,16	2,47	-0,21	146	1,02	2,47	0,42	76	0,83
201202												
cw	0,24	0,28	9	0,12	0,34	-0,09	34	1,04	0,26	0,05	55	0,81
all	0,24	0,09	50	0,42	0,41	-0,10	58	1,54	0,27	0,08	77	0,91
201203												
cw	0,08	0,03	4	0,05	0,11	0,06	24	0,81	0,08	0,09	10	0,27
all	0,08	0,03	11	0,17	0,11	0,06	26	0,81	0,08	0,09	11	0,26
201204												
cw	0,08	-0,03	3	0,05	0,08	-0,04	3	0,08	0,08	-0,02	6	0,21
all	0,10	-0,05	32	0,35	0,12	-0,05	27	0,55	0,09	-0,05	23	0,30

**Table A-20: Monthly numbers season 2011/2012 of rms (root mean square error), corr (correlation), number of icing hours and max ice load (kg/m) for site E14, all three models. First row using cloud water only in the icing calculation, second row with all condensates.**

	ARO				COA				WRF			
	rms	corr	ice hours	max load	rms	corr	ice hours	max load	rms	corr	ice hours	max load
201201												
cw	0,98	-0,19	19	0,59	0,95	-0,10	74	1,55	0,78	0,68	86	0,89
all	1,09	0,07	121	4,88	1,42	-0,05	150	5,73	1,57	0,44	218	8,99
201202												
cw	1,68	-0,14	22	0,28	1,59	0,11	99	0,93	1,57	0,12	103	1,37
all	1,59	0,19	132	1,29	1,58	0,04	150	2,42	1,67	0,11	183	6,36
201203												
cw	0,07	0,52	39	0,52	0,11	0,52	41	0,85	0,06	0,79	24	0,87
all	0,09	0,63	62	0,72	0,12	0,53	43	0,93	0,07	0,77	38	0,96
201204												
cw	0,01	0,00	7	0,08	0,12	0,00	27	0,49	0,06	0,00	29	0,32
all	0,34	0,00	91	1,85	0,37	0,00	102	1,64	0,38	0,00	75	2,35

## Appendix B

Tables B-1 to B-18, statistical scores for sites E4, E6, E7, E8, E9, and E11 for sensitivity experiments forcing, microphysics, and PBL in section 4.3.

### Forcing

**Table B-1: Observation and model statistics and statistical scores for site E5 from the forcing experiments.**

E5 2010/2011											
wind speed											
Data	mean	max	min	median	std	abse	corr	rmse	bias	bias std	dispe
wrf.3.2_FNL	7,40	23,75	0,07	7,07	3,64	2,03	0,72	2,61	-0,19	0,38	2,58
wrf.3.2_ERA	7,45	20,14	0,23	7,21	3,45	1,99	0,71	2,55	-0,15	0,18	2,54
wrf.3.2_NCAR	7,22	20,62	0,03	6,97	3,46	2,29	0,64	2,90	-0,37	0,19	2,87
obs80m	7,59	20,80	0,10	7,70	3,27	-	-	-	-	-	-
temperature											
Data	mean	max	min	median	std	abse	corr	rmse	bias	bias std	dispe
wrf.3.2_FNL	-2,02	13,64	-19,96	-2,16	6,39	1,40	0,96	1,89	-0,43	0,06	1,84
wrf.3.2_ERA	-2,18	13,79	-19,53	-2,26	6,51	1,41	0,95	2,02	-0,59	0,19	1,93
wrf.3.2_NCAR	-1,82	13,92	-18,49	-2,12	6,37	1,39	0,96	1,89	-0,23	0,04	1,87
obs80m	-1,59	19,50	-18,30	-2,40	6,33	-	-	-	-	-	-
pressure											
Data	mean	max	min	median	std	abse	corr	rmse	bias	bias std	dispe
wrf.3.2_FNL	911,2	935,8	884,8	910,9	11,99	3,06	1,00	3,22	3,05	0,19	1,01
wrf.3.2_ERA	911,5	936,4	885,0	911,2	11,86	3,29	1,00	3,45	3,29	0,32	1,01
wrf.3.2_NCAR	912,5	937,0	884,7	912,0	12,02	4,28	0,99	4,47	4,28	0,16	1,28
obs80m	908,2	934,0	883,0	908,0	12,18	-	-	-	-	-	-

**Table B-2: Observation and model statistics and statistical scores for site E6 from the forcing experiments.**

E6 2010/2011											
wind speed											
Data	mean	max	min	median	std	abse	corr	rmse	bias	bias std	dispe
wrf.3.2_FNL	8,24	21,97	0,18	7,94	3,53	2,18	0,70	2,92	1,26	0,28	2,62
wrf.3.2_ERA	8,07	22,43	0,20	7,87	3,52	2,10	0,71	2,81	1,10	0,27	2,57
wrf.3.2_NCAR	7,85	21,07	0,09	7,65	3,47	2,34	0,63	3,02	0,87	0,22	2,88
obs100m	6,97	19,70	0,10	7,10	3,24	-	-	-	-	-	-
temperature											
Data	mean	max	min	median	std	abse	corr	rmse	bias	bias std	dispe
wrf.3.2_FNL	-4,28	13,39	-20,84	-4,69	6,84	1,29	0,98	1,72	-0,87	0,31	1,46
wrf.3.2_ERA	-4,70	13,45	-21,97	-5,09	7,10	1,58	0,97	2,13	-1,29	0,56	1,60
wrf.3.2_NCAR	-4,23	14,39	-20,42	-4,65	6,86	1,44	0,97	1,89	-0,82	0,33	1,67
obs100m	-3,41	15,70	-19,50	-4,10	6,53	-	-	-	-	-	-
pressure											
Data	mean	max	min	median	std	abse	corr	rmse	bias	bias std	dispe
wrf.3.2_FNL	922,2	945,3	893,6	922,6	12,18	0,82	1,00	1,04	-0,45	0,05	0,93
wrf.3.2_ERA	922,5	945,9	893,9	923,0	12,07	0,75	1,00	0,97	-0,20	0,16	0,94
wrf.3.2_NCAR	923,3	946,6	893,8	923,6	12,15	1,09	0,99	1,43	0,66	0,08	1,26
obs100m	922,7	947,0	895,0	923,0	12,23	-	-	-	-	-	-

**Table B-3: Observation and model statistics and statistical scores for site E7 from the forcing experiments.**

E7 2010/2011											
wind speed											
Data	mean	max	min	median	std	abse	corr	rmse	bias	bias std	dispe
wrf.3.2_FNL	9,35	24,52	0,22	9,31	4,01	2,40	0,73	3,25	1,56	0,34	2,82
wrf.3.2_ERA	9,19	24,68	0,19	9,14	3,96	2,34	0,73	3,14	1,40	0,29	2,80
wrf.3.2_NCAR	8,82	23,33	0,23	8,78	3,90	2,55	0,66	3,30	1,04	0,23	3,12
obs200m	7,79	23,30	0,10	7,90	3,67	-	-	-	-	-	-
temperature											
Data	mean	max	min	median	std	abse	corr	rmse	bias	bias std	dispe
wrf.3.2_FNL	-4,44	12,69	-20,95	-4,91	6,53	1,14	0,98	1,52	-0,73	0,13	1,33
wrf.3.2_ERA	-4,83	12,86	-20,75	-5,33	6,75	1,36	0,98	1,84	-1,11	0,34	1,43
wrf.3.2_NCAR	-4,47	13,63	-20,31	-4,97	6,59	1,33	0,97	1,79	-0,76	0,18	1,62
obs200m	-3,72	15,40	-19,70	-4,20	6,41	-	-	-	-	-	-
pressure											
Data	mean	max	min	median	std	abse	corr	rmse	bias	bias std	dispe
wrf.3.2_FNL	910,6	933,9	882,4	910,8	12,04	0,74	1,00	0,95	-0,19	0,09	0,92
wrf.3.2_ERA	910,8	934,5	882,8	911,1	11,92	0,71	1,00	0,93	0,03	0,21	0,91
wrf.3.2_NCAR	911,7	935,1	882,3	911,9	12,00	1,23	0,99	1,58	0,91	0,13	1,28
obs200m	910,8	935,0	883,0	911,0	12,13	-	-	-	-	-	-

**Table B-4: Observation and model statistics and statistical scores for site E8 from the forcing experiments.**

E8 2010/2011											
wind speed											
Data	mean	max	min	median	std	abse	corr	rmse	bias	bias std	dispe
wrf.3.2_FNL	7,34	19,69	0,20	7,26	3,26	1,77	0,73	2,29	0,21	0,37	2,25
wrf.3.2_ERA	7,32	17,97	0,11	7,36	3,21	1,75	0,74	2,23	0,19	0,32	2,20
wrf.3.2_NCAR	7,32	19,38	0,13	7,24	3,21	1,96	0,68	2,48	0,19	0,33	2,46
obs70m	7,13	18,10	0,50	7,20	2,89	-	-	-	-	-	-
temperature											
Data	mean	max	min	median	std	abse	corr	rmse	bias	bias std	dispe
wrf.3.2_FNL	-3,11	14,31	-20,24	-3,40	6,80	1,36	0,96	1,88	-0,44	0,39	1,79
wrf.3.2_ERA	-3,48	14,60	-21,05	-3,52	7,04	1,50	0,96	2,14	-0,81	0,63	1,88
wrf.3.2_NCAR	-3,19	14,36	-20,06	-3,23	6,83	1,60	0,95	2,18	-0,52	0,42	2,08
obs70m	-2,67	17,10	-17,90	-3,20	6,41	-	-	-	-	-	-
pressure											
Data	mean	max	min	median	std	abse	corr	rmse	bias	bias std	dispe
wrf.3.2_FNL	917,0	941,5	884,6	917,6	11,72	2,56	1,00	2,68	-2,55	0,14	0,80
wrf.3.2_ERA	917,2	940,8	884,4	917,8	11,64	2,33	1,00	2,47	-2,32	0,22	0,82
wrf.3.2_NCAR	918,2	941,7	886,4	918,7	11,66	1,53	1,00	1,80	-1,37	0,20	1,14
obs70m	919,5	944,0	888,0	920,0	11,86	-	-	-	-	-	-

**Table B-5: Observation and model statistics and statistical scores for site E9 from the forcing experiments.**

E9 2010/2011											
wind speed											
Data	mean	max	min	median	std	abse	corr	rmse	bias	bias std	dispe
wrf.3.2_FNL	8,59	23,40	0,14	8,47	3,85	1,89	0,79	2,46	0,09	0,19	2,45
wrf.3.2_ERA	8,50	21,00	0,13	8,57	3,83	1,90	0,79	2,43	0,01	0,17	2,43
wrf.3.2_NCAR	8,51	22,53	0,12	8,39	3,79	2,13	0,73	2,73	0,01	0,13	2,73
obs155m	8,50	28,10	0,10	8,50	3,66	-	-	-	-	-	-
temperature											
Data	mean	max	min	median	std	abse	corr	rmse	bias	bias std	dispe
wrf.3.2_FNL	-3,43	13,66	-18,83	-3,76	6,57	1,26	0,97	1,76	-0,39	0,44	1,65
wrf.3.2_ERA	-3,74	14,16	-20,55	-3,86	6,78	1,38	0,96	1,99	-0,71	0,66	1,74
wrf.3.2_NCAR	-3,49	13,93	-19,09	-3,69	6,61	1,50	0,95	2,05	-0,45	0,48	1,94
obs155m	-3,04	14,80	-18,00	-3,50	6,12	-	-	-	-	-	-
pressure											
Data	mean	max	min	median	std	abse	corr	rmse	bias	bias std	dispe
wrf.3.2_FNL	907,1	931,5	875,2	907,5	11,65	0,93	1,00	1,14	-0,69	0,22	0,88
wrf.3.2_ERA	907,3	930,9	874,9	907,7	11,56	0,84	1,00	1,06	-0,47	0,30	0,90
wrf.3.2_NCAR	908,2	932,0	877,0	908,6	11,59	0,98	0,99	1,30	0,46	0,27	1,18
obs155m	907,8	932,0	877,0	908,0	11,86	-	-	-	-	-	-

**Table B-6: Observation and model statistics and statistical scores for site E11 from the forcing experiments.**

E11 2010/2011											
wind speed											
Data	mean	max	min	median	std	abse	corr	rmse	bias	bias std	dispe
wrf.3.2_FNL	8,67	24,36	0,25	8,46	3,64	2,14	0,78	2,79	1,61	0,51	2,23
wrf.3.2_ERA	8,70	22,42	0,13	8,64	3,65	2,22	0,78	2,82	1,63	0,53	2,24
wrf.3.2_NCAR	8,73	23,43	0,28	8,51	3,67	2,43	0,73	3,04	1,67	0,55	2,49
obs60m	7,07	22,60	0,10	7,10	3,13	-	-	-	-	-	-
temperature											
Data	mean	max	min	median	std	abse	corr	rmse	bias	bias std	dispe
wrf.3.2_FNL	-4,37	11,74	-19,64	-4,77	6,19	1,24	0,97	1,67	-0,90	0,12	1,40
wrf.3.2_ERA	-4,62	12,20	-21,30	-5,03	6,35	1,42	0,97	1,87	-1,15	0,28	1,45
wrf.3.2_NCAR	-4,39	11,37	-20,10	-5,00	6,19	1,41	0,97	1,85	-0,92	0,12	1,60
obs60m	-3,47	16,40	-19,40	-4,10	6,07	-	-	-	-	-	-
pressure											
Data	mean	max	min	median	std	abse	corr	rmse	bias	bias std	dispe
wrf.3.2_FNL	887,5	911,7	857,2	887,4	11,52	0,66	1,00	0,84	0,29	0,18	0,77
wrf.3.2_ERA	887,7	911,9	856,8	887,5	11,42	0,73	1,00	0,93	0,47	0,27	0,75
wrf.3.2_NCAR	888,7	913,2	858,5	888,4	11,51	1,57	0,99	1,88	1,45	0,19	1,18
obs60m	887,2	912,0	857,0	887,0	11,70	-	-	-	-	-	-

## Microphysics

**Table B-7: Observation and model statistics and statistical scores for site E5 from the microphysics experiments.**

E5 2010/2011											
wind speed											
Data	mean	max	min	median	std	abse	corr	rmse	bias	bias std	dispe
wrf.3.2_FNL	7,40	23,75	0,07	7,07	3,64	2,03	0,72	2,61	-0,19	0,38	2,58
wrf.3.2_wsm3	7,39	22,66	0,01	7,03	3,55	1,97	0,73	2,55	-0,21	0,29	2,52
wrf.3.2_wsm6	7,43	22,81	0,06	7,05	3,61	2,00	0,72	2,58	-0,17	0,34	2,55
wrf.3.2_Morr	7,42	23,37	0,06	7,06	3,62	2,02	0,72	2,59	-0,18	0,35	2,56
obs80m	7,59	20,80	0,10	7,70	3,27	-	-	-	-	-	-
temperature											
Data	mean	max	min	median	std	abse	corr	rmse	bias	bias std	dispe
wrf.3.2_FNL	-2,02	13,64	-19,96	-2,16	6,39	1,40	0,96	1,89	-0,43	0,06	1,84
wrf.3.2_wsm3	-2,19	13,65	-21,21	-2,20	6,42	1,43	0,96	1,90	-0,60	0,09	1,80
wrf.3.2_wsm6	-1,94	13,64	-19,60	-2,16	6,31	1,37	0,96	1,82	-0,35	0,02	1,78
wrf.3.2_Morr	-2,00	13,64	-19,75	-2,21	6,36	1,40	0,96	1,87	-0,41	0,03	1,82
obs80m	-1,59	19,50	-18,30	-2,40	6,33	-	-	-	-	-	-
pressure											
Data	mean	max	min	median	std	abse	corr	rmse	bias	bias std	dispe
wrf.3.2_FNL	911,24	935,76	884,82	910,91	11,99	3,06	1,00	3,22	3,05	0,19	1,01
wrf.3.2_wsm3	911,24	935,77	884,61	910,93	12,00	3,05	1,00	3,21	3,05	0,18	0,99
wrf.3.2_wsm6	911,12	935,63	884,56	910,83	12,01	2,94	1,00	3,09	2,93	0,17	1,00
wrf.3.2_Morr	911,11	935,66	884,50	910,84	12,01	2,93	1,00	3,09	2,92	0,17	1,00
obs80m	908,2	934,0	883,0	908,0	12,18	-	-	-	-	-	-

**Table B-8: Observation and model statistics and statistical scores for site E6 from the microphysics experiments.**

E6 2010/2011											
wind speed											
Data	mean	max	min	median	std	abse	corr	rmse	bias	bias std	dispe
wrf.3.2_FNL	8,24	21,97	0,18	7,94	3,53	2,18	0,70	2,92	1,26	0,28	2,62
wrf.3.2_wsm3	8,29	21,24	0,21	8,09	3,34	2,14	0,70	2,86	1,28	0,05	2,56
wrf.3.2_wsm6	8,31	23,05	0,18	8,10	3,44	2,19	0,69	2,95	1,32	0,17	2,63
wrf.3.2_Morr	8,24	21,04	0,06	8,01	3,42	2,19	0,69	2,94	1,29	0,16	2,64
obs100m	6,97	19,70	0,10	7,10	3,24	-	-	-	-	-	-
temperature											
Data	mean	max	min	median	std	abse	corr	rmse	bias	bias std	dispe
wrf.3.2_FNL	-4,28	13,39	-20,84	-4,69	6,84	1,29	0,98	1,72	-0,87	0,31	1,46
wrf.3.2_wsm3	-5,75	10,10	-22,02	-5,67	6,03	1,28	0,97	1,71	-0,88	0,38	1,42
wrf.3.2_wsm6	-5,61	10,33	-20,42	-5,55	6,01	1,22	0,97	1,63	-0,73	0,36	1,41
wrf.3.2_Morr	-5,57	13,33	-21,11	-5,62	6,17	1,29	0,97	1,72	-0,82	0,40	1,46
obs100m	-3,41	15,70	-19,50	-4,10	6,53	-	-	-	-	-	-
pressure											
Data	mean	max	min	median	std	abse	corr	rmse	bias	bias std	dispe
wrf.3.2_FNL	922,20	945,25	893,60	922,58	12,18	0,82	1,00	1,04	-0,45	0,05	0,93
wrf.3.2_wsm3	921,29	945,27	893,43	921,29	12,22	0,78	1,00	1,01	-0,41	0,01	0,92
wrf.3.2_wsm6	921,19	945,14	893,31	921,29	12,30	0,81	1,00	1,04	-0,49	0,03	0,91
wrf.3.2_Morr	921,29	945,15	893,26	921,22	12,23	0,82	1,00	1,05	-0,52	0,02	0,91
obs100m	922,7	947,0	895,0	923,0	12,23	-	-	-	-	-	-

**Table B-9: Observation and model statistics and statistical scores for site E7 from the microphysics experiments.**

E7 2010/2011											
wind speed											
Data	mean	max	min	median	std	abse	corr	rmse	bias	bias std	dispe
wrf.3.2_FNL	9,35	24,52	0,22	9,31	4,01	2,40	0,73	3,25	1,56	0,34	2,82
wrf.3.2_wsm3	9,43	23,80	0,07	9,53	3,87	2,37	0,74	3,15	1,57	0,11	2,73
wrf.3.2_wsm6	9,45	25,82	0,02	9,46	3,96	2,42	0,73	3,25	1,60	0,22	2,82
wrf.3.2_Morr	9,38	23,82	0,02	9,44	3,95	2,41	0,73	3,22	1,58	0,22	2,80
obs200m	7,79	23,30	0,10	7,90	3,67	-	-	-	-	-	-
temperature											
Data	mean	max	min	median	std	abse	corr	rmse	bias	bias std	dispe
wrf.3.2_FNL	-4,44	12,69	-20,95	-4,91	6,53	1,14	0,98	1,52	-0,73	0,13	1,33
wrf.3.2_wsm3	-5,73	10,38	-21,63	-5,61	5,73	1,10	0,97	1,49	-0,65	0,17	1,33
wrf.3.2_wsm6	-5,65	10,62	-21,07	-5,59	5,73	1,07	0,97	1,42	-0,55	0,16	1,30
wrf.3.2_Morr	-5,58	12,48	-21,21	-5,66	5,87	1,10	0,97	1,47	-0,60	0,19	1,33
obs200m	-3,72	15,40	-19,70	-4,20	6,41	-	-	-	-	-	-
pressure											
Data	mean	max	min	median	std	abse	corr	rmse	bias	bias std	dispe
wrf.3.2_FNL	910,56	933,88	882,37	910,81	12,04	0,74	1,00	0,95	-0,19	0,09	0,92
wrf.3.2_wsm3	909,62	933,89	882,15	909,41	12,06	0,73	1,00	0,95	-0,16	0,03	0,94
wrf.3.2_wsm6	909,54	933,77	882,04	909,45	12,13	0,74	1,00	0,96	-0,24	0,02	0,93
wrf.3.2_Morr	909,64	933,78	882,10	909,43	12,06	0,75	1,00	0,96	-0,27	0,02	0,92
obs200m	910,8	935,0	883,0	911,0	12,13	-	-	-	-	-	-

**Table B-10: Observation and model statistics and statistical scores for site E8 from the microphysics experiments.**

E8 2010/2011											
wind speed											
Data	mean	max	min	median	std	abse	corr	rmse	bias	bias std	dispe
wrf.3.2_FNL	7,34	19,69	0,20	7,26	3,26	1,77	0,73	2,29	0,21	0,37	2,25
wrf.3.2_wsm3	7,56	18,21	0,32	7,55	3,05	1,74	0,72	2,24	0,35	0,18	2,21
wrf.3.2_wsm6	7,54	18,49	0,18	7,54	3,12	1,77	0,72	2,28	0,31	0,23	2,25
wrf.3.2_Morr	7,46	19,58	0,16	7,50	3,21	1,81	0,72	2,33	0,27	0,31	2,30
obs70m	7,13	18,10	0,50	7,20	2,89	-	-	-	-	-	-
temperature											
Data	mean	max	min	median	std	abse	corr	rmse	bias	bias std	dispe
wrf.3.2_FNL	-3,11	14,31	-20,24	-3,40	6,80	1,36	0,96	1,88	-0,44	0,39	1,79
wrf.3.2_wsm3	-4,68	12,11	-19,33	-4,56	6,12	1,37	0,96	1,91	-0,66	0,47	1,74
wrf.3.2_wsm6	-4,40	12,28	-19,53	-4,45	6,02	1,32	0,95	1,83	-0,33	0,40	1,75
wrf.3.2_Morr	-4,44	12,44	-19,79	-4,46	6,19	1,40	0,95	1,94	-0,46	0,47	1,82
obs70m	-2,67	17,10	-17,90	-3,20	6,41	-	-	-	-	-	-
pressure											
Data	mean	max	min	median	std	abse	corr	rmse	bias	bias std	dispe
wrf.3.2_FNL	916,97	941,46	884,62	917,55	11,72	2,56	1,00	2,68	-2,55	0,14	0,80
wrf.3.2_wsm3	916,11	941,41	884,60	916,37	11,59	2,52	1,00	2,64	-2,52	0,12	0,78
wrf.3.2_wsm6	916,07	941,35	884,37	916,44	11,65	2,60	1,00	2,71	-2,60	0,09	0,78
wrf.3.2_Morr	916,16	941,33	884,28	916,39	11,61	2,61	1,00	2,73	-2,61	0,09	0,78
obs70m	919,5	944,0	888,0	920,0	11,86	-	-	-	-	-	-

**Table B-11: Observation and model statistics and statistical scores for site E9 from the microphysics experiments.**

E9 2010/2011											
wind speed											
Data	mean	max	min	median	std	abse	corr	rmse	bias	bias std	dispe
wrf.3.2_FNL	8,59	23,40	0,14	8,47	3,85	1,89	0,79	2,46	0,09	0,19	2,45
wrf.3.2_wsm3	8,76	21,29	0,11	8,76	3,60	1,87	0,78	2,42	0,14	0,08	2,42
wrf.3.2_wsm6	8,78	21,73	0,06	8,75	3,71	1,87	0,78	2,43	0,13	0,04	2,42
wrf.3.2_Morr	8,72	23,53	0,05	8,69	3,79	1,91	0,78	2,48	0,14	0,11	2,47
obs155m	8,50	28,10	0,10	8,50	3,66	-	-	-	-	-	-
temperature											
Data	mean	max	min	median	std	abse	corr	rmse	bias	bias std	dispe
wrf.3.2_FNL	-3,43	13,66	-18,83	-3,76	6,57	1,26	0,97	1,76	-0,39	0,44	1,65
wrf.3.2_wsm3	-4,90	11,62	-19,25	-4,67	5,82	1,27	0,96	1,79	-0,55	0,45	1,64
wrf.3.2_wsm6	-4,69	11,70	-19,17	-4,57	5,74	1,22	0,96	1,70	-0,29	0,40	1,63
wrf.3.2_Morr	-4,74	11,88	-18,57	-4,69	5,90	1,29	0,96	1,81	-0,42	0,47	1,69
obs155m	-3,04	14,80	-18,00	-3,50	6,12	-	-	-	-	-	-
pressure											
Data	mean	max	min	median	std	abse	corr	rmse	bias	bias std	dispe
wrf.3.2_FNL	907,06	931,49	875,21	907,52	11,65	0,93	1,00	1,14	-0,69	0,22	0,88
wrf.3.2_wsm3	906,07	931,45	875,17	906,20	11,50	0,88	1,00	1,08	-0,64	0,19	0,84
wrf.3.2_wsm6	906,04	931,39	874,96	906,33	11,55	0,91	1,00	1,11	-0,71	0,17	0,84
wrf.3.2_Morr	906,13	931,36	874,87	906,24	11,52	0,93	1,00	1,13	-0,72	0,17	0,85
obs155m	907,8	932,0	877,0	908,0	11,86	-	-	-	-	-	-

**Table B-12: Observation and model statistics and statistical scores for site E11 from the microphysics experiments.**

E11 2010/2011											
wind speed											
Data	mean	max	min	median	std	abse	corr	rmse	bias	bias std	dispe
wrf.3.2_FNL	8,67	24,36	0,25	8,46	3,64	2,14	0,78	2,79	1,61	0,51	2,23
wrf.3.2_wsm3	8,87	23,14	0,05	8,84	3,44	2,20	0,77	2,83	1,76	0,35	2,19
wrf.3.2_wsm6	8,88	23,50	0,09	8,74	3,55	2,20	0,78	2,86	1,73	0,41	2,24
wrf.3.2_Morr	8,81	23,41	0,20	8,63	3,60	2,19	0,78	2,84	1,68	0,46	2,24
obs60m	7,07	22,60	0,10	7,10	3,13	-	-	-	-	-	-
temperature											
Data	mean	max	min	median	std	abse	corr	rmse	bias	bias std	dispe
wrf.3.2_FNL	-4,37	11,74	-19,64	-4,77	6,19	1,24	0,97	1,67	-0,90	0,12	1,40
wrf.3.2_wsm3	-5,98	9,50	-20,66	-5,90	5,47	1,31	0,97	1,74	-1,06	0,19	1,37
wrf.3.2_wsm6	-5,75	9,65	-20,55	-5,75	5,40	1,16	0,97	1,57	-0,81	0,15	1,33
wrf.3.2_Morr	-5,73	9,75	-20,46	-5,78	5,56	1,22	0,97	1,66	-0,87	0,20	1,40
obs60m	-3,47	16,40	-19,40	-4,10	6,07	-	-	-	-	-	-
pressure											
Data	mean	max	min	median	std	abse	corr	rmse	bias	bias std	dispe
wrf.3.2_FNL	887,48	911,71	857,15	887,40	11,52	0,66	1,00	0,84	0,29	0,18	0,77
wrf.3.2_wsm3	886,21	911,66	857,05	886,13	11,28	0,68	1,00	0,87	0,34	0,15	0,79
wrf.3.2_wsm6	886,07	911,65	856,88	886,04	11,33	0,65	1,00	0,83	0,25	0,13	0,78
wrf.3.2_Morr	886,20	911,64	856,81	885,96	11,28	0,65	1,00	0,83	0,23	0,13	0,78
obs60m	887,2	912,0	857,0	887,0	11,70	-	-	-	-	-	-

**PBL****Table B-13: Observation and model statistics and statistical scores for site E5 from the PBL experiments.**

E5 2010/2011											
wind speed											
Data	mean	max	min	median	std	abse	corr	rmse	bias	bias std	dispe
wrf.3.2_FNL	7,40	23,75	0,07	7,07	3,64	2,03	0,72	2,61	-0,19	0,38	2,58
wrf.3.2_myj	7,34	23,59	0,05	7,16	3,39	1,99	0,70	2,58	-0,26	0,12	2,56
wrf.3.2_qnse	7,53	23,12	0,12	7,25	3,52	2,11	0,68	2,74	-0,07	0,25	2,73
wrf.3.2_mynn2	7,66	23,51	0,13	7,30	3,85	2,14	0,71	2,78	0,07	0,58	2,72
obs80m	7,59	20,80	0,10	7,70	3,27	-	-	-	-	-	-
temperature											
Data	mean	max	min	median	std	abse	corr	rmse	bias	bias std	dispe
wrf.3.2_FNL	-2,02	13,64	-19,96	-2,16	6,39	1,40	0,96	1,89	-0,43	0,06	1,84
wrf.3.2_myj	-2,80	13,59	-19,95	-3,16	6,41	1,56	0,96	2,16	-1,21	0,08	1,79
wrf.3.2_qnse	-2,82	13,44	-20,19	-3,23	6,39	1,62	0,96	2,24	-1,23	0,06	1,87
wrf.3.2_mynn2	-2,40	13,65	-20,05	-2,65	6,36	1,44	0,96	2,02	-0,81	0,03	1,85
obs80m	-1,59	19,50	-18,30	-2,40	6,33	-	-	-	-	-	-
pressure											
Data	mean	max	min	median	std	abse	corr	rmse	bias	bias std	dispe
wrf.3.2_FNL	911,24	935,76	884,82	910,91	11,99	3,06	1,00	3,22	3,05	0,19	1,01
wrf.3.2_myj	911,10	935,83	884,26	910,76	12,12	2,96	1,00	3,13	2,91	0,05	1,15
wrf.3.2_qnse	911,01	935,89	883,80	910,74	12,23	2,87	1,00	3,05	2,82	0,06	1,15
wrf.3.2_mynn2	911,04	935,82	884,01	910,78	12,17	2,91	1,00	3,07	2,85	0,01	1,13
obs80m	908,2	934,0	883,0	908,0	12,18	-	-	-	-	-	-

**Table B-14: Observation and model statistics and statistical scores for site E6 from the PBL experiments.**

E6 2010/2011											
wind speed											
Data	mean	max	min	median	std	abse	corr	rmse	bias	bias std	dispe
wrf.3.2_FNL	8,24	21,97	0,18	7,94	3,53	2,18	0,70	2,92	1,26	0,28	2,62
wrf.3.2_myj	8,72	20,50	0,21	8,70	3,47	2,42	0,69	3,17	1,73	0,19	2,64
wrf.3.2_qnse	9,05	21,55	0,21	9,00	3,68	2,71	0,68	3,49	2,06	0,41	2,79
wrf.3.2_mynn2	8,76	20,59	0,08	8,48	3,79	2,61	0,67	3,40	1,77	0,52	2,86
obs100m	6,97	19,70	0,10	7,10	3,24	-	-	-	-	-	-
temperature											
Data	mean	max	min	median	std	abse	corr	rmse	bias	bias std	dispe
wrf.3.2_FNL	-4,28	13,39	-20,84	-4,69	6,84	1,29	0,98	1,72	-0,87	0,31	1,46
wrf.3.2_myj	-6,31	8,75	-21,22	-6,06	5,78	1,47	0,97	1,90	-1,28	0,21	1,39
wrf.3.2_qnse	-6,32	8,69	-21,22	-6,01	5,79	1,51	0,97	1,96	-1,29	0,22	1,45
wrf.3.2_mynn2	-6,04	8,72	-20,78	-5,87	5,88	1,40	0,97	1,87	-1,06	0,31	1,51
obs100m	-3,41	15,70	-19,50	-4,10	6,53	-	-	-	-	-	-
pressure											
Data	mean	max	min	median	std	abse	corr	rmse	bias	bias std	dispe
wrf.3.2_FNL	922,20	945,25	893,60	922,58	12,18	0,82	1,00	1,04	-0,45	0,05	0,93
wrf.3.2_myj	921,42	945,35	893,16	921,60	12,38	0,84	1,00	1,15	-0,42	0,14	1,06
wrf.3.2_qnse	921,37	945,40	892,72	921,61	12,52	0,91	1,00	1,22	-0,48	0,26	1,09
wrf.3.2_mynn2	921,30	945,35	893,01	921,38	12,42	0,88	1,00	1,18	-0,48	0,19	1,06
obs100m	922,7	947,0	895,0	923,0	12,23	-	-	-	-	-	-

**Table B-15: Observation and model statistics and statistical scores for site E7 from the PBL experiments.**

E7 2010/2011											
wind speed											
Data	mean	max	min	median	std	abse	corr	rmse	bias	bias std	dispe
wrf.3.2_FNL	9,35	24,52	0,22	9,31	4,01	2,40	0,73	3,25	1,56	0,34	2,82
wrf.3.2_myj	10,29	24,80	0,22	10,48	4,45	3,06	0,74	3,90	2,46	0,71	2,94
wrf.3.2_qnse	10,75	24,88	0,28	10,72	4,85	3,49	0,72	4,43	2,90	1,11	3,16
wrf.3.2_mynn2	10,23	25,11	0,15	10,05	4,62	3,10	0,72	4,01	2,38	0,89	3,10
obs200m	7,79	23,30	0,10	7,90	3,67	-	-	-	-	-	-
temperature											
Data	mean	max	min	median	std	abse	corr	rmse	bias	bias std	dispe
wrf.3.2_FNL	-4,44	12,69	-20,95	-4,91	6,53	1,14	0,98	1,52	-0,73	0,13	1,33
wrf.3.2_myj	-6,11	8,95	-21,32	-5,95	5,56	1,17	0,97	1,57	-0,86	0,08	1,31
wrf.3.2_qnse	-6,08	8,90	-21,48	-5,82	5,57	1,21	0,97	1,62	-0,83	0,08	1,39
wrf.3.2_mynn2	-5,95	8,89	-21,33	-5,80	5,65	1,19	0,97	1,62	-0,74	0,16	1,43
obs200m	-3,72	15,40	-19,70	-4,20	6,41	-	-	-	-	-	-
pressure											
Data	mean	max	min	median	std	abse	corr	rmse	bias	bias std	dispe
wrf.3.2_FNL	910,56	933,88	882,37	910,81	12,04	0,74	1,00	0,95	-0,19	0,09	0,92
wrf.3.2_myj	909,75	933,99	881,91	909,73	12,22	0,79	1,00	1,08	-0,19	0,09	1,06
wrf.3.2_qnse	909,70	934,04	881,50	909,77	12,35	0,85	1,00	1,15	-0,25	0,21	1,10
wrf.3.2_mynn2	909,62	933,98	881,83	909,54	12,25	0,83	1,00	1,11	-0,24	0,14	1,08
obs200m	910,8	935,0	883,0	911,0	12,13	-	-	-	-	-	-

**Table B-16: Observation and model statistics and statistical scores for site E8 from the PBL experiments.**

E8 2010/2011											
wind speed											
Data	mean	max	min	median	std	abse	corr	rmse	bias	bias std	dispe
wrf.3.2_FNL	7,34	19,69	0,20	7,26	3,26	1,77	0,73	2,29	0,21	0,37	2,25
wrf.3.2_myj	7,59	19,03	0,27	7,81	3,09	1,77	0,71	2,30	0,36	0,20	2,26
wrf.3.2_qnse	7,82	19,11	0,12	8,12	3,24	1,88	0,71	2,42	0,59	0,34	2,32
wrf.3.2_mynn2	7,81	18,95	0,19	7,94	3,37	1,91	0,71	2,48	0,58	0,48	2,36
obs70m	7,13	18,10	0,50	7,20	2,89	-	-	-	-	-	-
temperature											
Data	mean	max	min	median	std	abse	corr	rmse	bias	bias std	dispe
wrf.3.2_FNL	-3,11	14,31	-20,24	-3,40	6,80	1,36	0,96	1,88	-0,44	0,39	1,79
wrf.3.2_myj	-5,32	10,07	-20,55	-5,12	5,75	1,48	0,95	2,10	-1,17	0,21	1,73
wrf.3.2_qnse	-5,36	9,66	-20,81	-5,21	5,69	1,53	0,95	2,16	-1,21	0,15	1,78
wrf.3.2_mynn2	-4,92	10,41	-20,36	-4,85	5,78	1,40	0,95	2,00	-0,77	0,24	1,83
obs70m	-2,67	17,10	-17,90	-3,20	6,41	-	-	-	-	-	-
pressure											
Data	mean	max	min	median	std	abse	corr	rmse	bias	bias std	dispe
wrf.3.2_FNL	916,97	941,46	884,62	917,55	11,72	2,56	1,00	2,68	-2,55	0,14	0,80
wrf.3.2_myj	916,19	941,76	884,44	916,52	11,79	2,55	1,00	2,72	-2,55	0,05	0,95
wrf.3.2_qnse	916,15	941,93	884,25	916,48	11,89	2,59	1,00	2,77	-2,59	0,15	0,97
wrf.3.2_mynn2	916,17	941,95	884,35	916,47	11,81	2,57	1,00	2,73	-2,56	0,07	0,94
obs70m	919,5	944,0	888,0	920,0	11,86	-	-	-	-	-	-

**Table B-17: Observation and model statistics and statistical scores for site E9 from the PBL experiments.**

E9 2010/2011											
wind speed											
Data	mean	max	min	median	std	abse	corr	rmse	bias	bias std	dispe
wrf.3.2_FNL	8,59	23,40	0,14	8,47	3,85	1,89	0,79	2,46	0,09	0,19	2,45
wrf.3.2_myj	9,48	22,88	0,13	9,79	4,03	2,06	0,78	2,69	0,84	0,36	2,53
wrf.3.2_qnse	9,98	23,45	0,26	10,29	4,39	2,34	0,79	3,03	1,34	0,72	2,62
wrf.3.2_mynn2	9,49	23,97	0,26	9,61	4,34	2,20	0,77	2,90	0,84	0,68	2,69
obs155m	8,50	28,10	0,10	8,50	3,66	-	-	-	-	-	-
temperature											
Data	mean	max	min	median	std	abse	corr	rmse	bias	bias std	dispe
wrf.3.2_FNL	-3,43	13,66	-18,83	-3,76	6,57	1,26	0,97	1,76	-0,39	0,44	1,65
wrf.3.2_myj	-5,31	9,74	-19,03	-4,98	5,59	1,32	0,95	1,91	-0,83	0,34	1,69
wrf.3.2_qnse	-5,30	10,10	-19,01	-5,02	5,52	1,34	0,95	1,94	-0,82	0,27	1,74
wrf.3.2_mynn2	-5,06	9,74	-18,73	-4,86	5,58	1,32	0,95	1,89	-0,58	0,33	1,77
obs155m	-3,04	14,80	-18,00	-3,50	6,12	-	-	-	-	-	-
pressure											
Data	mean	max	min	median	std	abse	corr	rmse	bias	bias std	dispe
wrf.3.2_FNL	907,06	931,49	875,21	907,52	11,65	0,93	1,00	1,14	-0,69	0,22	0,88
wrf.3.2_myj	906,15	931,83	875,03	906,33	11,69	0,90	1,00	1,22	-0,67	0,03	1,02
wrf.3.2_qnse	906,10	931,99	874,82	906,31	11,78	0,94	1,00	1,26	-0,71	0,07	1,04
wrf.3.2_mynn2	906,13	931,99	874,94	906,34	11,71	0,91	1,00	1,22	-0,68	0,01	1,01
obs155m	907,8	932,0	877,0	908,0	11,86	-	-	-	-	-	-

**Table B-18: Observation and model statistics and statistical scores for site E11 from the PBL experiments.**

E11 2010/2011											
wind speed											
Data	mean	max	min	median	std	abse	corr	rmse	bias	bias std	dispe
wrf.3.2_FNL	8,67	24,36	0,25	8,46	3,64	2,14	0,78	2,79	1,61	0,51	2,23
wrf.3.2_myj	9,21	25,04	0,31	9,35	3,50	2,40	0,78	3,01	2,02	0,36	2,20
wrf.3.2_qnse	9,54	23,65	0,17	9,65	3,68	2,68	0,76	3,37	2,35	0,54	2,34
wrf.3.2_mynn2	9,44	25,86	0,19	9,43	3,93	2,67	0,75	3,43	2,25	0,79	2,46
obs60m	7,07	22,60	0,10	7,10	3,13	-	-	-	-	-	-
temperature											
Data	mean	max	min	median	std	abse	corr	rmse	bias	bias std	dispe
wrf.3.2_FNL	-4,37	11,74	-19,64	-4,77	6,19	1,24	0,97	1,67	-0,90	0,12	1,40
wrf.3.2_myj	-6,52	8,03	-20,71	-6,41	5,26	1,61	0,96	2,08	-1,45	0,08	1,49
wrf.3.2_qnse	-6,52	7,70	-20,24	-6,46	5,24	1,62	0,96	2,11	-1,45	0,06	1,52
wrf.3.2_mynn2	-6,25	7,93	-19,72	-6,16	5,27	1,40	0,96	1,88	-1,18	0,10	1,47
obs60m	-3,47	16,40	-19,40	-4,10	6,07	-	-	-	-	-	-
pressure											
Data	mean	max	min	median	std	abse	corr	rmse	bias	bias std	dispe
wrf.3.2_FNL	887,48	911,71	857,15	887,40	11,52	0,66	1,00	0,84	0,29	0,18	0,77
wrf.3.2_myj	886,16	912,03	856,88	886,05	11,43	0,75	1,00	1,02	0,25	0,02	0,99
wrf.3.2_qnse	886,11	912,17	856,72	886,05	11,52	0,77	1,00	1,04	0,19	0,08	1,02
wrf.3.2_mynn2	886,12	912,16	856,89	886,00	11,45	0,75	1,00	1,01	0,22	0,01	0,98
obs60m	887,2	912,0	857,0	887,0	11,70	-	-	-	-	-	-

# **ELFORSK**

SVENSKA ELFÖRETAGENS FORSKNINGSG- OCH UTVECKLINGSG - ELFORSK - AB

**Elforsk AB, 101 53 Stockholm. Besöksadress: Olof Palmes Gata 31  
Telefon: 08-677 25 30, Telefax: 08-677 25 35  
[www.elforsk.se](http://www.elforsk.se)**